NOTE TO USERS

This reproduction is the best copy available.

Investigating the nucleotide-binding domains of Abcb1a (mouse P-glycoprotein/Mdr3): a mutational analysis approach

Isabelle Carrier

Department of Biochemistry
McGill University
Montréal, Québec, Canada

August 2008

A thesis submitted to McGill University in partial fulfillment of the requirements of the degree of Doctor of Philosophy

Your file Votre référence
ISBN: 978-0-494-66299-1
Our file Notre référence
ISBN: 978-0-494-66299-1

Abstract

ABC transporters consist of two transmembrane domains (TMDs) that form the transport channel and two cytosolic nucleotide-binding domains (NBDs) that energize transport via ATP binding and hydrolysis. Using site-directed mutagenesis, the role of highly conserved residues in the NBDs of Abcb1a was investigated.

In both NBDs of Abcb1a the A-loop aromatic residue is a tyrosine: Y397 in NBD1 and Y1040 in NBD2. Another tyrosine (618 in NBD1 and 1263 in NBD2) also appears to lie close to the ATP molecule. These four tyrosine residues were mutated to tryptophan and the effect of these substitutions on transport properties, ATP binding, and ATP hydrolysis was analyzed. Y618W and Y1263W enzymes had catalytic characteristics similar to wild-type (WT) Abcb1a. On the other hand, Y397W and Y1040W showed impaired transport and greatly reduced ATPase activity, including an ~10-fold increase in K_M(ATP). Thus, Y397 and Y1040 play an important role in Abcb1a catalysis.

Since it was speculated that ABC transporters utilize a catalytic base to hydrolyse the β-γ phosphodiester bond of ATP, a search for that residue was undertaken. Six pairs of highly conserved acidic residues in the NBDs of Abcb1a were investigated. Removal of the charge in D558N and D1203N as well as in E552Q and E1197Q produced enzymes with severely impaired transport. These mutants were purified and characterized with respect to ATPase activity. Mutants D558N and D1203N retained some drug-stimulated ATPase activity and vanadate (Vi) trapping of 8-azido-[α^{32}P]nucleotide confirmed slower basal and drug-stimulated hydrolysis. The E552Q and E1197Q mutants showed absence of ATPase activity but Vi trapping of 8-azido-[α^{32}P]nucleotide was observed, at a level similar to that of WT Abcb1a. Photolabelling by 8-azido-[α^{32}P]nucleotide, in the presence or absence of drug, was also detected in the absence of Vi. The ATPase activity, binding affinity, and trapping properties of these glutamate residues were further analyzed. In addition to the E→Q mutants, the glutamates were individually mutated to D, N, and A. The double mutants E552Q/E1197Q, E552Q/K1072R, and K429R/E552Q were also analyzed. The results obtained suggest that 1) the length of the side-chain is important for the catalytic activity, whereas the charge is critical for full turnover to occur, 2) formation of the catalytic transition state does occur in the mutant site in the

single-site mutants, suggesting that E552 and E1197 are not classical catalytic carboxylates, 3) steps after formation of the transition state are severely impaired in these mutant enzymes, 4) NBD1 and NBD2 are functionally asymmetric, and 5) the glutamates are involved both in NBD-NBD communication and transition-state formation through orientation of the linchpin residue.

Résumé

Les transporteurs ABC se composent de deux domaines transmembranaires (TMD) qui forment le canal de transport et deux domaines cytosoliques de fixation des nucléotides (NBD) fournissant l'énergie de transport via l'hydrolyse de l'ATP. Au moyen de la mutagénèse dirigée, nous avons étudié le rôle des résidus fortement préservés dans les NBDs de Abcb1a.

Dans les deux NBDs de Abcb1a, le résidu aromatique de la boucle-A est une tyrosine : Y397 dans NBD1 et Y1040 dans NBD2. Une autre tyrosine (618 dans NBD1 et 1263 dans NBD2) apparaît être également à proximité de la molécule d'ATP. Ces quatre résidus de tyrosine ont été mutés en tryptophane et l'effet de ces substitutions sur les propriétés de transport et de liaison et d'hydrolyse de l'ATP a été analysé. Les enzymes Y618W et Y1263W présentaient des caractéristiques catalytiques semblables à la protéine Abcb1a sauvage. D'un autre côté, Y397W et Y1040W montraient une déficience du transport et une activité ATPasique fortement réduite, incluant un accroissement d'environ 10 fois du K_M(ATP). Ainsi, Y397 et Y1040 jouent un rôle important dans la catalyse d'Abcb1a.

Puisqu'on supposait que les transporteurs ABC utilisent une base catalytique pour l'hydrolyse du γ-phosphate de l'ATP, nous avons entrepris la recherche de ce résidu. Six paires de résidus acides fortement préservés dans les NBDs de Abcb1a ont été étudiées. La suppression de la charge dans D558N et D1203N aussi bien que dans E552Q et E1197Q a produit des enzymes ayant une capacité de transport sérieusement affaiblie. Ces mutants ont été purifiés, et caractérisés selon l'activité ATPasique. Les mutants D558N et D1203N ont conservé une certaine activité ATPasique stimulée et la capture au vanadate (Vi) de 8-azido-[α^{32}P]nucléotide a confirmé une hydrolyse plus lente tant de base que stimulée par drogue. Les mutants E552Q et E1197Q ont montré une absence d'activité ATPasique mais la capture au Vi de 8-azido-[α^{32}P]nucléotide fut observée à un niveau semblable a la protéine Abcb1a sauvage. Le photo-marquage par 8-azido-[α^{32}P]nucléotide, en présence ou en absence de drogue, a également été détecté en absence de Vi. L'activité ATPasique, l'affinité de liaison et les propriétés de capture de ces résidus glutamates ont été analysées plus en profondeur. En plus des mutants E→Q, les glutamates furent mutés séparément en D, N et A. Les doubles mutants

E552Q/E1197Q, E552Q/K1072R et K429R/E552Q furent aussi analysés. Les résultats suggèrent que 1) la longueur de la chaîne latérale est importante pour l'activité catalytique, alors que la charge est critique pour un renouvellement complet, 2) la formation de l'état de transition catalytique prend place dans le site mutant chez les mutants à site simple, 3) les étapes qui suivent la formation de l'état de transition sont sérieusement diminuées dans ces enzymes mutants, 4) NBD1 et NBD2 sont fonctionnellement asymétriques et 5) les glutamates sont impliqués à la fois dans la communication NBD-NBD et dans la formation de l'état de transition grâce à l'orientation du résidu pivot.

Table of Contents

List of Figures

Chapter 3

Chapter 4

Chapter 5

Chapter 6

List of Tables

Preface

The work described in Chapters 2, 3, 4, and 5 of this thesis has been published as follows:

Chapter 2: **Carrier, I.**, Urbatsch, I. L., Senior, A. E., and Gros, P. Mutational Analysis of Conserved Aromatic Residues in the A-Loop of the ABC Transporter Abcb1a (Mouse Mdr3). *FEBS Letters*, **581(2)**: 301-308, 2007. © Federation of European Biochemical Societies. Reproduced here by permission from the publisher.

Chapter 3: Urbatsch, I. L., Julien, M., **Carrier, I.**, Rousseau, M.-É., Cayrol, R., and Gros, P. Mutational Analysis of Conserved Carboxylate Residues in the Nucleotide Binding Sites of P-Glycoprotein. *Biochemistry*, **39(46)**: 14138-14149, 2000. © American Chemical Society. Reproduced here by permission from the publisher.

Chapter 4: **Carrier, I.**, Julien, M., and Gros, P. Analysis of Catalytic Carboxylate Mutants E552Q and E1197Q Suggests Asymmetric ATP Hydrolysis by the Two Nucleotide-Binding Domains of P-Glycoprotein. *Biochemistry*, **42(44)**: 12875-12885, 2003. © American Chemical Society. Reproduced here by permission from the publisher.

Chapter 5: **Carrier, I.** and Gros, P. Investigating the Role of the Invariant Carboxylate Residues E552 and E1197 in the Catalytic Activity of Abcb1a (mouse Mdr3). *FEBS Journal*, **275(13)**: 3312-3324, 2008. © Federation of European Biochemical Societies. Reproduced here by permission from the publisher.

Contribution of Co-Authors

Chapter 2: In this chapter, the residues chosen for mutagenesis to tryptophan were selected by Ina L. Urbatsch and Philippe Gros based on results obtained in Dr. Alan E. Senior's laboratory (University of Rochester, Rochester, NY, USA). The mutagenesis was done by me, with the exception of the Y618W and Y1263W mutants which were began by Patrice Menard under the supervision of Ina L. Urbatsch. Subsequent subcloning into both yeast expression vectors was done by me, and all of the figures presented are based on experiments that I carried out. I prepared the published manuscript with the help and advice from my supervisor Dr. Philippe Gros.

Chapter 3: In this chapter, the first three authors contributed equally to the work. Ina Urbatsch used the server PredictProtein to search for and align the multiple NBD sequences in order to select the most conserved carboxylate residues in Abcb1a. cDNA modifications for all mutants was done by Ina Urbatsch, except E552Q and E1197Q which were done by Marc-Étienne Rousseau and Romain Cayrol. Transformation into the yeast strains JPY201 (*S. cerevisiae*) and GS115 (*P. pastoris*), as well as biological testing in JPY201 (FK506 resistance and mating assays) of all mutants, except E552Q and E1197Q, were carried out by Ina Urbatsch, with some of my help. E552Q and E1197Q were transformed into the yeast strains JPY201 and GS115 by Michel Julien. Testing of the biological activity of the E552Q and E1197Q mutants in JPY201 was done by me. Protein purification from GS115 membranes for WT Abcb1a and mutants D558N and D1203N was done by Ina Urbatsch, and the E552Q and E1197Q mutants were done by me. ATPase assays were carried out by Ina Urbatsch and Michel Julien. The time-dependence of vanadate trapping of Mg-8-azido-[α^{32}P]ATP on WT Abcb1a was done by me. Photolabeling was done by Ina Urbatsch (D558N and D1203N) and me (E552Q and E1197Q). Writing of the manuscript was essentially done by Ina Urbatsch, although additions pertaining to the mutants E552Q and E1197Q, and revisions, were done by me with the help and advice from my supervisor Dr. Philippe Gros.

Chapter 4: In this chapter, all of the figures presented are based on experiments that I carried out. Michel Julien provided useful insights for the writing of the manuscript. I prepared the published manuscript with the help and advice from my supervisor Dr. Philippe Gros.

Chapter 5: In this chapter, all of the figures presented are based on experiments that I carried out. I prepared the published manuscript with the help and advice from my supervisor Dr. Philippe Gros.

Philippe Gros provided excellent supervision and support throughout all of these studies.

Publications

Carrier, I. and Gros, P. (2008) Investigating the Role of the Invariant Carboxylate Residues E552 and E1197 in the Catalytic Activity of Abcb1a (Mouse Mdr3). *FEBS Journal*, **275(13)**: 3312-3324.

Carrier, I., Urbatsch, I. L., Senior, A. E., and Gros, P. (2007) Mutational Analysis of Conserved Aromatic Residues in the A-Loop of the ABC Transporter Abcb1a (Mouse Mdr3). *FEBS Letters*, **581(2)**: 301-308.

Carrier, I. Julien, M., and Gros, P. (2003) Analysis of Catalytic Carboxylate Mutants E552Q and E1197Q Suggests Asymmetric ATP Hydrolysis by the Two Nucleotide-Binding Domains of P-Glycoprotein. *Biochemistry*, **42(44)**: 12875-12885.

Vigano, C., Julien, M., **Carrier, I.**, Gros, P., and Ruysschaert, J.-M. (2002) Structural and Functional Asymmetry of the Nucleotide-Binding Domains of P-Glycoprotein Investigated by Attenuated Total Reflection Fourier Transform Infrared Spectroscopy. *J. Biol. Chem.*, **277(7)**: 5008-5016.

Urbatsch*, I. L., Julien*, M., **Carrier*, I.**, Rousseau, M.-É., Cayrol, R., and Gros, P. (2000) Mutational Analysis of Conserved Carboxylate Residues in the Nucleotide Binding Sites of P-Glycoprotein. *Biochemistry*, **39(46)**: 14138-14149. * Equal contribution.

Urbatsch, I. L., Beaudet, L., **Carrier, I.**, and Gros, P. (1998) Mutations in Either Nucleotide-Binding Site of P-Glycoprotein (Mdr3) Prevent Vanadate Trapping of Nucleotide at Both Sites. *Biochemistry*, **37(13)**: 4592-4602.

Acknowledgements

Firstly, I would like to thank my supervisor, Philippe Gros, for his support and guidance during my doctoral studies. I really enjoyed my time in the lab, with an interesting project and the chance to learn several different techniques. I am forever grateful for his kindness, understanding and patience. It was a relief to see that he was genuinely happy for me when I told him that I was expecting, and not just once, but twice!

Thanks to past and present members of the lab for their help, interesting discussions and friendship. In particular, Ina Urbatsch, who took me in as a summer student to help her with her project and trusted me to accomplish various tasks while teaching me the ABCs of ABC transporters and the techniques to study them. Also, Michel Julien, Jie Cai, and Tony Kwan who worked on ABC transporters as well, and with whom I could discuss my project and who provided answers to various questions that would pop into my mind. I am also grateful to Normand Groulx and Susan Gauthier for their help and willingness. Thanks to the many interesting persons from the department here at McGill as well as from so many different cities I had the chance to meet during my studies and conferences.

I am also grateful for the funding I received from FRSQ-FCAR and McGill Major Fellowships.

For their friendship and constant encouragements, I thank my very good friends Maria Ferraiuolo, Annie Boisclair, Lie Mittellehner, Julie Crowley and all the others.

Maman, Papa, je vous remercie énormément pour votre soutien et vos encouragements! Vous m'avez donné de merveilleuses opportunités dans la vie et j'ai pu poursuivre mon rêve de devenir biochimiste. Merci au reste de ma famille et à ma belle-famille aussi.

Eduardo, there aren't enough words to express my gratitude to you! Thank you so much for your love, patience, support (both moral and monetary), and in the last weeks, for giving me the chance to work on the week-ends without having to worry about family-related stuff! Thanks for making my task easier when you could. Finally, thanks to my two little "monsters", Romain and Arianne, for their liveliness and affection.

Objectives of the Presented Work

The translocation of molecules across cellular lipid membranes is critical for most aspects of cell physiology. ATP-binding cassette (ABC) transporters are one of the major classes of membrane transporters found in all cell types of all species studied so far (Holland *et al.*, 2003). Identified members of this protein superfamily include importers, exporters, channels, and receptors. Defects in a number of ABC transporters have been associated with serious hereditary disorders in humans. In addition, increased expression levels of certain members of this ubiquitous family are a common cause of multidrug resistance (MDR), which is of major concern in the treatment of many important human diseases such as cancer, schizophrenia, and infections by micro-organisms (viruses, bacteria, fungi, yeasts, and parasites). This family of proteins is therefore of particular economic, industrial, and medical importance and elucidation of the structure and mechanism of ABC transporters is essential to the rational design of agents to control their function.

The term "ATP-binding cassette" was not given to this large superfamily of proteins until 1990 (Higgins *et al.*, 1990), but the study of these transporters began decades earlier, with the discovery of ATP-dependent nutrient uptake mediated by systems associated with high-affinity binding proteins in the periplasm of Gram-negative bacteria (Weiner *et al.*, 1971). In bacteria, ABC importers can accumulate nutrients (sugars or amino acids typically) against gradients as large as 10^6:1 (Dippel and Boos, 2005), consistent with the use of ATP rather than the proton-motive force as a source of energy[1].

---

[1] **Primary versus secondary active transport**
Active transport refers to the movement of substrates against their electrochemical gradient, thereby requiring an input of energy. In primary active transport, the energy derives from a change in the chemical state of one of the reactants, a common example being the hydrolysis of ATP. In this case, as in ABC transporters, the energy from ATP hydrolysis is coupled to the movement of substrate by ATP-driven conformational changes in protein structure. In secondary active transport, energy is derived from a pre-existing electrochemical gradient, such as the bacterial proton-motive force. In the case of the lactose permease, accumulation of lactose in an energetically "uphill" direction is driven by the simultaneous downhill movement of protons into the cell. The number of protons associated with the reaction determines the extent to which lactose can accumulate because the size of the lactose gradient generated can never exceed the magnitude of the proton-motive gradient that drives the reaction. For LacY and most other secondary active transporters that accept sugars or amino acids, the coupling ratio is one proton per substrate, typically limiting the substrate gradient to 10^3 or less.

The objectives of the work presented in this thesis were to study specific conserved residues in the nucleotide binding sites (NBSs) of the NBDs of mouse Abcb1a in order to determine their role in the catalytic mechanism of the enzyme and thus provide insight into the mode of action of ABC transporters associated with MDR, such as mammalian P-glycoprotein (P-gp), as well as ABC proteins in general. When this thesis project was undertaken, some key features of the catalytic mechanism of human or rodent P-gp were already established. Thus, it was demonstrated that 1) drug transport is strictly ATP dependent (Ruetz and Gros, 1994; Shapiro and Ling, 1995), 2) purified human or rodent P-gp shows ATPase activity that can be further stimulated by certain MDR drugs and P-gp modulators (Sarkadi *et al.*, 1992; Urbatsch *et al.*, 1994), 3) both NBDs are essential for function, with complete cooperativity between the two sites for ATP hydrolysis and drug transport (Azzaria *et al.*, 1989; Loo and Clarke, 1995a; Urbatsch *et al.*, 1998), 4) both NBDs are catalytically active with equal probability of hydrolysis at NBD1 and NBD2 (Senior *et al.*, 1995b), and 5) ATP hydrolysis alternates between the two sites (Senior *et al.*, 1995b; Sauna and Ambudkar, 2000). However, many aspects of the catalytic activity of the protein were still not well understood, such as: 1) what is the mechanism of allocrite recognition and transport by the TMDs across the membrane lipid bilayer? 2) What are the exact structural determinants of the allocrite-binding site, and how exactly is this allocrite-binding site organized in the membrane lipid bilayer? 3) How does allocrite-binding to the TMDs result in the activation of the NBDs for ATP hydrolysis? 4) Which regions of the protein are critical for this signalling process between the two domains? 5) How is the energy of ATP hydrolysis coupled to allocrite transport and what kind of conformational changes take place during this process? 6) What is the nature of the mechanism by which the two NBDs hydrolyse ATP during the catalytic cycle? And 7) what are the structural and biochemical bases for the cooperativity between the two NBDs for ATP hydrolysis?

Mouse Abcb1a (P-gp, Mdr1a, Mdr3) is an integral membrane protein with two multiple-spanning TMDs and two large hydrophilic NBDs. The TMDs have been identified as the major site of allocrite binding and translocation, whereas the two NBDs have been determined to provide the energy for the translocation process, through hydrolysis of its substrate: ATP. Mouse Abcb1a is the orthologue of human ABCB1 and

these two proteins share 87% identity at the amino acid level, thus making Abcb1a a suitable model for ABCB1.

The first part of this thesis (Chapter 2) describes the investigation of the role of conserved aromatic residues (Y397, Y1040, Y618, and Y1263) in nucleotide binding. Two aromatic residues in human ABCB1 (one in each NBD) were identified as part of a conserved loop, the A-loop, responsible for stabilising the adenine moiety of ATP in the NBS (Ambudkar *et al.*, 2006; Kim *et al.*, 2006). By individually mutating all four tyrosine residues to tryptophan, it was established that the residues equivalent to the A-loop residues in ABCB1 (Y397 and Y1040) play a similar role in Abcb1a.

The focus of the rest of this thesis (Chapters 3, 4, and 5) was placed on the identification and characterisation of the catalytic residue(s) of the NBDs of Abcb1a. A catalytic carboxylate residue (acidic amino acid: aspartate or glutamate) was proposed earlier, based on sequence alignments and structural and biochemical analyses of Walker motif-containing enzymes, to be present in ABC transporters (Yoshida and Amano, 1995). By mutating seven pairs of conserved acidic amino acids in the NBDs of Abcb1a, a highly mutation sensitive glutamate pair was identified. When the invariant carboxylate residues E552 and E1197, in NBD1 and NBD2 respectively, were mutated to glutamine (Q) individually, the mutant enzymes became completely impaired for transport. The ATPase activity was also found to correspond to background levels in a Pi-release assay. Upon further characterization of these mutants using Vi-trapping of 8-azido[α^{32}P]ATP, a unique phenotype was identified. These mutants were still able to trap 8-azido-nucleotide in a drug-stimulated fashion at levels similar to wild-type (WT) Abcb1a. Importantly, this trapping also occurred in the absence of Vi, a characteristic unprecedented in ABC transporters (Chapter 3). Further characterization of these E→Q mutants (Chapter 4) using 8-azido-nucleotide trapping techniques suggested that single-site turnover occurred in the E552Q and E1197Q mutants and that ADP release from the mutant site, or another catalytic step, was impaired in these mutants. Functional asymmetry of the NBDs was also suggested by these results. To characterize the role of these residues in catalysis, the single-site mutants E552D, N, and A in NBD1, and E1197D, N, and A in NBD2, as well as the double mutant E552Q/E1197Q were created in Abcb1a. In addition, mutants in which the Walker A K→R mutation known to abolish ATPase activity was introduced in

the non-mutant NBD of E552Q and E1197Q were created. ATPase activity, binding affinity and trapping properties were tested for each Abcb1a variant (Chapter 5). The results suggested that the length of the invariant carboxylate residue is important for the catalytic activity, whereas the charge of the side chain is critical for full turnover to occur. Moreover, in the double-mutants where the K→R mutation is introduced in the WT NBD of the E→Q mutants, single-site turnover was observed, especially when NBD2 can undergo γ-Pi cleavage. The results further support the idea that the NBDs are not symmetric and suggest that the invariant carboxylates are involved both in NBD-NBD communication and transition-state formation through orientation of the linchpin residue.

Chapter 1

Introduction and Literature Review

Section 1.1 – Structure of ABC Transporters

ABC transporters are integral membrane proteins and consist of four core domains (Higgins *et al.*, 1986): two transmembrane domains, each normally (but not always) consisting of six transmembrane α-helices (TMD1 and TMD2) and two cytosolic nucleotide binding domains (NBD1 and NBD2). These four core domains form the minimal functional unit; however, there are many variations on this theme, as discussed in the next subsection.

1.1.1 Domain arrangements

Figure 1.1 depicts some of the domain arrangements found in ABC transporters. The four core domains of prokaryotic ABC transporters are most often encoded as separate polypeptides, but may also be fused in different arrangements to form the functional proteins. In mammals, the four domains may also be fused together in a number of ways, either as a single polypeptide or as two half transporters each consisting of one TMD and one NBD. In addition, some transporters have extra domains, including additional TMDs, intra- or extracellular loops, regulatory domains, and NBD insertions. For example, the ABCA subfamily comprises members that possess two large, sometimes extremely large, extracellular loops between the first two TM α-helices of each TMD (Tusnady *et al.*, 2006). Also, some members of the ABCC subfamily (ABCC1-3, 6, 8-10) have an additional transmembrane domain (TMD_0), consisting of five TM α-helices, at the amino terminus of the protein. The usual order of domains in a fused protein is NH_2-TMD-NBD-TMD-NBD-COOH, but this order is sometimes reversed, as is the case in the half-transporters of the ABCG subfamily.

For any given transporter, the two NBDs are often closely related to each other (they are sometimes identical), as are the two TMDs. Thus, it has long been predicted that ABC transporters are pseudodimers, with each half of the dimer consisting of one TMD and one NBD.

Abcb1a is a full-length transporter of 1278 amino acids containing two TMDs and two NBDs.

Figure 1.1:

Examples of domain arrangements found in ABC transporters

The basic transporter is represented as a four-subunit package with two TMDs and two NBDs. TMDs are represented as rounded-rectangles and NBDs as ovals. Where heterodimers of either TMD or NBD are present, these are distinguished by different shading of the subunits. Where rectangles and ovals are clearly shown to be independent, these are encoded by separate genes. The black lines represent the lipid bilayer.

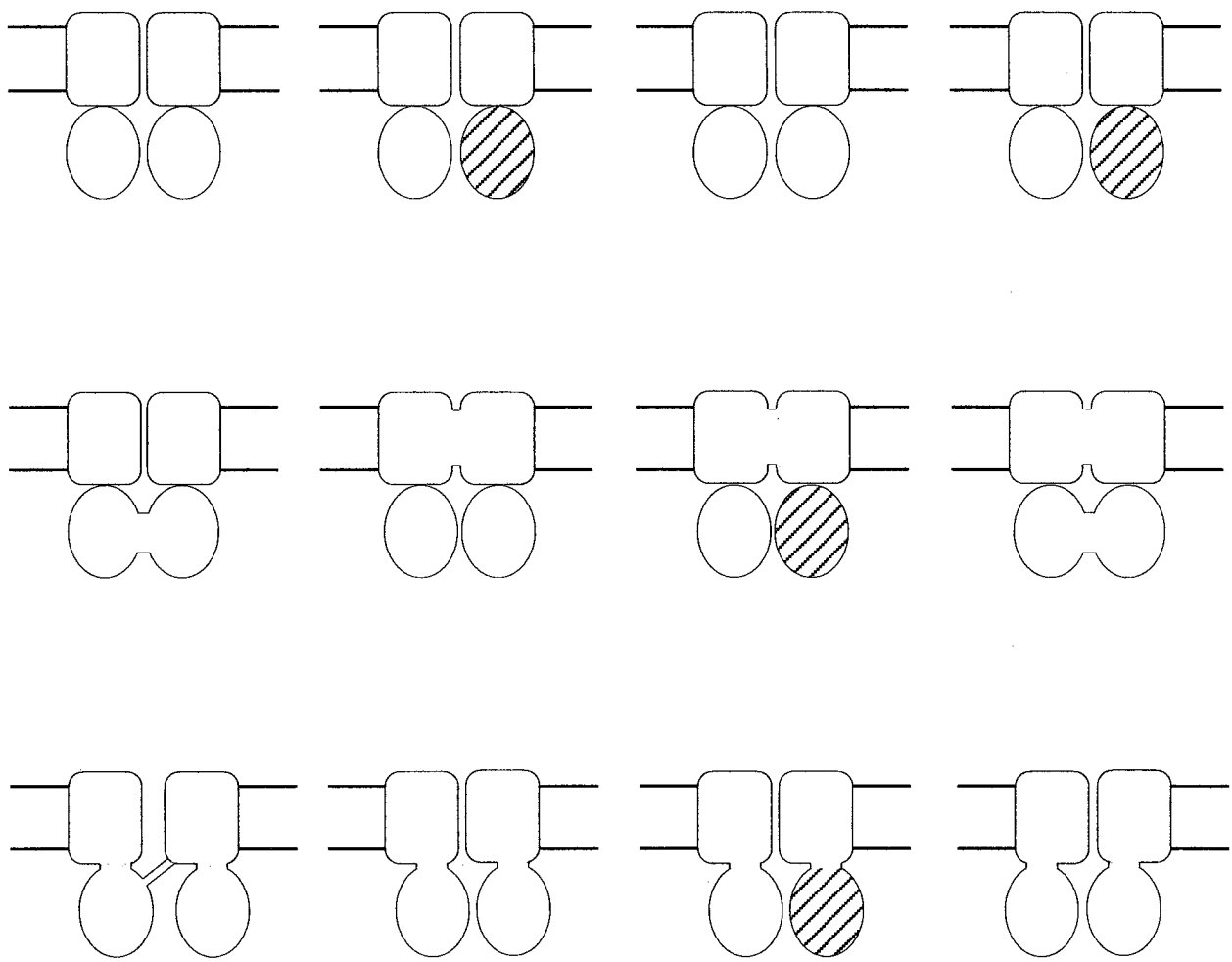

1.1.2 Topology

Unambiguously assessing the membrane topology of polytopic proteins is known to be difficult, and ABC transporters have not been an exception. Before crystal structures of complete ABC transporters became available, starting with the structure of the *E. coli* vitamin B_{12} importer BtuCD in May 2002, knowledge about the folds of their TMDs was limited to topological schemes based on hydropathy plots and mutational studies. Several computer-assisted empirical prediction methods are available to generate the hydrophobicity and other sequence-based profiles for a putative transmembrane protein. However, such analyses should be regarded only as ''educated guesses'', serving as good starting points for an experimental elucidation of the membrane topology. In a 2006 review, Tusnàdy *et al.* applied their topology prediction strategy (based on incorporation of experimental data into their prediction algorithm) to provide information for the most plausible membrane arrangements for the human ABC transporters (Tusnady *et al.*, 2006). In general, a typical pattern of six TM helices is preserved in the core transmembrane domains of all human ABC half transporters and this core structure is duplicated in the full transporters. Additional N-terminal regions may have important functions in the ABCC family members and in the ABCB half transporters. The homology models also indicate that most of the (predicted) extracellular regions of the ABC proteins are short. In contrast, members of the ABCA family possess two large, sometimes extremely large, extracellular loops in their TMDs. Also, the C-proximal extracellular loop in the ABCG subfamily is a relatively long segment.

At present, high-resolution structural data (including the TMDs) is available only for prokaryotic ABC transporters. Therefore, laborious biochemical experiments are necessary to elucidate the membrane topology of eukaryotic transporters. These methods include epitope insertion, localization of glycosylation sites, limited proteolysis, and immunochemical techniques. An example of the use of one of these methods is the determination of the membrane topology of mouse Abcb1a, which was accomplished by using epitope insertion (Kast *et al.*, 1995; Kast *et al.*, 1996).

Another experimental strategy is to predict the three-dimensional structure of a eukaryotic ABC transporter by homology modeling based on the available crystal structure of a prokaryotic ABC transporter. In principle this is a valid approach, as by

now six prokaryotic ABC-transporters have provided high-resolution structures which include the TMD(s). Four of them are importers: the vitamin B12 transporter BtuCD from *E. coli* (Locher *et al.*, 2002), the metal-chelate-type transporter HI1470/1 from *H. Influenzae* (Pinkett *et al.*, 2007), the molybdate/tungstate transporter $ModB_2C_2$ from *A. fulgidus* determined in complex with its cognate binding protein ModA (Hollenstein *et al.*, 2007b), and the maltose transporter complex $MalFGK_2$ from *E. coli* also determined in complex with its cognate binding protein maltose-binding protein (MBP) (Oldham *et al.*, 2007). Two of them are exporters: the multidrug transporter Sav1866 from *S. aureus* (Dawson and Locher, 2006; Dawson and Locher, 2007) and the bacterial lipid flippase MsbA from *E. coli*, *V. cholerae*, and *S. typhimurium* (Ward *et al.*, 2007). Figure 1.2 depicts a structural model of ABCB1 (Linton and Higgins, 2007) based on the crystal structure of MsbA (Ward *et al.*, 2007) and incorporation of experimental data from cysteine cross-linking studies in ABCB1 (Stenham *et al.*, 2003).

As stated above, six complete prokaryotic ABC transporters in their lipid environment have been crystallized to date (Locher *et al.*, 2002; Dawson and Locher, 2007; Hollenstein *et al.*, 2007b; Oldham *et al.*, 2007; Pinkett *et al.*, 2007; Ward *et al.*, 2007). Whereas ABC exporters contain a conserved core of 12 TM helices, ABC importers feature between 10 and 20 TM helices (Hollenstein *et al.*, 2007a) in the complete transporter. The variability in the number of transmembrane passes may reflect diverse architectures of the TMDs (where the sequence similarities are generally low between different transporters) and/or the need for fewer or more transmembrane passes to translocate allocrites of different sizes (Locher *et al.*, 2002). For example, vitamin B12 is a large compound and is transported by BtuCD which has a total of 20 TM helices.

Thus, the NBDs are located cytoplasmically and the TMDs span the membrane multiple times to form a translocation pathway which is adapted to its allocrite(s).

1.1.3 Three-dimensional crystal structures

As of July 2006, there were 35 three-dimensional (3-D) structures of ABC proteins in the protein database (Kelly *et al.*, 2007). The first crystal structures determined were of the soluble NBDs only, with or without nucleotide and nucleotide analogues bound at the nucleotide binding site. Hence, in 1998 the peripheral ATP-binding subunit,

Figure 1.2:

Schematic representation illustrated for ABCB1

The NBDs are coloured in cyan and yellow and shown in the closed dimer conformation with ATP at the interface in stick form and coloured elementally (carbon: white, nitrogen: blue, oxygen: red). The TMDs, shown in blue and red, form an aqueous chamber in the membrane (the plane of which is indicated by orange rectangles). Figure modified and reproduced with permission from (Linton and Higgins, 2007).

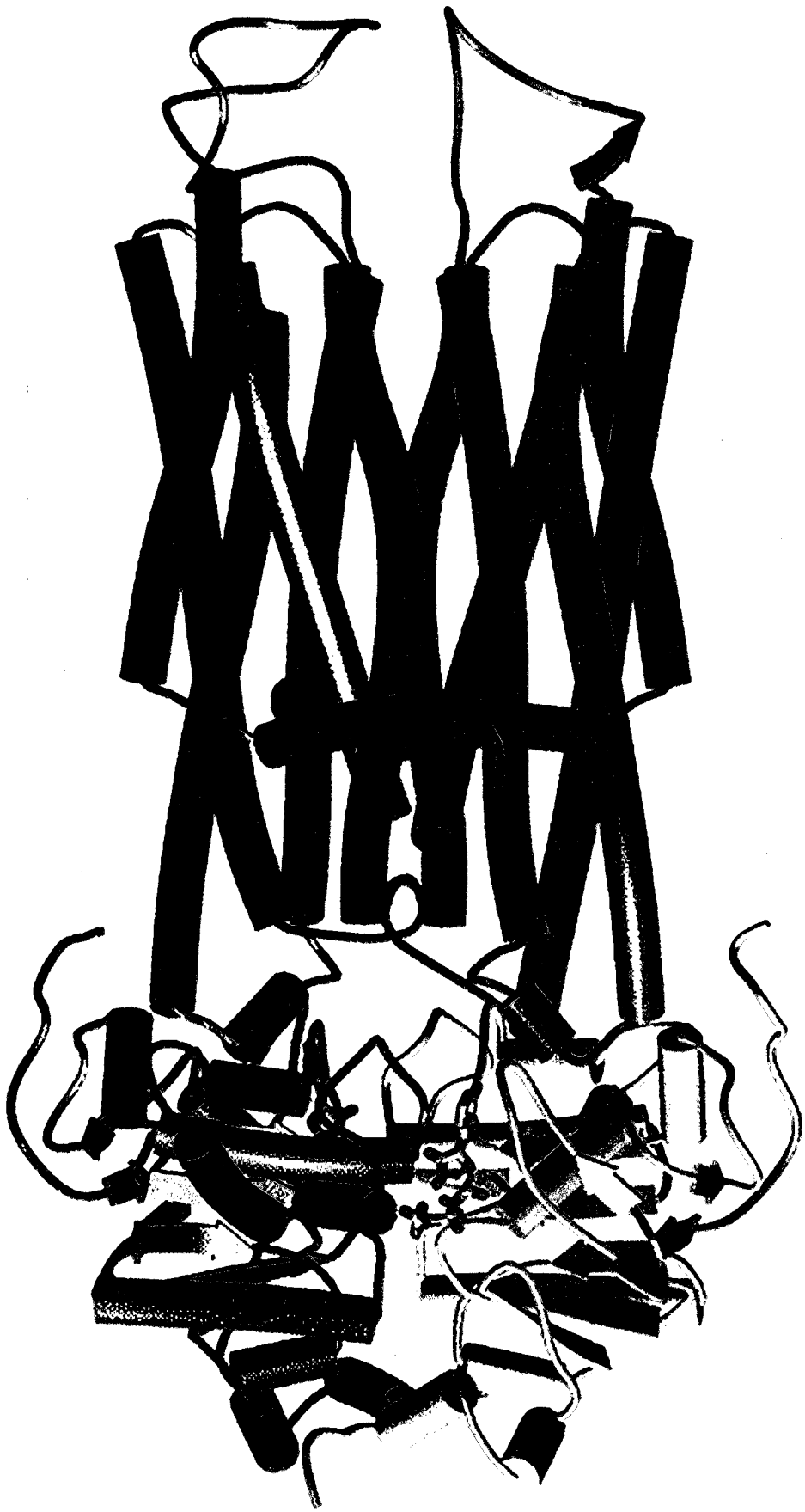
TMDs
NBDs

HisP, of the bacterial histidine permease from *Salmonella typhimurium* was the very first ABC transporter NBD to be crystallized (Figure 1.3 A & (Hung *et al.*, 1998)). Including HisP, several NBDs crystallized as dimers and, initially, several distinct dimer interfaces were observed. However, it is now clear from genetic and biochemical data that the dimer interface first observed in the Rad50 (Hopfner *et al.*, 2000), LolD (Smith *et al.*, 2002), and MutS (Obmolova *et al.*, 2000; Lamers *et al.*, 2004) structures, and subsequently in the complete BtuCD transporter (Locher *et al.*, 2002), reflect the physiological interface (Figure 1.3 B). In this dimer, the two nucleotide-binding pockets are located at the interface between the monomers, with both bound nucleotides coordinated by the conserved amino acids from both NBDs: the Walker A and B of one NBD and the signature motif of the other NBD. Thus, an ABC transporter (in the closed dimer form, at least) can be considered to have two ATP-binding pockets, with both NBDs contributing to each pocket, rather than each NBD having a separate ATP-binding site. Because it is sometimes convenient to refer to the activity of an individual NBD, the NBD that is referred to is the one with the catalytic site to which the said NBD contributes the ABC-core subdomain containing the Walker A and B motifs. The importance of the signature motif, as well as the basis for the cooperativity between the NBDs, has become clear through visualization of these dimers.

Recently, the crystal structures of six complete ABC transporters (including their cognate TMDs) have become available. As mentioned earlier, four of them are importers: the vitamin B12 transporter BtuCD from *E. coli* (Locher *et al.*, 2002), the metal-chelate-type transporter HI1470/1 from *H. Influenzae* (Pinkett *et al.*, 2007), the molybdate/tungstate transporter ModBC from *A. fulgidus* determined in complex with its cognate binding protein ModA (Hollenstein *et al.*, 2007b), and the maltose transporter complex $MalFGK_2$ from *E. coli* also determined in complex with its cognate binding protein maltose-binding protein (MBP) (Oldham *et al.*, 2007); and two of them are exporters: the multidrug transporter Sav1866 from *S. aureus* (Dawson and Locher, 2006; Dawson and Locher, 2007) and the bacterial lipid flippase MsbA from *E. coli*, *V. cholerae*, and *S. typhimurium* (Ward *et al.*, 2007). These structures reveal similar arrangements of the conserved ATP-hydrolysing NBDs, but unrelated architectures of the TMDs, with the notable exception of a common "coupling helix" that is essential for

Figure 1.3:

High-resolution structures of the NBD

(A) Crystal structure of ATP-bound HisP. View of a monomer from the side showing lobe I (multicoloured, left) and lobe II (green, right). ATP (ball-and stick model) is present in the ATP-binding pocket formed by lobe I. (B) Crystal structure of the ATP-bound Rad50cd dimer. View of Rad50cd dimer secondary structure and fold, with one Rad50cd domain in brown and green and the other domain in dark gray and light gray. Key loops are color-coded (P-loop: magenta, signature motif: yellow, D-loop: red, Q-loop: white). The two ATP molecules (CPK representation) are buried in the dimer interface and sandwiched between the P-loops (magenta) and signature motifs (yellow) of opposing domains. Figure reproduced with permission from (Hopfner *et al.*, 2000).


A)

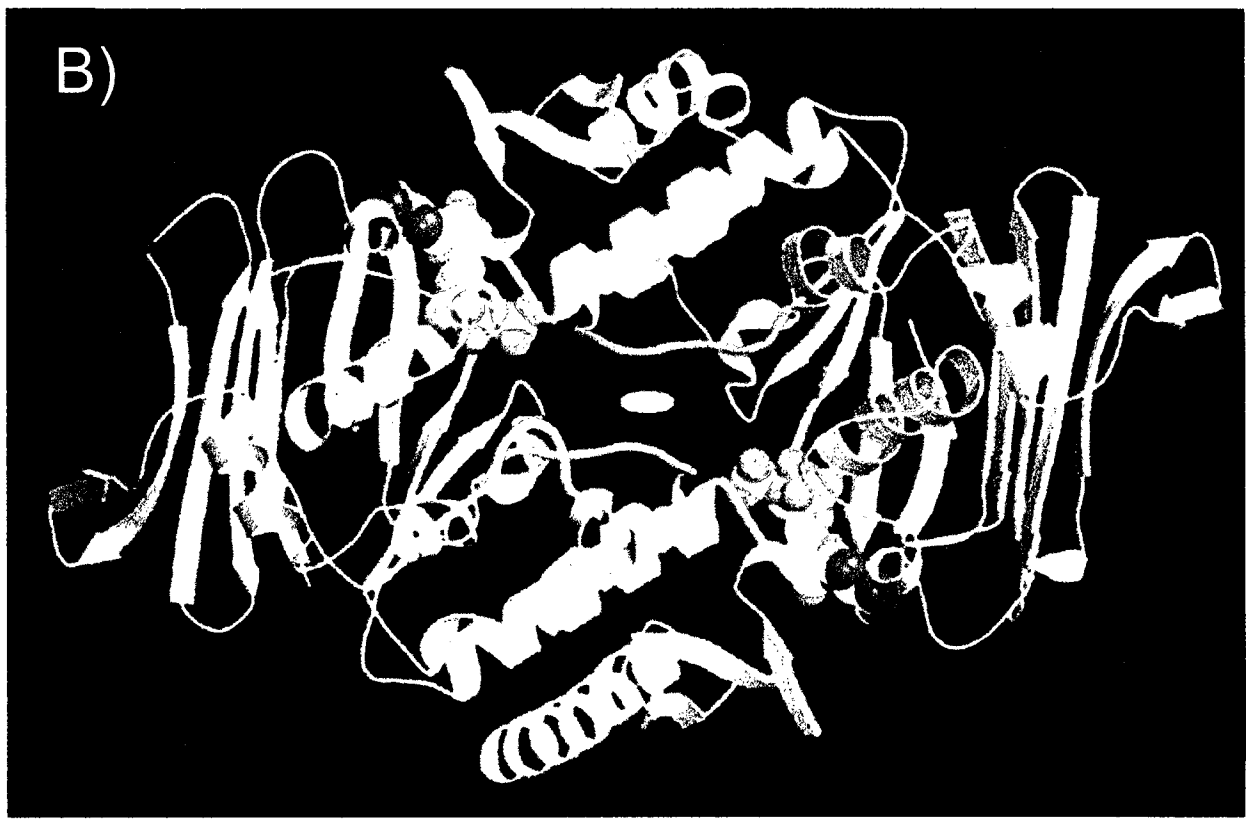
B)

transmitting conformational changes (Hollenstein *et al.*, 2007a). A central translocation pathway is observed in the crystal structures of all six transporters, but access is available from one side only, not from both. The structures thus suggest a mechanism that rationalizes ATP-driven transport; which will be discussed in a later section (see Chapter 6).

Structural details for the TMDs and NBDs will also be discussed in later sections pertaining to each domain respectively.

Section 1.2 – ABC-ATPase Protein Superfamily

The research described in this thesis was carried out with a specific member of this large superfamily of proteins: mouse Abcb1a (also known as P-glycoprotein, Mdr3, or Mdr1a). Abcb1a is a 1278-amino acids glycosylated membrane protein of ~140kDa. The aim of this section is to describe this ubiquitous family of proteins, the ABC-ATPase superfamily, with special emphasis on the members which, like Abcb1a, are mammalian transporters.

1.2.1 Members

ABC proteins are expressed in all kingdoms of life, whether prokaryotic (Monera) or eukaryotic (Protista, Fungi, Plantae, and Animalia) (Flugge and van Meer, 2006). ABC proteins form the largest and most conserved gene family known, with well over 300 members in bacteria, 31 in yeast, 129 in plants, 56 in the fly, 34 in the mouse, and 48 in humans (Dean *et al.*, 2001a; Gottesman and Ambudkar, 2001). In fact, by 2001, more than 2000 ABC ATPase domains or proteins had been identified in translated nucleic acid sequence databases (Dassa and Bouige, 2001). Most ABC proteins are membrane transporters, but some ABC proteins are involved in DNA binding/chromosome organisation (SMC proteins), DNA repair (MutS, Rad50), or mRNA export from the nucleus (Elf1p) (Linton and Higgins, 2007). Thus, a distinction is made between ABC proteins and ABC transporters, where only the latter contain TMDs. In prokaryotes, ABC transporters mediate mainly the influx (importers or permeases) of essential compounds

that cannot be obtained by simple diffusion (e.g., sugars, vitamins, metal ions, etc...), usually with the help of a soluble periplasmic binding protein (PBP), but they can also mediate the efflux of, among others, toxic substances. In eukaryotes, they function solely as exporters mediating the efflux of compounds from the cytosol to the extracellular space, or to the inside of intracellular compartments (i.e. endoplasmic reticulum, mitochondria, peroxisomes, or vacuoles). Thus, most of the known functions of eukaryotic ABC transporters involve the shuttling of hydrophobic compounds either within the cell as part of a metabolic process, or outside the cell for transport to other organs or secretion from the body (Dean *et al.*, 2001b). The range of compounds transported by ABC transporters is astounding and includes small ions, sugars, amino acids, vitamins, small peptides and large proteins, hormones, lipids, and xenobiotics. By definition, the compounds translocated by ABC transporters are not "substrates" since they are not enzymatically modified during translocation, and ATP is the true substrate. The term "allocrite" for unmodified compounds transported by proteins has been previously proposed (Young and Holland, 1999) and will be used throughout this thesis.

The ubiquitous distribution and primordial origin of ABC proteins reflect the fundamental requirement of cellular homeostasis to import and concentrate essential nutrients and expel toxins acquired from the environment or produced as metabolic by-products (Schneider and Hunke, 1998). ABC genes are dispersed widely in eukaryotic genomes and are highly conserved between species, indicating that most of these genes have existed since the beginning of eukaryotic evolution. The eukaryotic ABC genes are organized either as full transporters, containing two trans-membrane domains (TMDs) and two nucleotide binding domains (NBDs), or as half transporters (Hyde *et al.*, 1990), which must form either homo- or heterodimers to constitute a functional transporter. The genes can be divided into subfamilies based on similarity in gene structure, order of domains, and on sequence homology in the NBDs and TMDs. Moreover, comparison of the genomic organization and chromosomal localization indicates an autonomous evolution of each subfamily of human ABC transporters (Efferth, 2001). There are seven mammalian ABC gene subfamilies, and they are described in the next section.

1.2.2 Human ABC transporter superfamily

In humans, seven families of ABC protein genes, labelled *ABCA* through *ABCG*, have been defined, based on organization of domains and amino acid homology, coding for 48 individual ABC proteins (Table 1.1). Following is a brief overview of the members of each of the seven ABC protein subfamilies. A more detailed analysis can be found on the Web site http://www.nutrigene.4t.com/humanabc.htm.

ABCA: Phospholipid and cholesterol homeostasis

This subfamily comprises 12 full transporters that are further split into two subgroups based on phylogenetic analysis and intron structure (Broccardo *et al.*, 1999). This subfamily contains some of the largest ABC genes, many of which code for proteins which are >2100 amino acids in length. The first group includes seven genes (*ABCA1-4, 7, 12*, and *13*) that map to six different chromosomes. The second group (*ABCA5, 6*, and *8-10*) is organized into a cluster on chromosome 17 (Albrecht and Viturro, 2007); this cluster is also found in the murine genome. Of the ABCA subfamily members, the ABCA1 (ABC1) and ABCA4 (ABCR) proteins have been most extensively studied and are involved in cholesterol transport and high-density lipoprotein (HDL) biosynthesis (ABCA1), as well as transport of vitamin A derivatives in photoreceptor cells (ABCA4). ABCA1 is expressed in many organs and is thought to mediate HDL maturation by facilitating the efflux of cellular phospholipids and cholesterol onto apolipoproteins. Interestingly, despite near-ubiquitous expression of ABCA1 (Langmann *et al.*, 1999), the accumulation of cholesterol observed in Tangier disease (discussed later) or ABCA1-knockout mice appears to be restricted primarily to macrophages (Assmann *et al.*, 1995; McNeish *et al.*, 2000). In macrophages, ABCA1 appears to be localized at the plasma membrane and Golgi apparatus where it can export intracellular cholesterol and phospholipids (Brooks-Wilson *et al.*, 1999; Lawn *et al.*, 1999). A role for ABCA1 has also been suggested in apoptosis where it may be involved in the engulfment of apoptotic cells (Luciani and Chimini, 1996). ABCA4 is highly expressed in photoreceptor cells of the retina (Molday *et al.*, 2000) and experimental data suggests that ABCA4 functions as a flippase for N-retinylidene-phosphatidylethanolamine (Weng *et al.*, 1999), a component of the visual photo-transduction cycle, across the membrane of rod outer segment disks.

Table 1.1 List of human ABC genes and their function

Symbol	Alias	Protein Expression[a]	Function
ABCA1	ABC1	Ubiquitous (macrophages)	Cholesterol efflux onto HDL
ABCA2	ABC2	Brain (oligodendrocytes)	Lipid transport (& drug resistance)
ABCA3	ABC3	Lung (alveolar type II cells)	Pulmonary surfactant secretion
ABCA4	ABCR	Eye (rod photoreceptors)	N-retinyldiene-PE efflux
ABCA5		*Skeletal muscle, kidney, liver, placenta*	Lysosomal trafficking?
ABCA6		Diverse	
ABCA7		Myelolymphatic tissues, keratinocytes	Lipid trafficking?
ABCA8		Heart, skeletal muscle, liver	
ABCA9		Diverse	
ABCA10		Diverse	
ABCA12		Keratinocytes, stomach	
ABCA13		*Trachea, testis, bone marrow; at low levels*	
ABCB1	PGP, MDR1	Adrenal, kidney, brain	Multidrug resistance
ABCB2	TAP1	All cells	Peptide transport
ABCB3	TAP2	All cells	Peptide transport
ABCB4	MDR3, MDR2	Liver	PC transport
ABCB5		Ubiquitous	
ABCB6	MTABC3	Mitochondria	Iron transport
ABCB7	ABC7	Mitochondria	Fe/S cluster transport
ABCB8	MABC1	Mitochondria	
ABCB9		Heart, brain	
ABCB10	MTABC2	Mitochondria	
ABCB11	SPGP	Liver	Bile salt transport
ABCC1	MRP1	Lung, testes, PBMC[b]	Drug resistance
ABCC2	MRP2, cMOAT	Liver	Organic anion efflux
ABCC3	MRP3	Lung, intestine, liver	Drug resistance
ABCC4	MRP4	Prostate	Nucleoside transport
ABCC5	MRP5	Ubiquitous	Nucleoside transport
ABCC6	MRP6	Kidney, liver	
ABCC7	CFTR	Exocrine tissues	Chloride ion channel
ABCC8	SUR1	Pancreas	Sulfonyl urea receptor, K(ATP) regulator
ABCC9	SUR2	Heart, muscle	
ABCC10	MRP7	Low in all tissues	
ABCC11	MRP8	Low in all tissues	
ABCC12	MRP9	Low in all tissues	
ABCD1	ALD	Peroxisomes	VLCFA[b] transport regulation
ABCD2	ALDR	Peroxisomes	
ABCD3	PMP70	Peroxisomes	
ABCD4	PMP69	Peroxisomes	
ABCE1	OABP, RNaseL I	Ovary, testes, spleen	Oligoadenylate binding protein
ABCF1	ABC50	Ubiquitous	
ABCF2		Ubiquitous	
ABCF3		Ubiquitous	
ABCG1	ABC8, White	Ubiquitous	Cholesterol transport?
ABCG2	BCRP	Placenta, intestine	Toxin efflux, drug resistance
ABCG4		Liver	
ABCG5		Liver, intestine	Sterol transport
ABCG8		Liver, intestine	Sterol transport

a) For those transporters whose protein expression has not yet been determined the mRNA expression profile is given in italics.
b) PBMC = peripheral blood mononuclear cells; VLCFA = very long chain fatty acids

Adapted from (Dean *et al.*, 2001)

ABCA2 is predominantly expressed in the brain (Vulevic *et al.*, 2001) where it is located in lysosomes. High expression as a lysosome-associated protein was found only in the cell bodies of oligodendrocytes (Zhou *et al.*, 2001) and solely in restricted regions of the newborn spinal cord (Zhou *et al.*, 2002a). ABCA2 is thought to play an important role in controlling lipid trafficking from the neuronal cell body to the membrane (Vulevic *et al.*, 2001; Tanaka *et al.*, 2003). ABCA3 is predominantly expressed in alveolar type II cells in the lung (Yamano *et al.*, 2001) localized to lamellar bodies, lysosome-like structures storing pulmonary surfactant: a mixture of phospholipids and proteins. Pulmonary surfactant, produced by alveolar type II cells and stored intracellularly, forms a lipid-rich monolayer that coats the airways of the lung and is essential for proper inflation and function of the lung because it reduces surface tension at the air-liquid interface. ABCA3 is closely related to ABCA1 and ABCA4, proteins that transport phospholipids. Based on its expression profile, it was hypothesised that ABCA3 played a role in surfactant phospholipid metabolism and secretion. Indeed, it was established that ABCA3 is critical for the proper formation of lamellar bodies and surfactant function (Nagata *et al.*, 2004). ABCA12 appears to play a role in skin lipid homeostasis and high levels of the protein can be found in healthy keratinocytes (Yamanaka *et al.*, 2007). Moreover, mutations in *ABCA12* are associated with rare hereditary skin diseases (Annilo *et al.*, 2002; Lefevre *et al.*, 2003). ABCA7 is expressed in myelolymphatic tissues such as spleen and thymus (Kaminski *et al.*, 2000; Broccardo *et al.*, 2001) and ABCA13, the largest ABC protein described to date (5058 aa's), expresses its mRNA at low levels in all tissues (Prades *et al.*, 2002) and the resulting protein expression has not yet been studied. The function of ABCA7 and ABCA13 is still not known although they are speculated to participate in cellular lipid homeostasis in specialized environments (Dean *et al.*, 2001a; Abe-Dohmae *et al.*, 2006). Findings that ABCA7 shares a sterol dependent up-regulation with ABCA1 support its possible function (Kaminski *et al.*, 2000; Kaminski *et al.*, 2001). The protein expression pattern of the chromosome 17 subgroup is not well defined, but the expression pattern of the genes is restricted, with *ABCA5* and *ABCA10* expressed in skeletal muscle, *ABCA6* in the liver, *ABCA8* in the ovary, and *ABCA9* in the heart, suggesting that the protein may be expressed in these specific tissues. No diseases map to the corresponding region of the mouse and human genomes, and the functions of this group of genes are as

yet uncharacterized (Dean *et al.*, 2001a). But, since all steroid hormones are derived from cholesterol, and given the high level of expression of some of these genes in the ovary and other tissues, it has been speculated that the gene products may play a role in ovarian hormone biogenesis or transport (Dean and Allikmets, 2001). Interestingly, for these five members, the C-terminal NBD contains the Walker A and B motifs, but lacks the signature sequence (Albrecht and Viturro, 2007).

ABCB: Multidrug resistance and antigen presentation

This subfamily is unique since it contains both full and half transporters; namely, four full and seven half transporters are currently comprised in this subfamily. Though research interest in the ABC superfamily is widespread, the stimulus for much of the research on ABC proteins may be traced to ABCB1 (also known as PGP, MDR1, PGY1), discovered by Dr. Ling's group more than 30 years ago as an integral plasma membrane glycoprotein with the ability to confer a multidrug resistance (MDR) phenotype to cancer cells (Juliano and Ling, 1976). ABCB1 is the archetypal ABC transporter and has earned its reputation by being the first discovered, the most important medically, the most studied, and the one having arguably the broadest portfolio of allocrites and reversing agents. Thus, ABCB1, which is expressed primarily in the kidney and brain (at the blood-brain barrier), but also in the adrenal gland and placenta, appears to have a role in the normal secretion of metabolites as well as in detoxification (Thiebaut *et al.*, 1987). Studies on knock-out mice demonstrated that *ABCB1* is not an essential gene; the animals are vital, fertile, and do not show phenotypic abnormalities although they are hypersensitive to cytotoxic agents, especially in the brain (Schinkel *et al.*, 1994; Schinkel *et al.*, 1996). ABCB2 (TAP1) and ABCB3 (TAP2) are ubiquitously expressed half transporters that form a heterodimer which transports peptides of about 8 to 12 amino acids from the intracellular proteasome complex to the endoplasmic reticulum (ER) and thereby to the extracellular peptide binding site of major histocompatibility complex (MHC) class I molecules (Powis *et al.*, 1992). MHC class I proteins present peptides which originate from intracellularly degraded proteins. MHC class I (and II) gene products present peptides to immunocompetent lymphocytes thus implicating ABCB2 and 3 in immunity. ABCB4 (MDR3/MDR2) and ABCB11 (SPGP/BSEP) are both

expressed in the liver, and are involved in the secretion of phosphatidylcholine (PC) and bile salts, respectively (Smit *et al.*, 1993; Smit *et al.*, 1994; Gerloff *et al.*, 1998). ABCB9 (TAPL) is a half transporter homologous to ABCB2 and ABCB3. To date, ABCB9 has been localized to lysosomes of Sertoli cells (Zhang *et al.*, 2000), dendritic cells and macrophages (Demirel *et al.*, 2007). ABCB9 has been shown to homodimerise and transport peptides of various sizes with a preference for those of 23 residues (Wolters *et al.*, 2005). Although related to ABCB2 and ABCB3, ABCB9 is unique as far as its interaction partner(s), transport properties, and substrate specificities are concerned, thus excluding that it is part of the peptide-loading complex in the classic route of antigen processing via MHC class I molecules (Wolters *et al.*, 2005). The remaining members of this subfamily are all half transporters (ABCB5-8, 10) and, except ABCB5, localize to the mitochondria where they function in iron metabolism and transport of Fe/S protein precursors. *ABCB5* mRNA is expressed in normal melanocytes and in retinal pigment epithelial cells, suggesting that *ABCB5* expression is pigment cell-specific and might be involved in melanogenesis (Chen *et al.*, 2005). In an earlier study, ABCB5 was found to be expressed in a tissue-restricted manner on the plasma membrane of progenitor cells among human epidermal melanocytes and chemoresistant malignant melanoma cells. It was thus determined to function as a determinant of membrane potential and regulator of cell fusion in physiologic skin progenitor cells (Frank *et al.*, 2003) as well as a novel drug transporter and chemo-resistance mediator in human malignant melanoma (Frank *et al.*, 2005).

ABCC: Chloride ion channel, sulfonylurea receptor, and multidrug resistance-associated proteins (MRPs)

This subfamily comprises 12 full transporters of which some (ABCC1, 2, 3, 6, 8, 9, and 10) contain an extra TMD of five TM α-helices at their N-termini. These transporters perform functions in ion transport, signal transduction, and toxin secretion. ABCC7, better known as cystic fibrosis transmembrane conductance regulator (CFTR), is the best characterised of this subfamily. CFTR is the only ABC protein which acts as a channel; it is regulated by cAMP and transports chloride ions (Anderson *et al.*, 1991). Because CFTR does not mediate transport of its allocrite against an electrochemical

gradient, it cannot really be considered as a transporter. CFTR is expressed in all exocrine tissues and thus plays a role in all exocrine secretions (Trezise and Buchwald, 1991). Mutations in CFTR cause cystic fibrosis (Quinton, 2007) a very common disease in Caucasians. The sulphonylurea receptors (SURs) ABCC8 (SUR1, expressed in the pancreas (Inagaki *et al.*, 1995)) and ABCC9 (SUR2, expressed in heart and muscle (Chutkow *et al.*, 1996; Inagaki *et al.*, 1996)) are not true transporters either since, like CFTR, they are not known to mediate transport against an electrochemical gradient (Borst and Elferink, 2002); instead, evolution has matched these molecules with K^+ selective pores, either $K_{IR}6.2$ (ABCC8 and sometimes ABCC9) or $K_{IR}6.1$ (ABCC9), to assemble ATP-sensitive K^+ (K_{ATP}) channels found in endocrine cells, neurons, and both smooth and striated muscle (Bryan *et al.*, 2007). Pancreatic β-cell K_{ATP} channels, which comprise two subunits: ABCC8 and Kir6.2, play an important role in the regulation of glucose-induced insulin secretion (Burke *et al.*, 2008). The rest of the subfamily is composed of nine related transporters (ABCC1-6 and ABCC10-12) better known as the multidrug resistance proteins (MRPs, MRP1-9). Between them, the MRPs can transport a large range of organic anions, including anionic drugs and drugs conjugated to glutathione (GSH), sulphate, or glucuronate. No two MRPs have exactly the same substrate specificity or tissue distribution and the precise function or physiological role of most of the MRPs remains to be established. ABCC1 (MRP1) is the best characterized among the MRP family and is expressed ubiquitously in the body, with highest levels in the lung, testis, kidney, heart and placenta (Bakos and Homolya, 2007). ABCC2 (MRP2/cMOAT) and ABCC3 (MRP3) are expressed at highest levels in the liver and intestine (Mayer *et al.*, 1995; Kiuchi *et al.*, 1998; Dietrich *et al.*, 2003) although ABCC2 is localized exclusively to the apical membrane and ABCC3 to the basolateral membrane of hepatocytes (Stockel *et al.*, 2000). ABCC1, 2, and 3 are transporters of endo- or exogenous organic anions, leukotriene C4, as well as neutral or amphiphilic toxic compounds, alone or in conjugation or complexation with glutathione, glucuronate or sulphate (Zhang *et al.*, 1998; Robbiani *et al.*, 2000; Deeley and Cole, 2006). In addition, transported hydrophobic compounds may undergo co-transport with glutathione. These transporters thus represent an important defence mechanism against reactive toxic compounds, although this function may not be the primary role of these transporters. An

important physiological role for ABCC1 seems to be in dendritic cell development (differentiation) and functions (migration) (van de Ven *et al.*, 2006). ABCC2 is a hepatocellular canalicular transporter for endogenous organic anions, especially glucuronidated bilirubin (Paulusma and Oude Elferink, 1997) and contributes to bile formation and elimination of molecular waste (Konig *et al.*, 1999). For now, ABCC3 has been involved in transporting some endogenous glucuronosyl conjugates, such as bilirubin-glucuronides, out of cells (Borst *et al.*, 2007). The tissue expression profile for ABCC4 includes kidney, liver, erythrocytes, adrenal gland, platelets, brain, and pancreas (Borst *et al.*, 2007). ABCC5, a close structural homolog of ABCC4, is ubiquitously expressed albeit at low levels (Wijnholds *et al.*, 2000). ABCC4 and ABCC5 have been well characterized as transporters of modified nucleotide (nucleoside monophosphate) analogs (Jedlitschky *et al.*, 2000). They can thus confer cellular resistance to a range of base, nucleoside, and nucleotide analogs and participate in the transport of diverse chemotherapeutic and antiviral agents such as 6-mercaptopurine (6-MP) and 9-(2-phosphonyl-methoxyethyl) adenine (PMEA) (Ritter *et al.*, 2005). Though their ability to transport cyclic adenosine monophosphate and cyclic guanosine monophosphate (cGMP) suggests a possible role in cellular signaling (Russel *et al.*, 2008), ABCC4 and 5 are organic anion transporters whose biological functions are not known. Interestingly, the *ABCC6* gene is expressed primarily in the liver and to a lesser extent in the kidney (Matsuzaki *et al.*, 2005) while the protein is most highly expressed in enteroendocrine G cells of the stomach (Beck *et al.*, 2005). The function of ABCC6 is not yet defined, although mutations in the gene cause *pseudoxanthoma elasticum* (described in a later section), a disease which affects the skin, eyes, and cardiovascular system (Jiang and Uitto, 2006). ABCC10, 11, and 12 (MRP7, 8, 9) are recently identified members of this subfamily and protein expression in tissues has not yet appeared in the literature. On the other hand, gene expression for *ABCC10*, *11* and *12* appears to occur in many tissues. A physiological function has only been established for ABCC11, for which a single nucleotide polymorphism determines wet vs. dry earwax type (Yoshiura *et al.*, 2006). However, the constituent of earwax that is susceptible to transport by ABCC11 has not been identified. ABCC10 and 11 are lipophilic anion pumps that are able to confer

resistance to chemotherapeutic agents while the functional characteristics of ABCC12 are currently unknown (Kruh *et al.*, 2007).

ABCD: Fatty acid metabolism

There are four genes that encode half transporters in this subfamily. These half transporters are exclusively expressed in the peroxisome. Although the exact role of the ABCD proteins have yet to be elucidated, it appears that members of this subfamily are involved in fatty acid metabolism (Wanders *et al.*, 2007). In yeast, there are only two half transporters in this subfamily (PXA1 and PXA2) and these two proteins form a heterodimer involved in very long chain fatty acid oxidation in the peroxisome (Shani and Valle, 1998).

ABCE and ABCF: Non-membrane ABC proteins

These two subfamilies are composed of proteins which contain ATP-binding domains that are closely related to other ABC transporters but lack any TMDs. These proteins are therefore not known to be involved in any membrane transport functions. The ABCE subfamily only has one member, ABCE1 (RNase L inhibitor/OABP), which is perhaps the most evolutionary conserved member of the ABC protein superfamily as ABCE1 homologs are present in all organisms, except eubacteria (Barthelme *et al.*, 2007). Thus, the gene coding for ABCE1 is found in all Archaea and eukaryotes and human ABCE1 is expressed in most tissues, but most abundantly in the ovary, testes, spleen, and pancreas (Aubry *et al.*, 1996). ABCE1 has two ABC ATPase domains which are arranged in a head-to-tail orientation via a flexible linker and hinge region (Karcher *et al.*, 2005) and it is unique as it is the only ABC protein which contains an iron-sulphur cluster binding domain (Barthelme *et al.*, 2007). This ABC protein has been found to be essential in all organisms tested (Winzeler *et al.*, 1999; Estevez *et al.*, 2004; Coelho *et al.*, 2005). ABCE1 was first identified by its inhibition of the antiviral, interferon-activated ribonuclease (RNase) L (Bisbal *et al.*, 1995). Subsequently, it was shown that assembly of immature HIV1 capsids requires ATP hydrolysis by ABCE1 (Zimmerman *et al.*, 2002). Recent data suggest that the cellular and perhaps evolutionary and essential function of ABCE1 is found in ribosome biogenesis, translation initiation, and/or

formation of translation initiation components (Chen *et al.*, 2006; Andersen and Leevers, 2007). ABCE1 was found to interact with translation initiation factors eIF2, eIF3, eIF5, the 40S ribosomal subunit, and several ribosomal RNAs (Yarunin *et al.*, 2005; Chen *et al.*, 2006). Also, depletion of the protein causes defects in the assembly of the pre-initiation complex, rRNA processing, and accumulation of ribosomal subunits in the nucleus (Dong *et al.*, 2004). Nevertheless, the underlying molecular mechanism remains enigmatic. Each of the three ABCF proteins (ABCF1-3) also contains two NBDs and is expressed ubiquitously. The best characterized member is actually a yeast protein: GCN20 from *S. cerevisiae*, which mediates the activation of the eIF-2 α-kinase (Marton *et al.*, 1997). The human homolog, ABCF1 (ABC50), is part of the ribosome complex and appears to play a similar role (Tyzack *et al.*, 2000; Paytubi *et al.*, 2008).

ABCG: Sterol transport

The ABCG subfamily is composed of five "reverse" half transporters that have an NBD at the N-terminus and a TMD at the C-terminus. ABCG1, which is ubiquitously expressed, but at higher levels in macrophages, is involved in cholesterol transport regulation (Klucken *et al.*, 2000). ABCG2, better known as breast cancer resistance protein (BCRP), is involved in drug resistance and its normal function in cells is not well defined. Since its discovery in breast cancer cells, ABCG2 has been found in drug resistant ovary, colon and gastric cancer cells (Young *et al.*, 2003). ABCG2 is also expressed in normal cells, including the epithelia of the intestines and colon, duct and lobules of the breast, the endothelial cells of veins and capillaries of these tissues, and the syncytiotrophoblast of the placenta (Maliepaard *et al.*, 2001; Young *et al.*, 2003). Its high expression in placental trophoblast cells suggests that it may transport toxic metabolites from the fetal to the maternal blood supply (Jonker *et al.*, 2000). Also, a survival role for ABCG2 in the placenta, protecting the trophoblast against cytokine-induced apoptosis, has been proposed (Evseenko *et al.*, 2007). ABCG5 and ABCG8, both expressed in the liver and intestine, form a heterodimer which is important for sterol transport (Berge *et al.*, 2000). The ABCG4 protein is closely related to the Drosophila *white* and human ABCG1 genes. The function of ABCG4 has yet to be fully determined, but it has been found to be expressed in the brain (Annilo *et al.*, 2001) where it appears to have a

physiological role in mediating efflux of cholesterol and cholesterol biosynthetic intermediates from cells such as astrocytes to HDL (Wang *et al.*, 2007). Knockout mice of both *Abcg1* and *Abcg4* were required to see substantial accumulation of sterols in astrocytes and brain, indicating overlapping roles and mutual compensation of these two transporters in sterol efflux processes (Wang *et al.*, 2007).

1.2.3 ABC proteins: diseases and phenotypes

Besides being involved in a variety of basic cell functions, ABC proteins also contribute to microbial pathogenicity and drug resistance.

1.2.3.1 ABC genes and human genetic diseases

To date, there are a total of 17 ABC genes that are associated with both Mendelian and complex genetic disorders (Dean and Annilo, 2005) (Table 1.2). In fact, several ABC genes were originally discovered during the positional cloning of human genetic disease loci (Klein *et al.*, 1999; Dean *et al.*, 2001b). ABC genes predominantly encode structural proteins and as a result, all of the disorders are recessive and are attributable to a severe reduction or lack of function of the protein (Dean *et al.*, 2001a).

Tangier disease or high-density lipoprotein (HDL) deficiency type 2: Tangier disease is characterised by deficient efflux of lipids, especially cholesterol, from peripheral cells such as macrophages, and a very low level of circulating HDL (Dean *et al.*, 2001b). Clinical features of the disorder are very large orange tonsils, hepatosplenomegaly, enlarged lymph nodes caused by accumulation of cholesterylesters in macrophages, as well as increased incidence of atherosclerosis and peripheral neuropathy (Efferth, 2001). The gene responsible for this disease is *ABCA1*. ABCA1 is essential for high-density lipoprotein formation and, hence, for inter-organ trafficking of the highly water-insoluble cholesterol molecules (Plosch *et al.*, 2005). Current models for ABCA1 function place it at the plasma membrane where it mediates the transfer of phospholipid and cholesterol onto lipid-poor apolipoproteins to form nascent HDL particles (Young and Fielding, 1999). Patients with hypolipidemia have also been described that are heterozygous for *ABCA1* mutations, suggesting that variations in

Table 1.2 Diseases and Phenotypes Caused by ABC Genes

Gene	Mendelian disorder	Complex disease
ABCA1	Tangier disease, familial hypoapoproteinemia	
ABCA3	Respiratory distress syndrome	
ABCA4	Stargadt disease/ fundus flavimaculatus, retinitis pigmentosa, cone-rod dystrophy	Age-related macular degeneration
ABCA12	Lamellar and Harlequin ichthyosis	
ABCB2	Immune deficiency disorders	
ABCB3	Immune deficiency disorders	
ABCB4	Progressive familial intrahepatic cholestasis-3	Intrahepatic cholestasis of pregnancy
ABCB7	X-linked sideroblastic anemia and ataxia	
ABCB11	Progressive familial intrahepatic cholestasis-2	
ABCC2	Dubin-Johnson Syndrome	
ABCC6	Pseudoxanthoma elasticum	
ABCC7	Cystic fibrosis, CBAVD[a]	Pancreatitis, bronchiectasis
ABCC8	Familial persistent hyperinsulinemic hypoglycemia of infancy	
ABCC9	Dilated cardiomyopathy with ventricular tachycardia	
ABCD1	Adenoleukodystrophy	
ABCG5	Sitosterolemia	
ABCG8	Sitosterolemia	

a) CBAVD = congenital bilateral absence of vas deferens

Modified from (Dean and Annilo, 2005)

ABCA1 may play a role in regulating the level of HDLs in the blood (Marcil *et al.*, 1999). Persuasive experimental evidence for a causative link of ABCA1 to perturbations in lipoprotein metabolism has been provided with knock-out mice (Orso *et al.*, 2000).

Respiratory distress syndrome: Mutations in the *ABCA3* gene can result in fatal surfactant deficiency in term newborn infants (Shulenin *et al.*, 2004) and chronic interstitial lung disease in older children (Bullard *et al.*, 2006). Proper formation of lamellar bodies and surfactant function (Shulenin *et al.*, 2004; Cheong *et al.*, 2006) is highly dependent on ABCA3, a protein which is closely related to ABCA1 and ABCA4 which transport phospholipids in macrophages and photoreceptor cells, respectively. Consequently, a role in surfactant phospholipid metabolism is beginning to emerge for ABCA3 (Matsumura *et al.*, 2007).

Stargardt disease and other eye disorders: As mentioned earlier, the *ABCA4* gene is expressed exclusively in rod photoreceptors where it transports retinol (vitamin A) derivatives from the photoreceptor outer segment disks into the cytoplasm (Allikmets, 1997). Studies on *ABCA4* knock-out mice showed that ABCA4 is an export flippase for retinyl-derivatives (Weng *et al.*, 1999). To date >400 sequence variations in the *ABCA4* gene have been documented and linked to four degenerative retinal diseases including Stargardt disease (also known as fundus flavimaculatus), retinitis pigmentosa type 19 (RP19), cone-rod dystrophy type 3 (CRD3), and age-related macular degeneration (AMD) (Kaminski *et al.*, 2006). Analyses of *ABCA4* mutations in individuals with Stargardt disease, RP19, CRD3, or AMD led to the suggestion of a model in which *ABCA4* mutations can cause a spectrum of retinal disease, with the clinical phenotype determined by the level of residual ABCA4 protein activity (Rozet *et al.*, 1998). Thus, complete loss of ABCA4 function leads to RP19, whereas patients with "milder" alleles have Stargardt disease (Martinez-Mir *et al.*, 1997). Stargardt disease is characterised by juvenile to early adult onset of rapid retinal degeneration and loss of central vision (Bither and Berns, 1988). Carriers of *ABCA4* mutations are also increased in frequency in patients with AMD (Allikmets, 2000). AMD patients display loss of central vision after the age of 60 and the causes of the disease are poorly understood. The abnormal

accumulation of retinoids (in the form of lipofuscin), due to a deficiency in ABCA4, appears to be one mechanism by which the process of vision loss is initiated (Cideciyan *et al.*, 2004).

Lamellar and Harlequin ichthyosis: ABCA12 facilitates the delivery of lipids to lamellar bodies in keratinocytes, which is critical for permeability barrier function. Recently, *ABCA12* gene mutations were found to underlie lamellar and Harlequin ichthyosis (Lefevre *et al.*, 2003; Thomas *et al.*, 2006), two devastating skin disorders. Harlequin ichthyosis (HI) is the most severe and often lethal form of autosomal-recessive, congenital ichthyosis and is characterized by large diamond-shaped scales on the skin, as well as abnormal contraction of the eyes, ears, mouth, and other appendages (Hsu *et al.*, 1989). Affected infants have markedly impaired barrier function and are more susceptible to infection. Abnormalities in the localization of epidermal lipids as well as abnormal lamellar granule formation are features of HI skin (Thomas *et al.*, 2006).

Immune deficiency disorders: The transporter associated with antigen processing (TAP) genes *ABCB2* and *ABCB3* are involved in several diseases:

1) **Bare lymphocyte syndrome type I** (or histocompatibility lymphocyte antigen (HLA) class I antigen deficiency): a C→T point mutation that results in early truncation of the *ABCB3* gene (at position 253) has been identified in a major histocompatibility complex (MHC) class I deficient family from Morocco (de la Salle *et al.*, 1994). This deficiency did not lead to severe viral infections but was associated with susceptibility to bacterial infections of the respiratory mucosa (Donato *et al.*, 1995).

2) **Viral infections**: The *Herpes simplex* virus type I (HSV-1) immediate-early gene product ICP47 inhibits peptide translocation into the ER by blocking the peptide binding site(s) of the ABCB2/ABCB3 heteromeric transporter (Ahn *et al.*, 1996). The transmembrane class I glycoprotein US6 of human cytomegalovirus (HCMV) binds to the ER-luminal part of ABCB2/3 and inhibits peptide translocation, thus impairing MHC class I antigen presentation. The functional consequence of TAP inhibition is that infected cells are unable to present endogenous antigen to cytotoxic T lymphocytes and are

therefore resistant to cytotoxic T lymphocyte lysis (Ahn *et al.*, 1997; Hengel *et al.*, 1997; Lehner *et al.*, 1997).

3) **Cancer**: ABCB2 has been found to be down-regulated in renal cell carcinomas (Seliger *et al.*, 1997) and mutated close to the ATP-binding site (R659Q) in a small lung cancer cell line (Chen *et al.*, 1996). The presentation of endogenous antigens on the surface of tumor cells may be an immuno-surveillance mechanism, thus deficient presentation may aid cancer progression.

4) **Multiple sclerosis**: *ABCB3* gene polymorphisms contribute to the genetic susceptibility of MS (Moins-Teisserenc *et al.*, 1995).

5) **Diabetes mellitus**: an association of an ABCB2 allele with insulin-dependent diabetes mellitus has been reported (Jackson and Capra, 1993).

Progressive familial intrahepatic cholestasis (PFIC): Several ABC transporters are specifically expressed in the liver and have a role in the secretion of components of the bile. When dysfunctional, these transporters are responsible for many types of PFIC. PFICs are a heterogeneous group of autosomal recessive liver disorders which are characterised by early onset of cholestasis that leads to liver cirrhosis and failure (Alonso *et al.*, 1994). PFIC type 3 is characterized by high serum γ-glutamyltransferase activity and inflammation of the bile duct, as well as ductal proliferation in the liver. This type is closely related to the symptoms seen in *Abcb4-/-* knock-out mice. Human ABCB4 (MDR2) transports phosphatidylcholine across the canalicular membrane of hepatocytes into the bile (van Helvoort *et al.*, 1996). Missense and nonsense mutations in *ABCB4* cause PFIC3 (Deleuze *et al.*, 1996; de Vree *et al.*, 1998) and are also associated with intrahepatic cholestasis of pregnancy (Dixon *et al.*, 2000). The *ABCB11* gene was originally identified based on homology to *ABCB1* (Childs *et al.*, 1995). ABCB11 is highly expressed on the liver canalicular membrane and has been shown to be the major bile salt export pump. Mutations in *ABCB11* are found in patients with PFIC type 2 (Strautnieks *et al.*, 1998). PFIC2 is characterized by deficient bile salt secretion and retention of bile salts within hepatocytes causes hepatocellular damage and cholestasis.

X-linked sideroblastic anaemia and ataxia (ASAT): Two distinct missense mutations in *ABCB7* are associated with the ASAT phenotype (Allikmets *et al.*, 1999). ASAT is characterized by moderate anaemia and early-onset spinocerebellar syndrome in males. The ataxia has been described to be either non-progressive or slowly progressive.

Dubin-Johnson Syndrome: This disorder is associated with a defect in the ability of hepatocytes to secrete conjugated bilirubin and anionic conjugates into the bile, which causes conjugated hyperbilirubinemia in the liver without elevation of liver enzymes. Dubin-Johnson syndrome is characterized by chronic jaundice, bilirubinemia, and lysosomal accumulation of black pigment in the liver. Mutations in *ABCC2* have been identified in Dubin-Johnson syndrome patients (Wada *et al.*, 1998). The Dubin-Johnson syndrome is an inherited disturbance of bilirubin secretion across the gall capillary membranes of hepatocytes leading to increased bilirubin storage in the liver.

Pseudoxanthoma elasticum (PXE): PXE is an inherited systemic disease of connective tissue primarily affecting the skin, retina, and cardiovascular system (causing premature atherosclerosis). It is characterised pathologically by elastic fibre mineralisation and fragmentation, and clinically by high heterogeneity in age of onset and the extent and severity of organ system involvement. PXE is associated with mutations in the *ABCC6* gene and at least one *ABCC6* mutation is found in about 80% of patients. These mutations consist of missense, nonsense, and frameshift mutations, as well as large deletions. No correlation between the nature or location of the mutations and phenotype severity has yet been established. *ABCC6* encodes the protein ABCC6 (also known as MRP6), which is expressed only to a lesser extent in tissues affected by PXE. The physiological substrates of ABCC6 remain to be determined, but the current hypothesis is that PXE should be considered as a metabolic disease with undetermined circulating molecules interacting with the synthesis, turnover, or maintenance of elastic fibres (Chassaing *et al.*, 2005). Recently, it was suggested that vitamin K may be the circulating molecule involved that would be secreted by ABCC6 from the liver as a conjugated precursor (Borst *et al.*, 2008).

Cystic fibrosis (CF): Cystic fibrosis is characterized by abnormal exocrine secretions causing pancreatic degeneration and lung infections (Tsui, 1995). Cystic fibrosis is the most common lethal childhood disease in Caucasian populations. The gene responsible for this disease is *ABCC7* (*CFTR*) (Riordan *et al.*, 1989). The disease frequency correlates with the frequency of the major allele of the *ABCC7* gene, a deletion of three base pairs which leads to a protein lacking a phenylalanine residue at position 508 (ΔF508). There is a spectrum of severity in the phenotypes caused by *ABCC7* that is inversely related to the level of ABCC7 activity. Patients with two severe CFTR alleles typically display serious disease with inadequate secretion of pancreatic enzymes leading to nutritional deficiencies, bacterial infections of the lung, and obstruction of the vas deferens, leading to male infertility. Patients with at least one partially functional allele display enough residual pancreatic function to avoid the major nutritional and intestinal deficiencies (Dean *et al.*, 1990) and people with mild alleles display only congenital absence of the vas deferens with no other symptoms of CF.

Familial persistent hyperinsulinemic hypoglycaemia of infancy (FPHHI): The ATP-sensitive potassium channel $K_{(ATP)}$, a functional complex of the sulfonylurea receptor 1 (ABCC8) and an inward rectifier potassium channel subunit (Kir6.2) regulates insulin secretion in the pancreas. Mutations in the *ABCC8* gene are associated with persistent hyperinsulinemic hypoglycaemia of infancy (PHHI) (Thomas *et al.*, 1995), a disorder of pancreatic β-cell function characterized by excess insulin secretion and hypoglycaemia. Unless early and aggressive intervention is undertaken, brain damage from recurrent episodes of hypoglycaemia may occur (Siesjo, 1988).

Dilated cardiomyopathy with ventricular tachycardia: Stress tolerance of the heart requires high-fidelity metabolic sensing by $K_{(ATP)}$ channels that adjust membrane potential-dependent functions to match cellular energetic demand. Mutations in *ABCC9*, which encodes the regulatory SUR2A subunit of the cardiac $K_{(ATP)}$ channel, were identified in individuals with heart failure and rhythm disturbances due to idiopathic dilated cardiomyopathy (Bienengraeber *et al.*, 2004).

Adenoleukodystrophy (ALD): ALD is an X-linked recessive disorder characterised by neurodegenerative phenotypes with onset typically in late childhood (Mosser *et al.*, 1993). The gene responsible for this disease is *ABCD1*. ABCD1 is located in the peroxisome, where it is believed to be involved in the transport of very long chain fatty acids. Thus, ALD patients have an accumulation of unbranched, saturated fatty acids with a chain length of 24-30 carbons in the cholesterol esters of the brain and in the adrenal cortex. Adrenal deficiency commonly occurs and the presentation of ALD is highly variable.

Sitosterolemia: In healthy individuals, acute changes in cholesterol intake produce modest changes in plasma cholesterol levels. A striking exception occurs in sitosterolemia, an autosomal recessive disorder characterized by increased intestinal absorption and decreased biliary excretion of dietary sterols, hypercholesterolemia, and premature coronary atherosclerosis. *ABCG5* and *ABCG8* are both mutated in patients with sitosterolemia (Berge *et al.*, 2000). The genes *ABCG5* and *ABCG8* are located head-to-head and are regulated by the same promoter. They encode the half-transporters ABCG5 and ABCG8 that together form a functional heterodimer.

1.2.3.2 ABC genes and multidrug resistance

Cells exposed to toxic compounds can possess or develop resistance by a number of mechanisms including decreased uptake, increased detoxification, alteration of target proteins, or increased excretion. Several of these pathways can lead to multidrug resistance (MDR), in which the cell is resistant to several chemotherapeutic agents, in addition to the initial compound. Often, the mechanism of resistance involves overexpression of one or more proteins. But, even in non-over-expressing cells, drug efflux by multidrug transporters may interfere with the effective dosing of potentially efficacious drugs by altering the pharmacokinetic properties or intracellular concentrations of those drugs (Allen *et al.*, 2000).

Multidrug transporters exhibit broad allocrite specificity and are able to lower the intracellular drug concentration to sub-toxic levels by mediating the active extrusion of drugs from the cell. They are integral membrane proteins, which can be broadly classified

according to their bioenergetic requirements into primary- and secondary-active transporters (Venter *et al.*, 2005). In primary-active transport, as is the case for ABC transporters, the translocation of allocrite is coupled directly to the hydrolysis of ATP. The ever-increasing incidence of MDR due to (over)expression of multidrug transporters is an important cause of failure of the drug-based treatment of patients with cancers or infections by pathogenic micro-organisms (Borst and Elferink, 2002), as well as patients with conditions that are treated by chemotherapeutic agents, such as epilepsy (Sisodiya *et al.*, 2002) and schizophrenia (Bebawy and Chetty, 2008). Several ABC transporters have already been associated with drug transport:

ABCB1: The best characterized ABC drug pump is the ABCB1 transporter. *ABCB1* was the first human ABC transporter gene cloned and characterized through its ability to confer an MDR phenotype to cancer cells that had developed a defined pattern of resistance to chemotherapeutic drugs (Juliano and Ling, 1976). Thus, these cells were resistant to anthracyclines, anthracenediones, *vinca*-alkaloids, taxanes, and epipodophyllotoxins, but not to topoisomerase I poisons, antimetabolites, alkylating agents, or platinum compounds. Since then, ABCB1 has been shown to be an indiscriminate transporter of various hydrophobic compounds and drugs such as colchicine, VP16, adriamycin, and vinblastine. In addition, it can transport lipids, steroids, xenobiotics, and peptides (Ambudkar *et al.*, 1998). ABCB1 is thought to have an important role in removing toxic metabolites from cells, but its expression in cells at the blood-brain barrier implicates it in the transport of compounds that cannot be delivered by diffusion into the brain. ABCB1 confers drug resistance by lowering the intracellular drug concentrations to sub-lethal levels. The prognostic significance of ABCB1 as indicator for failure to chemotherapy and worse outcome has been demonstrated in a number of clinical studies (e.g. Chan *et al.*, 1991; Verrelle *et al.*, 1991; Holmes and West, 1994; Sauerbrey *et al.*, 1994). Apart from MDR in cancer cells, ABCB1 also appears to contribute to resistance of AIDS patients towards protease inhibitors like indinavir, nelfinavir, or saquinavir (Lee *et al.*, 1998; Jones *et al.*, 2001; Fellay *et al.*, 2002). Drug absorption after oral administration is also affected by the expression of ABCB1 in the normal gastrointestinal tract (Spahn-Langguth *et al.*, 1998; Fromm, 2000). Likewise,

ABCB1 expression in the brain prevents penetration of drugs across the blood-brain barrier (Schinkel, 1999) which has implications in the treatment of patients suffering from epilepsy (Sisodiya *et al.*, 2002) or schizophrenia (Bebawy and Chetty, 2008).

ABCA3: Intracellular drug sequestration also contributes to MDR and a genuine intracellular ABC transport protein with MDR function has just recently been identified. Analyzing the intrinsic drug efflux capacity of leukemic stem cells, Chapuy *et al.* found the ABC transporter ABCA3 to be expressed consistently in acute myeloid leukemia (AML) samples. Their results showed that greater expression of ABCA3 was associated with unfavourable treatment outcome and that elevated expression *in vitro* induced resistance toward a broad spectrum of cytostatic agents. Additionally, ABCA3 remained localized within the limiting membranes of lysosomes and multi-vesicular bodies, in which cytostatics are efficiently sequestered. In addition to AML, Chapuy *et al.* also detected ABCA3 in a panel of lymphohematopoietic tissues and transformed cell lines (Chapuy *et al.*, 2008).

ABCC1 and other Multidrug Resistance Proteins: The *ABCC1* gene was identified in a multidrug resistant small-cell lung carcinoma cell line that did not overexpress *ABCB1* (Cole *et al.*, 1992). ABCC1 confers resistance to doxorubicin, daunorubicin, vincristine, colchicines, and several other compounds, a profile that is very similar to that of ABCB1. However, unlike ABCB1, ABCC1 transports drugs that are conjugated to glutathione by the glutathione reductase pathway (Borst *et al.*, 2000). Many solid tumors and hematological malignancies show expression of ABCC1 (a few examples: Endo *et al.*, 1996; Campling *et al.*, 1997; Sullivan *et al.*, 1998). ABCC1 has been found to be a prognostic factor for response to chemotherapy and for poor outcome in neuroblastoma (Norris *et al.*, 1996). Frequently, an inversion on chromosome 16 (p13q22) can be observed in patients with acute myeloid leukemia subtype M4E0 (Le Beau *et al.*, 1983). Since the ABCC1 gene maps to chromosome 16, this inversion results in silencing of the *ABCC1* gene and renders patients more sensitive to chemotherapy (Kuss *et al.*, 1994). Additional evidence for a causative contribution of ABCC1 to drug resistance has come from transfection experiments (Cole *et al.*, 1994; Grant *et al.*, 1994).

Other ABCC subfamily members which have been implicated in MDR include ABCC2, 3, 5, and 10 (Kool *et al.*, 1997; Young *et al.*, 1999).

ABCG2: Analysis of cell lines resistant to mitoxantrone that neither overexpress ABCB1 nor ABCC1 led several laboratories to identify the *ABCG2* gene as a drug transporter (Allikmets *et al.*, 1998; Doyle *et al.*, 1998; Miyake *et al.*, 1999). The half-transporter ABCG2 confers resistance to anthracycline anticancer drugs and is amplified or involved in chromosomal translocations in cell lines selected with topotecan, mitoxantrone, or doxorubicin. The MDR phenotype due to ABCG2 expression is overlapping with, but distinct from the one due to ABCB1 (Litman *et al.*, 2000). It is suspected that ABCG2 functions as a homodimer because transfection of the gene into cells confers resistance to chemotherapeutic drugs (Kage *et al.*, 2002).

1.2.4 ABC gene subfamilies in characterized eukaryotes

ABC proteins form the largest and most conserved gene family known, with well over 300 members in bacteria, 31 in yeast, 129 in plants, 56 in the fly (*D. melanogaster*), 58 in the worm (*C. elegans*), 52 in the mouse (*M. musculus*), and 48 in humans (Dean *et al.*, 2001a; Gottesman and Ambudkar, 2001 and Web address: http://www.pasteur.fr/recherche/unites/pmtg/abc/database.iphtml). One of the interesting findings from the analysis of the ABC genes from eukaryotes whose genomes have been sequenced is the remarkable similarity in the number of ABC genes in higher eukaryotes (Table 1.3). Thus, it appears that humans do not have substantially more ABC genes than much simpler eukaryotes, suggesting that there is a core of essential ABC genes that are required for all multicellular eukaryotes. On the other hand, yeast does have only about half the number of ABC genes as the higher eukaryotes do, suggesting that the evolution of multicellularity was accompanied by the expansion in the number of ABC genes. It is clear, also, that certain species have expanded some subfamilies more than others (Dean *et al.*, 2001b). The structural homology detected between ABC transporters also translates into functional similarity, highlighting the conservation of this family of proteins. For example, mouse *Abcb1a* (multidrug transporter) can partially complement yeast *Ste6* ("**a**" mating pheromone transporter), thus restoring mating in a Δ*Ste6* sterile yeast strain

Table 1.3 Number of orthologues in each subfamily in some of the characterized eukaryotes

Subfamily	Human[a]	Mouse[b]	Yeast[c,d]	*D. melanogaster*[a]	*D. discoideum*[e]	*A. thaliana*[f]	*C. elegans*[f]
A	12	15	0	10	12	12	7
B	11	12	4	10	9	27	23
C	12	11	7	12	14	16	8
D	4	4	2	2	3	2	5
E	1	1	1	1	1	3	1
F	3	3	5	3	4	5	3
G	5	6	10	15	21	39	11
Other	0	0	3	3	4	10	0
Total	**48**	**52**	**31**	**56**	**68**	**114**	**58**

[a](Dean *et al.*, 2001)

[b](Schriml and Dean, 2000; Dean, 2002)

[c](Decottignies and Goffeau, 1997)

[d](Michaelis and Berkower, 1995)

[e](Anjard and Loomis, 2002)

[f](Rea, 2007)

(Raymond *et al.*, 1992). In addition, LmrA, an antibiotic-resistance ABC transporter from *L. lactis* (van Veen *et al.*, 1996), can confer multidrug resistance when transfected into human lung fibroblast cells, with characteristics very similar to human ABCB1 (van Veen *et al.*, 1998).

Most of the human genes have a clear mouse orthologue, although there are some exceptions (Table 1.4). Hence, the mouse ABC genes can also be grouped into the seven previously described human ABC protein subfamilies. In fact, examination of phylogenetic relationships of mouse and human ABC genes demonstrates that mouse and human ABC orthologues are more closely related than are human or mouse paralogues (Schriml and Dean, 2000). The closest orthologue of human ABCB1 is mouse Abcb1a and these two proteins share 87% identity at the amino acid level. Thus, results for both transporters can be used to devise a common model for the function and transport mechanism of these multidrug resistance proteins, which are of considerable interest for clinical reasons as well as for their relevance to the mechanisms of other ABC transporters. Several ABC genes have been disrupted in the mouse; these include some of the genes mutated in human diseases, as well as several of the known drug transporters. Some knock-out mice show compromised viability, such as Abca1$^{-/-}$, Abca3$^{-/-}$, and Cftr$^{-/-}$; however, most of the remaining knockouts are viable and fertile and many show either no phenotype or a phenotype only under stressed conditions.

Section 1.3 – Trans-Membrane Domains

The TMDs of ABC transporters have two central roles in the transport process. First, they form the pathway through which the allocrite is translocated across the membrane. Second, they provide the amino acid residues which interact directly with the allocrite and form the allocrite binding-site(s). In addition, the TMDs contain extracellular and intracellular loops that connect the TM helices and are important for interdomain communication and recognition. The TMDs vary considerably in primary sequence, length, architecture, and the number of TM helices, suggesting that they are adapted to their respective allocrite(s). Thus, TMDs only share significant sequence

Table 1.4 Mouse orthologues of human ABC transporters

Human gene	Mouse gene	Knockout	Reference
ABCA1	Abca1	Y	Orso *et al.*, 2000; McNeish *et al.*, 2000
ABCA2	Abca2	Y	Mack *et al.*, 2007
ABCA3	Abca3	Y	Fitzgerald *et al.*, 2007
ABCA4	Abca4	Y	Weng *et al.*, 1999
ABCA5	Abca5	Y	Kubo *et al*., 2005
ABCA6	Abca6	N	
ABCA7	Abca7	Y	Kim *et al.*, 2005
ABCA8	Abca8a	N	
	Abca8b	N	
ABCA9	Abca9	N	
ABCA10			
ABCA12	Abca12	N	
ABCA13	Abca13	N	
ABCB1	**Abcb1a** (Mdr3)	Y	Schinkel *et al.*, 1994
	Abcb1b (Mdr1)	Y	Schinkel *et al.*, 1997
ABCB2	Abcb2 (Tap1)	Y	Van Kaer *et al.*, 1992
ABCB3	Abcb3 (Tap2)	N	
ABCB4	Abcb4	Y	Smit *et al.*, 1993
ABCB5	Abcb5	N	
ABCB6	Abcb6	N	
ABCB7	Abcb7	Y	Pondarré *et al.*, 2006
ABCB8	Abcb8	N	
ABCB9	Abcb9	N	
ABCB10	Abcb10	N	
ABCB11	Abcb11	Y	Wang *et al.*, 2001
ABCC1	Abcc1	Y	Lorico *et al.*, 1997; Wijnholds *et al.*, 1997
ABCC2	Abcc2	Y	Paulusma *et al.*, 1996
ABCC3	Abcc3	Y	Zelcer *et al.*, 2005
ABCC4	Abcc4	Y	Leggas *et al.*, 2004
ABCC5	Abcc5	Y	Wijnholds et al., 2000
ABCC6	Abcc6	Y	Klement *et al.*, 2005
ABCC7	Abcc7 (Cftr)	Y	Dorin *et al.*, 1992; Snouwaert *et al.*, 1992
ABCC8	Abcc8	Y	Seghers et al., 2000
ABCC9	Abcc9	Y	Chutkow *et al*., 2001
ABCC10	Abcc10	N	
ABCC11			
ABCC12	Abcc12	N	
ABCD1	Abcd1	Y	Forss-Petter *et al.*, 1997
ABCD2	Abcd2	Y	Pujol *et al.*, 2004
ABCD3	Abcd3	N	
ABCD4	Abcd4	N	
ABCE1	Abce1	N	
ABCF1	Abcf1	N	
ABCF2	Abcf2	N	
ABCF3	Abcf3	N	
ABCG1	Abcg1	Y	Kennedy *et al.*, 2005
ABCG2	Abcg2	Y	Zhou *et al.*, 2002; Jonker *et al.*, 2002
	Abcg3	N	
ABCG4	Abcg4	N	
ABCG5	Abcg5	Y	Plosch *et al.*, 2004
ABCG8	Abcg8	Y	Klett *et al.*, 2004

similarity if they translocate the same (or a very similar) allocrite in the same direction across the membrane (Dawson *et al.*, 2007).

One way the TMDs of importers appear to have adapted to the size of their respective allocrite(s) is by varying the number of TM helices (5-10) present in each TMD. On the other hand, exporters contain a conserved core of 12 TM helices, and adaptation probably occurred as changes in primary sequence. Additional TM helices are found in several human homologues, but are likely facilitating regulatory functions rather than the principal transport reaction (Dawson *et al.*, 2007). For example, in the human ABC transporter associated with antigen processing (ABCB2/ABCB3) each half transporter has additional N-terminal TM helices that appear to be essential for the interaction with tapasin (TAP-binding protein) (Koch *et al.*, 2004; Procko *et al.*, 2005). These additional helices could be deleted without loss of peptide recognition or transport *in vitro*, even though the *in vivo* function of ABCB2/3 was affected due to the lost interaction with tapasin.

1.3.1 Allocrite binding site(s) and allocrite recognition

ABC importers require external binding proteins that capture allocrites with high affinity and specificity and feed them to the transporter. Because only the binding protein, not the transporter, binds the cargo effectively, this arrangement ensures unidirectional transport (Dawson *et al.*, 2007). The structures of many binding proteins with and without substrates have been determined at high resolution. A general feature of these proteins is a bi-lobed architecture with a central cleft that forms a specific binding site. Thus, in importers, substrate acquisition occurs on the periplasmic face of the TMD. In ABC exporters, on the other hand, the exact location of substrate acquisition is not fully understood since many of the substrates are exceedingly hydrophobic and might be located within the lipid bilayer. The classical pump model for transporters has been proposed for ABC exporters, where the allocrite initially interacts with the protein from the aqueous phase at an inward facing site and conformational changes result in an outward facing site that releases the allocrite outside the cell or compartment. However, when the allocrites are highly hydrophobic these tend to concentrate in the membrane, thus allowing the allocrite to be presented to the transporter within the lipid bilayer. The

broad range of allocrites transported by ABC transporters is astounding. While some transporters are very specific towards an allocrite, others transport a plethora of structurally and functionally different compounds. A major question concerning ABC transporters involved in transport of more than one allocrite is how these enzymes are able to recognize and transport such a diverse range of compounds. Although the answer is not yet fully contrived for ABC transporters, other multidrug-binding proteins have provided potential models for this phenomenon. For example, QacR is a multidrug-binding transcription repressor from *Staphylococcus aureus*, that does not belong to the ABC transporter superfamily, and is induced by structurally diverse cationic lipophilic drugs (Schumacher *et al.*, 2001). Crystal structures of multiple QacR-drug complexes reveal that its substrates bind in a large pocket, which is composed of smaller overlapping "minipockets", i.e. separate but linked drug-binding sites (Kaur, 2002). This multi-site drug binding mechanism provides a basis for the specific binding of multiple drugs to a single protein and is therefore consonant with studies on multidrug resistance transporters and other ABC transporters that carry diverse allocrites. Presentation to the transporter of the allocrite within the lipid bilayer could also explain the wide range of allocrites that can be transported by the members that are multidrug transporters. A popular mechanism proposed by Gottesman and colleagues, known as the "hydrophobic vacuum cleaner" model, is that these transporters (especially ABCB1) extract the various allocrites from the inner leaflet of the membrane bilayer and transport or flip them via a single channel through the protein to the outer leaflet of the membrane where they can diffuse out (Gottesman and Pastan, 1993).

The high-resolution structure of the $MalFGK_2$-MBP complex in the presence of ATP and maltose (Oldham *et al.*, 2007) is the first structural evidence for the presence of an allocrite-binding site inside the TM subunits of an ABC transporter, as was suggested by genetic data (Shuman, 1982). There is apparently only a single binding site and the mode of interaction between the allocrite and the residues in the cavity is interesting, but has limited use in the elucidation of the mechanism of allocrite recognition by multidrug transporters.

Identifying structural elements required by allocrite binding sites and their possible location within the TMDs are important not only in understanding the

mechanism by which allocrites interact with ABC transporters, but also in designing specific inhibitors or chemo-sensitizers capable of altering the function of ABC transporters involved in resistance.

Two approaches have been used to identify putative allocrite binding sites: 1) the use of photo-activatable analogs of the allocrite(s) which can bind to the transporter and 2) the analysis of naturally occurring or genetically engineered mutations that affect transport and allocrite specificity (reviewed in Gottesman and Pastan, 1993). For example, the TMDs of human ABCB1 can be photoaffinity-labelled by drug analogs, and mutations altering allocrite specificity map to these domains (Ueda *et al.*, 1997). The results from labelling studies with photolabelled analogs of drug substrates in hABCB1 (Bruggemann *et al.*, 1989; Bruggemann *et al.*, 1992; Greenberger, 1993), suggested that the labelled sites are closely associated with TM5 and 6 and TM11 and 12. These photolabelling studies also suggested that there may be two distinct drug-labelling sites or that the two labelled segments are part of a single drug-labelling site (Loo and Clarke, 1999c).

1.3.2 Allocrite transport

Historically, transporters located in the cytoplasmic membrane have been viewed as undergoing conformational changes in which a central binding site is exposed alternately to either the inside or to the outside of the cell, but never simultaneously to both sides (Figure 1.4). This simple allosteric model for membrane pumps (Jardetzky, 1966) ensures that there is never an open pathway that could permit unregulated movement of substrate down its concentration gradient, thereby preventing active accumulation. Indeed, in bacteria, a proton gradient is maintained by the cytoplasmic membrane, to synthesize ATP and drive other membrane activities, implying that transporters must be sealed so tightly that even a proton cannot pass freely (Davidson and Maloney, 2007). Presumably, the simple allosteric model for membrane pumps also holds true for ABC transporters.

In ABC transporters, allocrite recognition and binding is followed by movement (either inward or outward) of allocrites across the membrane (cytoplasmic or organellar). Many studies have demonstrated that active transport is energized by ATP hydrolysis at

Figure 1.4:

The simple allosteric model for membrane pumps

To function as a pump, a polymer molecule must meet three structural conditions only. (1) It must contain a slit or a cavity in the interior of the molecule, large enough to admit the transported molecule. (2) It must be able to assume two different configurations, such that the molecular cavity is open to one side of the membrane in one configuration (A) and to the opposite side in the other (B). (3) It must contain a binding site (shaded ovals) for the transported species in its molecular cavity, the affinity of which is different in the two configurations for the transported species (e.g. (A) high affinity; (B) low affinity).

A)

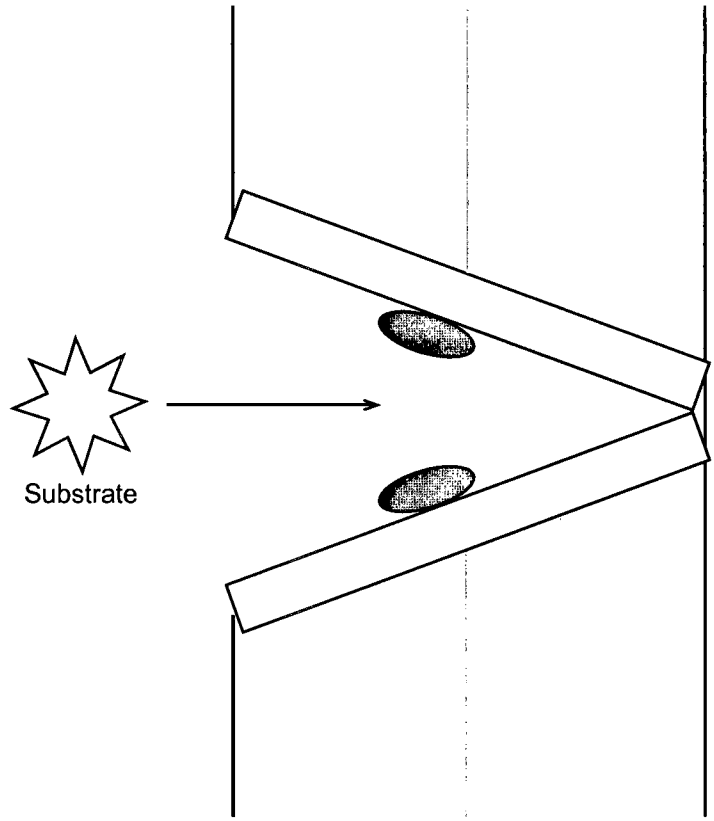

B)

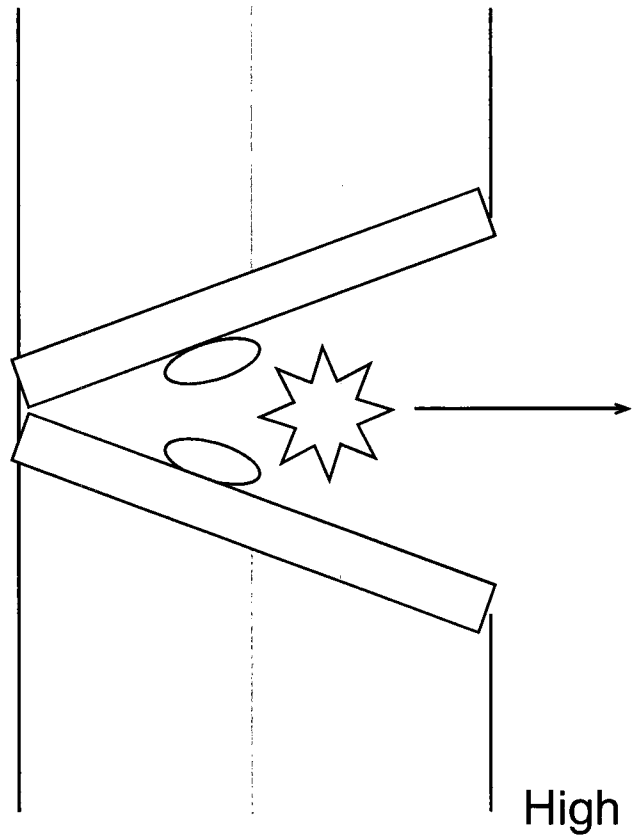

Low [substrate]

High [substrate]

the NBDs. The first such studies were carried out on the histidine and maltose permease complexes of *E. coli* using inside-out vesicles (Ames, 1989; Dean *et al.*, 1989). Subsequently, reconstitution studies with purified hABCB1 also showed that transport of hydrophobic drug substrates against a concentration gradient is coupled to ATP hydrolysis (Sharom *et al.*, 1993).

Recent high-resolution views of complete ABC transporters in different conformational states have provided further clues as to how ATP might be used to drive the structural reorganizations that accompany membrane transport. Importantly, a putative translocation pathway appears to run through the center of the transporter which might be gated alternately, either at the inside or the outside of the cytoplasmic membrane, coupling allocrite translocation to a cycle of ATP-dependent conformational changes (see Chapter 6).

1.3.3 Intra- and extracellular loops

In addition to physically connecting the TM α-helices, and therefore acting as hinges, the extra- and intra-cellular loops of the TMDs play important roles in interdomain communication and formation of the translocation pathway.

Interdomain communication is known to occur between the TMDs and NBDs since allocrite binding can significantly activate the ATPase activity of many ABC transporters and ATP hydrolysis energizes translocation of allocrite(s) by the TMDs. This signalling between the two domains is thought to occur through the conserved intracellular loops (ICLs) linking the individual TM helices of the TMDs. Both biochemical and structural data provide evidence for this interaction. Using a random mutagenesis approach in Abcb1a, mutations were identified in ICL1 affecting both allocrite specificity and allocrite-stimulated ATPase activity of this enzyme (Kwan, 1998). The finding that mutations in ICL1 can modulate the activity of two separate and distinct regions supports the proposed role for the ICLs. Recent high-resolution crystal structures of complete ABC transporters have confirmed these biochemical findings and have established the nature of the TMD-NBD contact surface which is referred to as the "transmission interface" (see Section 1.5).

In importers, the extracellular (or periplasmic) loops (ECLs) are important contact points for the periplasmic binding protein (PBP), which delivers the transporter's allocrite(s) to the TMDs. In the crystal structure of $ModB_2C_2$ in complex with its PBP: ModA, interactions of the TMDs (ModB) and the PBP (ModA) occur between several charged amino acid residues on the ModA surface and two ECLs of ModB (one between TM helices 3 and 4 and another between TM helices 5 and 6, Hollenstein *et al.*, 2007b). Similarly, in the crystal structure of $MalFGK_2$ in complex with its PBP: maltose binding protein (MBP), both lobes of MBP interact extensively with the TMDs (MalF and MalG). Two notable interactions include the insertion of the MalG ECL3 into the MBP sugar-binding cleft as well as contacts by mostly the N-lobe of MBP with a large periplasmic loop (ECL2) of MalF, which folds into an Ig-like domain and extends about 30Å away from the membrane surface. The insertion of the MalG ECL3 into the MBP sugar-binding site is a notable feature at the MBP–TMD interface relating to maltose transfer (Oldham *et al.*, 2007). If a sugar molecule is modelled into the binding site of the MBP based on the structures of substrate-bound open forms of MBP (Duan and Quiocho, 2002), even the smallest substrate: maltose, clashes with ECL3. Therefore, insertion of this loop appears to dislodge the sugar from the binding protein like a "scoop" and ensures efficient transfer of the sugar from the PBP to the TMDs. Consistently, a mutant containing a 31-residue insertion in this loop was defective in transport but retained the ability to assemble a $MalFGK_2$ complex (Nelson and Traxler, 1998). Insertion of periplasmic loops into the binding protein was also observed in the recent structure of BtuCD-BtuF (Hvorup *et al.*, 2007).

In some ABC transporters, ICLs and ECLs can also take part in the formation of the gates for the translocation pathway. For example, in Sav1866 (in the "closed NBD" state) the translocation pathway is open to the extracellular space. The ICLs between TM helices 2 and 3 and TM helices 4 and 5 in each TMD extend the helical secondary structure beyond the lipid bilayer, protruding approximately 25Å into the cytoplasm. No connection to the cytoplasm exists and the ICLs form the bottom of the cavity present between the two TMDs (Dawson and Locher, 2006). No inward facing conformation has been observed for this transporter yet. In BtuCD, (in the "closed NBD" state) the translocation pathway is open to the periplasm and residues in the ICL between TM

helices 4 and 5 from each TMD form a gate that blocks access to the cytoplasm (Locher *et al.*, 2002). By contrast, in BtuCD-BtuF, (in the "open NBD" state) the translocation pathway is open to the cytoplasm. The translocation pathway is gated at the periplasmic side through interactions with BtuF but also between residues in TM helix 5 and ECL3 (helix 5a between TM helices 5 and 6) of both TMDs (Hvorup *et al.*, 2007). Similarly, in HI1470/1, (in the "open NBD" state) the translocation pathway is open to the cytoplasm and residues in TM helix 5 and ECL3 (helix 5a between TM helices 5 and 6) in both TMD help restrict access to the translocation pathway from the periplasmic side (Pinkett *et al.*, 2007). No outward facing conformation has been observed for this transporter yet. (Atypically, in these last two ABC transporters the TMDs each have 10 spans, not the usual six.)

1.3.4 Three-dimensional structural details

With the high-resolution structures of full-length transporters now available it has become possible to view the probable TM helical packing of the TMDs into the membrane. Moreover, the diversity of the TMDs of the crystallized transporters provides insight into how different transporters (importers and exporters) may accommodate different allocrites which vary in nature (size, shape, charge, and polarity) by modifying the number and packing of the TM helices in their TMDs.

Amongst the high-resolution structures, four of the complete transporters have TMDs which contain 6 TM helices (Sav1866, ModBC, $MalFGK_2$ –although MalF has two extra TM helices, and MsbA), and of those only two are exporters (Sav1866 and MsbA). Thus, these transporters are better suited to model the TMDs of mammalian transporters such as Abcb1a.

The crystal structure of Sav1866 was the first to reveal the conserved core structure of an ABC exporter (Dawson and Locher, 2006). The TMDs of Sav1866 extend beyond the membrane boundary and protrude ~25Å into the cytoplasm. In the observed state (nucleotide-bound NBD dimer), Sav1866 exhibits a pronounced outward-facing conformation; the TM helices cluster toward the cytoplasm but diverge into two discrete wings toward the extracellular side of the membrane (Dawson and Locher, 2006; Dawson and Locher, 2007). Defying long-held models, these wings do not represent individual

TMDs. Rather, each wing consists of TM1–TM2 from one TMD and TM3–TM6 from the other. Cross-linking studies that identified neighbouring TM helices in human ABCB1 (Stenham *et al.*, 2003) are consistent with the helix arrangement observed in Sav1866, suggesting that Sav1866 probably serves as a good model for the core architecture of all ABC exporters (Hollenstein *et al.*, 2007a; Zolnerciks *et al.*, 2007). In the lipid exporter MsbA, which has been crystallized in different states (nucleotide-free open and less-open, and nucleotide-bound closed NBD dimer, Ward *et al.*, 2007), the TM helices of the TMD are arranged similarly to those of Sav1866, with a root mean square deviation (rmsd) of < 2.2Å between the Cα positions of monomers. As in Sav 1866, the TM helices extend into the cytoplasm. The most striking feature of the MsbA models is that TM4/TM5/ICL2 crosses over and associates with TM1-TM3/TM6 of the opposing monomer. This cross-over motif, as observed in Sav1866, is accentuated by the open-apo structure and provides the only means of interaction between the two monomers. The cross-over interaction likely holds the dimer together during the open inward-facing conformation. This type of interlocking mechanism, known as an intertwined interface, has been observed in cytokines and DNA-binding proteins and is thought to reinforce stability and symmetry (Larsen *et al.*, 1998).

Section 1.4 – Nucleotide-Binding Domains

The most prominent characteristic of the ATP-binding cassette (ABC) systems is that they share a highly conserved ATPase domain, the ABC or nucleotide-binding domain (NBD). NBDs are between 200 and 300 amino acids in length and an overall identity of 30% or more between different ABC proteins is typically observed (Holland and Blight, 1999). Sequence analysis of NBDs revealed the presence of two consensus Walker motifs (A and B). These motifs, originally described in bacterial ATPases, suggested that the NBD contains a site where ATP can possibly bind and be hydrolysed (Walker *et al.*, 1982). Initial evidence indicating that drug efflux from multidrug resistant cells was energy-dependent was obtained through experiments in which cellular ATP pools were depleted, which resulted in inhibition of drug efflux (Ling and Thompson, 1974; Fojo *et al.*, 1985). In addition, studies of bacterial ABC transporters showed that

the NBDs bind and hydrolyse ATP and that ATP hydrolysis is coupled to transport (e.g. Bishop *et al.*, 1989). Thus, ATP is the true substrate of ABC proteins and it is hydrolysed to ADP and P_i. Hence, consumption of ATP provides energy for a large number of biological processes (Dassa and Bouige, 2001).

The NBDs of all ABC transporters contain a number of conserved characteristic motifs, which define this superfamily of proteins and distinguish them from other ATP-binding proteins (Higgins *et al.*, 1986). These sequences are either involved in MgATP binding and hydrolysis or in facilitating crucial interfaces in the assembled transporter (Schneider and Hunke, 1998; Davidson and Chen, 2004).

1.4.1 Conserved sequence motifs

ABC-transporter NBDs contain the classical Walker A and Walker B consensus sequences first described by Walker and colleagues for nucleotide binding (Walker *et al.*, 1982). These sequence motifs have been identified in a range of proteins engaged in diverse cellular processes, such as receptor signalling, phosphoryl transfer reactions, motility, ATP synthesis/proton efflux, membrane transport, and DNA translation and maintenance or repair, which all have in common the binding and/or utilization of nucleotide (Ramakrishnan *et al.*, 2002). The presence of additional conserved consensus sequences defines the ABC-ATPases and these sequences include the signature motif and the equally characteristic D-loop. Figure 1.5 illustrates the relative position of the different conserved sequence motifs in the NBD, as well as the interaction of specific residues of these sequences with the bound ATP (as determined for HisP). Following is a brief description of the sequence and role of the conserved motifs found in the NBDs of ABC transporters.

The A-loop (for aromatic residue interacting with the adenine ring of ATP), contains a highly conserved aromatic residue (Y, W, F) approximately 25 amino acids upstream of the Walker A motif that is essential for ATP-binding (Kim *et al.*, 2006). Mutational analysis of this subdomain in several ABC transporters (including Abcb1a, see Chapter 2) as well as homology modeling, structural, and data mining studies have provided evidence for a functional role of the A-loop in ATP-binding in most members of the superfamily of ABC transporters (Kim *et al.*, 2006). The aromatic side chain of the A-

Figure 1.5:

Conserved sequence motifs in ABC-ATPase NBDs

(A) Relative position of the conserved sequence motifs in the NBDs of ABC-ATPases. A: A-loop, Q: Q-loop, P: Pro-loop, IC: invariant carboxylate, D: D-loop, H: H-loop. (B) Position of the residues of the conserved sequence motifs (coloured as in A) around the bound ATP as modeled by HisP (the equivalent residues in Abcb1a are also given beside the boxed HisP residues; NBD1/NBD2).

A)

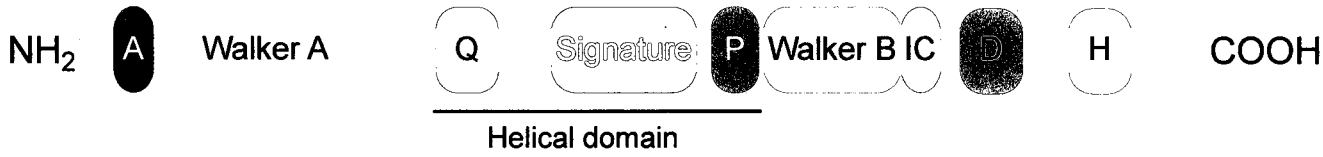
NH2
A
Walker A
Q
Signature
P
Walker B IC
D
H
COOH
Helical domain

B)

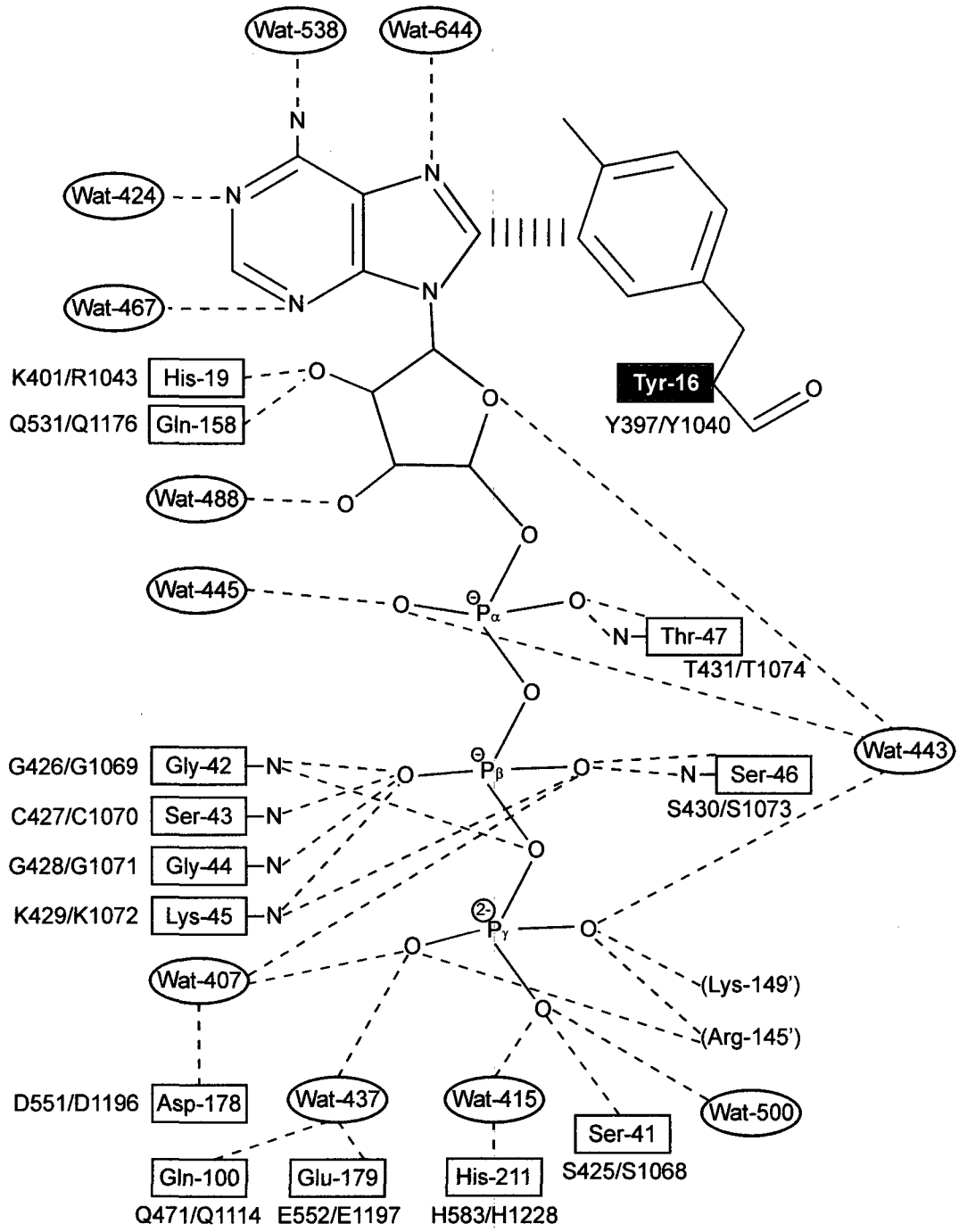
Wat-538
Wat-644
Wat-424
Wat-467
K401/R1043
His-19
Q531/Q1176
Gln-158
Tyr-16
Y397/Y1040
Wat-488
Wat-445
Thr-47
T431/T1074
Wat-443
G426/G1069
Gly-42
C427/C1070
Ser-43
G428/G1071
Gly-44
K429/K1072
Lys-45
Ser-46
S430/S1073
Wat-407
(Lys-149')
(Arg-145')
D551/D1196
Asp-178
Wat-437
Wat-415
Wat-500
Ser-41
S425/S1068
Gln-100
Q471/Q1114
Glu-179
E552/E1197
His-211
H583/H1228

loop residue π-stacks against the adenine moiety of bound nucleotide and serves to increase stability (Ambudkar *et al.*, 2006). The relatively non-specific π-stacking interaction with the adenine moiety explains the intrinsic promiscuity of ABC-NBDs for other nucleotides (Oswald *et al.*, 2006).

The Walker A motif (GXXGXGKS/T) embodies a structure known as the phosphate-binding loop or P-loop, a glycine-rich loop preceded by a β-strand and followed by an uncapped α-helix (Saraste *et al.*, 1990). This structure functions to bind the nucleotide through electrostatic interactions with the triphosphate moiety, in particular with the β-phosphate, of ATP. Detailed mutational analyses performed with numerous ABC transporters confirmed that amino acid changes in the Walker A motif, especially at the lysine residue, are generally not tolerated with respect to ATPase activity (Schneider *et al.*, 1994; Koronakis *et al.*, 1995; Loo and Clarke, 1995c; Urbatsch *et al.*, 1998). Conservative substitution of the invariant lysine by arginine in, for example, PrtD, MalK and Abcb1a abolished ATP hydrolysis but nucleotide-binding activity was retained (Azzaria *et al.*, 1989; Delepelaire, 1994; Schneider *et al.*, 1994; Urbatsch *et al.*, 1998). While other replacements of the lysine residues still allowed interaction with nucleotides as demonstrated by photocross-linking with the analog 8-azidoATP (Panagiotidis *et al.*, 1993; Carson *et al.*, 1995; Bliss *et al.*, 1996) or enhancement of fluorescence of trinitrophenyl-ATP (Koronakis *et al.*, 1995), a change to asparagine also eliminated the nucleotide-binding activity (Shyamala *et al.*, 1991; Panagiotidis *et al.*, 1993). This critical lysine residue is involved in hydrogen bonding with the β-phosphate of ATP.

The Q-loop or γ-phosphate linker contains a phylogenetically invariant glutamine (Q) residue that is located at the C-terminus of a β-strand and is followed by a flexible loop (Hopfner *et al.*, 2000; Yuan *et al.*, 2001). The Q-loop joins the catalytic domain (lobe I) to the N-terminal end of the helical domain (lobe II) of the NBD (see section 1.4.2). Comparative analysis of NBD crystal structures suggests that the conserved glutamine moves in and out of the active site during the catalytic cycle; engaging the MgATP-bound active site, and disengaging and moving away after ATP has been hydrolysed (Yuan *et al.*, 2001; Jones and George, 2002). This idea is consistent with the mechanism of other P-loop proteins in which the Mg^{2+}-coordinating protein ligand equivalent to the glutamine is situated on a switch region that mediates oligomeric

interactions in response to nucleotide binding and hydrolysis, such as in G proteins and the F_1-ATPase (Frasch, 2000; Spoerner *et al.*, 2001). The structural variability of this region amongst the ABC crystal structures supports the idea that the Q-loop may undergo conformational switching transitions. The structural data also indicate that the Q-loop forms part of the TMD-NBD interface, making contacts with a specific loop (the "coupling helix") of the TMDs in the six complete transporter structures (BtuCD, Sav1866, Hi1470/1, $ModB_2C_2$, $MalFGK_2$, and MsbA). The N- and C-termini of the Q-loop have high sequence variability amongst ABC transporters, consistent with the notion that these segments are involved in subunit-subunit interactions (Jones and George, 2002). Biochemical evidence that the conserved glutamine and Q-loop are involved in interdomain communication also exists (Hunke *et al.*, 2000a; Hunke *et al.*, 2000b; Urbatsch *et al.*, 2000b). Thus, it appears that through its interactions with the nucleotide and catalytic Mg^{2+} ion, the conserved glutamine may signal between the active site and the TMDs, possibly by moderating conformational transitions of the Q-loop, and thus TMD-NBD interactions. It was suggested by the group of Dr. Yuan that interaction of the conserved glutamine with the γ-phosphate of the bound nucleotide mediates rotation of the helical subdomain into the "closed" conformation where the LSGGQ motif is correctly oriented to engage the opposite catalytic site within the dimer (Yuan *et al.*, 2001). Interestingly, a recent crystal structure of the GlcV monomer with bound nucleotide analogue (Verdon *et al.*, 2003a) shows that the conserved glutamine can engage the catalytic Mg^{2+} ion when the helical domain is rotated outward, thus suggesting that the glutamine may not mediate rotation of the helical domain. Hence, the flexibility of the Q-loop may function, in part, to accommodate the outward rotation of the helical domain (similar to a hinge) while the glutamine remains engaged in the active site. The nature of the relationship between rotation of the helical domain and the Q-loop transitions thus remain uncertain.

The signature motif or C-loop (LSGGQ) is about 20 residues upstream of the Walker B motif and is composed of up to 15 residues, usually starting with LSGGQ. This motif is used as a diagnosis for ABC-ATPases. With the crystallization of the NBDs in their dimerized state, the role of the mutation-sensitive signature motif was finally revealed. Thus, it was shown that the signature motif completes the nucleotide binding

fold and interacts with the γ-phosphate of ATP across the dimer, in the ATP-bound state. In ABCB1, substitutions in this motif result in miscommunication between the TMDs and the NBDs (Szakacs *et al.*, 2001), suggesting that this motif plays a key role in the interdomain communication regulating allocrite-induced ATP hydrolysis.

The Pro-loop contains a near invariable proline (P) residue that is located immediately before the Walker B motif. This short loop (~5 residues) joins the C-terminal of the helical domain to the catalytic domain and is therefore believed to act as a hinge, similarly to the Q-loop, allowing rigid-body movement of the helical domain with respect to the catalytic domain. Substitutions of this proline residue have a severe impact on the thermal stability and amount of overexpression of the HlyB-NBD (Schmitt *et al.*, 2003). Moreover, substituting this proline with leucine in HlyB makes the secretion of HlyA temperature-sensitive *in vivo* (Blight *et al.*, 1994) and the corresponding mutation in HisP renders the ATPase constitutively active *in vitro* (Petronilli and Ames, 1991). These results imply an important role for this conserved proline in the structure and function of this second connecting loop, which is probably also involved in relaying conformational information between the helical and the catalytic domains.

The Walker B motif (ΦΦΦΦD, where Φ is a hydrophobic residue) constitutes a buried β strand within the core of the nucleotide binding fold of P-loop ATPases (Smith and Rayment, 1996a). The Walker B aspartate residue hydrogen-bonds to coordinating ligands of the catalytic Mg^{2+} ion, thereby assisting in the establishment and maintenance of the geometry of the active site. Mg^{2+} is an essential divalent metal cofactor in the catalysis of ABC-ATPases and substitutions of the conserved aspartate residue were generally shown to abolish ATPase activity and nucleotide binding (Shyamala *et al.*, 1991; Panagiotidis *et al.*, 1993; Koronakis *et al.*, 1995; Urbatsch *et al.*, 1998).

The invariant carboxylate (IC) is a highly conserved glutamate (or sometimes aspartate) located immediately after the Walker B aspartate. The importance of this acidic residue was not established prior to its mutagenesis in Abcb1a. The work described in Chapters 3, 4, and 5 of this thesis has helped to elucidate the role of this highly conserved residue, which appears to be involved in the catalytic reaction of ATP hydrolysis as well as NBD-NBD communication.

The D-loop is located just downstream of the Walker B motif and is composed of four conserved residues: SALD or similar. A backbone oxygen atom near the C-terminus of the D-loop interacts with the putative nucleophilic water in the active site of the opposite monomer in the crystal structures of two NBD dimers: Rad50cd (Hopfner *et al.*, 2000) and MJ0796-E171Q (Smith *et al.*, 2002). This loop is therefore thought to be involved in the contact interface between the two NBDs and possibly in other tasks, such as communication between the catalytic sites (Jones and George, 2004).

The H-loop or "switch motif" contains an almost invariant histidine residue. This histidine contacts the γ-phosphate of ATP, the invariant carboxylate residue, and residues in the D-loop of the opposite NBD (Hung *et al.*, 1998; Chen *et al.*, 2003; Zaitseva *et al.*, 2005a). This loop is also sometimes called the switch motif because the side chain of the His residue "swings in" to interact with the γ-phosphate on binding of the nucleotide. Mutations of this histidine in some prokaryotic ABC-ATPases abolished transport function, but not necessarily ATPase activity, suggesting a role for this region in coupling ATP hydrolysis to transport (Schneider and Hunke, 1998). Recently, the conserved histidine has also been implicated in the catalytic reaction of ATP hydrolysis by forming a catalytic dyad with the invariant carboxylate residue in the bacterial transporter HlyB. Hence, in HlyB, the H-loop histidine acts as a "linchpin" by holding together all required parts of a complicated network of interactions between ATP, Mg^{2+}, water molecules, and amino acids from both NBDs, necessary for transition-state formation and inter-monomer communication (Zaitseva *et al.*, 2005a).

1.4.2 Three-dimensional structural details

A plethora of 3-D crystal structures of NBDs have been determined since Dr. Kim's lab reported the first such structure, the HisP protein of the histidine transporter from *Salmonella typhimurium* in 1998 (Hung *et al.*, 1998). The crystal structures of isolated NBDs share a conserved fold containing two domains, the catalytic and helical domains. In addition, the arrangement of the NBDs in the functional ABC transporter is conserved. The arrangement is called 'head-to-tail' or 'Rad50-like', after the structure of the Rad50 protein in which it was first visualized (Hopfner *et al.*, 2000), and the key feature is that the two NBDs present their conserved sequence motifs at the shared

interface, forming two composite ATP-binding sites. The structures of the ATP-bound state of isolated NBDs (see, for example, Smith *et al.*, 2002; Zaitseva *et al.*, 2005a) and one full transporter (Sav1866, Dawson and Locher, 2006; Dawson and Locher, 2007) are very similar in structure and indeed show two ATP molecules (or non-hydrolysable analogues) sandwiched between the NBDs. Structural data is important for the identification of residues potentially involved in enzyme function, thus, the next subsections will describe the structural details of the NBD both at the monomeric and dimeric levels.

1.4.2.1 The NBD as a monomer

In 1998, the first 3-D crystal structure of an NBD was published: that of the HisP subunit of the histidine permease from *Salmonella typhimurium* (Hung *et al.*, 1998). The NBD subunit of the well-characterised bacterial histidine permease complex thus became the first structural model for ABC-ATPases. Since then, several other NBDs from different ABC proteins of various organisms have been crystallized, including MalK (Diederichs *et al.*, 2000), the NBD of ABCB2 (TAP1) (Gaudet and Wiley, 2001), HlyB (Schmitt *et al.*, 2003), and NBD1 of ABCC7 (CFTR) (Lewis *et al.*, 2004) to name a few.

In ABC transporters, the NBD adopts an L-shaped conformation with a two-domain architecture that consists of two lobes or arms (Figure 1.6 A). Lobe I, also called the catalytic domain, contains the core fold of P-loop ATPases which is characterised by a central, mostly parallel β sheet flanked by α-helices (Smith and Rayment, 1996a). This domain adopts a fold most similar to that of RecA (Story and Steitz, 1992) and parts of the bovine F_1-ATPase (Abrahams *et al.*, 1994) and contains the nucleotide binding site. Lobe II, also called the helical or signalling domain, is more structurally diverse. Because the catalytic domain can further be divided into two subdomains: the ABC-core and ABCβ subdomains, the NBDs are sometimes considered to have three structurally and functionally distinct subdomains. Figure 1.6 B depicts a generic topology and numbering system for the secondary structural elements of the NBD and the three subdomains are colour-coded as in figure 1.6 A. The central, mostly parallel β sheet forming the binding site for the nucleotide phosphates, and the α-helices flanking and joining these β strands, are referred to collectively as the ABC-core subdomain (Karpowich *et al.*, 2001) (in light

Figure 1.6:

Consensus ABC-transporter NBD fold

(A) Two-lobe domain structure of ABC-ATPase NBDs as modelled by HlyB-NBD. The ATP-binding core subdomain is shown in yellow, the antiparallel β-subdomain (ABCβ) in grey and the helical subdomain in beige. Conserved sequence motifs are coloured (Walker A: red; Q-loop: burgundy; C-loop: blue; Pro-loop: orange; Walker B: mauve; D-loop: black; H-loop: green) and labelled. This figure was modified and reproduced by permission from (Zaitseva *et al.*, 2005b). (B) Topology diagram of the consensus ABC transporter NBD fold. β-strands are depicted as arrows and α-helices as rectangles. Loops connecting secondary structural elements are depicted as lines. The ATP-binding core subdomain is shown in dark yellow (β-strands) and light yellow (α-helices), the antiparallel β-subdomain (ABCβ) in grey and the helical subdomain (lobe II) in beige. Loop regions are coloured black or orange to indicate continuity. Key loop regions discussed in the text are labelled with the appropriate letter(s) and colour-coded is in (A). A numbering system is introduced in which the variable β-strands which occur immediately C-terminal to β-strand 4 are numbered β4', β4'' etc. In addition, whilst consensus α-helix 2 does not occur in certain ABC-ATPase NBDs, the first helix of the ABCα subdomain is always referred to as α-helix 3.

A)

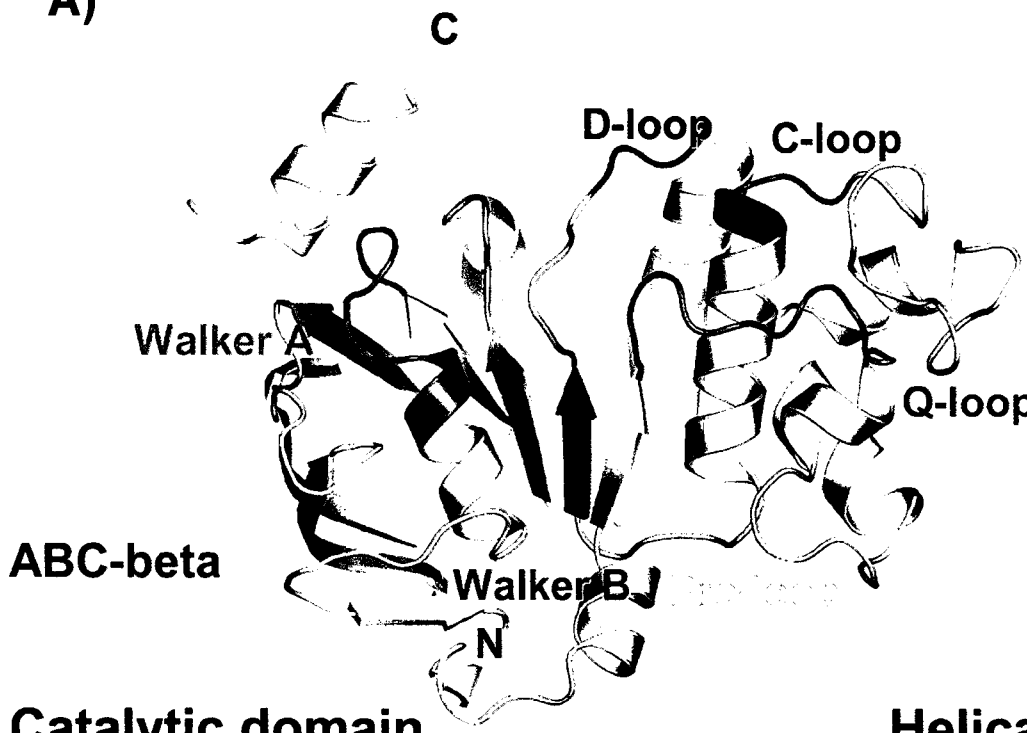
C
D-loop
C-loop
Walker A
Q-loop
ABC-beta
Walker B
N
Catalytic domain
Helical domain

B)

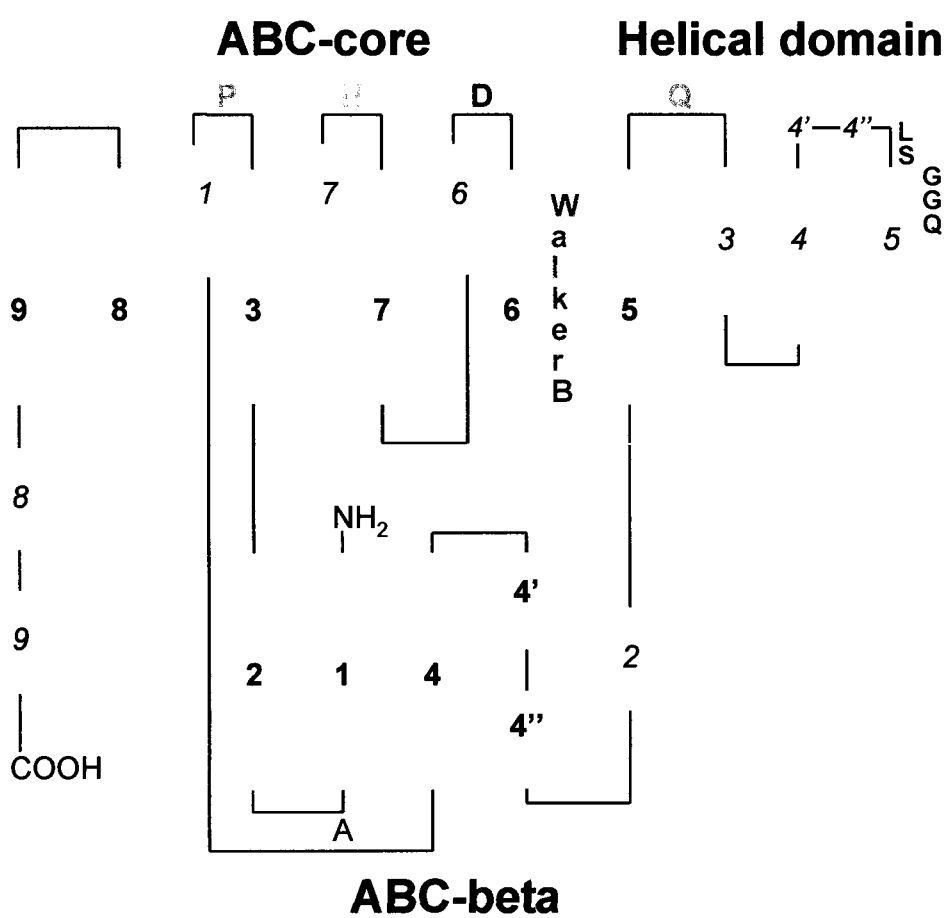
ABC-core
Helical domain
P
D
Q
4'—4"
LSGGQ
1
7
6
3
4
5
Walker B
9
8
3
7
6
5
8
NH2
4'
9
2
1
4
2
4"
COOH
A
ABC-beta

and dark yellow in figure 1.6 B). This subdomain contains the Walker A and B consensus motifs. The antiparallel β sheet, which functions in binding the ribose and adenine (A-loop) moieties of the bound nucleotide, is designated the ABCβ subdomain (in grey in figure 1.6 B). The ABCβ subdomain β sheet is characteristic of ABC-ATPases and is arranged approximately at right angles to the ABC-core subdomain β sheet, with helix 1 situated in the angle thus formed held in place by extensive hydrophobic contacts. Together, the two β sheets, comprising β-strands 1, 2, 3, 4, 6, 7, 8, and 9, and P-loop (Walker A) helix 1 form a structurally rigid core which has a root mean square deviation between the ABC transporter NBD structures of <1.3Å (Jones and George, 2004). The ABC-core subdomain and the ABCβ subdomain thus form lobe I of the ABC-ATPases. The ABC transporter NBD also contains a third subdomain with a structurally conserved core comprising a bundle of three α-helices, variously known as lobe II, the helical or signalling domain (Ames *et al.*, 1992), the ABCα subdomain or α-subdomain (Karpowich *et al.*, 2001) (in beige in figure 1.6 B). The helical domain is an insertion of ~70 residues between the β5 and β6 strands of the ABC-core subdomain. The N-terminal halves of helix 3 and helix 5 within the helical subdomain are composed of residues which are, for the most part, highly conserved amongst ABC transporters. The Q-loop is part of the protein sequence which links the ABC-core subdomain and the N-terminal end of the helical domain and acts as a hinge for movement of the helical domain with respect to the catalytic domain. The LSGGQ signature sequence forms the N-terminus of helix 5 within the bundle, with the serine side chain capping the helix. Helix 4 and the two loops at its N- and C-termini, which join the two conserved regions in the helical subdomain, are highly variable in sequence, length, and structure and the loop regions are the sites of transporter-specific insertions (Jones and George, 2002). In general, the region of the helical domain sandwiched between the Q-loop and the signature motif (30-40 residues) shows considerable variation between different NBDs and this has given rise to the term structurally diverse region (SDR) sometimes used to describe this region (Schmitt *et al.*, 2003). As this region interacts with the transmembrane part of ABC-transporters, the SDR may explain the selectivity and/or targeting of different NBDs to their cognate transmembrane domains. Finally, the Pro-loop is the sequence which links the C-terminal

end of the helical domain to the ABC-core subdomain and acts as the other hinge that allows movement of the helical domain with respect to the catalytic domain.

1.4.2.2 The NBDs as a dimer

One of the most significant questions answered by the structural studies on ABC transporters concerns the role of the ABC signature sequence and the mode of interaction of the two NBDs. The crystal structures of isolated NBDs have revealed a conserved fold, and it has become clear that the head-to-tail arrangement of the NBDs in the functional ABC transporter (i.e. full-length or complete) is also conserved. A key element of this arrangement is that the two NBDs present their conserved sequence motifs at the shared interface (Hopfner *et al.*, 2000; Smith *et al.*, 2002; Chen *et al.*, 2003; Dawson and Locher, 2006; Dawson and Locher, 2007). As a consequence, two ATP-binding sites are formed between the Walker A/P-loop and Walker B of one NBD and the signature motif and D-loop of the other and *vice versa* (Figure 1.7). In the ATP-bound state of isolated NBDs or complete transporters (usually containing a mutation that prevents ATP hydrolysis), two ATP molecules (or non-hydrolysable analogues) are sandwiched at the NBD-NBD interface. This arrangement is consistent with earlier predictions based on sequence analysis (Jones and George, 1999) and with a number of biochemical studies (Hrycyna *et al.*, 1998; Chen *et al.*, 2001; Mannering *et al.*, 2001; Vergani *et al.*, 2005). Binding of ATP by the Walker A mediates NBD-NBD interactions by altering the surface of the monomer, and this is achieved in two ways. First, ATP is sandwiched between the monomers in the NBD dimer and forms a significant part of the dimer interface (Figure 1.7), acting as the "glue" between the monomers, with NBD residues making direct contacts with the bound nucleotide rather than with residues from the opposite monomer (although some direct contacts are made). Second, comparative analysis of ABC NBDs suggests that ATP binding, and in particular the γ–phosphate, produces an induced-fit effect, altering the conformation of the D-, H-, P-, and Q-loops in the vicinity of the γ-phosphate, thereby altering or ordering the surface of the monomer (Karpowich *et al.*, 2001). As shown in the Rad50cd and MJ0796-E171Q dimer structures (Hopfner *et al.*, 2000; Smith *et al.*, 2002), the D-, H-, and P-loops form part of the NBD-NBD interface and share the binding of the γ-phosphate with the signature region of the opposite

Figure 1.7:

NBD dimer with nucleotide sandwiched at the interface

(A) The NBD dimer viewed from the membrane with two ATP molecules sandwiched at the dimer interface. The ATP binding pockets are composite sites comprised of the ABC-core subdomain of one NBD (orange and blue) and the helical subdomain of the other NBD (gold and turquoise). (B) The orange-gold NBD viewed from the blue-turquoise NBD. The elementally coloured ATP is cradled by the Walker A and B motifs, as well as the H-loop, A-loop, and Q-loop of the ABC-core subdomain. The Q-loop extends from the top surface of the NBD, where it will be in close proximity to the intracellular loops of the TMDs, making it a prime candidate for energy and signal transduction within the complex. The helical subdomain contains the signature motif, which contacts the dark-gray coloured ATP. The D-loop contains residues which hydrogen-bond with the blue-turquoise NBD. The NBDs shown are from ABCB1 (Stenham *et al.*, 2003) modelled on the dimer arrangement from MJ0796 (Smith *et al.*, 2002). Figure modified and reproduced by permission from (Linton, 2007).

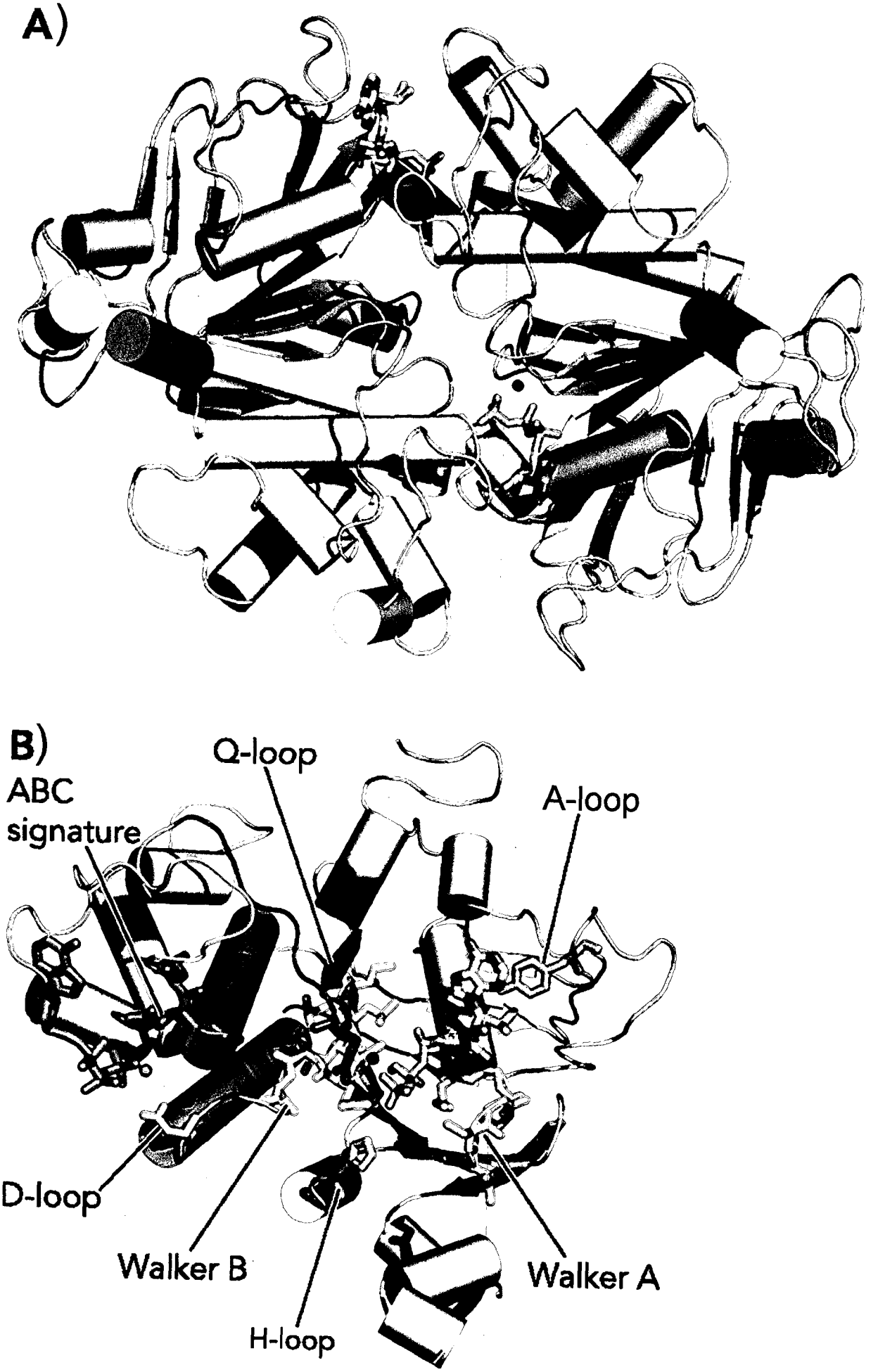
A)
B)
ABC
signature
Q-loop
A-loop
D-loop
Walker B
H-loop
Walker A

monomer, suggesting the induced-fit effect produced by nucleotide binding is also likely to be important for NBD dimer formation.

The structures of isolated NBDs trapped in the ATP-bound state reveal close superposition with each other, indicating strict geometric constraints. By contrast, the nucleotide-free states of full transporters or dimeric NBDs (Chen *et al.*, 2003; Oloo *et al.*, 2006) exhibit surprisingly large differences, suggesting that no strict geometric constraints exist in this state. Most of the isolated NBDs are monomers in the absence of TMDs. Addition of ATP, under non-hydrolysing conditions (or non-hydrolysable ATP analogues such as AMP-PNP), causes these monomeric NBDs to dimerize. The situation is different in some of the isolated NBDs and complete transporters, where the crystal structures reveal continued contact between the NBDs, mediated mostly by their C-termini, whether nucleotide is present or not. A nomenclature of 'open' and 'closed' NBD dimer conformations has been introduced to describe the nucleotide-free and the ATP-bound states (Higgins and Linton, 2004).

Thus, in the absence of nucleotide, the interface between the NBDs is open. Upon binding of ATP, closure of the dimer interface is induced through both rotation of the helical domain and closure of the entire cassette interface (Chen *et al.*, 2003). Close examination of this mobile interface reveals that most of the contacts in the closed conformation are between protein and nucleotide rather than protein and protein, indicating that ATP binding must precede stable closure of the domains. Notably, binding of MgADP fails to trigger closure of the dimer interface (Moody *et al.*, 2002; Lu *et al.*, 2005; Zaitseva *et al.*, 2005c), suggesting a cycle in which ATP binding triggers closure and, following ATP hydrolysis, the dimer interface opens because the contacts between ADP and protein are insufficient to stabilize the closed state (Chen *et al.*, 2003; Zaitseva *et al.*, 2006).

As will be discussed later, the head-to-tail arrangement rationalizes the cooperativity in ATP hydrolysis that was observed in the maltose transporters and in human ABCB1 (Davidson *et al.*, 1996; Senior and Bhagat, 1998).

1.4.3 ATP hydrolysis

Actual binding of ATP to ABC transporter NBDs was demonstrated in experiments where membrane vesicles or membrane-enriched fractions from cells over-expressing endogenous human ABCB1 or transfected with *ABCB1* cDNAs were able to bind the photo-activatable ATP analogue 8-azido-[α^{32}P]ATP in a specific and concentration-dependent manner (Cornwell *et al.*, 1987; Schurr *et al.*, 1989). The NBDs of Pgh1 (*Plasmodium falciparum* ABCB1 homologue) and KpsT (the NBD subunit of the KpsMT system involved in the export of capsular polysaccharide in *E. coli*) were also demonstrated to bind nucleotide in similar experiments using 8-azido-[^{32}P]ATP (Karcz *et al.*, 1993; Pavelka *et al.*, 1994).

Purification of membrane-enriched fractions or ABC proteins permitted formal demonstration of the ATPase activity of the ABC enzymes. Thus, purified plasma membranes from Chinese hamster ovary (CHO) cells enriched for Abcb1 showed significant ATPase activity (al-Shawi and Senior, 1993). The level of activity was increased when Abcb1 was purified from these membranes and reconstituted into a lipid environment (Shapiro and Ling, 1994; Urbatsch *et al.*, 1994). Over-expression of hABCB1 in the membrane of mammalian cells (HEK293) and other eukaryotic heterologous expression systems have also been used (Loo and Clarke, 1995c). For example, crude membranes from baculovirus-infected *Spodoptera frugiperda* ovary (Sf9) cells showed high levels of ATP hydrolysis activity when the infecting recombinant virus carried the *ABCB1* gene (Rao, 1995). Similarly, membranes and purified protein from the methylotrophic yeast *Pichia pastoris* over-expressing mouse Abcb1a show ATPase activity (Beaudet *et al.*, 1998a; Urbatsch *et al.*, 1998).

In most ABC-transporters, direct proof has been obtained that both catalytic sites hydrolyse ATP; although some transporters seem to have altered the activity of one of their NBDs to suit their needs (e.g. ABCB2/TAP1, ABCC1/MRP1, and ABCC7/CFTR). ATP hydrolysis in ABC transporters is often stimulated by allocrite binding and different compounds inhibit ATPase activity. In addition, full cooperativity has been observed between the NBDs for ATP hydrolysis.

Now that a general picture of ABC transporters has been painted, the following subsections will focus on the orthologous human and rodent ABC transporters ABCB1

and Abcb1a (mouse) or Abcb1 (hamster), generally known as P-glycoprotein (P-gp). P-gp is one of the most intensively studied members of the ABC superfamily. Human P-glycoprotein (P-gp, MDR1, or ABCB1) is a 170-180 kDa protein that was first discovered in the plasma membrane of mammalian cells that had been selected for resistance to drugs (Gottesman and Ling, 2006). Mouse P-gp (Mdr3, Mdr1a, or Abcb1a) and hamster P-gp (Abcb1) are the orthologues of human P-gp (PGY1 or ABCB1). The rodent proteins share 93% sequence identity at the amino acid level, and both share 87% identity with human P-gp. Hence, these transporters have been studied "interchangeably" and conclusions obtained with one are assumed to apply to the others. The following subsections will therefore focus mainly on these proteins, referred to collectively as P-gp.

1.4.3.1 Functional characterization

Evidence indicating that P-gp actually binds nucleotide was obtained from experiments in which the enzyme was labelled with a photo-activatable analogue of ATP: 8-azido[α^{32}P]ATP (Cornwell *et al.*, 1987; Schurr *et al.*, 1989). Tryptic mapping of the ATP-photoaffinity labelled protein indicated that ATP crosslinking was site-specific and limited to two discrete peptide fragments of the protein, suggesting that P-gp is capable of direct and specific ATP binding (Schurr *et al.*, 1989). Mg-8-azidoATP was later found to label P-gp at a stoichiometry of 2 moles of nucleotide per mole of protein, with the label equally distributed between both halves of the protein, suggesting that both NBSs, identified in the protein sequence deduced from the cDNA, could bind nucleotide (al-Shawi *et al.*, 1994). Labelling was specifically inhibited by MgATP, indicating that the NBSs can bind MgATP and Mg-8-azidoATP. Fluorescent derivatives of nucleotides, such as 2',3'-(2,4,6-trinitrophenyl) (TNP)-ATP and TNP-ADP can also bind both NBSs with high affinity and have been used in fluorescence spectroscopy studies to examine nucleotide binding properties (Lerner-Marmarosh *et al.*, 1999) as well as the stoichiometry of binding and the architecture of the NBSs (Liu and Sharom, 1997). Together, these studies indicate that a single molecule of P-gp is able to bind two ATP molecules and that binding occurs at each NBS within the two NBDs in a non-cooperative manner. Moreover, ATP-binding affinity appears to be equal for both NBSs (Baubichon-Cortay *et al.*, 1994; Dayan *et al.*, 1996; Lerner-Marmarosh *et al.*, 1999).

The demonstration that P-gp possesses ATPase activity was first done on immunoaffinity chromatography-purified P-gp (Hamada and Tsuruo, 1988). The hydrolysis of ATP was established by the formation of ADP from [α^{32}P]ATP, but the specific activity was very low and did not show stimulation by chemicals involved with MDR. Subsequent assays carried out with membrane-enriched or purified P-gp determined catalytic characteristics of this enzyme. Thus, it was demonstrated that ATPase activity follows Michaelis-Menten kinetics (Sarkadi *et al.*, 1992). In addition, ATPase activity was shown to be optimal at 37°C and pH 7.4, with MgATP as the preferred substrate, CaATP being poorly hydrolyzed, and MgADP and MgAMP not hydrolysed (al-Shawi and Senior, 1993).

P-gp has a relatively high "baseline" level of ATPase activity that varies depending on the preparation and cells of origin, with reported V_{max} values ranging from 0.1 to 2 μmol min^{-1} mg^{-1} of protein, and a K_M for ATP between 0.3 and 1.4 mM (Ambudkar *et al.*, 1992; Gottesman and Pastan, 1993; Beaudet *et al.*, 1998a). The ATPase activity of P-gp can be influenced by the lipid environment, which explains why different preparations can yield different activities (Urbatsch and Senior, 1995). A unique property of the "baseline" ATPase activity is that it can be significantly activated beyond basal levels in the presence of certain MDR drugs, such as vinblastine, verapamil, colchicine, rhodamine 123, paclitaxel, and dibromobimane, to name a few (Scarborough, 1995; Senior *et al.*, 1995a). Compounds which interact with P-gp have been divided into three classes based on their effects on ATPase activity (Ambudkar *et al.*, 1999). Class I agents stimulate ATPase activity at low concentrations but inhibit at high concentrations (e.g. verapamil, vinblastine, and paclitaxel). Class II agents enhance ATPase activity in a dose-dependent manner without inhibition (e.g. valinomycin, bisantrene, and tetraphenylphosphonium ion). Class III agents inhibit both basal and verapamil-stimulated ATPase activity (cyclosporine A, gramicidin D, and rapamycin). Furthermore, compounds which modulate ATPase activity can be subdivided into transported (allocrites) vs non-transported (modulators) drugs. Upon purification and reconstitution in the presence of lipids and DTT, P-gp shows maximal drug-stimulated ATPase activities ranging from 5-22 μmol min^{-1} mg^{-1} of protein while the K_M for ATP remains unchanged.

Assuming that ABC-ATPases are only activated when specific allocrites or modulators bind, purified NBDs separated from the transport complex would be expected to be inactive *in vitro*. However, this is clearly not the case, with many examples of "constitutive" ATPase activity of the isolated NBD being reported. Thus, several ABC-ATPases have been over-expressed and purified in active form. Examples include HisP (Nikaido, 1997) and MalK (Morbach *et al.*, 1993), as well as NBDs expressed separately from their normally fused TMD, e.g.: from mouse Abcb1a (Dayan *et al.*, 1996) or ABCC7 (CFTR) (in this case as a MalE-fusion, Ko and Pedersen, 1998). Reported ATPase activities vary widely and have high K_M values (low mM range), reflecting the relatively low affinity of this type of ATPase for ATP. These values for the isolated ATPase domain should be treated with caution, however, since they may reflect low specific activity preparations, or completely misleading values in the absence of membrane, other essential protein domains, and allocrites.

The paradox of constitutive activity in the absence of allocrite, in some cases at least, such as with HisP and MalK, might be explained by findings that assembly into a membrane complex with partner permease components in some way restrains or shuts down ATPase activity until the corresponding allocrite is added (Bishop *et al.*, 1989; Davidson and Nikaido, 1990; Liu and Ames, 1997; Liu, 1998). In other cases, such as with P-gp, where the intact molecule including the TMD has been purified and reconstituted into liposomes and still shown to have activity in the absence of drug molecules (the allocrites), the presence of a significant level of constitutive activity remains a mystery (Shapiro and Ling, 1994). One explanation is that the activity occurs due to interactions with endogenous lipids or chemicals.

The high K_M(ATP) reported for P-gp (0.3-1.4mM) indicates that the catalytic sites have low affinity for ATP as compared to other translocating ATPases such as F_1F_0-ATP synthase and vacuolar ATPase, which have K_M's in the μM range. The specificity of the NBS is also low, as ITP, GTP and CTP can substitute for ATP, albeit at reduced rates of hydrolysis (Senior *et al.*, 1995a). Hydrolysis of nucleotide is dependent on the presence of Mg^{2+}, but other divalent metal cations such as Co^{2+} or Mn^{2+} can substitute with a lower affinity (Doige and Sharom, 1992; Urbatsch *et al.*, 1995b). Competitive inhibition can be achieved by MgADP and non-hydrolysable ATP analogues such as MgAMP-PNP and

MgATPγS (Senior *et al.*, 1995a). Thus, the physiological substrate of P-gp appears to be MgATP, but because other nucleotides and divalent metal cations can be substituted, the catalytic sites appear to have low specificity for substrate.

As for most ABC-ATPases, the ATPase activity of P-gp can be inhibited by a number of compounds, and their use has proven very informative. P-gp ATPase activity was inactivated potently by 4-chloro-7-nitrobenzo-2-oxa-1,3-diazole (NBD-Cl) (al-Shawi and Senior, 1993). Inactivation of ATPase activity correlated linearly with covalent labelling, with 100% inactivation occurring at a stoichiometry of 1.1 mol NBD-Cl per mole of P-gp, and the characteristics of inactivation suggested that there was a single reactive lysine residue located within one of the NBDs of P-gp. Other inactivating compounds are sulfhydryl- (or thiol-) specific alkylating agents, which include *N*-ethylmaleimide (NEM) and 2-(4-maleimido anilino)naphthalene-6-sulfonic acid (MIANS). These thiol-specific reagents also inactivate the ATPase activity of P-gp by covalently attaching to the protein. As shown by labelling with radioactive NEM, this occurs at two sites: one in the N-terminal half and the other in the C-terminal half (al-Shawi *et al.*, 1994). Since MgATP protected against inhibition by these reagents, this suggested that the sites of reactivity and inhibition were cysteine residues located within the two NBSs. The use of single-cysteine mutants in the cysteine-less P-gp (Loo and Clarke, 1995b, ABCB1 has 7 endogenous cysteines) demonstrated that the two critical cysteine residues sensitive to inhibition by NEM, were those of the Walker A motif of the NBDs (Loo and Clarke, 1995a).

Orthovanadate (Vi), a structural analogue of inorganic phosphate (Pi), is a potent inhibitor of ATPases such as myosin ATPase, adenylate kinase, and the P-type ATPases of which F_1-ATPase is a member. Vi can also inhibit the basal and allocrite-stimulated ATPase activity of ABC-ATPases. Thus, it was shown that pre-incubation of P-gp (either in enriched membranes or purified and reconstituted) with Vi and MgATP or MgADP leads to inactivation of ATP hydrolysis (Urbatsch *et al.*, 1995b). The mechanism of inactivation by Vi is described as follows. Hydrolysis at either of the catalytic sites yields MgADP and Pi. When Pi is released out of the active site, Vi enters and non-covalently binds with significantly higher affinity than Pi, effectively trapping MgADP in the catalytic site. Trapping is dependent on the presence of divalent cations such as Mg^{2+},

Mn^{2+}, and Co^{2+}, and the stoichiometry of trapping is equivalent to 1 mole of nucleotide trapped per mole of enzyme. Incubation with Vi and either MgATP or MgADP yields only trapped MgADP, indicating that at least one turnover of the catalytic cycle has occurred. The Vi-trapped P-gp/MgADP complex is proposed to mimic the physiological transition state in which MgADP and Pi are bound to the enzyme before being released (i.e. a post-hydrolysis state Goodno, 1982). Two other Pi analogues, aluminium fluoride (AlF_4^-) and beryllium fluoride (BeF_x) can also trap nucleoside diphosphates (i.e. MgADP) in the catalytic site, and inhibit ATPase activity of the enzyme (Sankaran *et al.*, 1997b; Sankaran *et al.*, 1997a). As with Vi, the stoichiometry of trapping for these two Pi structural analogues is equivalent to 1 mole of nucleotide trapped per mole of enzyme. A feature of the Vi-induced catalytic transition state is that extended UV irradiation can cause photochemical cleavage of the peptide bond in the vicinity of the Vi (Hrycyna *et al.*, 1998). Additionally, trapping of radio-labelled Mg-8-azido-nucleotide using any of the Pi analogues, followed by UV crosslinking, results in covalent labelling of the enzyme with the radio-labelled nucleotide through the azido group. In such experiments, the enzyme becomes permanently inactivated and labelling occurs in both catalytic sites, further indication that both sites can hydrolyse ATP. The technique of nucleotide trapping has proven extremely useful in the study of the catalytic mechanism of ABC transporters.

1.4.3.2 Cooperativity of the NBDs

Many studies have shown that the two NBDs of ABC transporters function cooperatively. For example, expression of each half of P-gp separately showed that either half could hydrolyse ATP but the individual activities were not stimulated by allocrites (Loo and Clarke, 1994). On the other hand, when both half-molecules were co-expressed, the ATPase activity could now be stimulated by allocrites, suggesting that coupling of ATPase activity to drug binding requires interaction between both halves of P-gp.

The fact that inactivation of only one catalytic site at a time completely abolishes all ATPase activity was another observation that pointed to this cooperativity. Inactivation of a single catalytic site can be achieved in several ways. One way is to use single cysteine mutants in the Walker A motif of either of the two NBDs. Reaction with thiol-specific reagents blocks the NBS by preventing ATP binding at that site. Inactivation of any one of the NBSs with NEM completely blocked ATP hydrolysis by

the enzyme (Loo and Clarke, 1995a). Similar studies with NBD-Cl (which covalently labels a lysine residue in one NBS) arrived at the same results (al-Shawi and Senior, 1993). The observed stoichiometry of 1 mol inhibitor per mol P-gp for full inhibition by NEM or NBD-Cl suggested that inactivation occurred at one site and this inactive site interacted with the other intact site to prevent ATP hydrolysis. Similarly, using Vi-trapping experiments, Senior and colleagues demonstrated that trapping of nucleotide in only one NBS is sufficient to completely inhibit ATPase activity of P-gp (Urbatsch *et al.*, 1995b). Another way is the use of site-directed mutagenesis. Point mutations of key residues in the Walker A or B motifs in each NBD separately have shown that inactivation of one NBD abolishes drug resistance and ATPase activity (Azzaria *et al.*, 1989; Muller *et al.*, 1996; Urbatsch *et al.*, 1998). Mutation of a single NBD which affects activity of the other NBD strongly suggests that both domains are essential for the function of P-gp and that there is strong cooperativity between the two domains.

The fact that ATP hydrolysis by ABC transporters is highly cooperative lead to the suggestion that the two NBDs function as a dimer in the translocation process (Davidson *et al.*, 1996; Liu *et al.*, 1997). The basis for this cooperativity has now been determined by high-resolution crystal structures in which the NBDs are shown to dimerize in the ATP-bound state (Hopfner *et al.*, 2000; Smith *et al.*, 2002; Dawson and Locher, 2006). In these structures, the two NBSs are composed of residues contributed by both NBDs, high-lighting a possible means of communication between the two domains.

Unfortunately, the manner in which the cooperativity of the NBDs affects ATP hydrolysis by either NBS during the catalytic cycle remains largely unclear.

1.4.3.3 Catalytic cycle

In order to mediate the active translocation of allocrites across cellular membranes, ABC transporters must couple conformational changes in the NBDs to conformational changes in the TMDs, powered by the free energy released from the catalysis of ATP in the former. Just how the energy of ATP hydrolysis is coupled to allocrite transport is still unclear, although the crystal structures of complete transporters are starting to shed light on this issue (see Chapter 6). The number of ATP molecules required for the transport of one allocrite molecule across the membrane is still

disputable. In addition, we are only beginning to understand the catalytic mechanism for ATP hydrolysis by the NBDs.

ABC transporters catalyze the translocation of substrates at the expense of hydrolysis of ATP, but the actual ATP to allocrite stoichiometry is still controversial. Various reports have estimated the number of ATP molecules required per allocrite molecule transported to be between 1 and 5, although values up to 50 have been observed (e.g. Muir *et al.*, 1985; Davidson and Nikaido, 1990; Eytan *et al.*, 1996; Ambudkar *et al.*, 1997). The large variations observed are most likely the result of differences in experimental setup, and/or the need to correct for uncoupled ATP hydrolysis or substrate leak pathways. Because ATP hydrolysis in the OpuA system from *Lactococcus lactis* is tightly coupled to the osmotic signal and the presence of allocrite, this system affords optimal conditions for the determination of ATP to allocrite stoichiometries. Using proteoliposomes in which OpuA has been functionally reconstituted Poolman and colleagues accomplished stoichiometry measurements using two independent assays and elegantly demonstrated that two molecules of ATP are required to translocate one molecule of glycine betaine (Patzlaff *et al.*, 2003). Given the similarity in architecture between different members of the ABC superfamily, it is likely that a universal mechanistic stoichiometry is applicable to all members.

As mentioned earlier, direct proof has been obtained that both catalytic sites in P-gp bind and hydrolyse ATP and that hydrolysis occurs in a cooperative manner. Additional experiments using Vi-trapping of nucleotide and UV irradiation demonstrated that ATP hydrolysis only occurs at one site at once, never simultaneously at both sites (Senior *et al.*, 1995b; Hrycyna *et al.*, 1998). These observations led Senior and colleagues to propose a model of ATP hydrolysis that alternates equally between the two NBDs, with equal probability of hydrolysis at NBD1 and NBD2, implying that ATP bound at one NBS prevents hydrolysis at the second site (Senior *et al.*, 1995b). It is now accepted that the NBDs of ABC transporters dimerize upon binding of ATP (see Section 1.4.2.2). Consequently, it has been proposed that the NBD dimer conformation represents an intermediate in the catalytic cycle. Senior and colleagues investigated this dimerized intermediate using Abcb1a mutants known to form nucleotide-occluded dimers (Tombline *et al.*, 2004b; Tombline *et al.*, 2005). Incorporating these results into their

original model, they suggest a new model depicting a mechanism in which (1) loose binding of MgATP at two NBSs triggers formation of the closed, dimeric NBD conformation with one ATP bound more tightly than the other, committing it to hydrolysis. (2) The transition state occurs at the site of this tightly bound nucleotide, and ADP and Pi are formed. (3) Pi and ADP are released from this site as the dimer opens, which allows new ATP to bind; if the non-hydrolysed ATP that is present in the original dimer is retained after release of product ADP, then hydrolysis in alternating sites will still be operative. In this model it is assumed that the dimer re-opens transiently between each hydrolysis to release newly formed ADP and Pi. However, this has not been formally demonstrated. Thus, the dimer may also re-open only following hydrolysis of both molecules of ATP bound at the dimer interface and the implications for the catalytic mechanism will be presented in the discussion of this thesis (Chapter 6).

Despite major advances in the understanding of ABC proteins, the exact mechanism of ATP hydrolysis by the NBDs remains an enigma. Particularly, the exact function of conserved amino acid residues in the vicinity of the NBS, the reaction path of ATP hydrolysis, and the molecular communication between NBD monomers during ATP binding and hydrolysis are poorly understood. Within different nucleoside triphosphate-hydrolysing enzymes, the question as to whether a general base residue is essential to the catalytic mechanism of hydrolysis has been a matter of considerable debate. Yoshida and colleagues have proposed the presence of a catalytic carboxylate in ABC transporters (Yoshida and Amano, 1995). Studies with some ABC transporters, such as BmrA, have suggested that this is indeed the case (Orelle *et al.*, 2003). In contrast, ATP hydrolysis by ABC transporters has more recently been suggested to occur via a mechanism involving substrate-assisted catalysis (SAC) (Zaitseva *et al.*, 2005a). As presented in Chapter 3 of this thesis, an attempt at identifying the catalytic residue of P-gp has been made.

Section 1.5 – Interaction Interfaces

Because ABC transporters are integral membrane proteins, they can be subdivided into two domains: the membrane-associated domain (made-up of the transmembrane domains: TMDs) and the cytosolic domain (made-up of the nucleotide binding domains:

NBDs). Thus, three kinds of interactions are possible in this multi-domain arrangement: TMD-TMD, NBD-NBD, and TMD-NBD.

The TMD-TMD interaction has already been discussed in section 1.3.1 as it defines the allocrite binding site and transport channel. Similarly, the NBD-NBD interaction has already been discussed in section 1.4.2 as it is important in dimer formation and cooperativity of the NBDs. The TMD-NBD interface is extremely important for function, since it is the interface which connects the "engine" to the "channel". Thus, when the TMDs bind its allocrite or the allocrite-bound PBP, a signal is conveyed to the NBDs to activate ATP catalysis. Conversely, the conformational changes associated with ATP catalysis at the NBDs are then transmitted to the TMDs via this interface to effect allocrite transport and release. Additionally, targeting of NBDs to their cognate TMDs (in multi-domain transporters, at least) and proper folding of complete transporters is controlled by the interaction between these two domains.

1.5.1 Transmission interface: coupling the engine to the gates

Communication between the TMDs and NBDs appears to be bidirectional: allocrite binding enhances the catalytic activity of the NBDs and ATP catalysis at the NBDs powers transport of allocrites.

X-ray crystal analyses reveal that the orientation of the TMDs with respect to the NBD dimer, and the regions of the NBDs which form the oligomeric interfaces, are analogous in all ABC proteins (Jones and George, 2004). This indicates that not only the engines but also the transmission is architecturally conserved in ABC transporters (Hollenstein *et al.*, 2007a). To highlight its relevance in coupling mechanistically important conformational changes, the TMD-NBD contact surface is referred to as the "transmission interface". In the structures available so far (Locher *et al.*, 2002; Dawson and Locher, 2006; Dawson and Locher, 2007; Hollenstein *et al.*, 2007b; Hvorup *et al.*, 2007; Oldham *et al.*, 2007; Pinkett *et al.*, 2007; Ward *et al.*, 2007), each TMD is attached to an NBD through an ICL that emanates from two TM helices. This ICL is present in BtuCD between TM 6 and 7 (ICL 3), in Sav1866 between TM 4 and 5 (ICL2), in HI1471 between TM 6 and 7 (ICL3), in ModBC between TM 4 and 5 (ICL2), in MalG between TM 4 and 5 (ICL2), in MalF between TM 6 and 7 (ICL3, homologous to ICL2 of MalG),

and in MsbA between TM 4 and 5 (ICL2). This ICL usually contains two short α-helices, of which one makes direct and intensive contacts with the NBD and is referred to alternately as the L-loop, the EAA-loop, or the coupling helix. The coupling helix is grasped in a cleft lined by residues of the Q-loop on the surface of the NBD, at the boundary between the catalytic and the helical subdomains (Figure 1.8) (Hollenstein *et al.*, 2007a). Strikingly, the TMDs of these transporters, despite their vastly different topologies and architectures, all feature this coupling helix that provides the bulk of the contacts to the NBDs. Although the coupling helices share little or no sequence similarity when aligned, superimposing the NBDs results in a striking superposition of the coupling helices as well. Thus, it is assumed that conformational changes in the NBDs are transmitted to the TMDs, and *vice versa*, via non-covalent interactions at this interface (Dawson *et al.*, 2007). In-detail analysis of individual high-resolution structures, in particular the exporters, has identified other sites of interaction between TMDs and NBDs which also appear to be part of the transmission interface. For example, in Sav1866, ICL1 (between TM2 and 3) interacts with residues from both NBDs, including a glutamate from the NBD of the same subunit and a tyrosine residue downstream of the Walker A motif of the NBD of the opposite subunit. The glutamate, which also contacts the coupling helix (ICL2) of the opposite subunit, is part of a novel conserved sequence motif immediately upstream of the signature motif of the NBD. This new motif has been designated the x-loop to highlight its apparent function in cross-linking the ICLs (Dawson and Locher, 2006). The x-loop is a short sequence motif that appears conserved in ABC export proteins only and was shown previously to be important in TMD-NBD communication (Beaudet and Gros, 1995). In MsbA the first ICL (ICL1, between TM2 and TM3) contains a short helix which inserts down into a groove above the Walker A motif and makes contact with the A-loop and the nucleotide of the NBD of the same subunit.

Despite the similarity in the location of the coupling helices, there is an important difference between ABC importers and exporters. In the exporters Sav1866 and MsbA, the coupling helices are domain swapped, that is, the coupling helix from subunit A interacts with the NBD of subunit B and *vice versa*. By contrast, the importers ModBC, BtuCD, HI1470/71, and $MalFGK_2$ have no swapping, which results in a large gap at the

Figure 1.8:

Arrangement of the transmission interface between the TMDs and NBDs in the functional ABC transporter

The NBDs of the multidrug ABC transporter Sav1866, crystallized with bound AMP-PNP, are shown in a view from the side (A) or from the membrane (showing the surface facing the TMDs, B). The two NBDs are in green and yellow, with mechanistically important sequence motifs coloured and labelled with single letters: P (P-loop/Walker A), B (Walker B), Q (Q-loop), C (signature motif). Bound AMP-PNP is shown as black sticks. Note that two AMP-PNP molecules are sandwiched between the P-loop of one NBD and the signature motif of the other, and *vice versa* (head-to-tail arrangement). The short, black helices are the coupling helices from the TMDs, with arrows indicating the direction of the polypeptide chain from the N-terminus to the C-terminus. In Sav1866, the coupling helices are domain swapped. Figure reproduced with permission from (Hollenstein *et al.*, 2007a).

A)

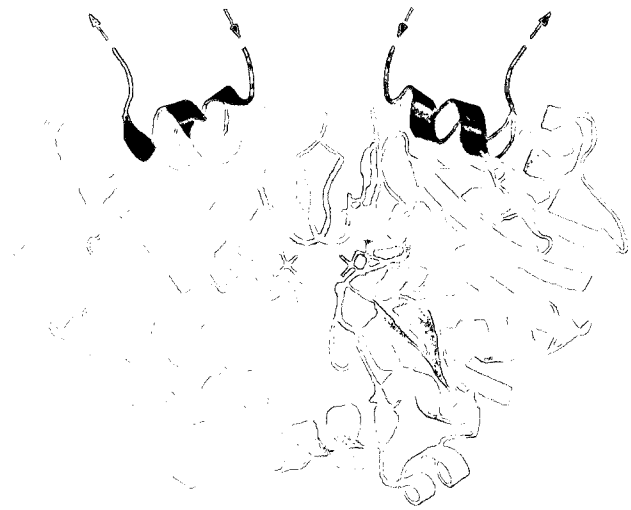

B)

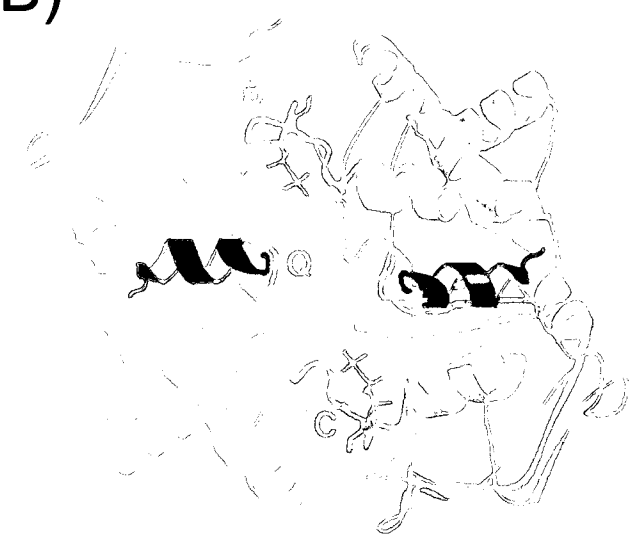

center of the assembled transporter, with no direct contact between diagonally positioned TMD-NBD pairs (Figure 1.9).

Mutations in the helical domain can cause uncoupling or misassembly of ABC transporters. There are well-documented cases for each defect: 1) the mutation R659Q (located in the NBD, between the signature and Walker B motifs) in ABCB2 of the human antigenic peptide transporter ABCB2/3 yields a fully assembled transporter that binds antigenic peptides and hydrolyses ATP, but is unable to transport the substrates, suggesting that the conformational changes induced by ATP hydrolysis are not properly transmitted to the TMDs (Chen *et al.*, 1996), and 2) in human ABCC7/CFTR, deletion of F508 (located in the NBD, downstream of the Q-loop) is responsible for 70% of cystic fibrosis cases. Here, the problem appears to be the inability of the mutant protein to fold efficiently, with only ~1% of the generated proteins reaching the plasma membrane (Tsui, 1992). Similarly, mutations in the coupling helix can cause uncoupling of ABC transporters: missense mutations introduced in the ICL corresponding to the coupling helix of Pxa1p, a *Saccharomyces cerevisiae* orthologue of ABCD1 (ALDP), demonstrated that this loop is important for Pxa1p function as measured in transport assays (Shani *et al.*, 1996). Interestingly, missense mutations in corresponding amino acids in ABCD1 cause adrenoleukodystrophy in humans (review Section 1.2).

The nature of the conformational changes involved in the bidirectional transmission of signals between the TMDs and the NBDs remain speculative; although it seems likely that the coupling helices of the TMDs and the Q-loops of the NBDs are involved. A model for the transport based on the structural data available to date is presented in the Discussion of this thesis (Chapter 6).

1.5.2 Recognition interface

Recently, a "structurally diverse region" (SDR) within the helical domain has been described for certain ABC transporters and appears to represent a specificity region that controls targeting of NBDs to their cognate TMDs (Schmitt *et al.*, 2003). In support of this, earlier studies of MalK-HisP chimeras indicated clearly that allocrite identity is conferred by specific recognition of the TMD by the NBD. This chimera, which was composed of the catalytic domain of HisP and the signalling domain of MalK, energized

Figure 1.9:

Ribbon representation of some of the available crystal structures of the complete ABC transporters

The source organism, transporter name, and putative function are indicated below each transporter. The gray box or black lines depicts the position of the membrane. ModA is the cognate molybdate/tungstate binding protein of ModBC, while MBP is the cognate maltose/maltodextrin binding protein of $MalFGK_2$. Figures reproduced with permission from (Hollenstein *et al.*, 2007a; Oldham *et al.*, 2007; Ward *et al.*, 2007).

S. aureus Sav1866
Multidrug exporter

A. fulgidus ModBC-A
MoO_4 / WO_4 importer

E. coli BtuCD
Vitamin B_{12} importer

H. influenzae HI1470/1
Metal-chelate importer

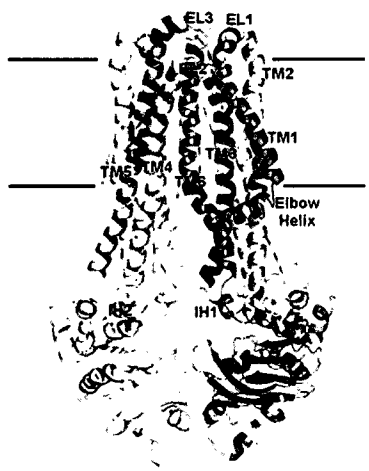

V. cholerae MsbA
Lipid A & LPS exporter

E. coli $MalFGK_2$
Maltose importer

the import of maltose but not of histidine (Schneider and Walter, 1991). Additionally, biochemical and genetic studies of HisP and MalK demonstrated that a sub-region of the helical domain is involved in specific and functional contacts between the TMDs and the NBDs (Mimura *et al.*, 1991; Schmees *et al.*, 1999; Hunke *et al.*, 2000b).

It is worth noting that the SDR is sandwiched between two conserved motifs, the Q-loop and the signature motif, regions that are involved in TMD contact (Locher *et al.*, 2002) and ATP-sensing, respectively (Fetsch and Davidson, 2002; Smith *et al.*, 2002). Such an arrangement is reminiscent of GTPases (Vetter and Wittinghofer, 2001) and Ras-effector proteins (Herrmann, 2003), where a bipartite recognition process has been postulated (Herrmann, 2003), with one part of the enzyme conserved to sense the functional state of the enzyme whilst the other part confers specificity.

Section 1.6 – Expression of Abcb1a in Heterologous Systems

Studies on ABC transporters, including human and rodent P-gp in transfected mammalian cells such as Chinese hamster ovary (CHO) cells or NIH-3T3 fibroblasts have proven informative; however transfection in mammalian cells is not efficient for carrying out biochemical analyses of many mutants simultaneously. The selection procedure is time-consuming and expensive, and does not generate large enough quantities of protein that can be reasonably purified for detailed kinetic measurements and binding studies. Consequently, a number of heterologous systems have been developed for the systematic study of a large number of mutants in a time- and cost-effective manner.

One of the first systems used was the yeast *Saccharomyces cerevisiae*. Human and rodent P-gp can be stably expressed and targeted to the plasma membrane of this yeast. *S. cerevisiae* expressing Abcb1a is able to confer cellular resistance to some antifungal drugs (macrolides FK506 and FK520, Raymond *et al.*, 1994). Abcb1a can also complement yeast that is null at the *Ste6* locus, transporting the ***a***-factor mating peptide pheromone (Raymond *et al.*, 1992). Mutations that affect the function of Abcb1a in mammalian cells have also been shown to affect FK506 resistance and ***a***-factor transport in *S. cerevisiae*. This makes the yeast system amenable to analyzing the effect of various

mutations in a qualitative and quantitative manner. Liquid assays for FK506 resistance as well as *Ste6* complementation (or mating) assays have been developed for monitoring growth of yeast expressing various Abcb1a mutants (Urbatsch *et al.*, 2000c).

More detailed biochemical analyses of ATPase activity of wild-type (WT) and mutant Abcb1a require much larger quantities of purified protein. Recombinant baculovirus-infected Sf9 cells are commonly used as a heterologous eukaryotic expression system. Sf9 cells are able to produce large quantities of ABCB1, totalling approximately 3% of the membrane proteins (Rao, 1995). Purification from these enriched membranes yields enough protein to carry out measurements of drug-stimulated ATPase activities. However, this system is difficult to manage due to possible recombination events of the infected virus with the endogenous genes. Also, this system is not really cost-effective due to the length of time required and the initial costs involved. Another expression system has involved the use of human embryonic kidney cells (HEK293) transiently transfected with the cDNA for the ABC transporter of interest, i.e. *ABCB1*, modified to contain a polyhistidine tag at the carboxyl terminus (Loo and Clarke, 1995c). This allows the protein to be purified by affinity nickel-chelate chromatography. The method is simple and quick, but does not yield great amounts of purified protein, and is difficult to scale-up. Generally, expression and large-scale purification from animal cell systems for detailed analysis of multiple mutants is time consuming and cost inefficient.

A newer method has employed another species of yeast, *Pichia pastoris*, as a heterologous system for large-scale purification of WT and mutant Abcb1a and ABCB1 (Beaudet *et al.*, 1998a; Lerner-Marmarosh *et al.*, 1999). *P. pastoris* is a methylotrophic yeast that is able to use methanol as its sole source of carbon. Under conditions where the cells are starved for glucose, the yeast switches to the methanol utilization pathway. The first enzyme in the pathway is alcohol oxidase (AOX1), which converts methanol to formaldehyde for use as carbon units for growth (van der Klei *et al.*, 1991). When *P. pastoris* is grown in methanol-containing medium, the AOX1 enzyme is induced and accounts for ~30% of total soluble protein (Veenhuis *et al.*, 1983; van der Klei *et al.*, 1991). An expression system has been devised whereby the gene encoding for the protein to be studied can be homologously recombined with the *AOX1* locus in the *P. pastoris* genome (Sreekrishna *et al.*, 1988). Growth in methanol-containing medium now drives

high-level expression of the protein, which is under control of the *AOX1* promoter. Large quantities of highly purified preparations of ABCB1 and Abcb1a from membranes of *P. pastoris* have been obtained by Nickel-affinity chromatography purification, due to the addition of a polyhistidine tag at the C-terminus of the protein, followed by DE52 anion exchange cellulose chromatography. After reconstitution into lipids in the presence of DTT, purified Abcb1a retains drug-stimulated ATPase activity of high specificity and the ability to bind photo-activatable ATP analogues.

Despite rapidly increasing knowledge of the biochemistry and the high-resolution three-dimensional structure of ABC-transporters, we are still far away from a thorough molecular understanding of the catalytic cycle of the NBDs. In order to better understand the catalytic mechanism of ABC-ATPases, it is important to identify residues that are key players in this mechanism. With the ability to purify Abcb1a to homogeneity and in large quantities, the basis for more detailed biochemical characterization has been put in place.

Chapter 2

Mutational Analysis of Conserved Aromatic Residues in the A-Loop of the ABC Transporter Abcb1a (Mouse Mdr3)

Modified version (expanded) of the published manuscript, by permission from the publisher and Philippe Gros (corresponding author):

Carrier, I., Urbatsch, I. L., Senior, A. E., and Gros, P. Mutational Analysis of Conserved Aromatic Residues in the A-Loop of the ABC Transporter Abcb1a (Mouse Mdr3). *FEBS Letters*, **581(2)**: 301-308, 2007.

2.1 Abstract

The A-loop is a recently described conserved region in the NBDs of ABC transporters (Ambudkar *et al.*, 2006; Kim *et al.*, 2006). In mouse P-glycoprotein (Abcb1a), the aromatic residue of the A-loop in both NBDs is a tyrosine: Y397 in NBD1 and Y1040 in NBD2. Another tyrosine residue (618 in NBD1 and 1263 in NBD2) also appears to lie in proximity to the ATP molecule. We have mutated residues Y397, Y618, Y1040, and Y1263 to tryptophan and analyzed the effect of these substitutions on transport properties, ATP binding, and ATP hydrolysis by Abcb1a (mouse Mdr3). Y618W and Y1263W enzymes had catalytic characteristics similar to WT Abcb1a. On the other hand, Y397W and Y1040W showed impaired transport and greatly reduced ATPase activity, including a ~10-fold increase in K_M for MgATP. Thus, Y397 and Y1040 play an important role in Abcb1a catalysis.

2.2 Introduction

Members of the ATP-binding cassette (ABC) family of membrane transporters use ATP hydrolysis to transport a variety of structurally dissimilar substrates including ions, peptides, lipids, nucleotides, and chemotherapeutic drugs, across the phospholipid bilayer (Gottesman and Ambudkar, 2001; Dean and Annilo, 2005). Mutations in almost half of the 48 human ABC transporters have severe pathophysiological effects and cause diseases in humans (Dean and Annilo, 2005).

The defining features of this family include two membrane-spanning domains (TMDs), usually consisting of six trans-membrane α-helices in each, and two cytoplasmic nucleotide-binding domains (NBDs) (Chen *et al.*, 1986; Gros *et al.*, 1986). While the TMDs are involved in substrate binding and transport, the NBDs bind and hydrolyse ATP and energize transport (Senior *et al.*, 1995b; Ambudkar *et al.*, 1997). The NBDs contain a number of conserved sequence motifs: the Walker A (GXSGCGKST) and B (ILLLDEA) motifs, the signature region (LSGGQ), and the A, D, H, and Q structural loops (Gottesman *et al.*, 1996). These highly conserved subdomains cluster around the bound nucleotide(s) and play important roles in positioning MgATP (Walker A and B motifs, signature region, and the A and H-loops), in the activation of the catalytic water molecule (extended Walker B, H-loop), and in the signal transduction between the NBDs, and the NBDs and TMDs (D and Q loops).

ABCB1, also known as P-glycoprotein/MDR1, functions as a flippase for phospholipids in normal cells, but can also act on xenobiotics, such as anti-cancer drugs, when they are inserted in the lipid bi-layer. It has been established that 1) drug transport is strictly ATP dependent (Ruetz and Gros, 1994; Shapiro and Ling, 1995), 2) purified Pgp shows ATPase activity that can be further stimulated by certain MDR drugs and Pgp modulators (Sarkadi *et al.*, 1992; Urbatsch *et al.*, 1994), 3) both NBDs are essential for function, with complete cooperativity between the two sites for ATP hydrolysis and drug transport (Azzaria *et al.*, 1989; Loo and Clarke, 1995a; Urbatsch *et al.*, 1998), 4) both NBDs are catalytically active with equal probability of hydrolysis at NBD1 and NBD2 (Senior *et al.*, 1995b), and 5) ATP hydrolysis alternates between the two sites (Senior *et al.*, 1995b; Sauna and Ambudkar, 2000). Other mechanistic aspects of Pgp function are not fully understood.

The increasing availability of high resolution three-dimensional (3-D) crystal structures has provided a structural framework to understand the function and mechanism of action of many proteins. For example, 3-D crystal structures for several ABC transporters and ABC-like proteins (HisP, Rad50, MalK, MJ0796, MJ1267, TAP1, MsbA, BtuCD, GlcV, HlyB, and CFTR) (Hung *et al.*, 1998; Diederichs *et al.*, 2000; Hopfner *et al.*, 2000; Chang and Roth, 2001; Gaudet and Wiley, 2001; Karpowich *et al.*, 2001; Yuan *et al.*, 2001; Locher *et al.*, 2002; Chang, 2003; Schmitt *et al.*, 2003; Verdon *et al.*, 2003a; Lewis *et al.*, 2004; Reyes and Chang, 2005; Zaitseva *et al.*, 2005a), in particular those with bound nucleotide, have helped to establish the fact that the NBDs form a dimer that sandwiches nucleotide(s) between the Walker A and B motifs of one NBD and the signature motif and D-loop of the other (Smith *et al.*, 2002). In addition, they have helped in the identification of the residues that appear to be critical for catalysis (Urbatsch *et al.*, 2000c; Zaitseva *et al.*, 2005a); as well as exposed the role of the aromatic amino acid ~25 residues upstream of the Walker A motif. Although previous findings by several groups (Shyamala *et al.*, 1991; Sankaran *et al.*, 1997c; Zhao and Chang, 2004; Zaitseva *et al.*, 2005c) had hinted at the role for this conserved aromatic residue, the 3-D structures have now confirmed its strategic location with respect to bound nucleotide (Figure 2.1). Indeed, as Ambudkar and colleagues have demonstrated, this residue contributes to the positioning of ATP in the active site of Pgp/ABCB1 via π-π interactions with the adenine ring of ATP (Ambudkar *et al.*, 2006; Kim *et al.*, 2006). This is also the case for the MRP1 and HlyB proteins (Zhao and Chang, 2004; Zaitseva *et al.*, 2005c). Although most of the binding energy for ATP appears to be contributed by the phosphate groups (Berger and Welsh, 2000), the nucleotide specificity and further stabilization of nucleotide binding may be contributed by residues which interact with the nucleoside moiety. A recent large-scale data-mining study of ATP-bound crystal structures (including some members of the ABC-transporter family) by Mao *et al.*, determined that the molecular determinants for recognition of the adenine moiety of ATP by proteins includes hydrogen bonding, Van der Waals, π-π stacking, and cation-π stacking interactions, of which aromatic residues are good candidates for π-π stacking (Mao *et al.*, 2004).

Figure 2.1:

Positioning and conservation of tyrosine residues in the NBDs of Pgp

(A) Crystal structure of HisP, the NBD of Histidine permease from *S. typhimurium*, showing the position of ATP, as determined by Hung *et al.* (Hung *et al.*, 1998). The protein is shown as a ribbon model and ATP as a ball-and-stick model. (B) Atomic details of the interactions of residues surrounding the ATP molecule in HisP; the equivalent residues in NBD1 and NBD2 of Abcb1a are shown. Modified from (Hung *et al.*, 1998). (C & D) Sequence alignment of HisP with mouse Abcb1a and human MDR1 NBD1 (C) and NBD2 (D). *Dots* indicate gaps that were introduced to optimize alignment. The numbers below the tyrosine residue thought to interact with the adenine ring of ATP represent the number of sequences of other NBDs where a Y (or any aromatic residue: Y, F, or W) is also present at that position, over the total number of sequences aligned at that position.

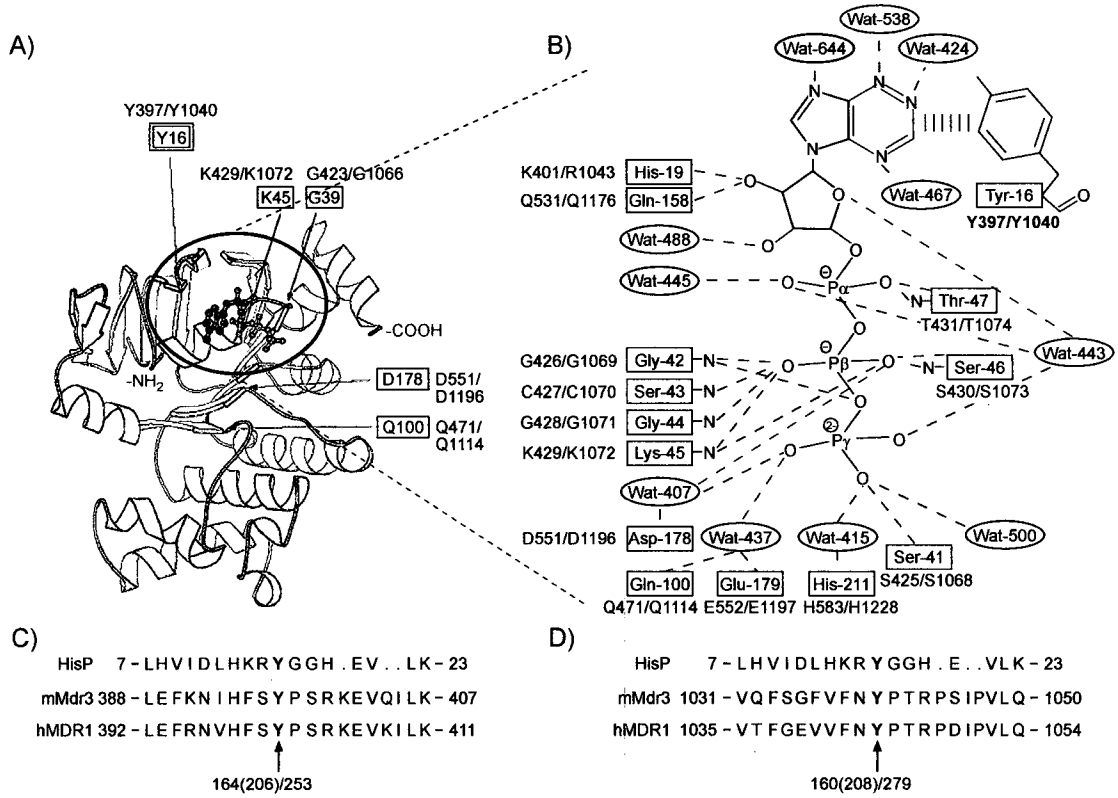
A)
B)
Y397/Y1040
Y16
K429/K1072
G423/G1066
K45
G39
-COOH
-NH2
D178
D551/
D1196
Q100
Q471/
Q1114
Wat-538
Wat-644
Wat-424
K401/R1043
His-19
Q531/Q1176
Gln-158
Wat-467
Tyr-16
Y397/Y1040
Wat-488
Wat-445
Thr-47
T431/T1074
Wat-443
G426/G1069
Gly-42
C427/C1070
Ser-43
G428/G1071
Gly-44
K429/K1072
Lys-45
Ser-46
S430/S1073
Wat-407
D551/D1196
Asp-178
Wat-437
Wat-415
Wat-500
Ser-41
Gln-100
Glu-179
His-211
S425/S1068
Q471/Q1114
E552/E1197
H583/H1228
C)
HisP 7-LHVIDLHKRYGGH.EV..LK-23
mMdr3 388-LEFKNIHFSYPSRKEVQILK-407
hMDR1 392-LEFRNVHFSYPSRKEVKILK-411
164(206)/253
D)
HisP 7-LHVIDLHKRYGGH.E..VLK-23
mMdr3 1031-VQFSGFVFNYPTRPSIPVLQ-1050
hMDR1 1035-VTFGEVVFNYPTRPDIPVLQ-1054
160(208)/279

An important but poorly understood aspect of catalysis by ABC transporters is the nucleotide occupancy of the two active sites during a full cycle of ATP hydrolysis. We wanted to investigate the NBD residues that were labelled by photoactive nucleotide analogs during the catalytic cycle of Pgp. These residues were labelled a) in the presence of the transition state analog vanadate (Vi), which traps ADP in the site undergoing catalysis, and b) in the absence of Vi to mimic the ATP-bound structure of the NBD. Under Vi trapping conditions, residues Y398 and Y1041 in NBD1 and NBD2 of hamster Pgp, respectively, were found to be covalently modified by 8-azido-[α^{32}P]ATP (Sankaran *et al.*, 1997c). Figure 2.1 shows the position of these residues in the NBD as modeled by HisP. Under binding conditions (absence of Vi) Y619 in NBD1 was covalently labelled by 8-azido-[α^{32}P]ATP (unpublished results[2]). The equivalent tyrosine residue in NBD2 is Y1264 and was not labelled in these experiments. Y619 and Y1264 are located near the C-terminal of both NBDs, following all conserved motifs. In the crystal structure of HisP, the equivalent position is located in the last alpha helix, which is about 18Å away from the adenine moiety in the crystal structure (Figure 2.1). These photo-labelling studies suggest that at least three aromatic residues, including those of the A-loop, are in the proximity of the ATP nucleotide during binding and hydrolysis. To further characterize the functional role of these four aromatic residues, we have replaced each residue in mouse P-glycoprotein (Abcb1a/Mdr3) by the bulkier aromatic residue tryptophan and studied the effect of these changes on transport function, ATP binding, and ATP hydrolysis by Pgp.

[2] Essentially same methodology as in Sankaran, B., Bhagat, S. and Senior, A. E. (1997c). Photoaffinity labelling of P-glycoprotein catalytic sites. *FEBS Lett.* **417**(1): 119-22. but omitting Vi. Plasma membranes were incubated at 1 mg/mL protein with 50μM 8-azido-[α^{32}P]ATP in 40mM Tris-HCl pH7.4, 0.1mM EGTA, 2mM $MgSO_4$, and 10μM verapamil at 0°C. Samples were subjected to UV-photolysis, and then precipitated by TCA. The protein was then digested with trypsin and radiolabelled peptides were separated by Al-chelate affinity chromatography. The radiolabelled peptides were then separated by HPLC on a C18 column. The sequence of the major radioactive peak produced Y619 as being covalently modified.

2.3 Materials and Methods

2.3.1 Abcb1a cDNA Modifications and Plasmid Constructions

Mutants Y397W and Y1040W were constructed by site-directed mutagenesis using a recombinant PCR approach as described previously (Vogan and Gros, 1997). To create the Y397W mutation in NBD1, the 5'-CGATGGCCAACTGAAGTGAATATTC-3' mutagenic oligo containing the *Nru*I site was used with the primer TK-5 (5'-GTGCTCATAGTTGCCTACA-3') on ssHL6 template DNA (*Abcb1a* with first six tryptophans replaced by phenylalanine). The 553bp *Msc*I-*Nru*I fragment carrying the mutated segment was purified and used to replace the corresponding fragment in the pVT-*mdr3* construct (Beaudet and Gros, 1995). For the homologous mutation Y1040W in NBD2, two overlapping fragments were synthesized using two pairs of primers: pair 1) 5'-GTGTTCAACTGGCCCACCCG-3' forward mutagenic oligo and primer *Hinc*II (5'-AGAAAGCTGTTAACGAAGCC-3'); pair 2) 5'-CGGGTGGGCCAGTTGAACAC-3' reverse mutagenic oligo and primer *Mfe*I (5'-CACACTGACAATTGAGAAG-3'). The overlapping fragments containing the inserted mutations were annealed, followed by a second PCR amplification using primers *Hinc*II and *Mfe*I. The 319bp *Spe*I-*Xho*I fragment carrying the mutated segment was purified and used to replace the corresponding fragment in the full length *Abcb1a* cDNA contained in the yeast expression construct pVT-*mdr3.5* (Urbatsch *et al.*, 1998). To create the Y618W mutation in NBD1, a 2.2kb *Eco*RI fragment of *Abcb1a* (positions 93-2248) was cloned in the corresponding site of phage vector M13mp18 (Urbatsch *et al.*, 1998), and single-stranded DNA was used as a template for site-directed mutagenesis using a commercially available kit (Amersham, Arlington Heights, IL), and the mutagenic oligonucleotide (5')-CATGACAAGTTT AAACCAAATGCCCTTTT-(3'). For the homologous NBD2 mutation Y1263W, a *Pst*I-*Hind*III *Abcb1a* fragment (positions 3511-4199) from pDR16 was inserted in the corresponding sites of M13mp18, with a *Sna*BI site introduced after the last amino acid (3889) (Urbatsch *et al.*, 1998). The Y1263W mutation was introduced using the mutagenic oligo (5')-GACCATTGAGAACCAAATGCCCTTCTG-(3'). The nucleotide sequence of the mutated segments was verified prior to their insertion in the corresponding sites of pVT-*mdr3* (NBD1 mutation, using *Eco*RI and *Msc*I) or pVT-*mdr3.5* (NBD2 mutation, using *Pst*I and *Sna*BI). pVT vectors containing either WT or

mutant DNA were then transformed into *S. cerevisiae* for biological testing, as previously described (Raymond *et al.*, 1992; Raymond *et al.*, 1994).

2.3.2 Testing of Abcb1a Function in Yeast Cells

pVT-*mdr3* plasmids carrying either wild-type (WT) or mutant versions of *Abcb1a* were transformed in the yeast *Saccharomyces cerevisiae* strain JPY201 (*MAT***a***ste6*Δ*ura3*) using a lithium acetate technique (Gietz *et al.*, 1995). The biological activity of mass populations of yeast cells transformed with individual plasmids was tested with respect to their capacity to convey cellular resistance to the anti-fungal agent FK506 (50 μg/mL) and to restore mating in the *ste6*Δ sterile yeast as previously described (Raymond *et al.*, 1992; Raymond *et al.*, 1994). Expression of WT and mutant Abcb1a proteins was monitored by immunoblotting using the monoclonal anti-Pgp antibody C219 (Signet Labs Inc.).

2.3.3 Plasmid Constructions and Transformation into Pichia pastoris

NBD1 mutants were excised from pVT-*mdr3* as *Afl*II-*Eco*RI fragments and NBD2 mutants were excised from pVT-*mdr3.5* as *Afl*II-*Sna*BI fragments, and substituted in the *Pichia pastoris* expression vector pHIL-*mdr3.5*-His_6. pHIL-*mdr3.5*-His_6 carrying either WT or mutant versions of *Abcb1a*, as well as the control pHIL-D2 vector, were transformed into *Pichia pastoris* strain GS115 according to the manufacturer instructions (In Vitrogen, license number 145457). His^+ transformants showing successful homologous recombination at the *AOX1* locus were identified as unable to grow on medium containing methanol (methanol utilizing slow, mut^S), as previously described (Beaudet *et al.*, 1998a).

2.3.4 Membrane Preparations

P. pastoris clones were picked and transferred to 10mL cultures followed by a 72h induction of *AOX1* with methanol, as previously described (Urbatsch *et al.*, 1998). Cells were then collected and lysed to obtain crude plasma membranes, as previously described (Urbatsch *et al.*, 1998). Abcb1a expression was monitored by immunoblotting with the anti-Pgp monoclonal antibody C219. For large-scale preparations of *P. pastoris* membranes, cultures were induced in 3L methanol-containing medium, and plasma membranes were isolated either by centrifugation on discontinuous sucrose density gradients (Beaudet *et al.*, 1998a) or by a modified protocol (Lerner-Marmarosh *et al.*,

1999). From a 1L culture we routinely obtained about 50mg of total membrane protein and ~350μg of pure Pgp.

2.3.5 Solubilization and Purification of Abcb1a

To obtain pure protein, 30mg of *P. pastoris* membranes (1-2mg/mL) were used in a protocol previously described (Urbatsch *et al.*, 1998), except that 1mL of packed Ni-NTA resin (Qiagen), 100mL of buffer A, 20mL of buffer B and 3 x 1mL of buffer C were employed. Also, Abcb1a was further eluted using 2 x 1.5mL of buffer D (50mM Tris-HCl, pH 8.0, 20% glycerol, 150mM imidazole, 0.1% DM). For reconstitution of Abcb1a, the 80mM and 150mM imidazole eluates were incubated with 0.3% *E. coli* lipids (w/v) (Avanti, acetone/ether preparation) for 30min on ice, followed by dialysis against 1L dialysis buffer (50mM Tris-HCl, pH 7.4, 0.1mM EGTA, and 1mM DTT). Abcb1a proteoliposomes were recuperated by centrifugation (100,000g, 30min), resuspended in dialysis buffer, aliquoted and stored at –80 °C until use. For the 8-azido-nucleotide trapping experiments, the protein was purified according to a more recent protocol where cultures were induced with 1% methanol for 72 hrs and plasma membranes isolated by centrifugation, as previously described in (Lerner-Marmarosh *et al.*, 1999). Solubilization and purification of WT and mutant Abcb1a variants by affinity chromatography on Ni-NTA resin (Qiagen) and DE52-cellulose (Whatman) was as described in (Lerner-Marmarosh *et al.*, 1999).

2.3.6 Assay of ATPase Activity

Reactions were carried out in 50μL of 50mM Tris-HCl, pH8.0, 0.1mM EGTA, 10mM Na_2ATP, and 10mM $MgCl_2$ at 37°C for appropriate times during which the reaction was linear, and $\leq$ 10% of added nucleotide was hydrolysed. Reactions were initiated by addition of purified reconstituted Abcb1a, and stopped by addition of 1mL of 20mM ice-cold H_2SO_4. P_i release was assayed by the method of Van Veldhoven and Mannaerts (Van Veldhoven and Mannaerts, 1987). For determination of kinetic parameters, an excess of 2mM $MgCl_2$ over MgATP concentrations was used. Drugs were added as dimethyl sulfoxide solutions, and the final solvent concentration in the assay was kept at $\leq$ 2% (v/v).

2.3.7 Photo-affinity Labelling with 8-Azido-[α^{32}P]ATP

8-Azido-[α^{32}P]ATP photo-affinity labelling was performed essentially as previously described (Carrier *et al.*, 2003) with minor modifications: FK506 was added to a final concentration of 30μM where indicated.

2.3.8 Materials

8-azido-[α^{32}P]ATP (~8.5 Ci/mmol) was purchased from ICN or Affinity Labelling Technologies, Inc.. Verapamil was purchased from ICN. Valinomycin and FK 506 were purchased from Calbiochem. Acetone/ether-precipitated *E. coli* lipids were from Avanti Polar Lipids. General chemicals were of reagent grade from Sigma.

2.4 Results

2.4.1 Expression and Characterization of Y397W, Y618W, Y1040W and Y1263W Abcb1a Mutants in S. cerevisiae

We have previously shown that expression of mouse Pgp (*Abcb1a*) in the yeast *Saccharomyces cerevisiae* can confer cellular resistance to the antifungal macrolides FK506 and FK520 (Raymond *et al.*, 1994), and complement the biological activity of the *a* factor pheromone ABC transporter *STE6*, restoring mating in an otherwise sterile yeast *ste6Δ* mutant (Raymond *et al.*, 1992). Mutants Y397W, Y618W, Y1040W and Y1263W were transformed in *S. cerevisiae* strain JPY201. Immunoblotting of crude membrane fractions from yeast transformants using the anti-Pgp antibody C219, showed similar levels of expression of the various mutants, comparable to WT (data not shown), suggesting that the mutations do not have a major effect on protein expression, stability or membrane targeting in yeast.

The ability of these mutants to confer resistance to the fungicide and Pgp substrate FK506 was tested in a growth inhibition assay in liquid medium (Figure 2.2). In drug-free medium, all transformants showed identical growth profiles (Figure 2.2 A). The growth rate of each transformant population was expressed as the percentage of growth in the presence of drug compared to growth in the absence of drug (Figure 2.2 B). While mutants Y618W and Y1263W showed growth rates similar to those measured in WT expressing cells (>85% growth of WT at 24hrs), mutant Y1040W showed a reduced growth phenotype (30% of WT at 24hrs) and mutant Y397W was severely impaired for growth in FK506 (<10% of WT at 24hrs). The ability of the Y397W, Y618W, Y1040W and Y1263W mutants to restore mating in the sterile *ste6Δ* yeast strain JPY201 was also tested (Figure 2.3). Mating was qualitatively assessed by the growth of diploid cells on selective medium (minimal plates) following mating of patches of JPY201 transformants with the tester strain DC17. The behaviour of the four mutants in the mating assay (Figure 2.3) paralleled that observed in the growth inhibition assay with FK506: mutants Y397W and Y1040W were functionally impaired while mutants Y618W and Y1263W behaved as WT Abcb1a.

Figure 2.2:

Effect of Y397W, Y618W, Y1040W and Y1263W mutations on Abcb1a-mediated resistance to FK506 in S. cerevisiae cells

The capacity of WT and mutant Abcb1a variants to confer cellular resistance to FK506 in the yeast *S. cerevisiae* was measured using a growth inhibition assay in liquid medium. (A) Growth of individual mass populations of transformants was measured over time in drug-free medium. (B) Growth of the same individual mass populations in medium containing FK506 at 50μg/mL; relative growth is expressed as percent of growth in FK506-containing vs drug-free medium. The pVT negative control does not express Abcb1a. Shown is one representative of three independent experiments.

A

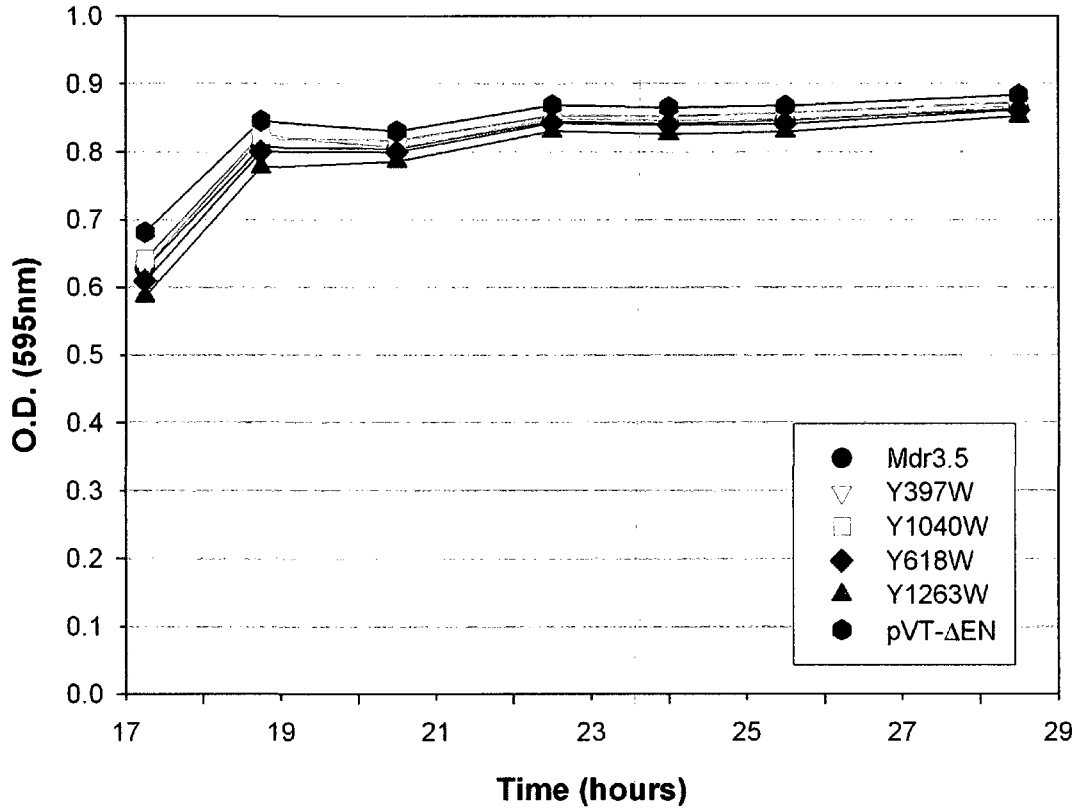
1.0
0.9
0.8
0.7
0.6
0.5
0.4
0.3
0.2
0.1
0.0
O.D. (595nm)
17
19
21
23
25
27
29
Time (hours)
Mdr3.5
Y397W
Y1040W
Y618W
Y1263W
pVT-ΔEN

B

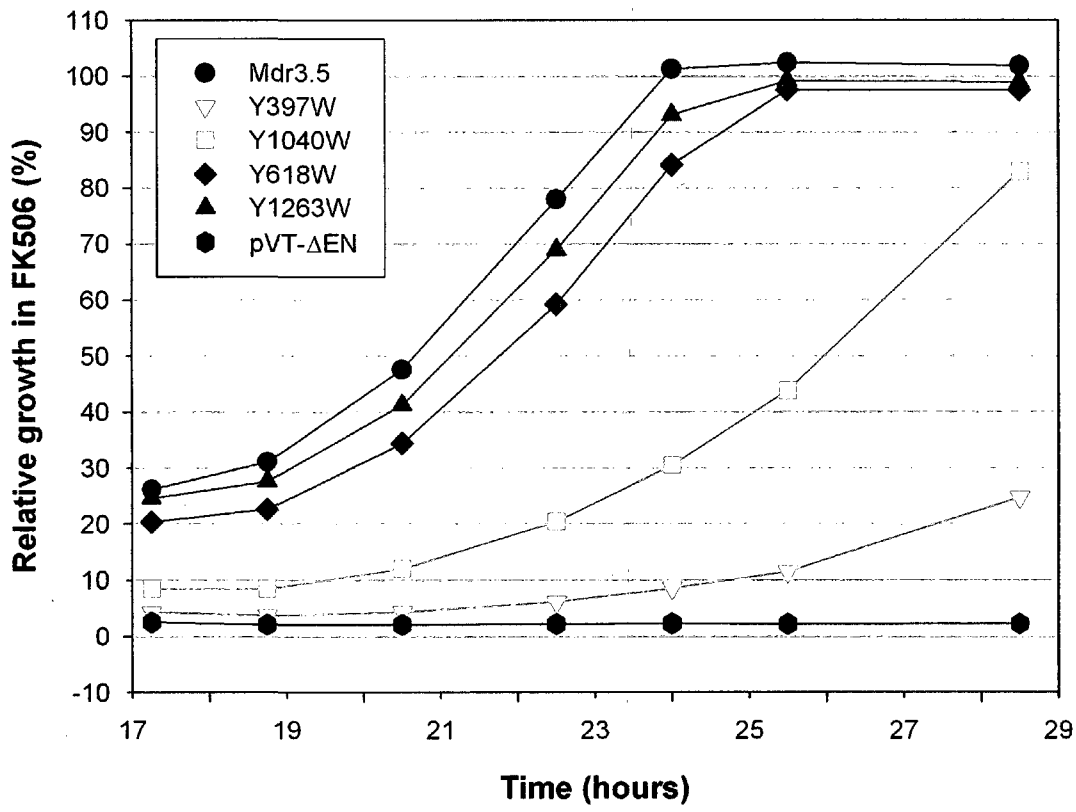
110
100
90
80
70
60
50
40
30
20
10
0
-10
Relative growth in FK506 (%)
17
19
21
23
25
27
29
Time (hours)
Mdr3.5
Y397W
Y1040W
Y618W
Y1263W
pVT-ΔEN

Figure 2.3:

Effect of Y397W, Y618W, Y1040W and Y1263W mutations on Abcb1a-mediated mating in S. cerevisiae cells

Patches of JPY201 cells transformed with either pVT-Mdr3, pVT-Y397W, pVT-Y1040W, pVT-Y618W, pVT-Y1263W, pVT-STE6 (positive control), or pVT-ΔEN (negative control) were mated to a lawn of DC17 tester stock (*MATαhis1*). Mating was allowed to proceed for 12hrs at 30°C before transfer onto minimal plates to assess diploid formation. Shown is one representative of two independent experiments.

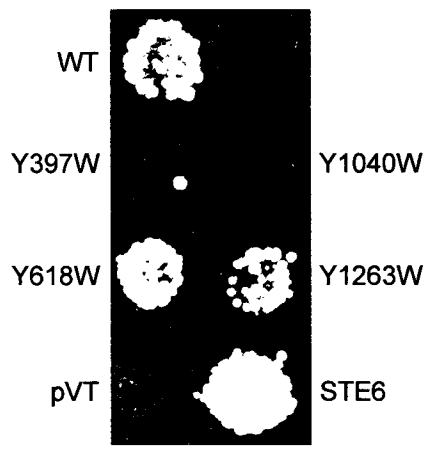
WT
Y397W
Y1040W
Y618W
Y1263W
pVT
STE6

2.4.2 Characterization of the ATPase Activity of Y397W, Y618W, Y1040W and Y1263W Abcb1a Mutants Expressed in P. pastoris

The effect of the Y397W, Y618W, Y1040W and Y1263W mutations on Abcb1a ATPase activity was measured following expression and purification of WT and mutant Abcb1a variants from *P. pastoris* membranes and reconstitution in *E. coli* lipids. ATPase activity was measured in the absence or presence of several Pgp substrates, including verapamil (VER), valinomycin (VAL), vinblastine (VBL), colchicine (COL), tetraphenylphosphonium bromide (TPP+), and FK506 (Gros and Hanna, 1996; Beaudet *et al.*, 1998a). Although the stimulation profiles for the four tryptophan mutants with the different Pgp substrates were qualitatively similar to the WT protein (Figure 2.4); mutants Y618W and Y1263W showed maximal levels of drug-stimulated ATP hydrolysis similar to WT, while mutants Y397W and Y1040W showed a significant reduction in maximal stimulation. The ATPase activity of the four mutants was also evaluated in increasing amounts of ATP. Purified reconstituted Abcb1a showed a single high K_M for MgATP hydrolysis (Figure 2.5 A) which was similar in the absence (0.2mM) or presence of verapamil (0.5mM), valinomycin (0.4mM), or FK506 (0.5mM). The K_M values for drug-stimulated ATP hydrolysis measured in the mutants Y618W and Y1263W were very similar to those obtained with WT Abcb1a (data not shown). However, K_M for drug-stimulated ATP hydrolysis was much higher (K_M ATP ~1.5-9mM) in the Y397W and Y1040W mutants (Figure 2.5 B and C). These results confirm that Y397 and Y1040 play an important role in ATP binding and/or hydrolysis by Pgp.

2.4.3 Photolabelling with Mg-8-azido-[α^{32}P]ATP

The altered K_M values for ATP hydrolysis detected in Y397W and Y1040W suggested alterations in nucleotide binding and/or hydrolysis in these mutants. The nucleotide-binding properties of the four mutants were monitored by photo-affinity labelling with the nucleotide analogue 8-azido-[α^{32}P]ATP (Carrier *et al.*, 2003). For this, purified mutants were exposed to increasing amounts of 8-azido-[α^{32}P]ATP, followed by cross-linking with UV, separation by SDS-PAGE and autoradiography. Results in figure 2.6 A suggest that none of the mutations had a major deleterious effect on the overall ATP binding properties of the protein.

Figure 2.4:

ATPase activity of purified reconstituted Y397W, Y618W, Y1040W and Y1263W variants in presence of various drugs

ATPase activities were assayed as described in Materials and Methods. All values are the means of at least three experiments ± the standard deviation. Verapamil (VER), valinomycin (VAL), vinblastine (VBL), colchicine (COL), FK506, and tetraphenylphosphonium bromide (TPP+) were added at concentrations of 100, 100, 100, 50, 30, and 50 μM respectively.

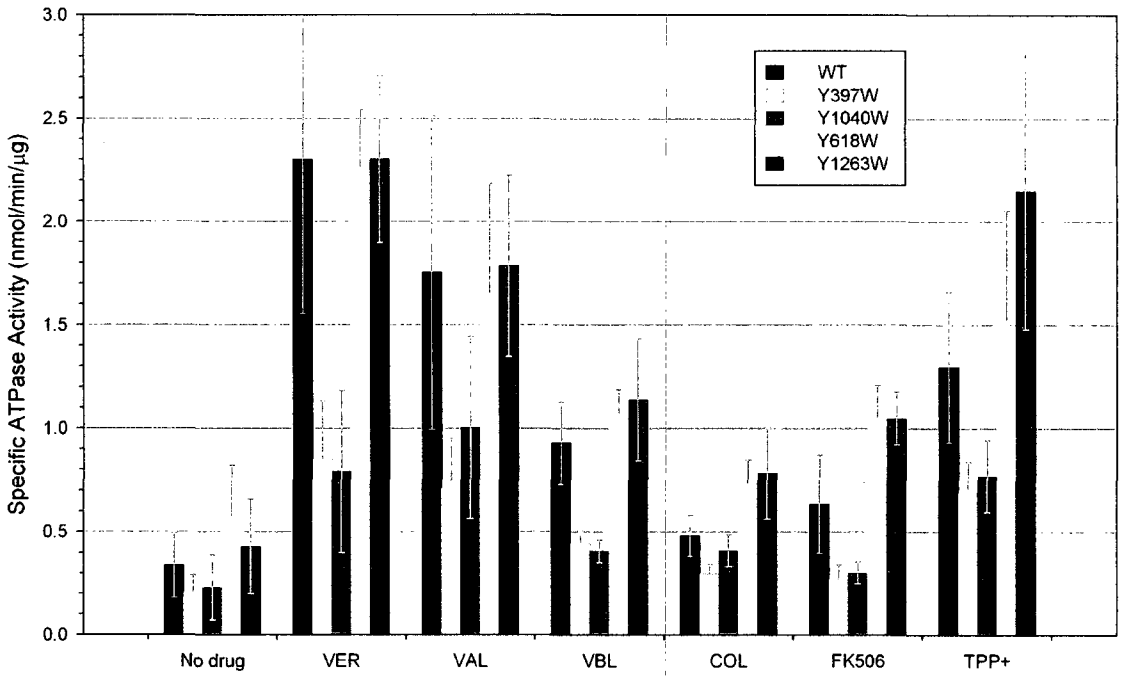
Specific ATPase Activity (nmol/min/μg)
3.0
2.5
2.0
1.5
1.0
0.5
0.0
WT
Y397W
Y1040W
Y618W
Y1263W
No drug
VER
VAL
VBL
COL
FK506
TPP+

Figure 2.5:

ATP hydrolysis by purified reconstituted Y397W and Y1040W mutants as a function of ATP concentration

The specific activity of purified reconstituted WT Abcb1a and Y397W and Y1040W variants was measured as a function of MgATP concentration in the absence or presence of 100μM verapamil (VER), 100μM valinomycin (VAL), or 30μM FK506. The points represent the mean of three or four independent experiments and the error bars represent the standard deviation. The curves are non-linear least-squares regression fits of the mean data points to the Michaelis-Menten equation which also provided the apparent K_M(ATP) values.

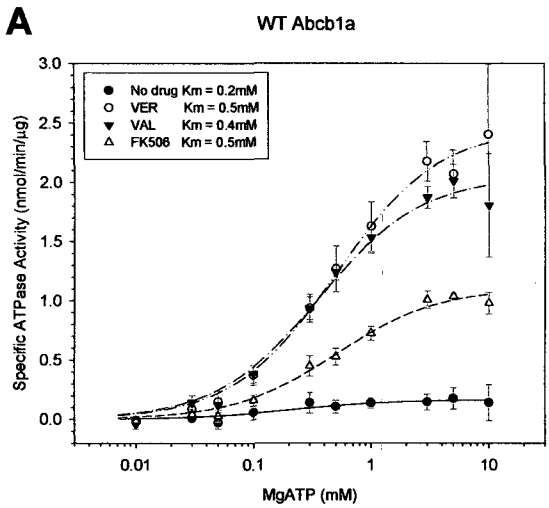
A
WT Abcb1a
No drug Km = 0.2mM
VER Km = 0.5mM
VAL Km = 0.4mM
FK506 Km = 0.5mM
Specific ATPase Activity (nmol/min/µg)
MgATP (mM)

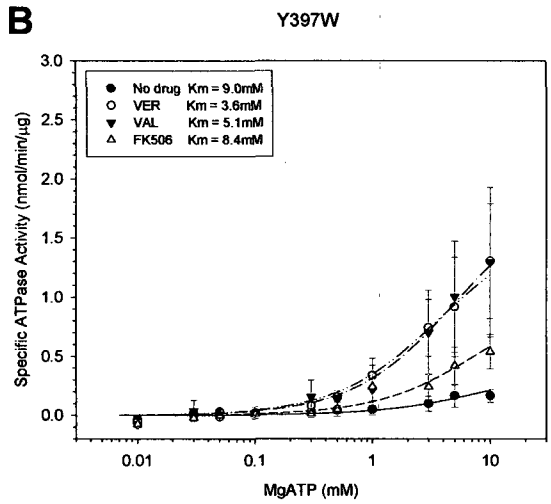
B
Y397W
No drug Km = 9.0mM
VER Km = 3.6mM
VAL Km = 5.1mM
FK506 Km = 8.4mM
Specific ATPase Activity (nmol/min/µg)
MgATP (mM)

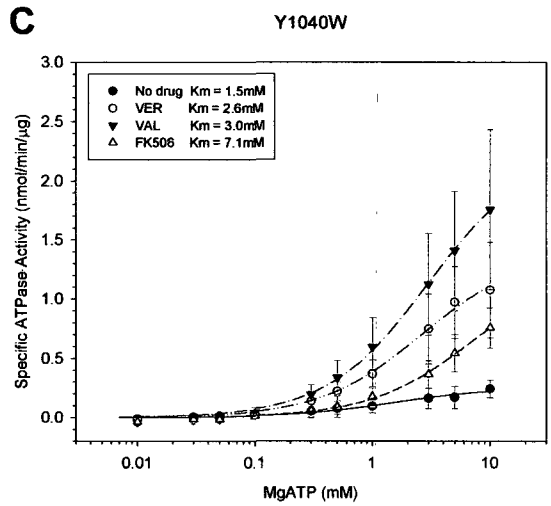
C
Y1040W
No drug Km = 1.5mM
VER Km = 2.6mM
VAL Km = 3.0mM
FK506 Km = 7.1mM
Specific ATPase Activity (nmol/min/µg)
MgATP (mM)

Figure 2.6:

Photo-labelling of purified reconstituted Y397W, Y618W, Y1040W and Y1263W variants with Mg-8-azido-[α^{32}P]ATP

(A) Three micrograms of purified reconstituted WT and mutant Abcb1a variants were UV-irradiated on ice in the presence of 3mM $MgCl_2$ and 5, 10, 20, 40, and 80 μM 8-azido-[α^{32}P]ATP. Photo-labelled samples were separated on 7.5% SDS-polyacrylamide gels and stained with Coomassie Blue followed by autoradiography. The position of the molecular mass markers is given on the left. Experiment was carried out in duplicate. (B) Purified activated WT and mutant Abcb1a variants were pre-incubated with 5 μM 8-azido-[α^{32}P]ATP and 3 mM $MgCl_2$ for 20 min at 37 °C with or without 200 μM vanadate. Verapamil (100 μM) or FK506 (50 μM) was included as indicated above the lanes. Unbound ligands were removed by ultracentrifugation and washing, and the samples were then UV irradiated. Photolabelled samples were then analyzed as described in (A).

A

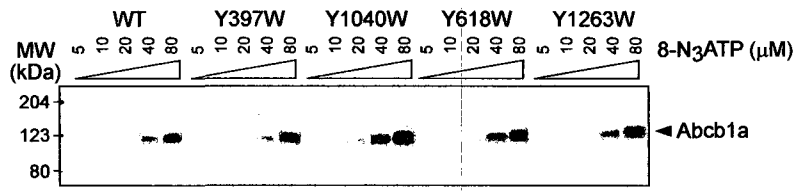
WT
Y397W
Y1040W
Y618W
Y1263W
MW (kDa)
5 10 20 40 80
8-N3ATP (μM)
204
123
80
Abcb1a

B

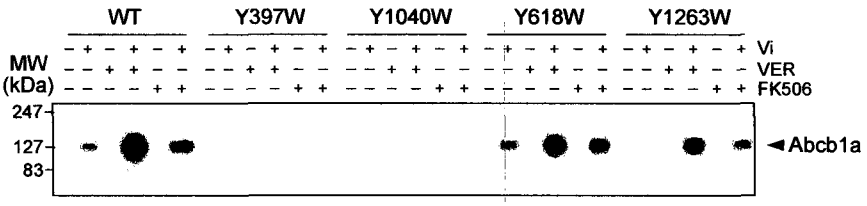
WT
Y397W
Y1040W
Y618W
Y1263W
Vi
VER
FK506
MW (kDa)
247
127
83
Abcb1a

Vi-induced trapping of 8-azido-[α^{32}P]ADP under hydrolysis conditions (37°C) has been used as an alternative and highly sensitive method to monitor ATPase activity in WT and mutant Pgp (Urbatsch *et al.*, 1998). Figure 2.6 B demonstrates that Y618W and Y1263W trap 8-azido-ADP at levels comparable to WT, whereas trapping by the mutants Y397W and Y1040W is greatly reduced (faint bands observed for Y397W and Y1040W in the presence of verapamil and vanadate upon overexposure of film, not shown). The reduction in labelling of the Y397W and Y1040W mutants is consistent with a lower rate of ATP hydrolysis (Figure 2.4), and with the effect of the mutations on K_M for the nucleotide substrate (Figure 2.5 B and C). Together, these results indicate that Y397 and Y1040 play an important role in ATP hydrolysis by Abcb1a, and highlight a critical role for residues of the A-loop in ATP hydrolysis by ABC transporters.

2.5 Discussion

In this study, we wanted to determine which amino acid side chains are in the vicinity of the adenine moiety of bound nucleotide under binding and hydrolysis conditions. We thus wanted to determine whether in Abcb1a an aromatic residue was also responsible for binding the adenine moiety of bound nucleotide as in HisP, ABCB1, MRP1, and HlyB. We also hypothesized that if the tryptophan substitution at these positions was tolerated, these residues could be used in a tryptophan-free enzyme to monitor nucleotide occupancy of the NBDs during the catalytic cycle, as was done for F1-ATPase, or dimer formation, as was done in MJ0796-E171Q. Two homologous pairs of tyrosine residues were investigated. The first pair is Y397 in NBD1 and its homolog in NBD2: Y1040, which are part of a conserved motif, the A-loop. The second pair is Y618 and its homolog in NBD2: Y1263, which are in the C-terminal portion of the NBD.

Preliminary assays in the yeast *S. cerevisiae* demonstrated that introduction of tryptophan residues at positions Y618 and Y1263 did not affect enzyme activity. On the other hand, introduction of tryptophan residues at positions Y397 and Y1040 appeared to have a significant effect on enzyme activity, since resistance to FK506 was significantly reduced and no mating was observed (Figures 2.2 and 2.3). The similar results obtained for the equivalent mutations in the two NBDs suggest that these residues play similar roles in both NBDs. Because expression at the plasma membrane was very similar for the WT and all mutants (data not shown), we concluded that enzyme activity must be impaired, and that these two residues were important for enzyme function. Although the activity of Y397W and Y1040W was strongly impaired, it was not fully abolished; therefore, we decided to determine the nature of the defect(s) of these two mutants. First, we evaluated the ATPase activity of the two enzymes in parallel with WT Abcb1a and the Y618W and Y1263W mutants. As seen in figure 2.4, Y397W and Y1040W do retain steady-state ATPase activity that can be stimulated by several drugs, although the basal and drug-stimulated activities are consistently lower than the WT and other two mutants. The lower ATPase activity observed for Y397W and Y1040W could thus account for the significant impairment of biological activity in *S. cerevisiae*, as a certain level of ATPase activity is necessary to maintain drug/pheromone transport (Urbatsch *et al.*, 2000c). Curiously, the basal activity of the Y618W and Y1263W mutants was seen to be

consistently higher than that of the WT. This may perhaps be due to a small change in conformation in the NBD, as a result of the bulkier side chain, that mimics the change associated with drug binding in the drug binding site(s), or which decreases the activation energy of the basal transition state, thereby increasing basal ATPase activity (Omote *et al.*, 2004). We next examined the enzyme kinetic parameters of the mutants (Figure 2.5). Whereas Y618W and Y1263W showed kinetic parameters very similar to the WT (not shown), Y397W and Y1040W revealed an important increase in K_M for ATP (~10-fold). Such high K_M values have not been previously described for any other point mutations in Abcb1a, but also suggest that these two tyrosine residues may in fact compare to the Y16 of HisP, which directly interacts with the adenine moiety of ATP (Figure 2.1), with Y401 and Y1044 in NBD1 and NBD2, respectively, of ABCB1, with W653 and Y1302 in NBD1 and NBD2, respectively, of MRP1, and with Y477 of HlyB. Indeed, mutation of Y16 to serine in HisP actually abolished ATP binding and transport activity (because the ATPase domain is a homodimer, only the double mutant was studied) (Shyamala *et al.*, 1991). Mutation of the equivalent residues in ABCB1, MRP1, and HlyB also caused an increase in K_M (Zhao and Chang, 2004; Zaitseva *et al.*, 2005c; Ambudkar *et al.*, 2006). Although K_M is generally used as a measure of the affinity of the enzyme for its substrate (in this case ATP), when ATP hydrolysis is used as readout, changes in K_M can also reflect changes in turnover rate. Using 8-azido-[α^{32}P]ATP binding assays (Figure 2.6 A), we determined that the initial affinity for nucleotide in these single mutant enzymes was not significantly different than the WT enzyme. On the other hand, trapping of 8-azido-[α^{32}P]ADP (Figure 2.6 B) was greatly reduced in Y397W and Y1040W. This is consistent with the decrease in overall steady-state ATPase activity (Figure 2.4), and mirrored by the increase in K_M (Figure 2.5). In fact, the 8-azido-[α^{32}P]ATP concentration used (5μM) in the trapping experiments is actually well below the K_M value for 8-azido-ATP (400-600μM) (Senior *et al.*, 1995a). With normal enzymes this allows for sensitive detection of drug-stimulated ATPase activity (Szabo *et al.*, 1998), but in the case of the Y397W and Y1040W mutants, where we have demonstrated a significantly higher K_M, this concentration is now 1000 times lower than the K_M, and thus 8-azido-nucleotide trapping becomes almost insignificant. Perhaps trapping similar to the WT enzyme could be obtained if a higher concentration of 8-azido-ATP was used in the assay with these

two enzymes. The increase in K_M could also explain the important effect of these mutations on transport activity as measured in yeast, since the cellular concentration of ATP in these organisms is around 5mM (a concentration about 10 times the normal K_M for the WT enzyme), which means that the mutant enzymes Y397W and Y1040W would then be functioning at sub-saturating concentrations of nucleotide.

In conclusion, although photolabeling experiments suggested that Y618 and Y1263, in NBD1 and NBD2 respectively, may be near the azido group of 8-azidoATP during nucleotide binding in the absence of vanadate, these residues do not seem to play a major role in nucleotide binding during catalysis, as the activity of the enzyme was not affected by their substitution to tryptophan. Mutagenesis to replace these residues by less conservative amino acids, singly or in combination, could determine whether they do actually have a role in catalysis. On the other hand, this suggests that the Y618W and Y1263W mutants may turn out to be good probes for nucleotide occupancy, or perhaps dimer formation, during the catalytic cycle, in tryptophan fluorescence assays, if their fluorescence becomes altered by the presence of nucleotide - or upon dimer formation; this will need to be tested in the future, following introduction in the tryptophan-less enzyme (Kwan *et al.*, 2000). Finally, the residues of the A-loop, Y397 and Y1040, in NBD1 and NBD2 respectively, seem to play an important role in ATP hydrolysis by Abcb1a by contributing significantly to the positioning and maintaining of the nucleotide in the active site. Our results are thus in agreement with those obtained by Kim *et al.* (Kim *et al.*, 2006) and Zhao *et al.* (Zhao and Chang, 2004) with the eukaryotic enzymes ABCB1 and MRP1, respectively. A major difference, though, is that in our eukaryotic enzyme, a simple substitution to a conserved amino acid produces a significant change in the catalytic properties of the enzyme, whereas these effects are only observed in ABCB1 and MRP1 when non-conserved substitutions are introduced in each NBD (ABCB1 and MRP1) or when the conserved substitutions are introduced simultaneously in both NBDs (W in ABCB1) (Zhao and Chang, 2004; Kim *et al.*, 2006). Perhaps the mouse enzyme is less tolerant of substitutions at this position because the NBD is more rigid and/or because there aren't (as many) other residues which contribute to the stabilization of ATP binding via the adenine moiety, as may be the case in ABCB1 or MRP1.

2.6 Acknowledgements

This work was supported by an FRSQ-FCAR-Santé scholarship to I. C. and by research grants to P.G. from the Canadian Institutes of Health Research (CIHR). P.G. is a Career Scientist of the CIHR.

Having determined that the tyrosine residues in Abcb1a, labelled by 8-azidoATP in the presence of Vi, are part of the A-loop which is responsible for π-stacking with the adenine moiety of ATP, our next focus was on the identification of the catalytic residues of the NBSs of Abcb1a which are responsible for the cleavage of the γ-phosphate of ATP.

Chapter 3

Mutational Analysis of Conserved Carboxylate Residues in the Nucleotide Binding Sites of P-Glycoprotein

Published manuscript reproduced by permission from the publisher:
Urbatsch, I. L., Julien, M., **Carrier, I.**, Rousseau, M.-É., Cayrol, R., and Gros, P. Mutational Analysis of Conserved Carboxylate Residues in the Nucleotide Binding Sites of P-Glycoprotein. *Biochemistry*, **39(46)**: 14138-14149, 2000.

3.1 Abstract

Mutagenesis was used to investigate the functional role of six pairs of aspartate and glutamate residues (D450/D1093, E482/E1125, E552/E1197, D558/D1203, D592/D1237, and E604/E1249) that are highly conserved in the nucleotide binding sites of P-glycoprotein (Mdr3) and of other ABC transporters. Removal of the charge in E552Q/E1197Q and D558N/D1203N produced proteins with severely impaired biological activity when the proteins were analyzed in yeast cells for cellular resistance to FK506 and restoration of mating in a *ste6*Δ mutant. Mutations at other acidic residues had no apparent effect in the same assays. These four mutants were expressed in *Pichia pastoris*, purified to homogeneity, and biochemically characterized with respect to ATPase activity. Studies with purified proteins showed that mutants D558N and D1203N retained 14 and 30% of the drug-stimulated ATPase activity of wild-type (WT) Mdr3, respectively, and vanadate trapping of 8-azido[α^{32}P]nucleotide confirmed slower basal and drug-stimulated 8-azido-ATP hydrolysis compared to that for WT Mdr3. The E552Q and E1197Q mutants showed no drug-stimulated ATPase activity. Surprisingly, drugs did stimulate vanadate trapping of 8-azido[α^{32}P]nucleotide in E552Q and E1197Q at a level similar to that of WT Mdr3. This suggests that formation of the catalytic transition state can occur in these mutants, and that the bond between the β- and γ-phosphates is hydrolysed. In addition, photolabelling by 8-azido[α^{32}P]nucleotide in the presence or absence of drug was also detected in the absence of vanadate in these mutants. These results suggest that steps after the transition state, possibly involved in release of MgADP, are severely impaired in these mutant enzymes.

3.2 Introduction

Multidrug resistance (MDR) in cultured cells in vitro and in tumour cells in vivo is often associated with the overexpression of P-glycoprotein (Pgp) (Ambudkar *et al.*, 1999). Pgp is a plasma membrane protein that functions as an energy-dependent drug efflux pump to reduce the level of intracellular drug accumulation (Ambudkar *et al.*, 1999). Drug transport by Pgp is strictly ATP-dependent and may be mechanistically related to the proposed phospholipid translocase activity of Pgp in normal tissues (Ruetz and Gros, 1994; van Helvoort *et al.*, 1996; Ambudkar *et al.*, 1999). Pgp is formed by two symmetrical halves with similar sequences, each encoding six transmembrane (TM) domains and one nucleotide binding (NB) site. These NB sites contain characteristic consensus Walker A and B sequence motifs, which have been described in a number of ATP binding proteins and ATPases (Walker *et al.*, 1982). The structural features encoded by each Pgp half (six TM domains and one NB domain) define a large protein superfamily known as the ABC (ATP binding cassette) family of membrane transporters (Holland and Blight, 1999). In addition to the three rodent (Mdr1, Mdr2, and Mdr3) and two human Pgp isoforms (MDR1 and MDR2) (Gros and Hanna, 1996), some of the best studied ABC transporters include the multidrug resistance-associated protein (MRP) family which transports glutathione and glucuronide adducts (Loe *et al.*, 1996), the CFTR chloride channel in which mutations cause cystic fibrosis in humans (Riordan *et al.*, 1989), the bacterial drug resistance protein LmrA (van Veen *et al.*, 1996), and the histidine permease (Hung *et al.*, 1998).

The key role of ATP binding and hydrolysis in Pgp-mediated drug transport has been demonstrated in transport studies with membrane vesicles from Pgp positive cells and with purified Pgp reconstituted in liposomes (Gros and Hanna, 1996; Ambudkar *et al.*, 1999). Furthermore, the ATPase activity of Pgp has been shown to be strongly modulated by substrates (drugs) or inhibitors of the protein (e.g., verapamil) (Urbatsch *et al.*, 1994; Loo and Clarke, 1995c; Shapiro and Ling, 1995; Sharom *et al.*, 1995). In addition, ATP binding and hydrolysis have been shown to occur at both NB sites of Pgp (Loo and Clarke, 1995a; Urbatsch *et al.*, 1995b), and a mechanistic model of the two sites alternating in catalysis has been proposed (Senior *et al.*, 1995b). Finally, single-point mutations at the key lysine residue in the Walker A motif (GCG**K**S) and at the key

aspartate in the Walker B motif (ILLL**D**) of each NB site have been shown previously to abolish the ability of Pgp to confer MDR in mammalian (Azzaria *et al.*, 1989; Loo and Clarke, 1995c; Muller *et al.*, 1996; Hrycyna *et al.*, 1999) and yeast (Urbatsch *et al.*, 1998) cells, and abrogate ATPase activity as assessed by standard P_i release, and by vanadate-induced trapping of nucleotides (Urbatsch *et al.*, 1998). Although significant structural and functional differences are likely to exist among different ABC proteins, it has been proposed that the overall structures of the NB sites of ABC proteins and of other proteins containing the Walker A and B signatures are probably very similar (Hyde *et al.*, 1990; Mimura *et al.*, 1991). Thus, additional key catalytic residues involved in ATP hydrolysis are probably conserved in the NB sites of these proteins as well, and candidates for these residues can be suggested by multiple sequence alignments.

Central to the nucleotide binding site of ABC transporters are the two Walker homology sequences (Walker A and B). The amino acids of the Walker A motif (GCGKS) form the phosphate binding loop, or P loop, which wraps around and provides tight binding for the phosphates of ATP (Walker *et al.*, 1982). The Walker B motif (ILLLD) is involved in the coordination of Mg^{2+}, a mandatory cofactor in the hydrolysis of ATP. In ATPases where a structure is known, such as recA, and the F_1 portion of F_1F_0-ATP synthase, the positions of residues that play key roles in hydrolysis have been determined by both site-directed mutagenesis and biochemical studies (Nadanaciva *et al.*, 1999b; Nayak and Bryant, 1999). For example, a key carboxylate residue includes D144 of recA, or D256 of the β-subunit of F_1-ATPase, which is present at the C-terminus of the Walker B motif β-strand, and is the residue that coordinates Mg^{2+} (Story and Steitz, 1992; Abrahams *et al.*, 1994; Weber and Senior, 1997). Also included is E96 of recA, or βE188 of F_1-ATPase, which is found in a loop region following a β-strand between the Walker A and B motifs. This carboxylate is responsible for activating the catalytic water molecule and thus initiating hydrolysis (Yoshida and Amano, 1995). In other words, E96 of recA and βE188 of F_1-ATPase are catalytic carboxylates.

Recently, a crystal structure has been determined for an ABC transporter, the nucleotide binding subunit, HisP, of the bacterial histidine permease (Hung *et al.*, 1998). Overall, the structure of the HisP dimer is quite different from that of recA and F_1-ATPase. However, several carboxylates that appear to be structurally and functionally

related to the activating carboxylates of F_1 and recA are found in proximity to the ATP molecule, in the ATP binding pocket. In HisP, residue D178 hydrogen bonds a water molecule in proximity to the γ-phosphate of ATP. This water molecule has been proposed to replace Mg^{2+} in the crystal structure (Hung *et al.*, 1998), implying that D178 and its homologue in Pgp (D551/D1196) coordinate Mg^{2+} in the NB site. In addition, the adjacent residue, E179, hydrogen bonds a water molecule, possibly activating it to promote nucleophilic attack and hydrolysis of the γ-phosphate, implying that E179 may be the catalytic carboxylate in histidine permease. However, unlike in recA or F_1-ATPase, the catalytic glutamate E179 is not located between the Walker A and B sequences, but within the extended Walker B motif (Hung *et al.*, 1998). Yoshida et al. have proposed the presence of a catalytic carboxylate in ABC transporters (Yoshida and Amano, 1995); as a result, the presence of such a residue in Pgp was investigated.

In the study presented here, we have identified 14 acidic amino acids in the nucleotide binding (NB) sites of Pgp (mouse Mdr3) that are highly conserved in the NB sites of ABC transporters. The importance of these conserved carboxylates was tested by mutagenesis followed by functional analysis in yeast cells and after purification and reconstitution of the enzymes. A cluster of three acidic residues within and adjacent to the Walker B motif are shown to be highly mutation sensitive (D551/D1196, E552/E1197, and D558/D1203), with the negative charge at these positions playing a key role in ATP hydrolysis and ADP release.

3.3 Materials and Methods

3.3.1 Multiple Sequence Alignments and Secondary Structure Prediction

We used the server PredictProtein (http://www.embl.heidelberg.de/predict protein) (Rost and Sander, 1993) to search the SwissProt database for the closest relatives of the NB1 and NB2 sequences of the mouse Mdr3 protein. Two hundred sixty-nine (NB1) and 321 (NB2) partial or complete sequences corresponding to other ABC transporters were found whose amino acid sequences were more than 30% identical with those of the NB1 and NB2 of Pgp, respectively, a percentage proposed as the threshold for structural similarity (Rost and Sander, 1994). The program then aligned the sequences of the ABC transporters with the neural network MAXHOM (Rost, 1996). These multiple sequence alignments are available as Supporting Information.

3.3.2 mdr3 cDNA Modifications

Mutations in NB1 were created by site-directed mutagenesis using a recombinant PCR approach as described previously (Vogan and Gros, 1997) with a primer TK-5 (5'-GTGCTCATAGTTGCCTACA) and the mutagenic oligos for the D450N, E482Q, and D558N mutations: 5'-CTGTCCGTTGATACTGAC-3', 5'-CGAATGTTCTGGGCA-ATCGTGGTG-3', and 5'-CTTTCTGTATTCAGGGCTG-3', respectively. A second overlapping *mdr3* cDNA fragment was amplified using primer pairs *Hin*cII (5'-GAAAGCTGTCAACGAAGCC-3') and primer A (5'-CTGTGTCATGACAAGTTTG-AA-3'). The amplification products were purified on gel, mixed, denatured at 94 °C for 2 min, and then incubated at 72 °C for 5 min with Vent DNA polymerase (New England Biolabs) in a reaction mixture without primers to generate hybrid DNA fragments. The hybrid products were then amplified using primers TK-5 and oligoA, and a 552 bp *Nru*I-*Sal*I fragment carrying the mutated segment was purified and used to replace the corresponding fragment in the pVT-*mdr3* construct (Beaudet and Gros, 1995) which had served as a template in the PCR. This template contains engineered *Nru*I (position 1346) and *Sal*I sites (position 1908) to facilitate cloning of the mutated cDNA portion. To screen for the desired mutations, individual plasmids were isolated and the nucleotide sequence of the entire 552 bp *Nru*I-*Sal*I fragment was determined. A similar strategy was used to create mutants D592N and E604Q. The mutagenic oligos were 5'-CAATGACGTTAGCATTACG-3' and 5'-GTCATTGTGCAGCAGCAAGGAAA-3',

respectively, and an overlapping cDNA fragment was amplified with the primer pair *Hinc*II and CK-19 (5'-CATTTCAACCACTCCTG-3'). Here, a 340 bp *Sal*I-*Eco*RI fragment carrying the mutated segment was cloned into the corresponding sites of the pVT-*mdr3* construct. All amplification reactions were performed with Vent DNA polymerase. Mutations in NB2 were created by site-directed mutagenesis using a commercially available kit (Amersham, Arlington Heigths, IL) and single-stranded *mdr3.5* cDNA as a template, as previously described (Urbatsch *et al.*, 1998). These templates contained engineered *Nru*I (position 2724), *Sal*I (position 2480), *Spe*I (position 2914), *Sna*BI (position 3889), and *Age*I sites (position 4199) to facilitate subsequent cloning of the mutated cDNA portions. Mutagenic oligos for the D1093N, E1125Q, D1203, and E1249Q mutations were 5'-CTTTGCCATTTAGAAACAC-3', 5'-GGCAATGTTCTGCGCAATGCTGCAG-TC-3', 5'-TCAGCTCTGAATACAGAAAG-3', and 5'-AAGGTCAAGCAGCACGGC-3', respectively. The nucleotide sequence of the mutated segments was verified prior to their insertion in the corresponding sites of pVT-*mdr3.5* (Urbatsch *et al.*, 1998).

For the E552Q and E1197Q mutants, the *Mlu*I-*Sal*I cassette and the previously described *Pst*I-*Age*I cassette were used. The mutants were created by site-directed mutagenesis using a standard recombinant PCR method (Vogan and Gros, 1997). The PCR conditions were optimized for each primer set; the annealing temperature was usually between 52 and 56 °C with the $MgCl_2$ concentration within the range of 0.5-2.5 mM. The general cycles were as follows: denaturation (94 °C) for 1 min, annealing for 1 min, and DNA synthesis (72 °C) for 2 min. For E552Q, complementary primers were 5'-GGTGGCCTGGTCCAACAAAAG-3' (E552Q/r) and 5'-GTTGGACCAGGCCACCTC A-3' (E552Q/f) with two additional anchor primers, 5'-GACAACATACAAGGA-3' (L-12/f) and 5'-TCATGACAAGTTTGAA-3' (OligoA/r). For E1197Q, complementary primers were 5'-TGATGTTGCTTGGTCCAGAAG-3' (E1197Q/r) and 5'-CTTCTG GACCAAGCAACATC-3' (E1197Q/f) with two additional anchor primers, 5'-CAGC ATCCCACATCATC-3' (mer9f/f) and 5'-CCTTGATTGGAGACTTG-3' (pVTBamHI/r).

3.3.3 Testing of Mdr3 Function in Yeast Cells

pVT-*mdr3* plasmids carrying either wild-type or mutant versions of *mdr3* were transformed in the yeast *Saccharomyces cerevisiae* strain JPY201 (*MAT***a***ste6*Δ*ura3*)

using a lithium chloride technique (Gietz *et al.*, 1995). The biological activity of individual mass populations was tested with respect to their capacity to convey cellular resistance to the fungicidal agent FK506 (50 μg/mL) and to restore mating in the *ste6*Δ sterile yeast as previously described (Raymond *et al.*, 1994). Mating efficiency was calculated from the ratio of diploid colonies grown on minimal plates to the total number of haploid JPY201 transformants introduced into the mating assay, and is expressed as the percentage of the mating efficiency of WT *mdr3* transformants. Expression of wild-type and mutant Pgp variants in *S. cerevisiae* membranes was monitored by Western blot analysis of crude plasma membrane preparations, using the monoclonal anti-Pgp antibody C219 (Signet Labs Inc.).

3.3.4 Purification of P-Glycoprotein

For expression and purification of D558N and E552Q, *Afl*II-*Eco*RI cDNA subfragments were excised from pVT-*mdr3* and subcloned into the corresponding sites of pHIL-*mdr3.5*-His_6 as previously described (Urbatsch *et al.*, 1998). In the case of the D1203N and E1197Q mutants, they were introduced into pHIL-*mdr3.5*-His_6 as *Eco*RI-*Sna*BI fragments. pHIL-*mdr3.5*-His_6 carrying either wild-type or mutant versions of *mdr3* as well as the control pHIL-D2 vector were transformed into *Pichia pastoris* strain GS115, according to the manufacturer's instructions (InVitrogen, license number 145457). His^+ transformants exhibiting successful homologous recombination at the *AOX1* locus were identified as being unable to grow on medium containing methanol (methanol utilizing slow or mut^s). More than 90% of the His^+mut^s transformants that were identified were found to express Pgp, and expression levels of wild-type and mutant Mdr3 variants in these clones were very similar. For large-scale preparations of *P. pastoris* membranes, cultures were induced with methanol and plasma membranes were isolated by centrifugation on discontinuous sucrose density gradients, as previously described (Beaudet *et al.*, 1998b). From a 3 L culture, we routinely obtained between 40 and 50 mg of membrane protein at the 16 to 31% sucrose gradient interface. Solubilization and purification of wild-type and mutant Mdr3 variants on Ni-NTA resin (Qiagen) was essentially as described (Urbatsch *et al.*, 1998) and recently modified (Lerner-Marmarosh *et al.*, 1999).

3.3.5 Assay of ATPase Activity

For ATPase assays, the 80 mM imidazole eluate from the Ni-NTA resin was incubated with 1% *Escherichia coli* lipids (Avanti, acetone/ether preparation) and 1 mM DTT for 30 min at 20 °C, followed by sonication at 4 °C for 30 s in a bath sonicator (Ultrasonic Inc., Plainview, NY). Omission of DTT resulted in a completely inactive Pgp ATPase. Aliquots of 2-5 μL were added into 50 μL of 50 mM Tris-HCl (pH 8.0), 0.1 mM EGTA, 10 mM Na_2ATP, and 10 mM $MgCl_2$, and the mixture was incubated at 37 °C for the appropriate amount of time, during which the reaction was linear, and ≤10% of the added nucleotide was hydrolysed. Reactions were stopped by addition of 1 mL of 20 mM ice-cold H_2SO_4, and P_i release was assayed as described previously (Van Veldhoven and Mannaerts, 1987). For the determination of kinetic parameters, an excess of 2 mM $MgCl_2$ over MgATP concentrations was used. Drugs were added as dimethyl sulfoxide solutions, and the final solvent concentration in the assay was kept at ≤2% (v/v).

3.3.6 Vanadate Trapping and Photoaffinity Labelling with 8-Azido[α^{32}P]ATP

8-Azido[α^{32}P]ATP photoaffinity labelling was performed as previously described (Urbatsch *et al.*, 1998) with minor modifications. The 80 mM imidazole eluate containing purified Pgp was incubated with 1% *E. coli* lipids (Avanti, acetone/ether preparation) and 1 mM DTT for 30 min on ice, and reconstituted by dialysis at 4 °C (16 h) against 20 volumes of 50 mM Tris-HCl (pH 7.4), 0.1 mM EGTA, and 1 mM DTT. Proteoliposomes were concentrated by centrifugation for 2 h at 4 °C and 100000*g*, resuspended in the same dialysis buffer, and stored as aliquots at -80 °C. DTT concentrations of ≤1 mM did not interfere with subsequent photolabelling. Proteoliposomes containing wild-type or mutant Mdr3 variants were incubated with 5 μM 8-azido[α^{32}P]ATP (8.5 Ci/mmol), 3 mM $MgCl_2$, 50 mM Tris-HCl (pH 8.0), and 0.1 mM EGTA, with or without 200 μM vanadate in a total volume of 50 μL at 37 °C for the indicated periods of time. Verapamil or valinomycin (either at 100 μM) was included where indicated. The incubations were started by addition of 8-azido[α^{32}P]ATP and stopped by transfer on ice. Free label was promptly removed by centrifugation at 200000*g* for 30 min at 4 °C in a TL-100 rotor (Beckman), and proteoliposomes were washed and resuspended in 50 μL of ice-cold 50 mM Tris-HCl (pH 8.0) and 0.1 mM EGTA. Samples were kept on ice and irradiated with UV for 5 min {UVS-II Minerallight (260 nm) placed directly above the samples}. At an

8-azido[α^{32}P]ATP concentration of 5 μM, hydrolysis and subsequent vanadate-induced trapping of nucleotide are about 20 times slower than at 80 μM 8-azido[α^{32}P]ATP, a concentration we previously used in vanadate trapping experiments. This appreciably slower hydrolysis rate allows the demonstration of drug-stimulated 8-azido[α^{32}P]ATP hydrolysis and vanadate trapping as described previously (Szabo *et al.*, 1998). Upon UV irradiation, up to 10% of the mouse Mdr3 molecules became covalently labelled by 8-azido[α^{32}P]nucleotide and could be detected by gel electrophoresis (Urbatsch *et al.*, 1998). Orthovanadate solutions (100 mM) were prepared from Na_3VO_4 (Fisher Scientific) at pH 10 as described previously (Goodno, 1982) and boiled for 2 min before each use to break down polymeric species.

3.3.7 Routine Procedures

Protein concentrations were determined by the bicinchoninic acid method in the presence of 1% SDS using bovine serum albumin as a standard. SDS-PAGE was carried out according to Laemmli (Laemmli, 1970) using the Mini-PROTEAN II gel and Electrotransfer system (Bio-Rad). Samples were dissolved in 5% (w/v) SDS, 25% (v/v) glycerol, 0.125 M Tris-HCl (pH 6.8), 40 mM DTT, and 0.01% pyronin Y for 30 min at 37 °C and separated on 7.5% polyacrylamide gels. For immunodetection of Pgp, the mouse monoclonal antibody C219 (Signet laboratories Inc.) was used with the ECL detection system (Amersham). For autoradiography, SDS gels were stained with Coomassie Blue, dried, and exposed overnight at -80 °C to Kodak BioMax films with intensifying screens.

3.3.8 Materials

8-Azido[α^{32}P]ATP (8.5 Ci/mmol) and verapamil were purchased from ICN, while valinomycin and FK506 were from Calbiochem. L-α-Lysophosphatidylcholine and acetone/ether-precipitated *E. coli* lipids were from Avanti Polar Lipids, and general reagent grade chemicals were from Sigma.

3.4 Results

3.4.1 Identification of Highly Conserved Carboxylate Residues in Mdr3 and Other ABC Transporters

In this study, we aimed to identify catalytically important acidic amino acids present in each of the two NB sites of the Mdr3 ATPase. For this, we searched the SwissProt database and found 269 and 321 other ABC transporters whose amino acid sequences were more than 30% identical to those of the NB1 and NB2 of Pgp, respectively, a percentage proposed as the threshold for structural similarity (Rost and Sander, 1994). Table 3.1 lists the most conserved acidic amino acids (aspartate and glutamate) among these sequences and identifies seven sets of acidic amino acids (bold) with a high degree ($\geq$50%) of conservation in both NB sites (Table 3.1).

Although there may be significant structural differences among NB sites of ABC transporters, the high degree of primary sequence similarity between HisP and the two NB sites of Pgp (48% similar; *43*) has prompted us to use the recently determined crystal structure of the HisP dimer (Hung *et al.*, 1998) as a model for Pgp. Figure 3.1 shows an alignment of the amino acid sequences of the two NB sites of Mdr3 and HisP, and the location of α-helices and β-strands based on the HisP structure is also indicated. In the case of Mdr3, the beginning of NB1 and NB2 was assigned as the first residue after TM6 and TM12, respectively; the end of NB2 was the carboxy terminus of Mdr3, and alignment with NB2 defined the end of NB1 (Figure 3.1). The most conserved acidic amino acids and their location relative to the Walker A and B motifs are shown (Figure 3.1 and Table 3.1). The first set, D450 and D1093, is located 21 residues downstream of the Walker A motif and located at the C-terminal end of a β-strand. A second set, E482 and D1125, is found 53 residues downstream of the Walker A motif; these residues have previously been suggested as candidate II for a catalytic carboxylate based on alignments of ABC transporters with the F_1-ATPase (Yoshida and Amano, 1995) and also by alignment of the NB sites of CFTR with F_1-ATPase (Bianchet *et al.*, 1997). Aspartate D551 and D1196, respectively, are part of the well-described Walker B motif and have previously been mutated in our laboratory (Urbatsch *et al.*, 1998). By analogy to other ATPases, these aspartates are suggested to form a complex with Mg^{2+} of MgATP. Two

Table 3.1 Conservation of Acidic Amino Acids in the Nucleotide Binding Sites of Mdr3 and Other ABC Transporters

NBD1					NBD2				
	D	E	% D + E	no. of sequences aligned[a]		D	E	% D + E	no. of sequences aligned[a]
D366	55	20	58	129	E1009	26	40	46	143
D441	54	50	39	267	D1084	58	59	36	328
D450	**138**	**11**	**56**	**267**	**D1093**	**142**	**15**	**50**	**317**
D453[b]	102	26	48	267	E1096[b]	114	44	50	317
E472	29	39	25	269	E1115	90	59	47	319
E482[c]	**50**	**109**	**59**	**269**	**E1125[c]**	**60**	**146**	**64**	**320**
D494	47	78	46	269	E1139	33	109	44	320
E495	25	93	44	269	E1140	24	112	43	320
D551	**266**	**0**	**100[d]**	**266**	**D1196**	**317**	**0**	**100[d]**	**317**
E552	**9**	**256**	**100[e]**	**266**	**E1197**	**10**	**306**	**100[e]**	**317**
D558	**260**	**1**	**98[e]**	**266**	**D1203**	**307**	**0**	**97[e]**	**317**
E562	18	85	39	266	E1207	20	89	34	317
D592	**173**	**12**	**70**	**264**	**D1237**	**227**	**9**	**74**	**317**
E604	**1**	**151**	**62[f]**	**246**	**E1249**	**2**	**166**	**54[g]**	**310**

[a] Total number of sequences aligned for each position (because some sequences are only partial, not all sequences can be aligned for each position). [b] Predicted by Yoshida (Yoshida & Amano, 1995) to be candidate I for a catalytic carboxylate. [c] Predicted by Yoshida (Yoshida & Amano, 1995) to be candidate II for a catalytic carboxylate. [d] Residues of the classical Walker B motifs. Previous substitutions D551N and D1196N revealed completely inactive enzymes. By analogy to other ATPases, these residues are involved in forming a complex with Mg^{2+} of MgATP (Nadanaciva *et al.*, 1999). [e] These residues are part of the extended Walker B motif typically found in ABC transporters (Holland & Blight, 1999). [f] Present in only 246 of the 270 aligned ABC transporters. [g] Present in only 310 of the 321 aligned ABC transporters.

Figure 3.1:

Nucleotide binding sites of the mouse Mdr3 ATPase

The amino acid sequences of the N-terminal (NB1) and C-terminal nucleotide binding sites (NB2) of mouse Mdr3 and HisP are aligned (van Veen *et al.*, 1996). The beginning of NB1 or NB2 was defined as the first residue after the transmembrane region TM6 or TM12, respectively; the end of NB2 was defined as the carboxy terminus of Mdr3, and alignment with NB2 was used to define the end of NB1. Residues which were $\geq$50% conserved among ABC transporters (see Table 1) are shown. α-Helices and β-strands from the crystal structure of HisP are identified (van Veen *et al.*, 1996). Small letters indicate gaps in the HisP sequence.

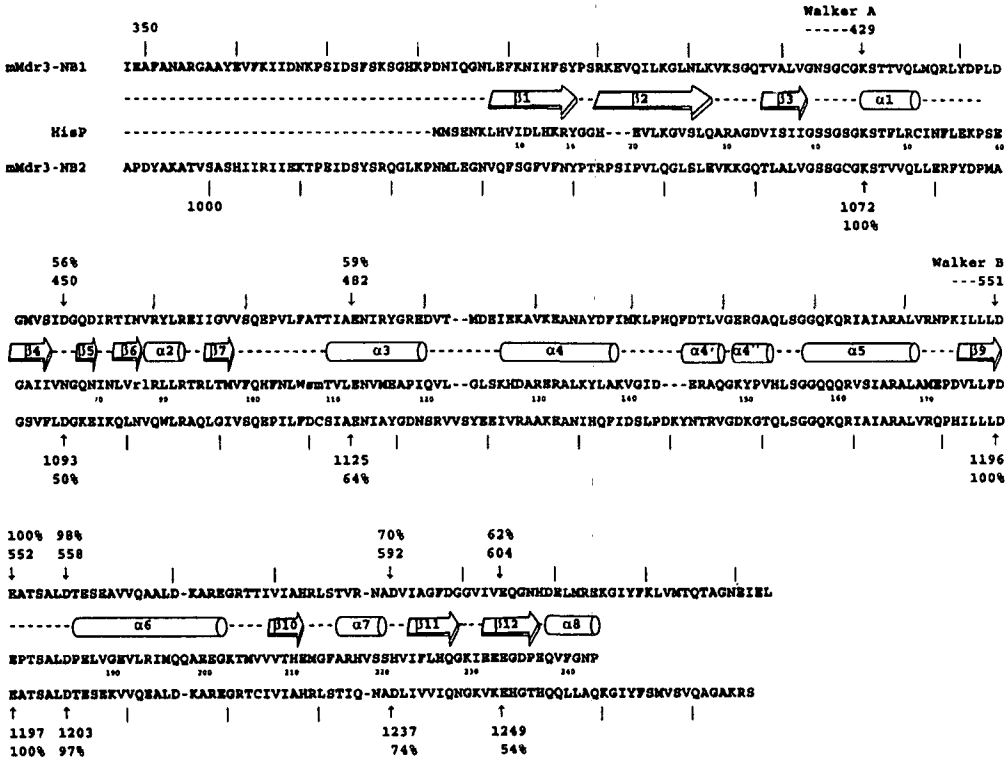
Walker A
350
429
mMdr3-NB1
IEAPANARGAAYEVFKIIDNKPSIDSFSKSGHKPDNIQGNLEFKNIHFSYPSRKEVQILKGLNLKVKSGQTVALVGNSGCGKSTTVQLMQRLYDPLD
β1
β2
β3
α1
HisP
MNSENKLHVIDLHKRYGGH---EVLKGVSLQARAGDVISIIGSSGSGKSTFLRCINFLEKPSE
mMdr3-NB2
APDYAKATVSASHIIRIIEKTPEIDSYSRQGLKPNMLEGNVQFSGFVFNYPTRPSIPVLQGLSLEVKKGQTLALVGSSGCGKSTVVQLLERFYDPMA
1000
1072
100%
56%
59%
Walker B
450
482
551
GMVSIDGQDIRTINVRYLREIIGVVSQEPVLFATTIAENIRYGREDVT--MDEIEKAVKEANAYDFIMKLPHQFDTLVGERGAQLSGGQKQRIAIARALVRNPKILLLD
β4
β5
β6
α2
β7
α3
α4
α4'
α4''
α5
β9
GAIIVNGQNINLVrlRLLRTRLTMVFQHFNLWsmTVLENVMEAPIQVL--GLSKHDARERALKYLAKVGID---ERAQGKYPVHLSGGQQQRVSIARALAMEPDVLLFD
GSVFLDGKEIKQLNVQWLRAQLGIVSQEPILFDCSIAENIAYGDNSRVVSYEEIVRAAKEANIHQFIDSLPDKYNTRVGDKGTQLSGGQKQRIAIARALVRQPHILLLD
1093
1125
1196
50%
64%
100%
100%
98%
70%
62%
552
558
592
604
EATSALDTESEAVVQAALD-KAREGRTTIVIAHRLSTVR-NADVIAGFDGGVIVEQGNHDELMREKGIYFKLVMTQTAGNEIEL
α6
β10
α7
β11
β12
α8
EPTSALDPELVGEVLRIMQQAREGKTMVVVTHEMGFARHVSSHVIFLHQGKIEEEGDPEQVFGNP
EATSALDTESEKVVQEALD-KAREGRTCIVIAHRLSTIQ-NADLIVVIQNGKVKEHGTHQQLLAQKGIYFSMVSVQAGAKRS
1197
1203
1237
1249
100%
97%
74%
54%

more sets, glutamate E552 and E1197, and aspartate D558 and D1203, respectively, are part of an "extended" Walker B motif typical of ABC transporters (Holland and Blight, 1999), and both sets of carboxylate residues are completely conserved in all ABC transporters that have been analyzed (Table 3.1). In addition, in the crystal structure of HisP, a glutamate (E179) is located within 4.3 Å of ATP and has been suggested to position the water molecule for a hydrolytic attack on the γ-phosphate (catalytic carboxylate) (Hung *et al.*, 1998). Glutamates E552 and E1197 appear to map at the homologous position of E179 in HisP. Finally, two more sets of conserved carboxylates, D592 and D1237 and E604 and E1249, are situated 40 and 52 amino acids downstream from the Walker B motifs, respectively (Figure 3.1).

3.4.2 Effects of NB Site Mutations on Mdr3 Function.

Single-point mutations D450N, E482Q, E552Q, D558N, D592N, and E604Q were introduced into the NB1 of Mdr3, and mutations D1093N, E1125Q, E1197Q, D1203N, D1237N, and E1249Q were introduced independently into the NB2. Mutations were inserted into pVT-*mdr3* and transformed in yeast *S. cerevisiae* strain JPY201. {The Walker B motif mutants D551N and D1196N have previously been shown to abrogate the ability of Mdr3 to confer MDR in vivo, as well as to abolish ATPase activity of the purified enzymes (Urbatsch *et al.*, 1998), and were included here for comparison.} Immunoblotting of crude membrane fractions from yeast transformants expressing individual mutants using the anti-Pgp antibody C219 showed similar levels of expression of the various Pgp mutants (Figure 3.2), suggesting that these mutations do not have a major effect on Mdr3 stability or membrane targeting in yeast. To assess the biological activity of these mutants, their ability to confer resistance to the fungicide FK506 was tested in a growth inhibition assay in liquid medium (Raymond *et al.*, 1994). Cells expressing WT Mdr3 or the NB1 mutants D450N, E482Q, D592N, and E604Q (Figure 3.3 A) or their NB2 counterparts D1093N, E1125Q, D1237N, and E1249Q (Figure 3.3 B) were all resistant to FK506. However, E552Q and D558N (NB1) failed to grow in FK506 and were indistinguishable from negative control *S. cerevisiae* cells transformed with either pVT vector, or with the Walker B motif mutant D551N (Figure 3.3 A). On the other hand, cells expressing D1203N (the NB2 counterpart of the D558N mutant) were also severely impaired for growth in FK506, although they retained some growth

Figure 3.2:

Expression of wild-type and mutant Mdr3 variants in S. cerevisiae

Western blot analysis of crude plasma membranes from mass populations of individual Mdr3 mutants (identified) in the yeast *S. cerevisiae* using the mouse monoclonal anti-Pgp antibody C219. pVT corresponds to control yeast cells transformed with the plasmid vector. Pgp is identified by an arrow, and the position of molecular mass markers is identified.

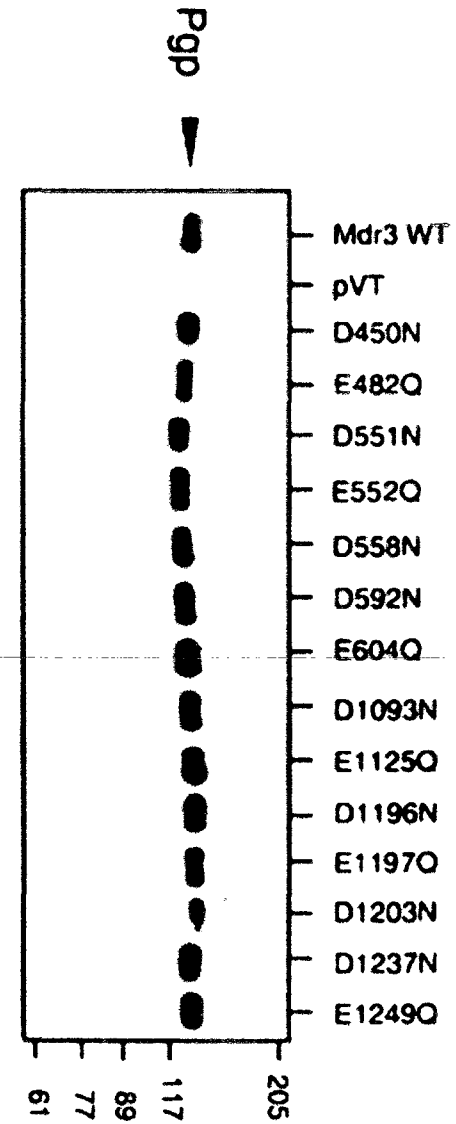
Pgp
Mdr3 WT
pVT
D450N
E482Q
D551N
E552Q
D558N
D592N
E604Q
D1093N
E1125Q
D1196N
E1197Q
D1203N
D1237N
E1249Q
61
77
89
117
205

Figure 3.3:

Drug resistance of wild-type and mutant Mdr3 variants

The capacity of WT and mutant Mdr3 variants to confer cellular resistance to FK506 in the yeast *S. cerevisiae* was measured by a growth inhibition assay. Growth of individual mass populations in 50 μg/mL FK506 is expressed as the relative growth compared to growth of the same cell populations in drug-free medium (expressed as a percentage). D551N and D1196N are mutations of the classical Walker B motifs previously described (Hrycyna *et al.*, 1999) and were included for comparison. Mutants D551N (*inverted light-grey triangle*), E552Q (*black square*), and D558N (*grey square*) in NB1 (A) and D1196N (*inverted light-grey triangle*) and E1197Q (*black square*) in NB2 (B) were indistinguishable from the pVT negative control which does not express Mdr3. Shown is one representative of at least three independent experiments.

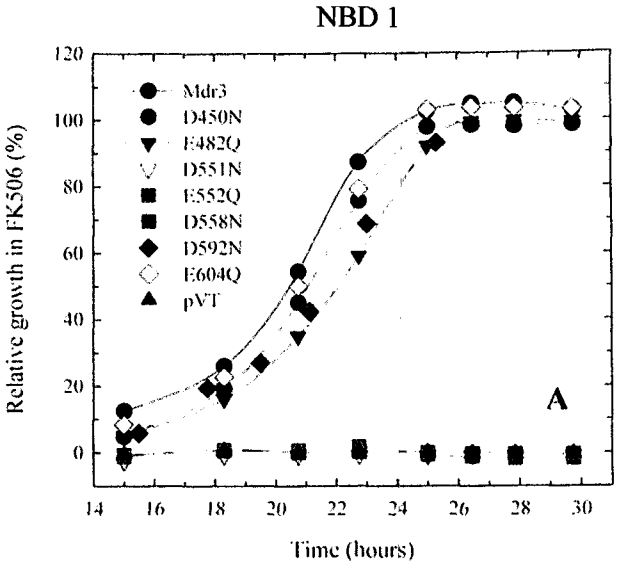
NBD 1
Relative growth in FK506 (%)
Time (hours)
Mdr3
D450N
E482Q
D551N
E552Q
D558N
D592N
E604Q
pVT
A
120
100
80
60
40
20
0
14
16
18
20
22
24
26
28
30

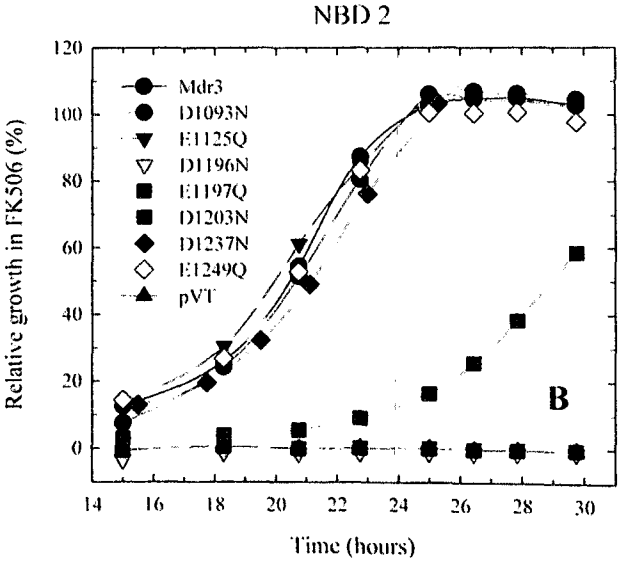
NBD 2
Relative growth in FK506 (%)
Time (hours)
Mdr3
D1093N
E1125Q
D1196N
E1197Q
D1203N
D1237N
E1249Q
pVT
B
120
100
80
60
40
20
0
14
16
18
20
22
24
26
28
30

potential which was detectable only upon extended incubation (>26 h) (Figure 3.3 B). In the NB2 group, only mutant E1197Q did not convey resistance to FK506 and showed growth characteristics similar to those of its NB1 counterpart E552Q, the pVT vector control, and the Walker B motif mutant D1196N (Figure 3.3 B). We also measured the capacity of the various Mdr3 mutants to restore mating in the sterile *ste6*Δ yeast strain JPY201 (Raymond *et al.*, 1994). The mating frequency was calculated as the fraction of transformed JPY201 cells forming diploid colonies on selective medium (over the total number of cells introduced in the assay) and was expressed as a percentage of the mating frequency displayed by WT Mdr3 cells. Mating frequencies of mutants D450N (104%), E482Q (127%), D592N (22%), and E604Q (85%) in NB1 (Figure 3.4) or their counterparts D1093N (72%), E1125Q (101%), D1237N (68%), and E1249Q (118%) in NB2 (Figure 3.4) were similar to that of the Mdr3 WT control. However, mating was completely impaired in the NB1 mutants E552Q (<0.1%) and D558N (0.15%), and the frequencies were similar to those measured in the pVT negative control (<0.2%) and for the Walker B mutant D551N (<0.2%) (Figure 3.4). Mutant E1197Q in the NB2 was completely impaired (<0.1%), similar to its counterpart E552Q in the NB1. In contrast, mutant D1203N in the NB2 (counterpart of D558N) was severely impaired (2.4%), but still retained some residual activity above the background levels seen in pVT or in Walker B motif mutant D1196N (<0.2%) (Figure 3.4).

Taken together, functional analysis of mutations of the six most conserved carboxylate residues in either NB site identified two sets of carboxylate residues, E552 and E1197 and D558 and D1203, as required for Mdr3 biological activity. These results suggest that these residues play a key role in Pgp function. For further analysis, mutants E552Q and E1197Q as well as D558N and D1203N were expressed in the yeast *P. pastoris* followed by purification and ATPase activity measurements.

3.4.3 Expression and Purification of NB Site Mutants in P. pastoris.

For large-scale production of plasma membranes and subsequent Mdr3 purification, we reconstructed E552Q and E1197Q, and D558N and D1203N, in plasmid vector pHIL-*mdr3*-His_6 and expressed the corresponding Pgp variants in the yeast *P. pastoris* (Urbatsch *et al.*, 1998). Crude membrane fractions were prepared from independent colonies of *P. pastoris* transformants and analyzed for Mdr3 protein

Figure 3.4:

Mating frequencies of yeast mass populations expressing wild-type and mutant Mdr3 variants

Mating frequency represents the proportion of transformed **a**-type JPY201 cells that formed diploids upon mating with α-type tester cells DC17, followed by plating on minimal medium. Values are the average of at least three independent experiments and are expressed as percentage of the wild-type frequency ± the standard error of the mean. D551N and D1196N are mutations of the classical Walker B motifs previously characterized (Hrycyna *et al.*, 1999).

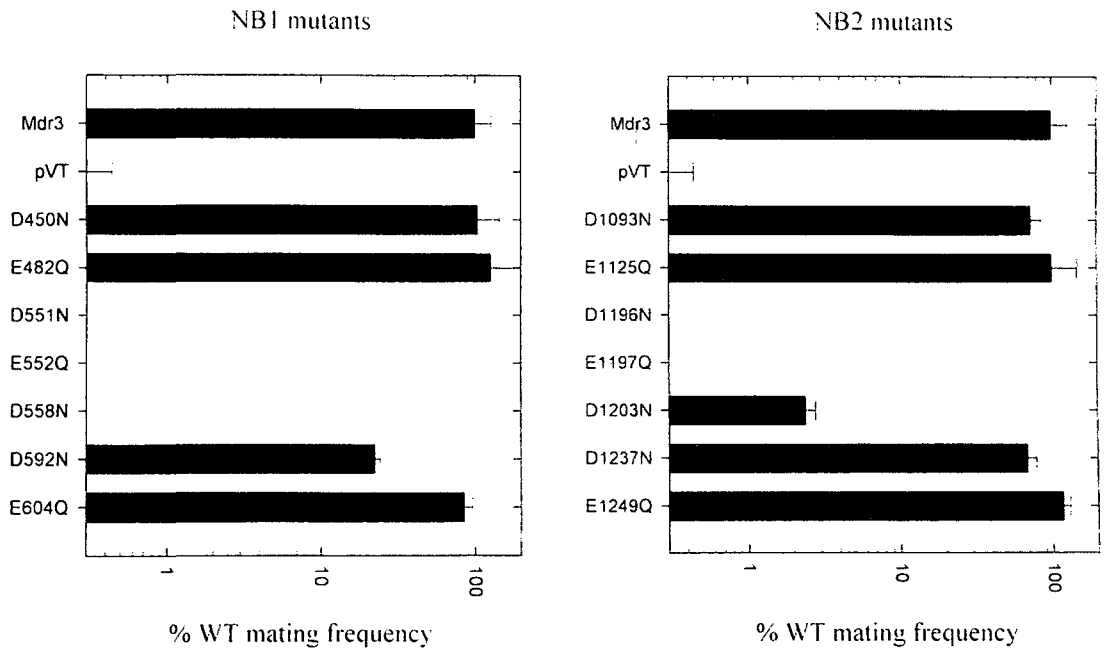
NB1 mutants
Mdr3
pVT
D450N
E482Q
D551N
E552Q
D558N
D592N
E604Q
1
10
100
% WT mating frequency
NB2 mutants
Mdr3
pVT
D1093N
E1125Q
D1196N
E1197Q
D1203N
D1237N
E1249Q
1
10
100
% WT mating frequency

expression. All Mdr3 mutants could be stably expressed in membrane fractions of *P. pastoris*, and the levels of expression of the mutants were very similar to that seen in cells expressing WT Mdr3 (data not shown). Individual Mdr3 mutants were purified from large-scale plasma membrane preparations by Ni-NTA chromatography as previously described (Urbatsch *et al.*, 1998). All mutant proteins yielded Mdr3 with equal purities and in similar amounts, comparable to those seen for the wild-type protein, as judged by Coomassie Blue-stained SDS gels and Western blot analysis (Figure 3.5).

3.4.4 ATPase Activity of Mdr3 and NB Site Mutants.

Steady-state ATP hydrolysis by the purified proteins was assessed, following reconstitution in *E. coli* lipids, in the absence and presence of different drugs (Table 3.2). The very low level of ATPase activity of the negative control pHIL-D2 proteoliposomes ranged from 0.05 to 0.10 μmol min^{-1} mg^{-1} (averages from two purifications), was not stimulated by verapamil, valinomycin, or FK506, and was probably caused by low-level contamination from residual plasma membrane ATPases. On the other hand, WT Mdr3 exhibited a basal ATPase activity {0.34 μmol min^{-1} (mg of protein)$^{-1}$} that could be strongly stimulated by verapamil, valinomycin, and FK506 (3.1-12-fold stimulation). Mutants E552Q and E1197Q exhibited very low basal ATPase activity that was similar to that detected in the pHIL-D2 negative control. However, unlike WT Mdr3, the ATPase activity was not stimulated by any of the drugs that were tested (Table 3.2). Thus, the loss of drug resistance and *ste*6 complementation seen in the E552Q and E1197Q mutants is associated with a complete loss of drug-stimulated ATPase activity (as measured by standard P_i release assays). These results indicate that carboxylates E552 and E1197 are essential for drug-stimulated ATP hydrolysis by Pgp. Since the mutants did not display any drug stimulation of ATP hydrolysis over a range of drug concentrations that were tested (1-200 μM, data not shown), we could not determine the K_M values as a measure for the binding affinities for MgATP. Preliminary data for 8-azido-ATP binding and drug binding to Pgp did not show major differences from WT Mdr3, suggesting proper folding of the purified enzymes (data not shown).

Mutants D558N and D1203N displayed significant drug-stimulated ATPase activity (Table 3.2). In the mutant D558N, the K_M (MgATP) was 0.66 and 0.79 mM in the presence of verapamil and valinomycin, respectively, and in the D1203N mutant, the

Figure 3.5:

Purification of NB site mutants from P. pastoris membranes

Wild-type and mutant Mdr3-His_6 variants (identified at the top of panel A) were expressed in the yeast *P. pastoris* and purified by Ni-NTA chromatography. Three micrograms (protein) from the 80 mM imidazole elution fractions was precipitated with TCA, subjected to SDS gel electrophoresis, and stained with Coomassie Blue (A). Western blot analysis of purified proteins with the mouse monoclonal anti-P-glycoprotein antibody C219 (B). The positions of molecular mass markers are given in kilo-Daltons on the right.

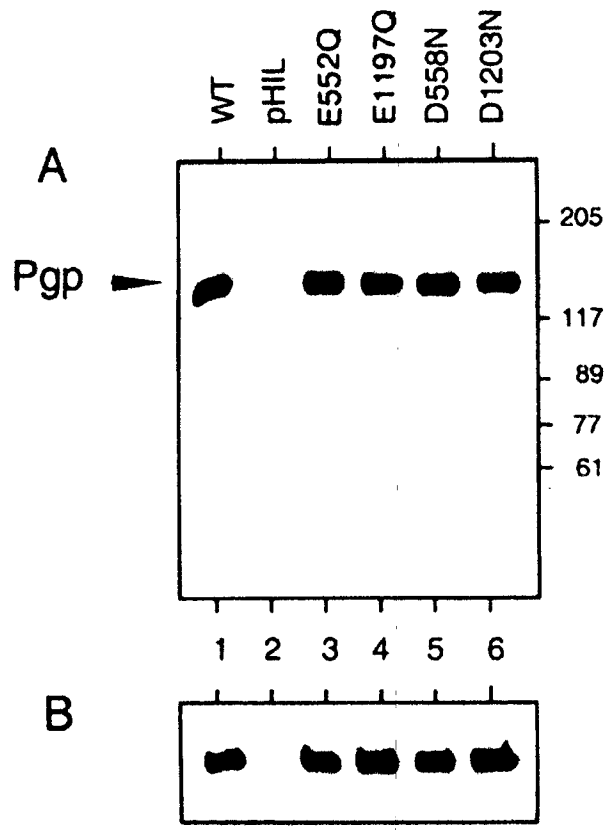
WT
pHIL
E552Q
E1197Q
D558N
D1203N
A
Pgp
205
117
89
77
61
1 2 3 4 5 6
B

Table 3.2 Characteristics of ATPase Activity of Wild-Type Mdr3 and NB Site Mutants

	Specific ATPase activity (μmol min^{-1} mg^{-1})[a]			
	No drug	Verapamil	Valinomycin	FK506
WT	0.34 ± 0.10	3.95 ± 0.10 (12-fold)	3.33 ± 0.33 (10-fold)	1.06 ± 0.073 (3.1-fold)
pHIL-D2[b]	0.066 ± 0.024	0.059 ± 0.004	0.053 ± 0.03	0.097 ± 0.056
E552Q	0.072 ± 0.031	0.077 ± 0.022 (1-fold) (2%[c])	0.084 ± 0.028 (1-fold) (3%)	0.067 ± 0.034 (1-fold) (6%)
E1197Q	0.054 ± 0.026	0.062 ± 0.019 (1-fold) (2%)	0.051 ± 0.022 (1-fold) (2%)	0.059 ± 0.033 (1-fold) (6%)
D558N	0.049 ± 0.044	0.45 ± 0.083 (9.2-fold) (11%)	0.44 ± 0.067 (9.0-fold) (13%)	0.19 ± 0.088 (93.9-fold) (18%)
D1203N	0.093 ± 0.034	1.02 ± 0.146 (11-fold) (26%)	0.95 ± 0.084 (10-fold) (29%)	0.37 ± 0.066 (4-fold) (35%)

[a] ATPase activities were assayed as described in Materials and Methods. All values are the mean of at least three experiments ± the standard error of the mean. Values in parentheses are the stimulation over basal activity in the absence of drug. Verapamil, valinomycin, and FK506 were added at concentrations of 100, 100, and 40 μM, respectively. [b] Please note that wild-type and Mdr3 mutants consist of >90% of P-glycoprotein and <10% impurities. Negative control proteoliposomes prepared from vector transformants pHIL-D2 consist of 100% impurities. [c] ATPase activity of individual mutants expressed as a fraction (percentage) of that of wild-type Mdr3.

K_M (MgATP) was 0.49, 0.53, and 0.46 mM in the presence of verapamil, valinomycin, and FK506, respectively (the ATPase activity of D558N in FK506 was too low to calculate a K_M accurately). These values were similar to those for WT Mdr3 for all the drugs that were assayed, indicating that the binding affinities for MgATP were not affected. However, V_{max} values varied considerably in these mutant enzymes, and in most cases, there was a good correlation between the activity of these mutants in drug resistance and mating assays and their ATPase activity. In the absence of drug, the ATPase activity of D558N was indistinguishable from that seen in control pHIL-D2 proteoliposomes, and as such was 10 times lower than that for WT Mdr3. However, in the presence of verapamil (100 μM), valinomycin (100 μM), or FK506 (40 μM), this mutant could hydrolyse ATP with a specific activity corresponding to 11, 12, or 18% of WT Mdr3, respectively (Table 3.2). From this, it appears that an 80-90% reduction in ATPase activity is sufficient to abolish Mdr3 biological activity (in mutant D558N), as assessed by FK506 resistance and *ste6* complementation. The homologous D1203N substitution in the NB2 displayed 26, 29, and 35% of the drug-stimulated ATPase activity of WT Mdr3 (Table 3.2). Thus, reduced drug resistance and mating activity caused by the D1203N mutation were associated with reduced ATPase activity. Moreover, the more severe effect of the D558N mutation on biological activity (drug resistance) when compared to D1203N was also paralleled by a more severe loss of ATPase activity.

Finally, E552Q, E1197Q, D558N, and D1203N are located just downstream of Walker B motif aspartates D551 and D1196 (Figure 3.1); thus, we were interested in determining whether these Mdr3 residues may also be involved in forming a complex with Mg^{2+} of MgATP, and whether impaired Mg^{2+} binding may be in part responsible for loss of activity in those mutants. Varying the Mg^{2+} concentration from 0.1 to 100 mM did not restore drug stimulation of ATPase activity in E552Q or E1197Q, and did not increase the drug-stimulated ATPase activity of D558N or D1203N (data not shown). From this, we conclude that both residues are important for efficient ATP hydrolysis to occur in the NB sites of the Mdr3 ATPase, although they are probably not directly involved in complexing Mg^{2+}.

3.4.5 Vanadate Trapping with Mg-8-Azido[α^{32}P]ATP.

We used the technique of vanadate (V_i) trapping of nucleotide to monitor hydrolysis of Mg-8-azido[α^{32}P]ATP in each of the NB site mutants of Mdr3. It has been previously established that vanadate trapping requires hydrolysis of ATP and that the trapped nucleotide species in Pgp is ADP (Shyamala *et al.*, 1991; Urbatsch *et al.*, 1995b). The mechanism of vanadate trapping requires first hydrolysis of the bond between the β- and γ-phosphates followed by dissociation of the terminal phosphate (P_i). This allows V_i to come in while MgADP is still bound in the site. V_i then occupies essentially the same position as the γ-phosphate previously did, and a long-lived intermediate is thus formed with bound {Mg·8-azido-ADP·V_i}, which resembles the normal transition state (Urbatsch *et al.*, 1995b). In initial experiments, WT Mdr3 was preincubated for 0.5-20 min at 37 °C with 5 μM Mg-8-azido[α^{32}P]ATP in the presence of vanadate (and in the absence or presence of verapamil) to allow trapping, followed by removal of unbound ligands by centrifugation, and finally cross-linking of the trapped nucleotide by UV irradiation. Photolabelling by the radionucleotide was readily detectable in WT Mdr3 after trapping for only 0.5 min, in the presence of verapamil, and this level of labelling increased rapidly upon augmenting the trapping periods (Figure 3.6). In the absence of drug, trapping and photolabelling were significantly slower, in agreement with a lower rate of ATP hydrolysis. At an 8-azido[α^{32}P]ATP concentration of 5 μM, the hydrolysis is slow, allowing one to distinguish between basal and drug-stimulated trapping and photolabelling (Szabo *et al.*, 1998; Urbatsch *et al.*, 1998). Under these conditions, vanadate-induced trapping of labelled nucleotide that can be strongly stimulated by verapamil and valinomycin was readily seen in WT Mdr3 (Figure 3.7 A). Trapping and photolabelling were completely absent in control pHIL-D2 proteoliposomes (not shown). As we previously reported (Urbatsch *et al.*, 1998), a mutation at the highly conserved Walker B aspartate of Mdr3 D551 (D551N), which is known to completely impair ATP hydrolysis and drug resistance, also abrogates vanadate-induced trapping of nucleotide in the presence or absence of drugs (Figure 3.7 A).

The purified and reconstituted mutants D558N and D1203N showed basal as well as drug-stimulated trapping and photolabelling in the presence of verapamil or valinomycin (Figure 3.7 B). We overexposed this autoradiograph to show the low level of

Figure 3.6:

Time dependence of vanadate trapping of Mg-8-azido-[α^{32}P]ATP in wild-type Mdr3

Purified reconstituted wild-type Mdr3 was preincubated with 5 μM 8-azido[α^{32}P]ATP, 3 mM $MgCl_2$, and 200 μM vanadate in the absence or presence of 100 μM verapamil. The times of preincubation at 37 °C are shown above the lanes. Unbound ligands were removed by ultracentrifugation and washing followed by UV irradiation. Photolabeled samples were separated by electrophoresis on SDS gels and subjected to autoradiography. Experiments were carried out in duplicate.

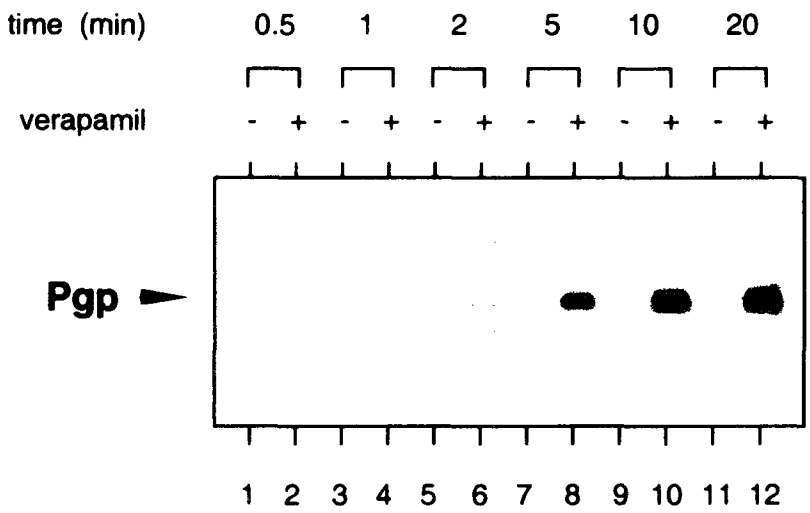
time (min)
0.5
1
2
5
10
20
verapamil
- + - + - + - + - + - +
Pgp
1 2 3 4 5 6 7 8 9 10 11 12

Figure 3.7:

Photolabelling of Mdr3 NB site mutants by vanadate trapping with Mg-8-azido-[α^{32}P]ATP

Purified reconstituted wild-type and mutant Mdr3 variants were preincubated with 5 μM 8-azido[α^{32}P]ATP and 3 mM $MgCl_2$ for 20 min at 37 °C in the absence or presence of 200 μM vanadate. Verapamil (100 μM) or valinomycin (100 μM) was included as indicated above the lanes. Unbound ligands were removed by ultracentrifugation and washing followed by UV irradiation (Materials and Methods). Photolabeled samples were separated by electrophoresis on SDS gels, transferred to a nitrocellulose membrane, and subjected to autoradiography. Experiments were carried out in duplicate.

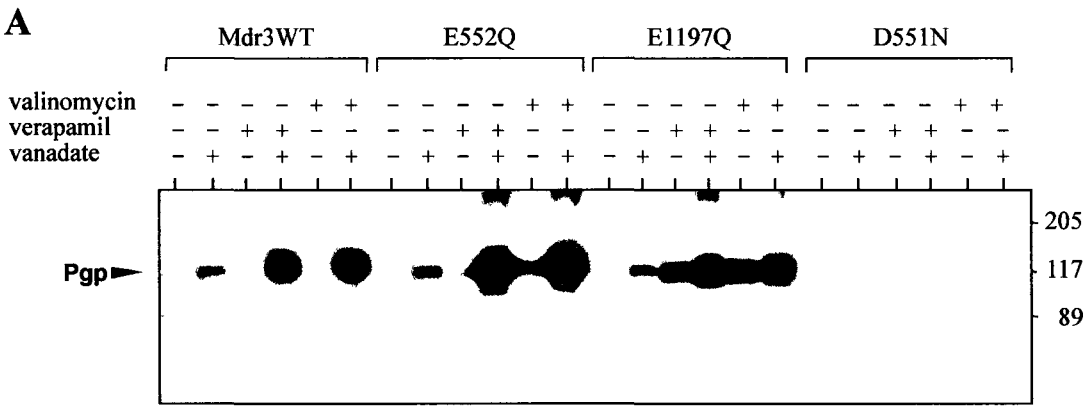
A
Mdr3WT
E552Q
E1197Q
D551N
valinomycin
verapamil
vanadate
Pgp
205
117
89

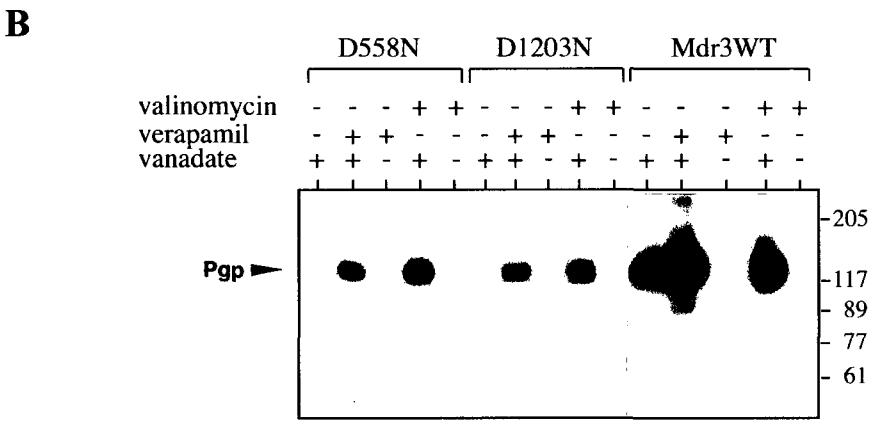
B
D558N
D1203N
Mdr3WT
valinomycin
verapamil
vanadate
Pgp
205
117
89
77
61

vanadate-induced trapping of 8-azidonucleotide and photolabelling of the 140 kDa P-glycoprotein in the absence of verapamil or valinomycin (lane 1, Figure 3.7 B), which strongly suggests that the low level of ATP hydrolysis exhibited by D558N (Table 3.2) is a true reflection of residual Mdr3 ATPase in this mutant, as opposed to contaminating ATPase activities. Increased levels of trapping and photolabelling in the presence of different drugs were noted in the D558N, D1203N, and WT Mdr3 proteins (Figure 3.7 B), in agreement with direct ATP hydrolysis data (Table 3.2).

Analysis of the E552Q and E1197Q mutants revealed unique and unexpected nucleotide trapping properties. Although E552Q is catalytically inactive in the standard ATPase assay (P_i release), vanadate-induced trapping of 8-azido[α^{32}P]nucleotide and subsequent photo-cross-linking were seen in E552Q, with trapping strongly stimulated by verapamil and valinomycin (Figure 3.7 A). This drug-stimulated trapping was similar to that detected for WTMdr3, and suggests that this mutant is capable of completing partial reactions of the ATP hydrolysis cycle. An additional unique feature of E552Q is that photolabelling with 8-azido-ATP could also be induced by drug molecules in the absence of vanadate. Under these conditions, the amount of labelled nucleotide bound was smaller than that seen in the presence of vanadate, but was still clearly greater than the very low background levels seen in control conditions lacking vanadate and drugs (Figure 3.7 A). This behavior is clearly distinct from that seen in WT Mdr3, where vanadate is required to observe nucleotide trapping under any condition. The nucleotide trapping properties of the homologous mutant in NBD2, E1197Q, were very similar to those of E552Q with respect to vanadate-induced trapping, and stimulation of trapping by drugs. Interestingly, E1197Q, in addition to being photolabelled in the absence of vanadate and presence of drugs (like E552Q), can also be photolabelled to a low level in the absence of vanadate and of drug molecules, a behavior distinct from that of E552Q and WT Mdr3. Parallel immunoblotting analysis of the photolabelled WT and mutant Mdr3 indicates equal amounts of protein loaded on gels, and transferred to membrane (data not shown).

3.5 Discussion

The aim of the study presented here was to identify catalytically important acidic amino acids in the two NB sites of the Mdr3 ATPase. Sequence alignments of the Mdr3 NB sites with other ABC transporters pointed out seven sets of acidic amino acids which were well conserved (Figure 3.1). These residues were studied by mutational analysis. Single-point mutations D450N, E482Q, D592N, and E604Q were introduced in NB1 and their homologous substitutions D1093N, E1125Q, D1237N, and E1249Q created in NB2, and the mutants were transformed in the yeast *S. cerevisiae* to assess their biological activity. These four sets of Mdr3 mutants were fully functional in two independent assays, cellular resistance to FK506 (Figure 3.3), and restoration of mating in an otherwise sterile *ste6*Δ yeast mutant (Figure 3.4). The results indicate that acidic amino acids at these positions in both NB sites are not critical for Mdr3 transport activity, and thus are unlikely to serve as catalytic carboxylate residues. Several acidic amino acids perfectly conserved among ABC transporters are found in the "extended" Walker B motif which incorporates a highly distinctive signature motif, the consensus HbHbHbHbD (Hb, hydrophobic) followed by "EA/PTSALD" or similar (Figure 3.1) (Holland and Blight, 1999). Removal of the charge in D551N and D1196N (previously analyzed in ref. Urbatsch *et al.*, 1998), E552Q and E1197Q (this study), and D558N and D1203N (this study) severely impaired transport activity in yeast, and steady-state ATP hydrolysis indicating that these residues are important for Mdr3 function. The negative charge of the glutamate residue at positions 551 and 1196 is completely conserved in the Walker B motif of ABC transporters (Table 3.1). Mutations at that site have previously been shown to abrogate function by impairing ATPase activity, as measured both in ATPase assays (P_i release) and by vanadate-induced trapping of nucleotides (completion of reaction steps leading to occlusion of $MgADP{\cdot}V_i$) (Urbatsch *et al.*, 1998). While E552Q (NB1), E1197Q (NB2), and D558N (NB1) failed to grow in FK506 (Figure 3.3) and were completely impaired in mating (Figure 3.4), D1203N (NB2) retained residual activity in both assays. We purified the mutant enzymes from the yeast *P. pastoris* to monitor Mdr3 specific ATP hydrolysis. Mutants D558N and D1203N both retained readily detectable but low levels of steady-state ATP hydrolysis in the presence of verapamil, valinomycin, and FK506 (Table 3.2), while mutants E552Q and E1197Q had no drug-stimulated

ATPase activity. Thus, the biological activity in yeast seemed to correlate well with the ATPase activity of the purified mutant enzymes. Overall, it appears that a drug-stimulated ATPase activity of ≤18% is insufficient to energize drug transport and show biological activity in yeast; e.g., the biological assay shows sensitivity to impairment of ATPase. Interestingly, a drug-stimulated ATPase activity of 30% in the D1203N mutant supported some biological activity, indicating that interactions may be different for NB1 and NB2, since the mutant at the homologous residue in the NB1 had more severe effects. Possible functional differences between the NB1 and NB2 of Pgp have recently been documented by Hrycyna et al. (Hrycyna *et al.*, 1999), while studying human MDR1 by photolabelling with 8-azido-ATP under binding and hydrolysis conditions. Finally, an important role for acidic residues in the extended Walker B motifs has been independently noted at the homologous position of distantly related bacterial ABC transporters HisP (Shyamala *et al.*, 1991), KpsT (Bliss *et al.*, 1996), and MalK (Stein *et al.*, 1997).

To further investigate the mechanistic basis for the partial or complete loss of function seen in these mutants, we applied the technique of vanadate trapping of nucleotide in the purified reconstituted NB site mutants. Previous studies have demonstrated that vanadate-induced trapping requires hydrolysis of 8-azido-ATP to 8-azido-ADP and that a stable {Pgp**·Mg·8-azido-ADP·V_i} transition-state complex forms, which can be cross-linked to the protein (Urbatsch *et al.*, 1995a; Urbatsch *et al.*, 1995b). In the D558N mutant, vanadate trapping and photolabelling of the140 kDa P-glycoprotein band by the 8-azidonucleotide proved that the low level of ATP hydrolysis seen in the absence of drug was clearly associated with the mutant Mdr3 ATPase activity (Figure 3.7 B). Increased levels of trapping and photolabelling in the presence of different drugs in the D558N and D1203N mutants reflected an increased level of MgATP hydrolysis; however, the extent of accumulation of 8-azidonucleotide was much lower in these mutants than in WT Mdr3. The significant but low level of ATP and 8-azido-ATP hydrolysis distinguished both mutants from Walker B motif mutants D551N and D1196N that have no ATPase activity and do not show any vanadate-induced nucleotide trapping in the NB sites (Figure 3.7 A; (Urbatsch *et al.*, 1998)).

Within different nucleoside triphosphate-hydrolysing enzymes, the question as to whether a general base residue is essential to the catalytic mechanism of hydrolysis has

been a matter of considerable debate. Spatial considerations in the crystal structure of F_1-ATPase suggest that βE188 serves as a general base to activate the water molecule promoting an in-line nucleophilic attack on the γ-phosphate for ATP hydrolysis (Abrahams *et al.*, 1994). The catalytic power of Mdr3 (k_{cat} = 10 s^{-1}) is 1 order of magnitude lower than that of F_1-ATPase (k_{cat} = 180 s^{-1}). Thus, according to the concept proposed by Mildvan (Mildvan, 1997), the Mdr3 ATPase may rely on a catalytic carboxylate by a mechanism related to F_1-ATPase. Mutants D558N and D1203N still retained 14 and 30% of their drug-stimulated ATPase activity, respectively. This relatively high ATPase activity does not compare with the loss of activity expected for such a catalytic carboxylate in Mdr3. In the crystal structure of HisP, the residue homologous to D558/D1203 is D185. It is located >19 Å away from the γ-phosphate of bound ATP, which is too far away for a direct interaction between the carboxylate of D185 and the γ-phosphate (Hung *et al.*, 1998). Thus, by analogy with F_1-ATPase, it is unlikely to function as a so-called catalytic carboxylate. D185 is located at the interface between β-sheets and the α-helical domain, which has been proposed to interact with the membrane domain, suggesting that D558 and D1203 in Mdr3 might be involved in coupling ATP hydrolysis and drug transport. Alternatively, they might simply be involved in "cross-talk" between the two NB sites to efficiently hydrolyse ATP to energize drug transport.

The parallel analysis of mutants E552Q and E1197Q revealed unique biochemical properties that together provide novel insight into the catalytic cycle of Pgp. Indeed, both mutants share a similar phenotype, which includes a complete loss of steady-state ATP hydrolysis, as assessed by P_i release in a standard assay. However, both mutants show vanadate-induced trapping of nucleotide, which can be strongly stimulated by drugs such as verapamil and valinomycin. Surprisingly, both mutants also exhibit drug-induced labelling by 8-azido-ATP even in the absence of vanadate (Figure 3.7 A). Several observations suggest that the unusual character of these mutants is a true reflection of the loss of negative charge at these positions, as opposed to a nonspecific effect of the mutation on overall three-dimensional structure of the protein, or through other possible artifacts associated with purification or testing procedures. First, this phenotype is very similar for the two mutants. Second, it is associated with a very discrete mutation in the

protein, the replacement of a negative charge with an uncharged amino group while retaining a similar size of the residue. Third, an identical mutation at the adjacent residue (D551N and D1196N) has a completely different phenotype, with a loss of both ATP hydrolysis and vanadate-induced nucleotide trapping (Figure 3.7 A). Fourth, both E552Q and E1197Q mutants display drug stimulation of photolabelling by 8-azido-ATP (in the presence or absence of vanadate), suggesting that drug binding and the overall structure of the protein are not grossly affected. Fifth, all mutant and wild-type proteins were purified by the same protocol and tested concurrently and repeatedly with very similar results.

In the presence of vanadate, increased levels of trapping and photolabelling in the E552Q and E1197Q mutants after addition of verapamil or valinomycin were seen and were comparable to WT levels, and reflected formation of the {Pgp**·Mg·8-azido-ADP·V_i} transition-state complex (Figure 3.7 A). The fact that these mutants were deficient in drug-stimulated steady-state ATP hydrolysis, yet fully retained their capability to form the transition-state complex in a drug-dependent manner, suggested that binding of 8-azido-ATP and initiation of hydrolysis leading to formation of the transition-state complex were normal in the E552Q and E1197Q mutant enzymes. However, steps after the formation of the transition state, including release of MgADP and/or P_i, were severely affected. Since the amount of photolabel incorporated in the E552Q and E1197Q mutants under conditions of vanadate alone or vanadate with drug was similar to that detected in the WT protein, it appears unlikely that a major defect in P_i release is present in these mutants. We favor a model in which release of MgADP is severely impaired, and the mutant enzymes are incapable of performing a single complete catalytic cycle. This phenotype is clearly distinct from that of mutants at the adjacent residues in the Walker B motif (D551N and D1196N), which did not show any steady-state ATPase activity and completely lost their capacity to trap 8-azido-ATP with vanadate to form the {Pgp**·Mg·8-azido-ADP·V_i} transition-state complex (Muller *et al.*, 1996; Urbatsch *et al.*, 1998).

Another interesting and distinguishing feature of the E552Q and E1197Q mutant enzymes is the observed drug-induced labelling of the proteins by 8-azidonucleotide in the absence of vanadate, which is clearly absent in the WT Pgp (Figure 3.7 A). We have

not yet established whether 8-azido-ATP or 8-azido-ADP (or both) is the nucleotide cross-linked in these mutants under such conditions. Preliminary experiments with direct photolabelling by 8-azido-ATP under binding conditions (4 °C) failed to detect major differences between E552Q, E1197Q, and WT Mdr3 (data not shown), suggesting that the affinity of the mutants for 8-azido-ATP is similar to that of WT Mdr3; in other words, increased affinity for 8-azido-ATP does not seem to be responsible for labelling in the mutant enzymes. It is tempting to speculate that the mutants are capable of cleaving the bond between the β- and γ-phosphates and hence undergo partial reactions toward a full cycle of 8-azido-ATP hydrolysis. However, it remains to be shown whether 8-azido-ADP is the bound nucleotide in the absence of vanadate. If so, MgADP release in these mutants may be sufficiently impaired to provide conditions necessary for cross-linking ADP in the NB sites in the absence of vanadate, a phenomenon not detectable in WT Mdr3 due to rapid turnover of ADP and/or ATP during the normal catalytic cycle. Additionally, it is not known at present in which NB site (or both) of E552Q and E1197Q the nucleotide is occluded. Preliminary trypsin digestion experiments suggest labelling at both NB1 and NB2 in E552Q and E1197Q (data not shown). Finally, the differences in photolabelling of E552Q and E1197Q by the radionucleotide in the absence of vanadate and in the absence or presence of drugs (E1197Q > E552Q) may reflect functional differences between the two NB sites of Pgp. Such differences would not be detected in the presence of vanadate that would stabilize the transition-state complex. Functional differences between the two NB sites of Pgp have been previously noted in photolabelling (Hrycyna *et al.*, 1999) and in trypsin sensitivity experiments (Julien and Gros, 2000). Additional experiments will be required to further test this hypothesis.

In the crystal structure of HisP, a glutamate (E179) is located within 4.3 Å of the γ-phosphate of bound ATP and forms a hydrogen bond with a water molecule (water 437), which interacts with the γ-phosphate through a hydrogen bond that is nearly parallel to the Pγ-Oβ bond, the bond that breaks upon hydrolysis. Therefore, this residue has been proposed to be the activating residue (catalytic carboxylate) (Hung *et al.*, 1998). Multiple sequence alignments identify E552 and E1197 as Pgp homologues of HisP E179. The loss of drug-stimulated steady-state ATP hydrolysis observed in the E552Q and E1197Q Pgp mutants detected here suggests a similar critical role of these residues in ATP hydrolysis

by Pgp. However, substitution of the charged glutamate by its uncharged homologue still allowed formation of the catalytic transition state with bound {Pgp**·Mg·8-azido-ADP·V_i} in the mutant enzymes. This situation is clearly different from that of the catalytic carboxylate mutant βE188Q of F_1-ATPase, where loss of ATPase activity is associated with loss of formation of the catalytic transition state with fluoroaluminate (Nadanaciva *et al.*, 1999a). Further biochemical and mutational analyses of these residues are warranted, and future crystal structures of ABC transporters in the presence of Mg^{2+} and/or transition-state analogues may give a more precise orientation for the two residues in question, and may provide better insights into this issue.

Together, the identification of two highly mutation-sensitive carboxylate residues at positions 552 and 1197, and 558 and 1203, reported here clearly points at a key functional role for the short helical loop located immediately downstream of the Walker B motif in the catalytic activity of the ATP binding sites of ABC transporters.

3.6 Acknowledgments

We thank Drs. Alan Senior and Joachim Weber (University of Rochester, Rochester, NY) for helpful discussions and for critical reading of the manuscript.

The identification of mutation-sensitive residues immediately following the Walker B motif suggested that these residues are important in Abcb1a function. Characterization of the E552Q and E1197Q mutants was undertaken to try to identify their underlying defect(s).

Chapter 4

Analysis of Catalytic Carboxylate Mutants E552Q and E1197Q Suggests Asymmetric ATP Hydrolysis by the Two Nucleotide-Binding Domains of P-Glycoprotein

Published manuscript reproduced by permission from the publisher:

Carrier, I., Julien, M., and Gros, P. Analysis of Catalytic Carboxylate Mutants E552Q and E1197Q Suggests Asymmetric ATP Hydrolysis by the Two Nucleotide-Binding Domains of P-Glycoprotein. *Biochemistry*, **42(44)**: 12875-12885, 2003.

4.1 Abstract

In the nucleotide binding domains (NBDs) of ABC transporters, such as mouse Mdr3 P-glycoprotein (P-gp), an invariant carboxylate residue (E552 in NBD1; E1197 in NBD2) immediately follows the Walker B motif (hyd_4**DE/D**). Removal of the negative charge in mutants E552Q and E1197Q abolishes drug-stimulated ATPase activity measured by Pi release. Surprisingly, drug-stimulated trapping of 8-azido-[α^{32}P]ATP is still observed in the mutants both in the presence and absence of the transition state analogue vanadate (Vi), and ADP can be recovered from the trapped enzymes. The E552Q and E1197Q mutants show characteristics similar to the wild-type (WT) enzyme with respect to 8-azido-[α^{32}P]ATP binding and 8-azido-[α^{32}P]nucleotide trapping, with the latter being both Mg^{2+} and temperature dependent. Importantly, drug-stimulated nucleotide trapping in E552Q is stimulated by Vi and resembles the WT enzyme, while it is almost completely Vi insensitive in E1197Q. Similar nucleotide trapping properties are observed when aluminum fluoride or beryllium fluoride is used as an alternate transition state-analogue. Partial proteolytic cleavage of photolabelled enzymes indicates that, in the absence of Vi, nucleotide trapping occurs exclusively at the mutant NBD, whereas in the presence of Vi, nucleotide trapping occurs at both NBDs. Together, these results suggest that there is single-site turnover occurring in the E552Q and E1197Q mutants and that ADP release from the mutant site, or another catalytic step, is impaired in these mutants. Furthermore, our results support a model in which the two NBDs of P-gp are not functionally equivalent.

4.2 Introduction

The successful chemotherapeutic treatment of many human tumors is often impeded by the emergence of multidrug-resistant cells (Gottesman *et al.*, 2002). Multidrug resistance (MDR) is characterized by cross-resistance to structurally and functionally unrelated compounds and is often associated with the overexpression of membrane transporters of wide substrate specificity, such as members of the ATP-binding cassette (ABC) protein superfamily, which include P-glycoprotein (P-gp), multidrug resistance-associated protein (MRP), and breast cancer resistance protein (BCRP) (Gottesman, 2002). ABC transporters form one of the largest and most conserved gene families known, with 48 members in humans, 56 in the fly, 129 in plants, and over 300 in bacteria (Gottesman and Ambudkar, 2001). In humans, multiple sequence alignments divide these transporters into 7 subfamilies designated ABCA to ABCG. There is great clinical interest in ABC transporters not only because of their involvement in multidrug resistance but also because many disease-causing mutations have been identified in proteins of this family in humans, causing diseases such as Tangier disease (ABCA1), progressive intrahepatic cholestasis (ABCB11), pseudoxanthoma elasticum (ABCC6), cystic fibrosis (ABCC7), persistent hyperinsulinemic hypoglycemia (ABCC8), adrenoleukodystrophy (ABCD1), and sitosterolemia (ABCG5, ABCG8) among others. The substrates for ABC transporters are very diverse and include drugs (ABCB1), lipids (ABCA4, ABCA7, ABCB4), fatty acids (ABCD1-4), sterols (ABCG5, ABCG8), anionic conjugates (ABCC1-3), peptides (ABCB2, ABCB3), nucleotides (ABCC4, ABCC5), and ions (ABCB6, ABCB7, ABCC7) (http://humanabc.4t.com/humanabc.htm), which are all transported across the phospholipid bilayer at the expense of ATP (Gottesman and Ambudkar, 2001).

ABC transporters are defined by a structural unit composed of six putative transmembrane α-helices that form one transmembrane domain (TMD) and one cytosolic nucleotide-binding domain (NBD) (Chen *et al.*, 1986; Gros *et al.*, 1986). In prokaryotes, the TMDs and NBDs are most often encoded by separate structural genes of the same operon (Linton and Higgins, 1998). In eukaryotes, many ABC transporters, including P-gp, show a duplication of this unit in a single polypeptide, while others appear to function as homo- or heterodimers of the 1TMD/1NBD unit (TAP1/2, ABCB2/3, ABCG5/8).

Also, members of the ABCC subfamily (MRP, SUR1) show an additional hydrophobic domain of five TM helices fused at the N-terminus of the classical 2TMD/2NBD backbone. The major topological features of P-gp, including the carboxy and amino termini, the glycosylated loop, and the NBDs, have been oriented with respect to the cell membrane, and the number, position, and polarity of the 12 TM helices have been established using biochemical and immunological methods (Loo and Clarke, 1995b; Kast *et al.*, 1996). Recently, a high-resolution structure was obtained for the ABC transporter MsbA (homodimer, 1TMD/1NBD) of *Escherichia coli* (*E. coli*) (Chang and Roth, 2001), which confirmed at 6 the number of TM helices present in each TMD of ABC transporters. Peptide mapping with photoactive substrate analogues (Safa, 1993) and studies in chimeric (Buschman and Gros, 1991; Zhou *et al.*, 1999), naturally occurring (Choi *et al.*, 1988; Devine *et al.*, 1992), or experimentally induced (Shustik *et al.*, 1995; Loo and Clarke, 1999a) P-gp mutants with altered substrate specificities, as well as site-specific modifications in single-cysteine mutants (Loo and Clarke, 1999b), suggest that the TMDs of P-gp, and of other ABC transporters, form the substrate-binding site in the lipid bilayer.

Drug transport is strictly ATP dependent, and considerable evidence suggests that ATP hydrolysis by the NBDs provides the energy required for this process (Ambudkar *et al.*, 1992; Sarkadi *et al.*, 1992; al-Shawi and Senior, 1993; Sharom *et al.*, 1993; Senior *et al.*, 1995b; Ambudkar *et al.*, 1997). Purified P-gp shows robust ATPase activity {measured by the release of inorganic phosphate (P_i) or by vanadate- (V_i-) induced trapping of nucleotide} that can be further stimulated by certain MDR drugs and P-gp inhibitors (Ambudkar *et al.*, 1992; Sarkadi *et al.*, 1992; Sharom *et al.*, 1993; Shapiro and Ling, 1994). Both NBDs have been shown, through mutagenesis (Azzaria *et al.*, 1989), site-specific modification in single-cysteine mutants (Loo and Clarke, 1995a), and studies in half-molecules (Loo and Clarke, 1994), to be essential for function, with complete cooperativity between the two sites for ATP hydrolysis and drug transport. In the "alternate site" catalysis model proposed by Senior and co-workers (Senior *et al.*, 1995b), both NBDs are catalytically active with equal probability of hydrolysis at NBD1 and NBD2. In this model, one drug molecule is transported per ATP molecule hydrolysed. The experiments that support this model include V_i-induced nucleotide trapping, in which

equal trapping of nucleotide occurs in NBD1 and NBD2, with complete inhibition of ATPase activity occurring with one molecule of V_i trapped per P-gp molecule (Urbatsch *et al.*, 1995a; Urbatsch *et al.*, 1995b). Thus, when one site enters the transition state (P-gp·MgADP·P_i/V_i), the other cannot do so, implying alternate hydrolysis. In the expanded model proposed by Ambudkar and co-workers, two ATP molecules need to be hydrolysed for one substrate molecule to be transported (Sauna and Ambudkar, 2000). This model is based on the observations that V_i-inhibited P-gp has reduced affinity for drugs (Ramachandra *et al.*, 1998; Sauna and Ambudkar, 2000; Sauna and Ambudkar, 2001) and that a second ATP hydrolysis event is required to restore normal drug-binding properties (Sauna and Ambudkar, 2000). Hence, drug binding induces hydrolysis of a first ATP and translocation of substrate to a low-affinity site, as well as substrate release, while binding and hydrolysis of a second ATP is required to recreate a high-affinity drug-binding site.

In ABC proteins, each NBD contains the consensus Walker A (GX_4GKS/T) and Walker B (hyd_4D, where hyd = hydrophobic residue) sequence motifs that have been previously described in various ATP-binding proteins and ATP-hydrolysing enzymes (ATPases) (Walker *et al.*, 1982). The high-resolution crystal structures of several NBDs of ABC transporters and proteins have been solved, including HisP, Rad50cd, MalK, MJ0796 (LolD), MJ1267 (LivG), TAP1, BtuCD, and HlyB (Hung *et al.*, 1998; Diederichs *et al.*, 2000; Hopfner *et al.*, 2000; Karpowich *et al.*, 2001; Yuan *et al.*, 2001). In most cases, structural information has been obtained for the protein bound to different nucleotides, revealing the location of the nucleotide complexes and defining the amino acid residues that form the active site. For example, the Walker A motif, also known as the P-loop, is seen to wrap around the phosphate chain of ATP with the main chain nitrogens of the residues within this motif making extensive hydrogen bonding with the β-phosphate. The Walker B motif is shown to provide the carboxylate residue that coordinates and stabilizes the magnesium ion indispensable for ATP hydrolysis. In addition, the recent crystal structure of the stable MJ0796-E171Q dimer (Smith *et al.*, 2002) shows that the signature motif of the opposite NBD also contributes to the active site by forming hydrogen bonds with the ribose and γ-phosphate of ATP. Finally, multiple sequence alignments identified another highly conserved carboxylate residue that

immediately follows the Walker B aspartate (Urbatsch *et al.*, 2000c). This carboxylate has been proposed to play a key role in catalysis since, in the HisP structure, the negatively charged side chain of this glutamate (E179) appears to polarize a water molecule for an in-line attack on the terminal phosphate of ATP (Hung *et al.*, 1998).

In an effort to gain insight into the mechanism of ATP hydrolysis by P-gp, including testing the role of the two NBDs in catalysis, we have previously mutated the glutamate residues homologous to E179 of HisP in the mouse Mdr3 enzyme (E552Q and E1197Q in NBD1 and NBD2, respectively) (Urbatsch *et al.*, 2000c). We observed that although no ATPase activity could be measured by P_i release for either of these mutants, 8-azido-[α^{32}P]nucleotide could still be trapped. These observations have suggested that a step during ATP hydrolysis is impaired in the mutant enzymes, providing a unique opportunity to study intermediate steps in the catalytic cycle of the enzyme. In this study, we have attempted to characterize the molecular basis of the defect in the E552Q and E1197Q mutants.

4.3 Materials and Methods

4.3.1 Purification of Mouse Mdr3

The wild-type mouse Mdr3 (WT) and the E552Q, E1197Q, and D551N mutants were created by site-directed mutagenesis and modified by in-frame addition of a six-histidine tag (His_6) at the C-terminus of the protein and were expressed in the yeast *Pichia pastoris* after cloning in the expression plasmid pHIL-D2 (Invitrogen, license 145457), as previously described (Urbatsch *et al.*, 2000c). For expression and purification, glycerol stocks of *P. pastoris* GS115 transformants were streaked on YPD plates, and single colonies were used to inoculate 6 L liquid cultures. For preparation of *P. pastoris* membranes, cultures were induced with 1% methanol for 72 h, and plasma membranes were isolated by centrifugation, as previously described (Lerner-Marmarosh *et al.*, 1999). Solubilization and purification of WT and mutant Mdr3 variants by affinity chromatography on Ni-NTA resin (Qiagen) and DE52-cellulose (Whatman) were as described (Lerner-Marmarosh *et al.*, 1999). This procedure routinely yielded between 1 and 1.6 mg of protein, with 95% minimum purity.

4.3.2 Assay of ATPase Activity

For ATPase assays, purified WT or mutant Mdr3 enzymes (concentrated DE52 eluate) were activated by incubating with 1% *E. coli* lipids (w/v; Avanti, acetone/ether preparation) and 5 mM dithiothreitol (DTT) for 30 min at 20 °C at a final protein concentration of 0.07 μg/μL (WT) or 0.1 μg/μL (mutants). Aliquots of 5 μL were added into 50 mM Tris-HCl (pH 8.0), 0.1 mM EGTA, 10 mM Na_2ATP, and 10 mM $MgCl_2$, to a final volume of 250 μL, and the mixture was incubated at 37 °C. At the appropriate time, a 50 μL aliquot was removed and quenched in 1 mL of ice-cold 20 mM H_2SO_4. Inorganic phosphate (P_i) release was assayed as described previously (Van Veldhoven and Mannaerts, 1987). Drugs were added as dimethyl sulfoxide stock solutions, and the final solvent concentration in the assay was kept at ≤2% (v/v).

4.3.3 Photoaffinity Labelling with 8-Azido-[α^{32}P]ATP

8-Azido-[α^{32}P]ATP photoaffinity labelling was performed as previously described (Urbatsch *et al.*, 2000c) with minor modifications. The purified Mdr3 proteins (concentrated DE52 eluate) were activated by incubating with 1% *E. coli* lipids (w/v; Avanti, acetone/ether preparation) and 5 mM DTT at a final concentration of 0.2 mg/mL

at 20 °C for 30 min immediately prior to starting the photolabelling reactions. For direct labelling experiments, activated WT or mutant Mdr3 variants were incubated on ice for ~10 min with 3 mM $MgCl_2$, 50 mM Tris-HCl (pH 8.0), 0.1 mM EGTA, and varying concentrations of 8-azido-[α^{32}P]ATP (5, 10, 20, 40, and 80 μM final concentrations at ~0.2 Ci/mmol specific activity) in a total volume of 50 μL. In some experiments, requirement for divalent cations was assayed by addition of EDTA (5 mM) to the reaction mixture. The samples were kept on ice and immediately UV-irradiated for 5 min {UVS-II Minerallight (260 nm) placed directly above the samples}. Unreacted nucleotides were then removed by centrifugation at 200000*g* for 30 min at 4 °C in a TL-100 rotor (Beckman), and protein-containing pellets were washed with 100 μL of ice-cold 50 mM Tris-HCl (pH 8.0) and 0.1 mM EGTA. The pellets were then dissolved in sample buffer {5% (w/v) SDS, 25% (v/v) glycerol, 0.125 M Tris-HCl (pH 6.8), 40 mM DTT, 0.01% pyronin Y} and separated by SDS-polyacrylamide gel electrophoresis (SDS-PAGE) on 7.5% gels, followed by autoradiography to Kodak BioMax MS film. For nucleotide trapping experiments, activated WT or mutant Mdr3 variants were incubated at 37 °C for 20 min with 5 μM 8-azido-[α^{32}P]ATP (0.2-0.5 Ci/mmol), 3 mM $MgCl_2$, 50 mM Tris-HCl (pH 8.0), and 0.1 mM EGTA, with or without vanadate (V_i, 200 μM), $AlCl_3$ (1 mM)-NaF (5 mM), or $BeSO_4$ (200 μM)-NaF (1 mM), in a total volume of 50 μL. Verapamil (100 μM) or valinomycin (100 μM) was included where indicated. Divalent cation dependence was assayed by addition of EDTA (5 mM). Modifications to the normal procedure are indicated in the figure legends. The incubations were started by addition of 8-azido-[α^{32}P]ATP and stopped by transfer on ice. Free label was then removed by centrifugation at 200000*g* for 30 min at 4 °C in a TL-100 rotor (Beckman), and pellets were washed and resuspended in 30 μL of ice-cold 50 mM Tris-HCl (pH 8.0) and 0.1 mM EGTA. Samples were kept on ice and irradiated with UV for 5 min. Labelled samples were resolved by SDS-PAGE on 7.5% gels and subjected to autoradiography. Orthovanadate solutions (100 mM) were prepared from Na_3VO_4 (Fisher Scientific) at pH 10 and boiled for 2 min before use to break down polymeric species.

4.3.4 Thin-Layer Chromatography Analysis of Vanadate-Trapped Nucleotides in Mouse Mdr3

Five micrograms of activated WT or mutant Mdr3 variants was incubated at 37 or 4 °C for 10 min with 5 μM 8-azido-[α^{32}P]ATP (0.4 Ci/mmol), 3 mM $MgCl_2$, 200 μM vanadate, 100 μM verapamil, 50 mM Tris-HCl (pH 8.0), and 0.1 mM EGTA in a total volume of 50 μL. The incubations were started by addition of 8-azido-[α^{32}P]ATP and stopped by transfer on ice. The free label was removed by centrifugation at 200000*g* for 30 min at 4 °C in a TL-100 rotor (Beckman), and the pellets were washed with ice-cold 50 mM Tris-HCl (pH 8.0) and 0.1 mM EGTA. The protein pellets were then resuspended in 15 μL of 50 μM 8-azido-ATP, and 2 μL of ice-cold 50% (w/v) trichloroacetic acid was added. The samples were centrifuged to precipitate the protein, and 1 μL of 50 mM EDTA was added to 20 μL of the supernatant. Samples (0.5 μL) were applied to a poly(ethylenimine)-cellulose plate along with 125 dpm of each nucleotide standard (8-azido-ATP, 8-azido-ADP, and a mixture of both ± protein) and developed in 3.2% (w/v) fresh NH_4HCO_3; the plate was then subjected to autoradiography.

4.3.5 Partial Trypsin Digestion of Photolabelled Mouse Mdr3

To detect radiolabelled nucleotide trapped in NBD1 and/or NBD2 of Mdr3 following photolabelling of the protein with 8-azido-[α^{32}P]ATP, we took advantage of the protease-hypersensitive site located in the linker region joining the two halves of P-gp (Bruggemann *et al.*, 1989). Photoaffinity-labelled proteins were resuspended in 30 μL of 50 mM Tris-HCl (pH 8.0) and 0.1 mM EGTA and kept on ice. The incubation with trypsin (2 μL of each stock solution) was then carried out for 10 min at 37 °C at enzyme-to-protein mass ratios of 1:75, 1:37.5, 1:18.75, 1:9.38, 1:4.69, 1:2.34, and 1:1.17. The digestion was stopped by addition of 15 μL of sample buffer. For the experiment carried out in the absence of V_i all ratios were used, whereas in the presence of V_i only the 1:37.5, 1:18.75, 1:9.38, and 1:4.69 ratios were used. Finally, the Mdr3 halves were resolved by SDS-PAGE on 10% gels, followed by transfer onto nitrocellulose membranes and exposition to film. Immunoblotting with the mouse monoclonal antibody C219 (Signet) that recognizes both halves of Mdr3, as well as with N-terminal and C-terminal half specific mouse monoclonal antibodies {MD13 with its epitope in NBD1 (494-504)

and MD7 with its epitope in the intracellular (IC) loop 3 (805-815)}, respectively (gift of Dr. V. Ling from The B.C. Cancer Research Centre, Vancouver, Canada) (Shapiro *et al.*, 1996), was then performed on the membranes.

4.3.6 Routine Procedures

Protein concentrations were determined by the bicinchoninic acid method in the presence of 0.5% SDS using bovine serum albumin as a standard. SDS-PAGE was carried out according to Laemmli (Laemmli, 1970) using the mini-PROTEAN II gel and Electrotransfer system (Bio-Rad). Samples were dissolved in sample buffer {5% SDS (w/v), 25% glycerol (v/v), 125 mM Tris-HCl (pH 6.8), 40 mM DTT, and 0.01% pyronin Y}. For immunodetection of Mdr3, the mouse monoclonal antibody C219 (Signet Laboratories Inc.) was used with the enhanced chemiluminescence (ECL) detection system (NEN Renaissance, PerkinElmer). To recognize NBD1 specifically, the mouse monoclonal antibody MD13 was used, and for NBD2 the mouse monoclonal antibody MD7 was employed. For autoradiography, SDS gels were stained with Coomassie Blue, dried, and exposed at -80 °C to Kodak BioMax MS film with an intensifying screen for the appropriate amount of time.

4.3.7 Materials

8-Azido-[α^{32}P]ATP was purchased from Affinity Labelling Technologies, Inc. (Lexington, KY). 8-Azido-ATP and verapamil were from ICN while valinomycin was from Calbiochem. Acetone/ether-precipitated *E. coli* lipids were from Avanti Polar Lipids. The PEI-cellulose TLC plates and general reagent grade chemicals were from Sigma or Fisher.

4.4 Results

During a previous search for catalytic carboxylate residues in the NBDs of P-glycoprotein two mutants of the mouse Mdr3 isoform at homologous positions in NBD1 and NBD2 (E552Q and E1197Q) showed a similar loss-of-function phenotype, which featured inability to convey multidrug resistance and abrogation of steady-state ATPase activity (Urbatsch *et al.*, 2000c). In the present study, we have investigated the mechanistic basis of the defect in those mutants. For this, wild-type (WT) Mdr3 and the E552Q and E1197Q mutants were expressed in the yeast *P. pastoris* as recombinant proteins bearing an in-frame polyhistidine tail (His_6) at the carboxyl terminus. The NBD1 Walker B motif mutant D551N, in which ATP hydrolysis is completely impaired (Urbatsch *et al.*, 1998; Hrycyna *et al.*, 1999, hMDR1), was also included as a negative control in the experiments. Protein purification from large-scale methanol-induced liquid cultures of *P. pastoris* was done by detergent extraction from enriched membrane fractions, followed by affinity and anion-exchange chromatography on Ni^{2+}-NTA and DE52-cellulose resins, respectively (Lerner-Marmarosh *et al.*, 1999). Using this protocol, all proteins could be purified in large amounts (1-1.6 mg/6 L culture) in a stable form and at a high degree of purity (>95%) (Figure 4.1 A).

Steady-state ATP hydrolysis by the purified proteins activated with *E. coli* lipids and DTT was determined by measuring P_i release, in the absence or presence of MDR drugs or P-gp inhibitors that are known to stimulate the ATPase activity of P-gp (Van Veldhoven and Mannaerts, 1987). As shown previously (Urbatsch *et al.*, 2000c), WT Mdr3 has low basal ATPase activity (0.35 μmol min^{-1} mg^{-1}), which can be strongly stimulated (6-9-fold) by verapamil and valinomycin (3.16 and 2.18 μmol min^{-1} mg^{-1}). As before, the purified E552Q and E1197Q mutants show a very low basal ATPase activity (0.13-0.18 μmol min^{-1} mg^{-1}) that is not stimulated by drugs (0.13-0.20 μmol min^{-1} mg^{-1}) and which is comparable to the activity seen in the ATPase inactive mutant D551N (Beaudet *et al.*, 1998b; Urbatsch *et al.*, 1998) that is considered to be background.

To determine whether the loss of ATPase activity seen in E552Q and E1197Q was caused by an effect of the mutations on affinity for nucleotides, the nucleotide-binding properties of the WT and Mdr3 variants were compared by photoaffinity labelling. Purified and activated proteins were incubated with increasing concentrations of 8-azido-

Figure 4.1:

Direct photolabeling of purified Mdr3 NB site mutants with Mg-8-azido-[α^{32}P]ATP

Purified and activated wild-type (WT) and mutant Mdr3 variants (E552Q, E1197Q, D551N) were UV-irradiated on ice in the presence of 3 mM $MgCl_2$ and 5, 10, 20, 40, and 80 μM 8-azido-[α^{32}P]ATP. Photolabeled samples were separated on 7.5% SDS-polyacrylamide gels and stained with Coomassie Blue (A) followed by autoradiography (B) (Materials and Methods). The position of the molecular mass markers is given on the left.

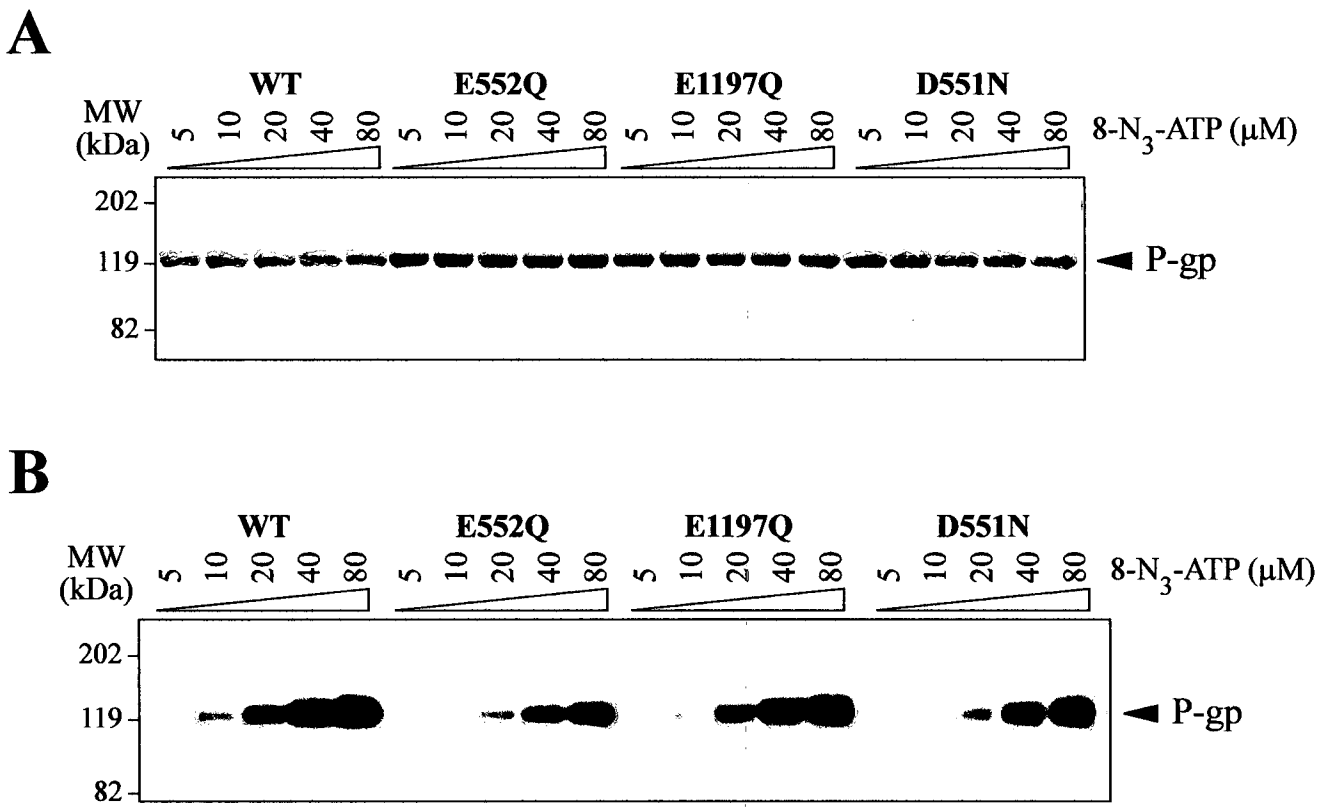
A
WT
E552Q
E1197Q
D551N
MW (kDa)
5 10 20 40 80 5 10 20 40 80 5 10 20 40 80 5 10 20 40 80
8-N3-ATP (μM)
202
119
82
P-gp
B
WT
E552Q
E1197Q
D551N
MW (kDa)
5 10 20 40 80 5 10 20 40 80 5 10 20 40 80 5 10 20 40 80
8-N3-ATP (μM)
202
119
82
P-gp

[α^{32}P]ATP in the presence of Mg^{2+} (~10 min on ice), followed by UV irradiation. Unincorporated ligand was removed by centrifugation, and labelled proteins were resolved by SDS-PAGE. The gels were stained with Coomassie Blue to verify comparable loading (Figure 4.1 A) and then subjected to autoradiography (Figure 4.1 B). Binding and subsequent photo-cross-linking of 8-azido-[α^{32}P]ATP was specific to Mdr3 and increased proportionally with the amount of 8-azido-[α^{32}P]ATP present in the reaction. The profile of ^{32}P incorporation over several experiments was quantitatively similar for all mutants and was also very similar to that seen for WT Mdr3. Similar results were obtained when the WT and mutant proteins were labelled at 4 °C with 8-azido-[γ^{32}P]ATP (data not shown). Together, these results suggest that the E552Q, E1197Q, and D551N mutations do not have a major effect on nucleotide binding to Mdr3 and are therefore unlikely to cause major nonspecific structural changes in the NBDs. This is in agreement with previous studies of catalytic residue mutants of the Walker A and B signature motifs (K429R, K1072R, D551N, and D1196N) which severely affect the catalytic activity of mouse Mdr3 but have little effect on the nucleotide-binding affinity of the protein (Urbatsch *et al.*, 1998). Thus, residues E552 and E1197 seem to participate in the hydrolysis steps after the initial binding of ATP to the NBDs.

Vanadate (V_i) is a transition-state analogue structurally related to phosphate (P_i) that can stably inhibit P-gp ATPase activity (Horio *et al.*, 1988). V_i trapping of nucleotide requires both hydrolysis of the bond between the β- and γ-phosphates of ATP and release of P_i. Once P_i is released, it is replaced by V_i, capturing ADP in the NB site and forming a long-lived intermediate that resembles the normal transition state {MgADP·V_i} (Urbatsch *et al.*, 1995b). This intermediate can be visualized by UV cross-linking when 8-azido-[α^{32}P]ATP is used as a substrate (Urbatsch *et al.*, 1995b). Indeed, V_i-induced trapping of 8-azido-[α^{32}P]ADP under hydrolysis conditions (37 °C) has been used as an alternative and highly sensitive method to monitor ATPase activity in WT and mutant P-gp (Urbatsch *et al.*, 1995b; Urbatsch *et al.*, 1998). For WT Mdr3, nucleotide trapping is dependent on the presence of V_i and is stimulated by VER and VAL. In contrast to WT, nucleotide trapping is completely absent from the Walker B mutant D551N under any of the conditions tested, as suggested by the absence of ATPase activity of this mutant. Despite the observed lack of ATPase activity of E552Q and E1197Q measured by P_i

release, 8-azidonucleotide trapping that is stimulated both by drug and by V_i is readily detectable in these mutants. Interestingly, drug-stimulated V_i-independent trapping is also seen in the mutants. We proposed previously that these mutants can only complete part of the ATP hydrolysis cycle of P-gp, such that binding of 8-azido-ATP and initiation of hydrolysis leading to formation of the transition-state complex are normal, but subsequent steps, such as release of MgADP and/or P_i, or others are impaired (Urbatsch *et al.*, 2000c).

Although studies of WT Mdr3 (Urbatsch *et al.*, 2000c) and of the inactive mutant D551N (Urbatsch *et al.*, 2000c) suggest that under the hydrolysis conditions used (37 °C; see Materials and Methods) little if any of the photolabelling is due to 8-azido-[α^{32}P]ATP binding, additional experiments were undertaken to verify that the labelling seen in E552Q and E1197Q ($\pm V_i$) was due to trapping of hydrolysed nucleotide, as opposed to simple binding of the label to Mdr3. As formation of the Mg-8-azido-ADP·V_i complex is optimum at 37 °C and requires Mg^{2+} ions (Urbatsch *et al.*, 1995b; Sauna *et al.*, 2001a), the temperature dependence and EDTA sensitivity of E552Q and E1197Q photolabelling by 8-azido-[α^{32}P]ATP were investigated. Results in Figure 4.2 A and B show that labelling of WT, E552Q, and E1197Q by 8-azido-[α^{32}P]ATP under all conditions tested ($\pm V_i$, ±drugs) was either completely eliminated or largely reduced (>90%) when the incubation and washing steps of the labelling reaction were carried out at 4 °C (Figure 4.2 B) as opposed to 37 °C (Figure 4.2 A). Parallel studies of Mg^{2+} ion dependence of 8-azido-[α^{32}P]ATP labelling under hydrolysis conditions, shown in Figure 4.2 D, indicate that addition of the chelator EDTA completely abrogates photolabelling of the WT and mutant proteins, under all conditions tested ($\pm V_i$, ±drugs). On the other hand, addition of EDTA to the reaction mixture is without effect on labelling of WT and mutant variants under nucleotide-binding conditions (4 °C; see Materials and Methods) (Figure 4.2 C), in agreement with previous studies showing that nucleotide binding to P-gp is largely Mg^{2+} independent (Hrycyna *et al.*, 1999; Lerner-Marmarosh *et al.*, 1999). These results are consistent with 8-azido-[α^{32}P]ATP hydrolysis in the WT and E552Q and E1197Q mutants with concomitant trapping of 8-azido-[α^{32}P]ADP. The differences in signal intensity that can be observed for the WT protein in the presence of vanadate and in the absence of drug between different experiments are likely due in part to different times of

Figure 4.2:

Temperature and divalent cation dependence of photolabeling of Mdr3 NB site mutants by vanadate trapping with Mg-8-azido-[α^{32}P]ATP

Purified and activated wild-type and mutant Mdr3 variants were preincubated with 5 μM 8-azido-[α^{32}P]ATP and 3 mM $MgCl_2$ for 20 min at either 37 °C (A and D) or on ice (4 °C; B) in the absence or presence of 200 μM vanadate, 100 μM verapamil or 100 μM valinomycin, and 5 mM EDTA (D only), as indicated above the lanes. Unbound ligands were removed by ultracentrifugation and washing, and the samples were then UV-irradiated and separated by SDS-PAGE. The autoradiographs in panels A and B were exposed to film for the same amount of time. (C) Purified and activated wild-type and mutant P-gp variants were UV-irradiated on ice in the presence of 20 μM 8-azido-[α^{32}P]ATP and 3 mM $MgCl_2$, with or without 5 mM EDTA, as indicated above the lanes. Photolabeled samples were separated on 7.5% SDS-polyacrylamide gels and stained with Coomassie Blue followed by autoradiography.

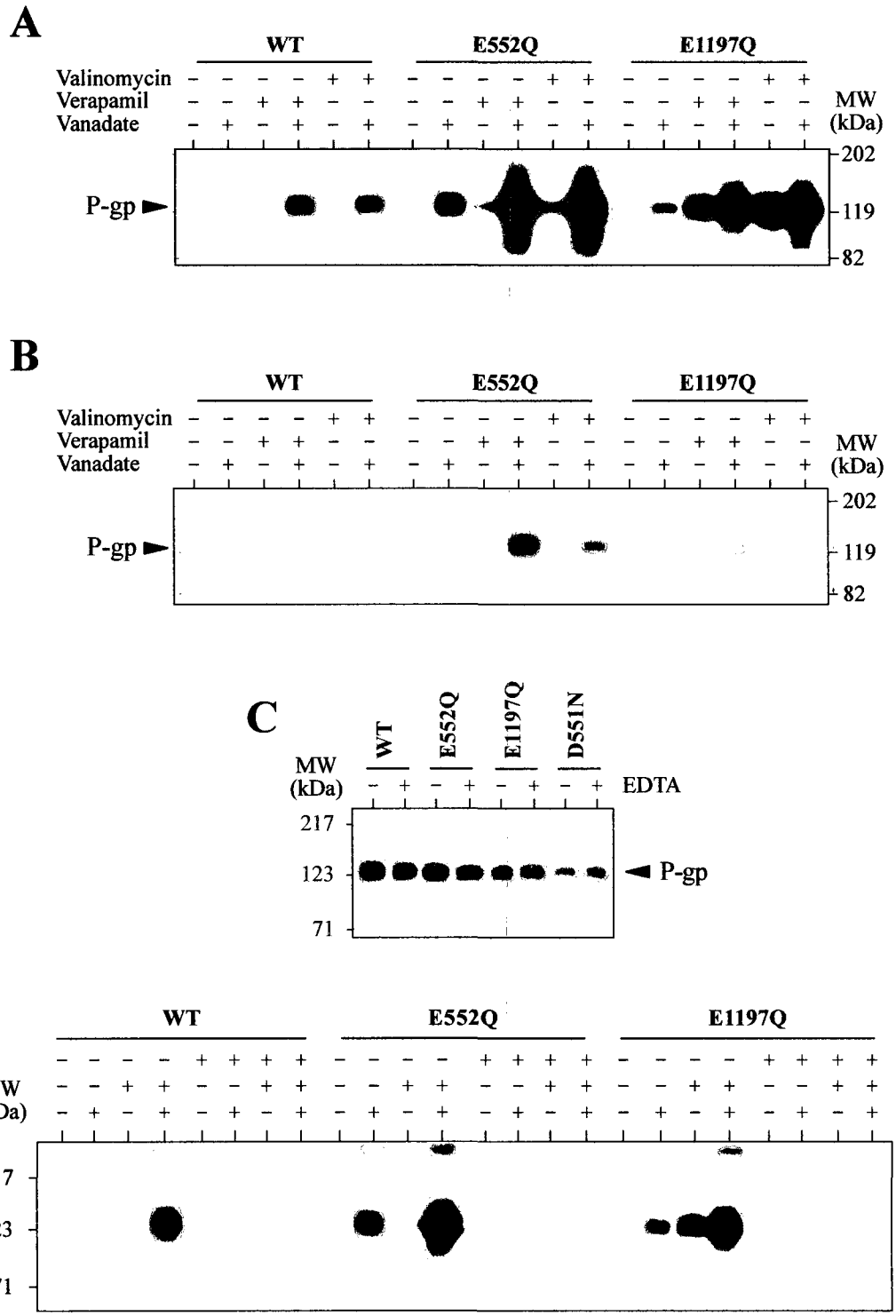
A
WT
E552Q
E1197Q
Valinomycin
Verapamil
Vanadate
MW
(kDa)
202
119
82
P-gp
B
WT
E552Q
E1197Q
Valinomycin
Verapamil
Vanadate
MW
(kDa)
202
119
82
P-gp
C
WT
E552Q
E1197Q
D551N
MW
(kDa)
EDTA
217
123
71
P-gp
D
WT
E552Q
E1197Q
EDTA
Verapamil
Vanadate
MW
(kDa)
217
123
71
P-gp

exposure and also to small differences in experimental conditions (such as different protein preparations).

To obtain further evidence that the E552Q and E1197Q mutants can form the {MgADP·V_i} transition-state complex, similar nucleotide trapping experiments were carried out in the presence of two other transition-state analogues: aluminum fluoride (AlF_4^-) and beryllium fluoride (BeF_x). Crystallographic studies of the myosin motor domain from *Dictyostelium discoideum* complexed to these P_i analogues show that the V_i- and AlF_4^--inhibited complexes are very similar and display a bond length of 2.0 Å between the V or Al atom and the pseudo-bridging oxygen (O) of the β-phosphorus of ADP. This bond length is significantly longer than the 1.56 and 1.67 Å bond lengths for the O atoms between the α- and β-phosphate groups of ADP, an observation strongly supporting the proposal that MgADP·V_i and MgADP·AlF_4^- complexes are true analogues of the MgADP·P_i transition state. On the other hand, the bond length measured for the Be to βO bond in the MgADP·BeF_x-inhibited complex is 1.57 Å, which is very similar to that seen for the P-O bond linking the α- and β-phosphates. This indicates that the MgADP·BeF_x complex more closely resembles ATP bound in the active site, reflecting the ground state of the enzyme prior to hydrolysis (Fisher *et al.*, 1995; Smith and Rayment, 1996b). Results in Figure 4.3 A indicate that AlF_4^- can also induce nucleotide trapping in the WT and E552Q and E1197Q mutants, with characteristics similar to those observed when V_i is used to induce trapping (Urbatsch *et al.*, 2000c). BeF_x can also induce nucleotide trapping in the WT and mutant Mdr3 enzymes (Figure 4.3 B). On the other hand, neither BeF_x nor AlF_4^- could induce nucleotide trapping in the inactive Walker B mutant D551N (Figure 4.3 A, B), in agreement with the V_i-induced trapping data (Urbatsch *et al.*, 2000c). These results show that the different transition states revealed by distinct P_i analogues can all be formed in the E552Q and E1197Q mutants in a comparable manner to WT Mdr3. Finally, results in Figure 4.3 C show that BeF_x- and AlF_4^--induced nucleotide trapping in the WT and E552Q and E1197Q mutants is EDTA sensitive. Together, these results expand observations with V_i (Figure 4.3, Urbatsch *et al.*, 2000c), showing that in the mutants E552Q and E1197Q activation and cleavage of the bond between the β- and γ-phosphates of ATP seem to take place.

Figure 4.3:

Photolabeling of Mdr3 NB site mutants by aluminum fluoride and beryllium fluoride trapping with Mg-8-azido-[α^{32}P]ATP

Purified and activated wild-type and mutant Mdr3 variants were preincubated for 20 min at 37 °C with 5 μM 8-azido-[α^{32}P]ATP and 3 mM $MgCl_2$ in the absence or presence of 100 μM verapamil, 1 mM aluminum chloride, and 5 mM sodium fluoride (A; AlF_4^-) or 0.2 mM beryllium sulfate and 1 mM sodium fluoride (B; BeF_x), as indicated above the lanes. Samples were processed for photolabeling as described in Materials and Methods and analyzed by SDS-PAGE. (C) The EDTA sensitivity of AlF_4^-, BeF_x, and vanadate (V_i) induced trapping of nucleotide in WT and mutant Mdr3 variants was tested as described in the legend to Figure 4.2. The gel in (C) was overexposed to ascertain the absence of labeling in all +EDTA lanes.

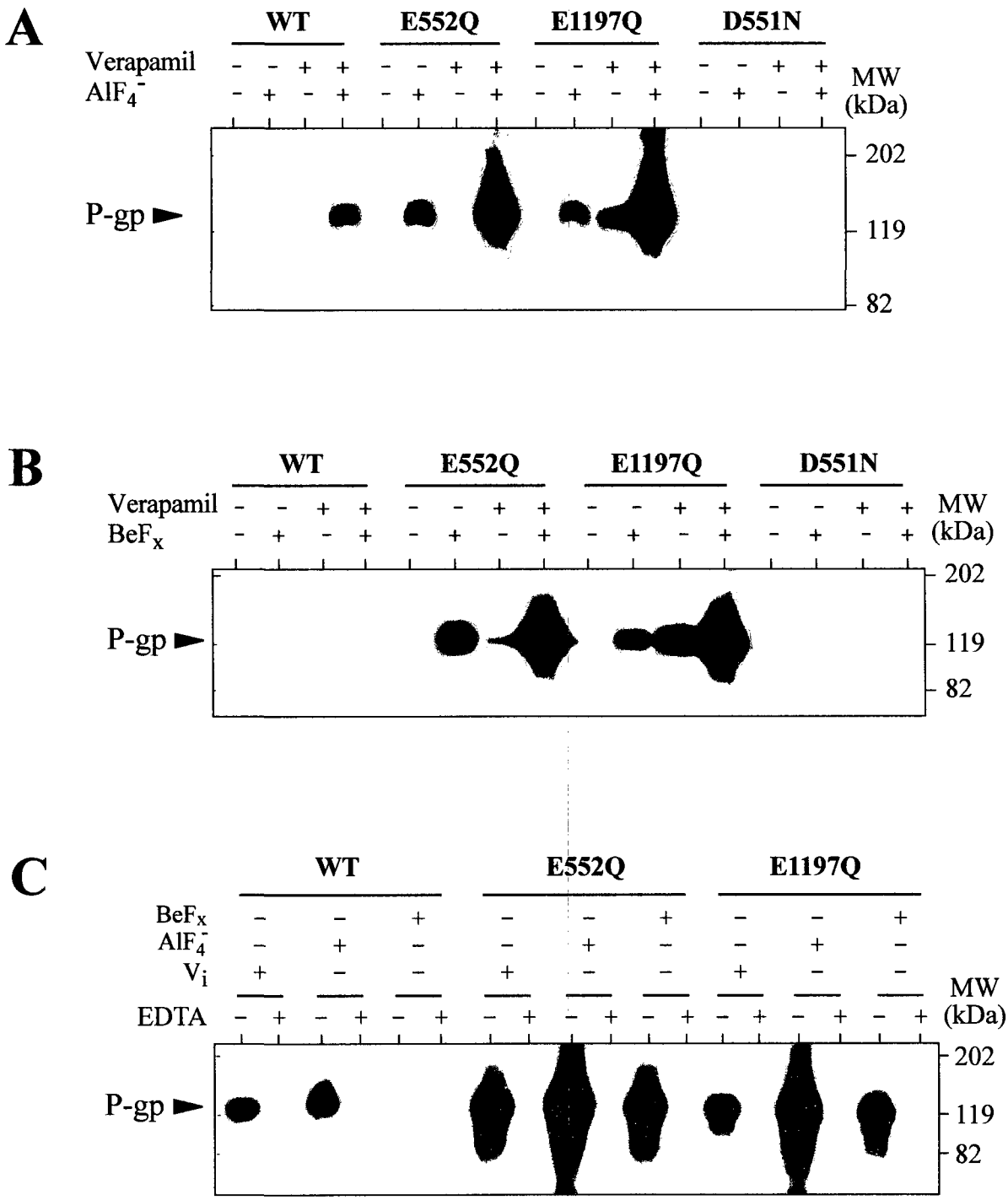
A
WT
E552Q
E1197Q
D551N
Verapamil
AlF4-
MW
(kDa)
P-gp
202
119
82
B
WT
E552Q
E1197Q
D551N
Verapamil
BeFx
MW
(kDa)
P-gp
202
119
82
C
WT
E552Q
E1197Q
BeFx
AlF4-
Vi
EDTA
MW
(kDa)
P-gp
202
119
82

Additionally, thin-layer chromatography (TLC) was used to identify the nucleotides bound to the enzymes following trapping in the presence of V_i. As seen in figure 4.4, 8-azido-[α^{32}P]ADP can be detected following incubation of the WT and E552Q and E1197Q mutants with 8-azido-[α^{32}P]ATP and vanadate, while it is absent in the catalytically inactive D551N mutant. Furthermore, formation of ADP does not occur in any of the enzymes when the trapping reaction is carried out at 4 °C. Thus, it appears that the E552Q and E1197Q mutants are able to hydrolyse at least one molecule of ATP. In these experiments, we also detected the presence of ATP in both WT and the E552Q and E1197Q mutants. Senior and colleagues have previously reported that only ADP could be recovered from WT protein following V_i-induced trapping of nucleotide (Urbatsch *et al.*, 1995b; Sankaran *et al.*, 1997b; Sankaran *et al.*, 1997a). The reason for the apparent discrepancy has not yet been determined but could be due to different experimental procedures used to eliminate unreacted nucleotides from the incubation reaction prior to recovery and analysis of bound nucleotides. An additional radioactive spot of slower mobility is also observed in each protein-containing lane, at both 37 and 4 °C, and to a lesser extent in the diluted commercial preparation of 8-azido-[α^{32}P]ATP (Figure 4.4, *). The identity of this radioactive spot is currently unknown; however, its presence in all protein-containing lanes, together with the lack of temperature dependence, strongly suggests that it corresponds to a nonspecific contaminant of the commercial preparation of 8-azido-[α^{32}P]ATP that becomes slightly enriched upon incubation with protein.

The nature of the molecular defect in the E552Q and E1197Q mutants was further investigated by comparing the V_i dependence of nucleotide trapping of the WT and the E552Q and E1197Q mutants in a dose-response experiment (0, 0.05 μM $\leq V_i \leq$100 μM) (Figure 4.5). For WT Mdr3, no trapping was observed for V_i concentrations below 10 μM (K_i ~5-10 μM) while robust trapping was seen at 100 μM V_i, a concentration known to completely inhibit P-gp ATPase activity (Ambudkar *et al.*, 1992; Sarkadi *et al.*, 1992; al-Shawi and Senior, 1993; Shapiro and Ling, 1994; Urbatsch *et al.*, 1995b). As expected from the results in our previous publication (Urbatsch *et al.*, 2000c), both E552Q and E1197Q could trap 8-azido-[α^{32}P]nucleotide at all V_i concentrations tested. However, clear differences were noted in the response of each mutant to increasing V_i

Figure 4.4:

Thin-layer chromatography analysis of vanadate-trapped nucleotides in Mdr3 NB site mutants

Purified and activated wild-type and mutant Mdr3 variants were preincubated with 5 μM 8-azido-[α^{32}P]ATP and 3 mM $MgCl_2$ for 10 min at either 37 or 4 °C in the presence of 200 μM vanadate and 100 μM verapamil. Unbound ligands were removed by ultracentrifugation and washing. The protein pellets were then resuspended in 8-azido-ATP and precipitated by TCA. The supernatant (0.5 μL) and 125 dpm of standards were applied to a PEI-cellulose plate following magnesium chelation with EDTA. The plate was developed in 3.2% (w/v) NH_4HCO_3 and exposed to film. The asterisk (*) indicates the position of a non-specific radioactive contaminant present in the commercial preparation of 8-azido-[α^{32}P]ATP.

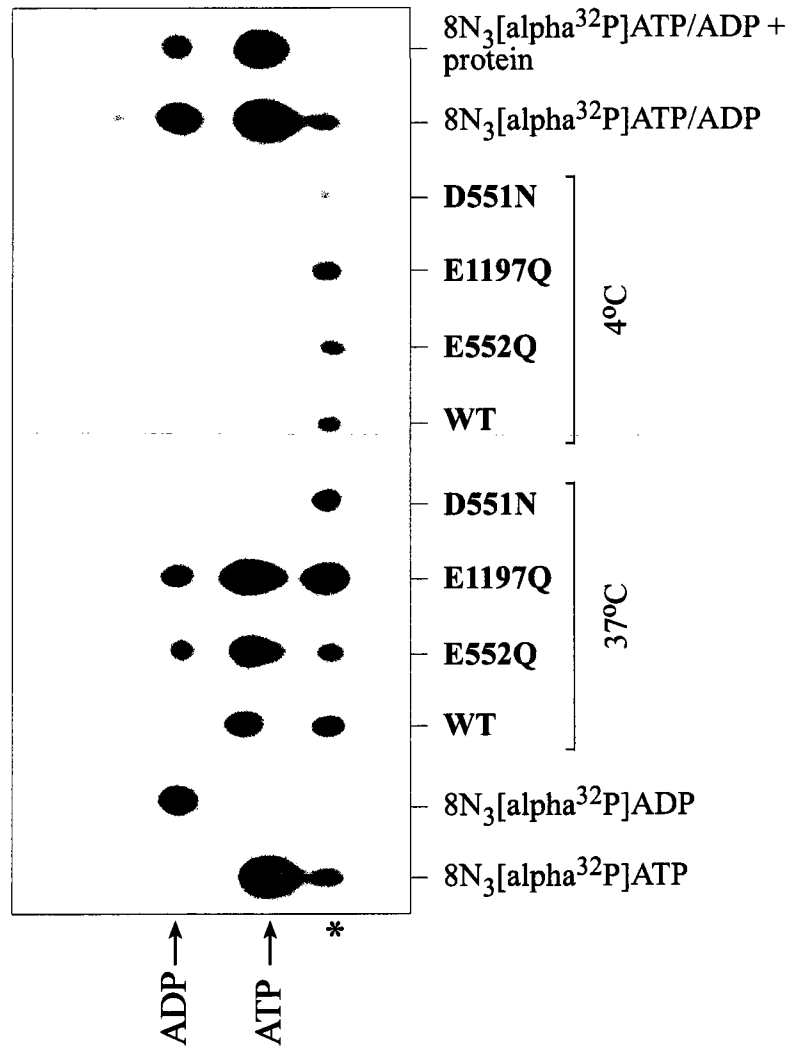
8N3[alpha32P]ATP/ADP + protein
8N3[alpha32P]ATP/ADP
D551N
E1197Q
E552Q
WT
4°C
D551N
E1197Q
E552Q
WT
37°C
8N3[alpha32P]ADP
8N3[alpha32P]ATP
ADP
ATP
*

Figure 4.5:

Photolabeling of Mdr3 NB site mutants with Mg-8-azido-[α^{32}P]ATP and varying concentrations of vanadate

Purified and activated wild-type and mutant Mdr3 variants were preincubated with 5 μM 8-azido-[α^{32}P]ATP, 3 mM $MgCl_2$, and 100 μM verapamil for 20 min at 37 °C in the absence or presence of increasing concentrations of vanadate, as indicated above the lanes. Samples were processed for photolabeling as described in Materials and Methods and analyzed by SDS-PAGE.

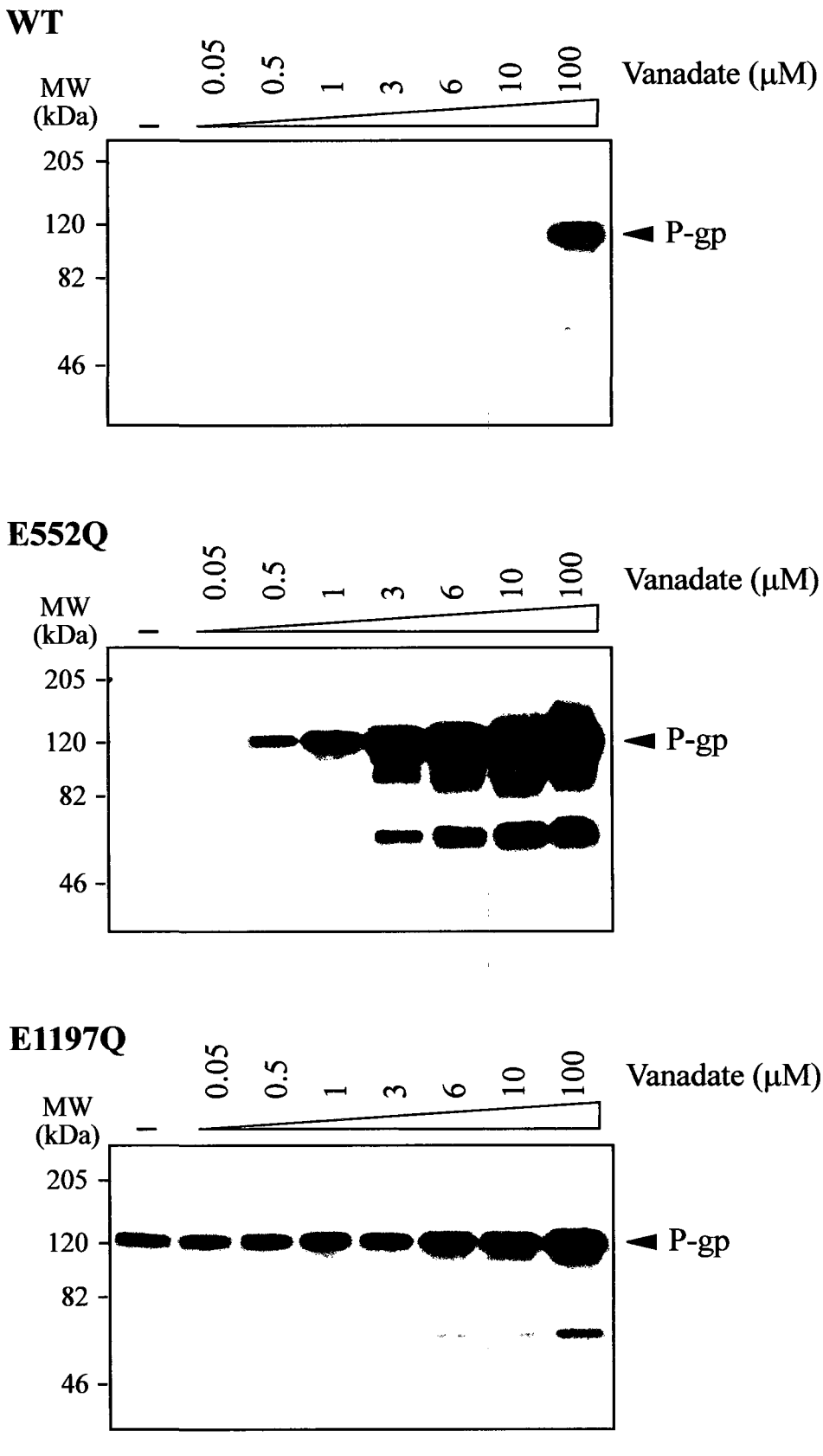
WT
MW
(kDa)
–
0.05
0.5
1
3
6
10
100
Vanadate (μM)
205
120
82
46
P-gp
E552Q
MW
(kDa)
–
0.05
0.5
1
3
6
10
100
Vanadate (μM)
205
120
82
46
P-gp
E1197Q
MW
(kDa)
–
0.05
0.5
1
3
6
10
100
Vanadate (μM)
205
120
82
46
P-gp

concentrations. E552Q showed low levels of trapping in absence of V_i, but labelling increased in a dose-dependent fashion (similar to the WT enzyme) with very intense labelling seen at 100 μM V_i (>50-fold stimulation). On the other hand, nucleotide trapping in E1197Q appeared to be largely V_i independent, appearing robust in the absence of V_i and showing only a modest increase even at the highest V_i concentration tested (100 μM; 2-3-fold stimulation). The distinct V_i dose-response behaviours of the two homologous mutants E552Q and E1197Q suggest that NBD1 and NBD2 are not catalytically symmetrical, with NBD2 (intact in E552Q) showing a more robust V_i-dependent trapping than its NBD1 counterpart (intact in E1197Q).

To further investigate a possible functional asymmetry between NBD1 and NBD2, suggested by the V_i dose-response study (Figure 4.5), we attempted to semi-quantitatively assess in which of the NBD(s) of E552Q and E1197Q the nucleotide was trapped, in both the absence and presence of V_i. For this, a protease-hypersensitive site present in the highly charged linker domain of the protein (Bruggemann *et al.*, 1989) was used to generate two Mdr3 halves that can be resolved on the gel and identified by antibodies specific for each half of the protein (Figure 4.6 A) (Julien and Gros, 2000). Briefly, WT and mutant enzymes were photolabelled with 8-azido-[α^{32}P]ATP in the presence of VER to stimulate labelling, in either the absence (Figure 4.6) or presence (Figure 4.7) of V_i, followed by proteolytic cleavage in increasing trypsin concentrations and analysis by SDS-PAGE. The gel was then blotted onto a nitrocellulose membrane, exposed to film to reveal the ^{32}P-labelled tryptic fragments (Figure 4.6 B), and analyzed by immunoblotting with two monoclonal antibodies specific for the amino-terminal (MD13; Figure 4.6 C) and carboxyl-terminal (MD7; Figure 4.6 E) halves of the protein (Shapiro *et al.*, 1996). The photolabelling signal (autoradiograph) was colorized to green, while the respective immunoblotting signals were colorized to red. Overlays of the two images are shown in panels D and F and identify in yellow the ^{32}P photolabelled Mdr3 tryptic fragments recognized by each antibody. For E1197Q, results in panels F and H clearly show that all of the label is in the MD7-reactive, C-terminal half of the protein, with little, if any, overlap with the MD13 reactive species detected in panel D. Conversely, and although the overall photolabelling signal is much weaker than that seen for E1197Q, the label incorporated in E552Q colocalizes with the N-terminal and MD13-

Figure 4.6:

Trypsin digestion of Mdr3 NB site mutants photolabeled with Mg-8-azido-[α^{32}P]ATP in the absence of vanadate

Purified and activated mutant Mdr3 variants were preincubated with 5 μM 8-azido-[α^{32}P]ATP, 3 mM $MgCl_2$, and 100 μM verapamil for 20 min at 37 °C. Unbound ligands were removed by ultracentrifugation and washing, and the samples were then UV-irradiated. The samples were promptly digested with trypsin (see Materials and Methods) at varying trypsin-to-protein ratios (lane 1, 1:75; lane 2, 1:37.5; lane 3, 1:18.75; lane 4, 1:9.38; lane 5, 1:4.69; lane 6, 1:2.34; lane 7, 1:1.17) and photolabeled; trypsinized samples were separated by electrophoresis on a 10% SDS-polyacrylamide gel, transferred onto a nitrocellulose membrane, and subjected to autoradiography (B). The membrane was then analyzed by immunoblotting using mouse monoclonal anti-P-glycoprotein antibodies that recognize either the N-terminal half (MD13, C) or the C-terminal half (MD7, E) or both halves of P-gp (C219, G) to identify fragments corresponding to NBD1 or NBD2. The scans of the autoradiograph (B) and of the NBD-specific immunoblots (C, E) were colorized in green and red, respectively, using Adobe Photoshop. The photolabeled tryptic peptides immunoreactive with either MD13 or MD7 are seen in yellow color in (D) and (F), respectively. Some of the predicted structural features of P-gp, including the position of the protease-hypersensitive site, as well as the epitopes for MD13, MD7, and C219 are identified in (A).

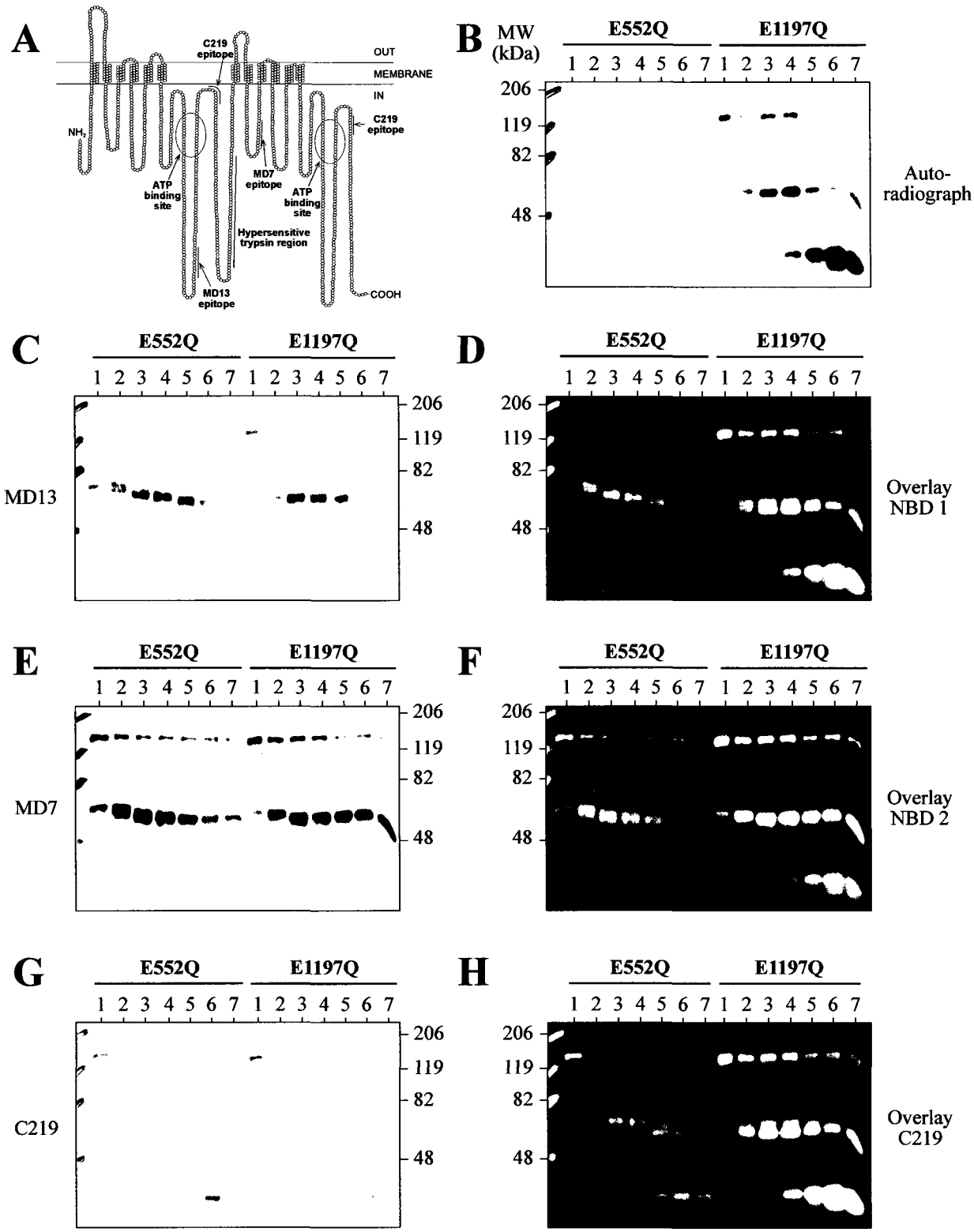
A
C219 epitope
OUT
MEMBRANE
IN
NH2
C219 epitope
ATP binding site
MD7 epitope
ATP binding site
Hypersensitive trypsin region
MD13 epitope
COOH
B
MW (kDa)
E552Q
E1197Q
1 2 3 4 5 6 7 1 2 3 4 5 6 7
206
119
82
48
Auto-radiograph
C
E552Q
E1197Q
1 2 3 4 5 6 7 1 2 3 4 5 6 7
MD13
206
119
82
48
D
E552Q
E1197Q
1 2 3 4 5 6 7 1 2 3 4 5 6 7
206
119
82
48
Overlay NBD 1
E
E552Q
E1197Q
1 2 3 4 5 6 7 1 2 3 4 5 6 7
MD7
206
119
82
48
F
E552Q
E1197Q
1 2 3 4 5 6 7 1 2 3 4 5 6 7
206
119
82
48
Overlay NBD 2
G
E552Q
E1197Q
1 2 3 4 5 6 7 1 2 3 4 5 6 7
C219
206
119
82
48
H
E552Q
E1197Q
1 2 3 4 5 6 7 1 2 3 4 5 6 7
206
119
82
48
Overlay C219

Figure 4.7:

Trypsin digestion of Mdr3 NB site mutants photolabeled with Mg-8-azido-[α^{32}P]ATP in the presence of vanadate

Purified and activated wild-type and mutant Mdr3 variants were preincubated with 5 μM 8-azido-[α^{32}P]ATP, 3 mM $MgCl_2$, and 100 μM verapamil in the presence of 200 μM vanadate for 20 min at 37 °C. Unbound ligands were removed by ultracentrifugation and washing, and the samples were then UV-irradiated. The samples were promptly digested with trypsin at varying trypsin-to-protein ratios (lane 1, 1:37.5; lane 2, 1:18.75; lane 3, 1:9.38; lane 4, 1:4.69). Photolabeled, trypsinized samples were separated by electrophoresis on 10% SDS-polyacrylamide gels, transferred onto nitrocellulose membranes, and subjected to autoradiography. The position of tryptic fragments corresponding to photolabeled NBD1 and NBD2 is indicated and was deduced by immunoblotting using MD13 and MD7 antibodies as described in the legend to Figure 4.6.

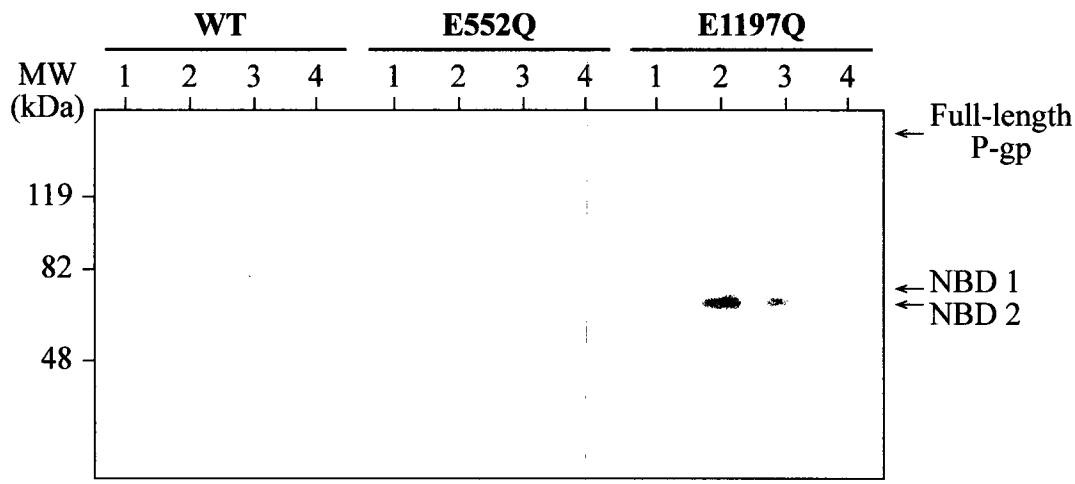
WT
E552Q
E1197Q
MW
(kDa)
1 2 3 4 1 2 3 4 1 2 3 4
119
82
48
Full-length
P-gp
NBD 1
NBD 2

reactive half (panels D and H) and does not overlap with the faster migrating MD7 positive fragment (panel F). Importantly, these results show that, in the absence of V_i, nucleotide trapping occurs exclusively in the mutated NBD of each mutant. Although the two Mdr3 halves generated by limited trypsin digestion differ only by a few kilodaltons (62 vs 76 kDa), they can be separated by the gel system used in this and previous studies (Julien and Gros, 2000). This is verified (Figure 4.6 G, H) by immunoblotting the same membrane with the monoclonal antibody C219 that recognizes a peptide epitope (VVQE/AALD) conserved in both halves of Mdr3 and present in the MD13 and MD7 immunoreactive fragments. This control also identifies the lane where the MD13 and MD7 immunoreactive fragments are present at equivalent amounts in the digest (lane 4). Because the WT protein is not labelled by 8-azido-[α^{32}P]ATP in the absence of V_i, it could not be analyzed in figure 4.6.

A similar proteolytic cleavage experiment was carried out in the presence of V_i (Figure 4.7). Results show that in the WT protein V_i stimulates nucleotide trapping in both NBDs with a slight preference for NBD2, in agreement with previous results (Hrycyna *et al.*, 1999). In the presence of V_i, nucleotide trapping was seen in both NBD1 and NBD2 of the E552Q and E1197Q mutants (albeit at different ratios, depending on the position of the mutation). Control immunoblotting experiments with the C219 antibody indicate that the two Mdr3 halves are separated by the gel system and that lane 2 contains almost equal amounts of MD13 (NBD1) and MD7 (NBD2) immunoreactive species (data not shown). These results indicate that, in WT Mdr3 and the E552Q and E1197Q mutants, both NBDs can hydrolyse at least one molecule of ATP with subsequent trapping of ADP in the presence of V_i and inhibition.

4.5 Discussion

Several aspects of the mechanism of action of P-gp remain poorly understood; these include the exact catalytic cycle, the equivalent or nonequivalent nature of the NBDs for ATP binding and hydrolysis, and the type of signal produced at the NBDs by ATP hydrolysis that is transmitted to the drug-binding sites in the TMDs to mediate substrate efflux. We have previously identified glutamates E552 and E1197 in NBD1 and NBD2, respectively, of mouse Mdr3 as highly conserved carboxylate residues possibly involved in initiation or in other aspects of catalysis (Urbatsch *et al.*, 2000c). These homologous residues map to the extended Walker B motif (or the D-loop) of the NBD and immediately follow the aspartate residues D551 and D1196, which coordinate Mg^{2+} in the site. Multiple sequence alignments suggest that E552 and E1197 are homologous to E179 of the *Salmonella typhimurium* ABC transporter HisP. Crystallographic analysis of HisP strongly suggests that E179 positions a water molecule for in-line nucleophilic attack on the terminal phosphate of ATP (Hung *et al.*, 1998). Indeed, E179 is mutation sensitive, and replacement to aspartate abrogates ATPase activity and transport activity (Hung *et al.*, 1998). Therefore, it is highly likely that E552 and E1197 play a similar role in P-gp.

Results expressed in the present study suggest that the E552Q and E1197Q mutants are not completely inactive (as opposed to the Walker B mutant D551N) and that these mutants can indeed cleave ATP to ADP and P_i, undergoing partial reactions toward a full cycle of catalysis but never fully turning over. First, although neither mutant has ATPase activity that can be detected by P_i release, both show V_i-induced trapping of 8-azido-[α^{32}P]nucleotide that can be stimulated by drugs, a behaviour clearly distinct from that of the D551N mutant. Previous studies have shown that hydrolysis of 8-azido-ATP to 8-azido-ADP is a prerequisite to V_i-induced trapping, resulting in the formation of a stable {P-gp·Mg-8-azido-ADP·V_i} transition-state complex that can be cross-linked to the protein (Urbatsch *et al.*, 1995a; Urbatsch *et al.*, 1995b). Second, 8-azidonucleotide trapping in the mutant enzymes in the absence and presence of V_i is both temperature dependent and EDTA sensitive, as in the WT enzyme (Figure 4.2). Third, other transition-state analogues of P_i can also support nucleotide trapping in the mutants, and this trapping is EDTA sensitive as well (Figure 4.3). Fourth, in the absence of V_i,

nucleotide trapping takes place at the mutant NBD only (Figure 4.6). Finally, TLC analysis of the nucleotides bound to the enzymes following V_i trapping of 8-azido-ATP shows formation of 8-azido-ADP by the WT and E552Q and E1197Q mutants (Figure 4.4). Together, these results indicate that E552Q and E1197Q can indeed cleave ATP to ADP and P_i and that 8-azido-ADP is the nucleotide trapped in the photolabelled enzymes. Moreover, in their recent work, Sauna and colleagues also demonstrated using α- and γ-labelled 8-azido-[^{32}P]ATP that mutants at the equivalent positions of the human MDR1 protein (E556Q and E556A, E1201Q and E1201A, and the double mutants) are indeed capable of ATP hydrolysis and single-site catalysis (Sauna *et al.*, 2002). Therefore, in the E552Q and E1197Q mutants, steps downstream from the formation of the transition state, such as the release of MgADP and/or P_i, or others, must be impaired. The observation that similar amounts of 8-azido-[α^{32}P]ADP are incorporated in the WT and mutant enzymes in the presence of V_i under conditions of drug stimulation (Urbatsch *et al.*, 2000c) strongly argues that P_i release is normal and that another step downstream of P_i release is impaired in the mutant enzymes. The finding that in the absence of V_i nucleotide trapping (ADP) occurs in the mutant NBD exclusively supports the contention that ADP release from the mutant NBD is the key catalytic step impaired in the mutant enzymes. Although our interpretation favors ADP release as the mechanistic step impaired in the mutants, the work by Sauna and colleagues (Sauna *et al.*, 2002) suggests that ADP release is impaired only in the double mutants but not in the single mutants. Indeed, they suggest that the single E556A/Q and E1202A/Q mutants are defective in the second ATP hydrolysis event of the catalytic cycle, which should reset the protein after hydrolysis at the first site. Additional experiments will be required to determine whether ADP release is in fact occurring in the mouse Mdr3 mutants described in the present report.

The question of whether NBD1 and NBD2 of P-gp are structurally and functionally equivalent and whether they play distinct roles during catalysis and transport is still being debated. In support of functional equivalence of the two sites are the observations that (1) there is no evidence for binding site heterogeneity in ATP- and ADP-binding studies with purified P-gp (Sharom *et al.*, 1999; Urbatsch *et al.*, 2000a), (2) mutations in Walker A or B residues in either NBD completely abolish drug transport and

ATPase activity (Azzaria *et al.*, 1989; Urbatsch *et al.*, 1998), (3) each P-gp half shows low intrinsic ATPase activity (Loo and Clarke, 1994), (4) V_i inhibits ATP hydrolysis and can induce trapping of 8-azido-[α^{32}P]ADP·V_i in P-gp with seemingly equal labelling of NBD1 and NBD2 (Urbatsch *et al.*, 1995a; Urbatsch *et al.*, 1995b; Sauna and Ambudkar, 2001), and (5) NEM inhibits P-gp ATPase activity by binding to a cysteine present in the Walker A motif of NBD1 and NBD2 (al-Shawi *et al.*, 1994; Sharom *et al.*, 1999), and NEM-sensitive ATPase activity is inhibited by similar ATP concentrations in single-cysteine P-gp mutants in NBD1 and NBD2 (Loo and Clarke, 1995a). Opposing data in support of structurally and functionally distinct NBDs include the observations that (1) under binding conditions (4 °C), 8-azido-[α^{32}P]ATP preferentially labels NBD1, while under hydrolysis conditions (37 °C and V_i), NBD2 is preferentially labelled in P-gp (Hrycyna *et al.*, 1999), (2) equivalent mutations in Walker B residues of NBD1 and NBD2 (D551N, D1196N) cause different conformational changes in Mdr3 as measured by trypsin sensitivity (Julien and Gros, 2000), (3) median inhibition of ATPase activity in cysteine-less P-gp mutants bearing single-cysteine replacements in NBD1 or NBD2 occurs at different NEM concentrations (Loo and Clarke, 1995a), and (4) functional studies of CFTR (Szabo *et al.*, 1999; Aleksandrov *et al.*, 2001; Aleksandrov *et al.*, 2002; Powe Jr. *et al.*, 2002), of MRP1 (Gao *et al.*, 2000; Hou *et al.*, 2000; Nagata *et al.*, 2000; Cui *et al.*, 2001; Hou *et al.*, 2002), and of the NBDs of the bacterial arsenite transporter ArsA (Zhou and Rosen, 1997) show that NBD1 and NBD2 have different ATP-binding and hydrolysis properties. The study of E552Q and E1197Q reported here clearly argues in favour of two NBDs that are not functionally equivalent in full-length P-gp. This is most clearly illustrated by results from the V_i dose-response experiment (Figure 4.5). In this experiment it can be observed that E552Q and E1197Q trap nucleotide in the absence of V_i and that the response of each mutant to V_i is completely different, with E552Q showing a strongly dose-dependent increase in labelling (similar to WT), while V_i has little effect on nucleotide trapping in E1197Q. This behaviour is inconsistent with the presence of two functionally equivalent NBDs in the protein. Since nucleotide trapping in the mutants occurs after cleavage of ATP (with ADP trapped; see above), the differential V_i dose-response observed in E552Q and E1197Q is most easily explained by differential sensitivity of the nonmutant site to inhibition by V_i. Finally, proteolytic cleavage studies

of photolabelled WT and mutant proteins have shown that (a) in the absence of V_i, only the mutant NBD is occluded, and (b) in the presence of V_i, both NBDs are occluded (albeit at a different degree; Figure 4.7). The idea of asymmetrical NBDs in P-gp is in agreement with the results previously reported by Hrycyna et al. (Hrycyna *et al.*, 1999) and Aleksandrov et al. (Aleksandrov *et al.*, 2001; Aleksandrov *et al.*, 2002; Powe Jr. *et al.*, 2002), and the results in this study are reminiscent of parallel studies of MRP1 (Gao *et al.*, 2000; Hou *et al.*, 2000; Nagata *et al.*, 2000; Cui *et al.*, 2001; Hou *et al.*, 2002) that also suggest nonequivalence of the two NBDs since it was observed for MRP1 that (1) mutation at the Walker A lysine of NBD2 has a more severe effect on transport than the homologous mutation at NBD1, (2) there is preferential binding of 8-azido-[γ^{32}P]ATP at NBD1, (3) there is preferential V_i-induced trapping of 8-azido-[α^{32}P]nucleotide at NBD2, and (4) NBD2 is also preferentially labelled by 8-azido-[α^{32}P]ADP.

In summary, the present work supports the finding that both NBDs are essential for function with complete cooperativity between the two sites and suggests that the E552 and E1197 residues of mouse Mdr3 are probably not the catalytic residues, as the E552Q and E1197Q mutants can hydrolyse ATP in both nucleotide-binding domains. Furthermore, our results support a model in which the two NBDs of P-gp are not functionally equivalent.

4.6 Acknowledgments

We especially thank Lian Wee Ler for growing the large cultures of all of the WT and mutant yeast clones. We are indebted to Cédric Orelle and Dr. John Hanrahan (Physiology Department, McGill University) for critical reading of the manuscript. We are also grateful to Dr. Victor Ling (The B.C. Cancer Research Centre, Vancouver, Canada) for the generous gift of mouse monoclonal antibodies MD13 and MD7.

Having determined that residues E552 and E1197 in Abcb1a are not classical catalytic residues, we next wanted to investigate the actual role of these invariant carboxylates in Abcb1a catalysis. The crystal structure of the NBD of HlyB (Kranitz *et al.*, 2002; Schmitt *et al.*, 2003) suggested that the invariant carboxylate immediately following the Walker B aspartate residue is part of a catalytic dyad, with the conserved histidine of the H-loop as partner. In HlyB-NBD this catalytic dyad appears to cause substrate-assisted hydrolysis of bound ATP. Thus, we used site-directed mutagenesis to analyse different substitutions at the invariant carboxylates in Abcb1a to gain more insight into the function of these residues and obtain more details on the catalytic mechanism of Abcb1a.

Chapter 5

Investigating the Role of the Invariant Carboxylate Residues E552 and E1197 in the Catalytic Activity of Abcb1a (Mouse Mdr3)

Published manuscript reproduced by permission from the publisher:

Carrier, I. and Gros, P. Investigating the Role of the Invariant Carboxylate Residues E552 and E1197 in the Catalytic Activity of Abcb1a (Mouse Mdr3). *FEBS Journal*, **275(13)**: 3312-3324, 2008.

5.1 Abstract

The invariant carboxylate residue which follows the Walker B motif (hyd_4DE/**D**) in the nucleotide binding domains (NBDs) of ABC transporters is thought to be involved in the hydrolysis of the γ-phosphate of MgATP, either by activating the attacking water molecule or by promoting substrate-assisted catalysis. In Abcb1a, this invariant carboxylate residue corresponds to E552 in NBD1 and E1197 in NBD2. To further characterize the role of these residues in catalysis, we created in Abcb1a the single-site mutants E552D, N, and A in NBD1, and E1197D, N, and A in NBD2, as well as the double mutant E552Q/E1197Q. In addition, we created mutants in which the Walker A K→R mutation known to abolish ATPase activity was introduced in the non-mutant NBD of E552Q and E1197Q. ATPase activity, binding affinity and trapping properties were tested for each Abcb1a variant. The results suggest that the length of the invariant carboxylate residue is important for the catalytic activity, whereas the charge of the side chain is critical for full turnover to occur. Moreover, in the double-mutants where the K→R mutation is introduced in the "wild-type" NBD of the E→Q mutants, single-site turnover is observed, especially when NBD2 can undergo γ-Pi cleavage. The results further support the idea that the NBDs are not symmetric and suggest that the invariant carboxylates are involved both in NBD-NBD communication and transition-state formation through orientation of the linchpin residue.

5.2 Introduction

Multidrug resistance (MDR) is of major concern in the treatment of many important human diseases such as cancer, schizophrenia and infections by micro-organisms, including HIV (Avendano, 2000; Loo and Clarke, 2005; Yasui-Furukori *et al.*, 2006). MDR is characterized by cross-resistance to structurally and functionally unrelated chemicals. Overexpression of membrane transporters of wide substrate specificity is the most common cause of MDR. These transporters include members of the ATP-binding cassette (ABC) protein superfamily, such as P-glycoprotein (Pgp, ABCB1), multidrug resistance-associated protein (MRP, ABCC1) and breast cancer resistance protein (BCRP, ABCG2) (Gottesman, 2002). With 48 members in humans, 56 in the fly (*Drosophila melanogaster*), 129 in plants and well over 300 in bacteria, the ABC transporter superfamily is one of the largest and most conserved gene families known (Gottesman and Ambudkar, 2001; Sanchez-Fernandez *et al.*, 2001). Mutations in about half of the 48 human members cause diseases and phenotypes including MDR, and make this family of proteins of great clinical interest (Dean and Annilo, 2005). Diseases include Tangier disease (ABCA1), cystic fibrosis (ABCC7) and sitosterolemia (ABCG5, ABCG8), to name a few.

The structural subunit which defines ABC transporters is composed of one transmembrane domain (TMD), formed by six putative transmembrane α helices and one cytosolic nucleotide-binding domain (NBD) (Chen *et al.*, 1986; Gros *et al.*, 1986). Usually, a complete ABC transporter is represented by various combinations of four domains, of which two are TMDs and two are NBDs (Holland and Blight, 1999). The four domains of this membrane-associated complex can be assembled from two to four separate protein subunits (most prokaryotes) or arranged in one single polypeptide (most eukaryotes). Crystallization of the ABC transporters Sav1866 and ModBC, in the absence and presence of nucleotide, has provided good structural models for ABC transporters in the lipid bilayer and the changes associated with dimerization and opening of the NBDs (Dawson and Locher, 2006; Dawson and Locher, 2007; Hollenstein *et al.*, 2007b; Zolnerciks *et al.*, 2007). In these 3D structures, it is thus possible to observe the position of each α helix in the TMD and establish which helices interact. Also, in the structures where nucleotide is present, dimerization of the NBDs is demonstrated, as observed for

other NBDs that were purified without their TMDs (Diederichs *et al.*, 2000; Hopfner *et al.*, 2000; Smith *et al.*, 2002; Verdon *et al.*, 2003b; Zaitseva *et al.*, 2005c). In ABC transporters, the TMDs form the translocation pathway and the NBDs hydrolyse ATP to energize transport. Based on the fact that ATP hydrolysis by ABC transporters is highly cooperative, it has been suggested that the two NBDs function as a dimer in the translocation process (Davidson *et al.*, 1996; Liu *et al.*, 1997); this has now been firmly established by several crystal structures (Hopfner *et al.*, 2000; Smith *et al.*, 2002; Dawson and Locher, 2006).

Whereas the TMDs are responsible for allocrite transport, it is the energy from ATP binding and hydrolysis, by the NBDs, that drives this transport. A high degree of sequence and structural conservation is observed for NBDs across the family. The NBD is an L-shaped protein with a two-domain architecture: the first is the catalytic domain, composed of an ABC (ABCβ) and a RecA-like subdomain, and contains the nucleotide binding site; the second is the helical domain (ABCα), which interacts with the TMD and is unique to ABC transporters because of an insertion of ~70 residues between the two Walker motifs (Walker *et al.*, 1982; Hung *et al.*, 1998). Each NBD contains several conserved sequence motifs: the Walker A and B motifs, the signature or LSGGQ motif and the A-, D-, H-, and Q-loops. These motifs are positioned around the bound nucleotide and help to position and maintain it in the active site. In particular, the Walker A motif wraps around the β-phosphate of bound nucleotide (Walker *et al.*, 1982), the Walker B motif is responsible for coordinating the essential Mg^{2+} cofactor (Walker *et al.*, 1982; Urbatsch *et al.*, 1998; Hrycyna *et al.*, 1999), the signature sequence contacts the γ-phosphate of the bound nucleotide across the dimer (Hopfner *et al.*, 2000) and the aromatic residue of the A-loop stacks against the adenine moiety of bound nucleotide and provides further stabilization and specificity (Ambudkar *et al.*, 2006; Kim *et al.*, 2006). The D-loop is thought to be involved in NBD-NBD communication (Zaitseva *et al.*, 2005a; Oloo *et al.*, 2006). The H-loop has recently been hypothesised to be directly involved in hydrolysis of the γ-phosphate by positioning the terminal phosphate in the correct orientation for attack by the catalytic water molecule (Hanekop *et al.*, 2006). And finally, the Q-loop, whose glutamine residue interacts with the putative catalytic water and a helix extending from the TMD, may be involved in signal transduction between the

TMD and NBD, by sensing either hydrolysis of the terminal phosphate or the presence of substrate in the drug-binding site (Urbatsch *et al.*, 2000b; Dalmas *et al.*, 2005).

Although recent successes in solving the crystal structures of ABC transporters have laid the foundation for a new era of studies using structure-guided mutagenesis, many issues relating to the mechanism of action of ABC transporters remain obscure. An important issue is the catalytic mechanism of ATP hydrolysis by the two NBDs, which can be further subdivided into two major components. The first pertains to the actual cleavage of the terminal phosphate and the second to NBD-NBD communication. Two models of catalysis by ABC transporters are currently accepted: (a) general base (Yoshida and Amano, 1995; Hung *et al.*, 1998; Moody *et al.*, 2002) and (b) substrate-assisted (Zaitseva *et al.*, 2005a; Hanekop *et al.*, 2006). Interestingly, both models involve the invariant carboxylate (IC) residue which immediately follows the Walker B aspartate, although it performs different tasks in each case. In the former model, the IC is the catalytic residue which coordinates and activates the attacking water molecule that cleaves the terminal phosphate of bound ATP. In the latter model, the IC is part of a catalytic dyad, along with the histidine residue of the H-loop, and positions the "linchpin" histidine in the correct orientation such that all atoms are then in position to favour abstraction of a proton from the attacking water molecule by the bound ATP, which results in cleavage of the terminal phosphate by the aforementioned water molecule. At present, it is tempting to favor substrate-assisted catalysis as the mechanism of action of ABC transporters because mutating the IC(s) in different enzymes is incompatible with a role for this residue in general base catalysis (Urbatsch *et al.*, 2000c; Sauna *et al.*, 2002; Verdon *et al.*, 2003a; Tombline *et al.*, 2004a).

In order to investigate further the role of the IC in the catalysis of ABC transporters, we created, in Abcb1a, six single-site mutants (E552D, N, and A, and E1197D, N, and A,) and three double-mutants (E552Q/E1197Q, E552Q/K1072R, K429R/E1197Q). The ATPase activity, binding affinity and trapping properties were tested for each Abcb1a variant.

5.3 Materials and Methods

5.3.1 Abcb1a cDNA Modifications

All mutations were created by site-directed mutagenesis using a recombinant PCR approach as described previously (Vogan and Gros, 1997). Mutations in NBD1 at position E552 were introduced using primer TK-5 (5'-GTGCTCATAGTTGCCTACA-3') and the following mutagenic oligos: E552Ar (5'-GTGGCCGCGTCCAAC-3'), E552Dr (5'-GTGGCGTCGTCCAAC-3'), and E552Nr (5'-AGGTGGCGTTGTCCAAC-3'). A second overlapping *mdr3* cDNA fragment was amplified using primer pairs HincII (5'-GAAAGCTGTCAACGAAGCC-3') and primer Mdr3-2008r (5'-CTGTGTCATGACA AGTTTG-3'). The amplification products were purified on gel, mixed, denatured at 94°C for 5 min followed by annealing at 54°C for 5 min and elongation at 72°C for 5 min (repeated 3 times) with VENT DNA polymerase in a reaction mixture without primers to generate hybrid DNA fragments. The hybrid products were then amplified using primers TK-5 and Mdr3-2008r, and a 1113 bp *Msc*I-*Sal*I fragment carrying the mutated segment was purified and used to replace the corresponding fragment in the pVT-*mdr3* construct (Beaudet and Gros, 1995) which had served as template in the PCR. To screen for the desired mutations, individual plasmids were isolated and the nucleotide sequence of the entire 1113 bp *Msc*I-*Sal*I fragment was determined. The mutations were then transferred to pHIL-*mdr3.5*-His_6 (Urbatsch *et al.*, 1998) using the restriction enzymes *Afl*II and *Eco*RI, as previously described (Urbatsch *et al.*, 2000c). Mutations in NBD2 at position E1197 were introduced using primer Y1040Wf (5'-GTGTTCAACTGGCCCACCCG-3') and the following mutagenic oligos: E1197Ar (5'-GATGTTGCTGCGTCCAGAAG-3'), E1197Dr (5'-GATGTTGCATCGTCCAGAAG-3'), and E1197Nr (5'-GATGTTGCGT TGTCCAGAAG-3'). A second overlapping *mdr3* cDNA fragment was amplified using mutagenic oligos E1197Af (5'-CTGGACGCAGCAACATC-3'), E1197Df (5'-CTGGACGATGCAACATC-3'), and E1197Nf (5'-CTGGACAACGCAACATCAG-3') with primer pHIL-3'r (5'-GCAAATGGCATTCTGACATCC-3'). The amplification products were purified on gel, mixed, denatured at 94°C for 5 min followed by annealing at 52°C for 5 min and elongation at 68°C for 5 min (repeated 3 times) with *Taq* HiFi polymerase in a reaction mixture without primers to generate hybrid DNA fragments. The hybrid products were then amplified using primers Y1040Wf and pHIL-3'r, and a 617 bp

*Xho*I(3386)-*Xho*I(4003) fragment carrying the mutated segment was purified and used to replace the corresponding fragment in the pHIL-*mdr3.5*-His_6 construct which had served as template in the PCR. To screen for the desired mutations and correct orientation of the inserted fragment, individual plasmids were isolated and the nucleotide sequence of the entire 617 bp *Xho*I(3386)-*Xho*I(4003) fragment was determined. For the double mutant E552Q/E1197Q, the E552Q mutation was excised from pHIL-E552Q using the restriction enzymes *Xma*I and *Eco*RI, and the 485 bp fragment containing the mutation was introduced in the corresponding sites of pHIL-E1197Q. For the double mutant E552Q/K1072R, the K1072R mutation was introduced into the E552Q template using a standard PCR approach with primer HincII and the mutagenic oligo which contains the *Xho*I site K1072R-*Xho*Ir (5'-CCGCTCGAGCAGCTGGACCACTGTGCTCCTCCCGC-3'). The 1622 bp *Xma*I-*Xho*I fragment containing both mutations was then introduced into pHIL-*Mdr3*. To screen for the desired mutations, individual plasmids were isolated and the nucleotide sequence of the entire 1622 bp *Xma*I-*Xho*I fragment was determined. For the double mutant K429R/E1197Q, a recombinant PCR technique was used to create the K429R mutation using pHIL-*mdr3.5* as template. A first fragment was created using primer Mdr3-1202f (5'-TTCGCCAATGCACGAGG-3') and mutagenic oligo K429Rr (5'-GTTGTGC TTCTTCCACAG-3'). A second overlapping *mdr3* cDNA fragment was amplified using mutagenic oligo K429Rf (5'-CTGTGGAAGAAGCACAAC-3') and primer E552Qr (5'-GGTGGCCTGGTCCAACAAAAG-3'). The amplification products were purified on gel, mixed, denatured at 98°C for 5 min and allowed to cool slowly to room temperature in a reaction mixture without primers to generate hybrid DNA fragments. Klenow polymerase and dNTPs were added to fill-in the single-stranded overhangs. The hybrid products were then amplified with VENT DNA polymerase using primers Mdr3-1202f and E552Qr, and a 402 bp *Bgl*II-*Xma*I fragment carrying the mutated segment was purified and used to replace the corresponding fragment in the pHIL-E1197Q construct. To screen for the desired mutation, individual plasmids were isolated and the nucleotide sequence of the entire 402 bp *Bgl*II-*Xma*I fragment was determined.

5.3.2 Purification of Abcb1a

For expression and purification of the six single and three double mutants, pHIL-*mdr3*-His_6 or pHIL-*mdr3.5*-His_6 carrying either a wild-type or mutant version of *Abcb1a* was transformed into *Pichia pastoris* strain GS115, according to the manufacturer's instructions (InVitrogen, license number 145457), and screened for expression as previously described (Urbatsch *et al.*, 2000c). Glycerol stocks of *P. pastoris* GS115 transformants were streaked on YPD plates and single colonies were used to inoculate 6 L liquid cultures. For preparation of *P. pastoris* membranes, cultures were induced with 1% methanol for 72 hrs and plasma membranes were isolated by centrifugation, as previously described (Lerner-Marmarosh *et al.*, 1999). Solubilization and purification of wild-type and mutant Abcb1a variants by affinity chromatography on Ni-NTA resin (Qiagen) and DE52-cellulose (Whatman) was as described (Lerner-Marmarosh *et al.*, 1999). This procedure routinely yielded between 0.4 to 2.5 mg of protein, with 95% minimum purity.

5.3.3 Assay of ATPase Activity

For ATPase assays, purified wild-type or mutant Abcb1a enzymes (concentrated DE52 eluate) were activated by incubating with 0.5% *E. coli* lipids (w/v; Avanti, acetone/ether preparation; equivalent to 50:1 w/w lipid to protein ratio) and 5 mM dithiothreitol for 30 min at 20°C at a final protein concentration of 0.07 $\mu g.\mu L^{-1}$ (wild-type) or 0.1 $\mu g.\mu L^{-1}$ (mutants). Aliquots of 5 µL were added into 50 mM Tris-HCl (pH 8.0), 0.1 mM EGTA, 10 mM Na_2ATP, and 10 mM $MgCl_2$, to a final volume of 250 µL and the mixture was incubated at 37°C. At the appropriate time, a 50 µL aliquot was removed and quenched in 1 mL of ice-cold 20 mM H_2SO_4. Inorganic phosphate (Pi) release was assayed as described previously (Van Veldhoven and Mannaerts, 1987). Drugs were added as dimethyl sulfoxide stock solutions, and the final solvent concentration in the assay was kept at $\leq$2% (v/v).

5.3.4 Photoaffinity Labeling with 8-azido-[α^{32}P]ATP

8-Azido-[α^{32}P]ATP photoaffinity labeling was performed as described previously (Urbatsch *et al.*, 2000c) with minor modifications. The purified Abcb1a proteins (concentrated DE52 eluate) were activated by incubating with *E. coli* lipids at a 50:1 lipid/protein ratio (w/w; Avanti, acetone/ether preparation) and 5 mM dithiothreitol, at a final concentration of 0.2 $mg.mL^{-1}$, at 20°C for 30 min immediately prior to starting the

photolabeling reactions. For direct labeling experiments, activated wild-type or mutant Abcb1a variants were incubated on ice for ~10 min with 3 mM $MgCl_2$, 50 mM Tris-HCl (pH 8.0), 0.1 mM EGTA and varying concentrations of 8-azido-[α^{32}P]ATP (5, 20, and 80 μM final concentrations at 0.2 Ci.mmol^{-1} specific activity) in a total volume of 50 μL (3 μg protein per sample). The samples were kept on ice and immediately UV-irradiated for 5 min {UVS-II Minerallight (260 nm) placed directly above the samples}. Unreacted nucleotides were then removed by centrifugation at 200 000 *g* for 30 min at 4°C in a TL-100 rotor (Beckman) and protein-containing pellets were washed with 100 μL ice-cold 50 mM Tris-HCl (pH 8.0) and 0.1 mM EGTA. The pellets were dissolved in sample buffer (5% w/v SDS, 25% v/v glycerol, 0.125 M Tris/HCl pH 6.8, 40 mM dithiothreitol, 0.01% pyronin Y) and separated by SDS/PAGE on 7.5% gels, followed by autoradiography to Kodak BioMax MS film. For nucleotide-trapping experiments, activated wild-type or mutant Abcb1a variants were incubated at 37°C for 20 minutes with 5 μM 8-azido-[α^{32}P]ATP, 3 mM $MgCl_2$, 50 mM Tris/HCl (pH 8.0), and 0.1 mM EGTA, with or without vanadate (Vi, 200 μM) in a total volume of 50 μL (3 μg protein per sample). Verapamil (100 μM) or valinomycin (100 μM) were included where indicated. Modifications to the normal procedure are indicated in the figure legends. The incubations were started by addition of 8-azido-[^{32}P]ATP and stopped by transfer on ice. Free label was then removed by centrifugation at 200 000 *g* for 30 min at 4°C in a TL-100 rotor (Beckman) and pellets were washed and resuspended in 30 μL of ice-cold 50 mM Tris/HCl (pH 8.0) and 0.1 mM EGTA. Samples were kept on ice and irradiated with UV light for 5 min. Labeled samples were resolved by SDS/PAGE on 7.5% gels and subjected to autoradiography. Orthovanadate solutions (100 mM) were prepared from Na_3VO_4 (Fisher Scientific) at pH10 and boiled for 2 min before use to break down polymeric species.

5.3.5 TLC Analysis of Vanadate-Trapped Nucleotides in Abcb1a

TLC was performed exactly as in Carrier *et al.* (Carrier *et al.*, 2003).

5.3.6 Partial Trypsin Digestion of Photolabeled Abcb1a

In order to detect radiolabeled nucleotide trapped in NBD1 and/or NBD2 of Abcb1a following photolabeling of the protein with 8-azido-[α^{32}P]ATP in the presence or absence of Vi, we took advantage of the protease hypersensitive site located in the linker region joining the two halves of Pgp (Bruggemann *et al.*, 1989). Photoaffinity-labeled proteins

were resuspended in 30 µL of 50 mM Tris/HCl (pH 8.0) and 0.1 mM EGTA and kept on ice. The incubation with trypsin (2 µL of each stock solution) was then carried out for 6 min at 37°C at enzyme-to-protein mass ratios of 1: 75, 1: 37.5, 1: 18.75, 1: 9.38, 1: 4.69, and 1: 2.34. Digestion was stopped by the addition of 15 µL of sample buffer. Finally, the Abcb1a fragments were resolved by SDS/PAGE on 10% gels, followed by transfer onto nitrocellulose membranes and exposition to film. Immunoblotting with the mouse mAb *C219* (Signet) that recognises both halves of Abcb1a, as well as with N- and C-terminal half specific mouse mAbs {*MD13* with its epitope in NBD1 (494-504), and *MD7* with its epitope in the intracellular loop 3 (805-815)}, respectively (gift of Dr. V. Ling, The B.C. Cancer Research Centre, Vancouver, Canada) (Shapiro *et al.*, 1996) was then performed on the membranes.

5.3.7 Routine Procedures

Protein concentrations were determined by the bicinchoninic acid method in the presence of 0.5% SDS using BSA as a standard. SDS/PAGE was carried out according to Laemmli (Laemmli, 1970) using the mini-PROTEAN II gel and Electrotransfer system (Bio-Rad). Samples were dissolved in sample buffer (5% SDS w/v, 25% glycerol v/v, 125 mM Tris/HCl pH 6.8, 40 mM dithiothreitol and 0.01% pyronin Y). For immunodetection of Abcb1a, the mouse mAb *C219* (Signet laboratories Inc.) was used with the enhanced chemiluminescence (ECL) detection system (NEN *Renaissance*, Perkin-Elmer). To recognize NBD1 specifically, the mouse mAb *MD13* was used and for NBD2 the mouse mAb *MD7* was employed. For autoradiography, SDS gels were stained with Coomassie Brilliant Blue, dried and exposed at –80°C to Kodak BioMax MS film with an intensifying screen for the appropriate time.

5.3.8 Materials

8-azido-[α^{32}P]ATP was purchased from Affinity Labeling Technologies, Inc. (Lexington, KY, USA). 8-azido-ATP and verapamil were from ICN, and valinomycin was from Calbiochem. Acetone/ether-precipitated *E. coli* lipids were from Avanti Polar Lipids. The PEI-cellulose TLC plates and general reagent grade chemicals were from Sigma or Fisher Scientific.

5.4 Results

In a previous study, analysis of mutants E552Q and E1197Q of mouse Abcb1a suggested that single-site turnover did occur in these mutant enzymes and that ADP release was the most likely step impaired by the mutations. Interpretation of these results also suggested that the two NBDs of Pgp were not functionally equivalent (Carrier *et al.*, 2003). Studies by other groups also showed that these IC residues are not directly involved in the hydrolysis of the terminal phosphate of ATP and it was determined that the ICs either played a role in NBD-NBD communication (Sauna *et al.*, 2002) and/or normal transition state formation following NBD dimerization (Tombline *et al.*, 2004a; Tombline *et al.*, 2004b). In this study, we investigated further the role of these two IC residues in the catalytic mechanism of Abcb1a. For this, wild-type and the Abcb1a mutants E552D, E552N, E552A, E1197D, E1197N, E1197A, E552Q/E1197Q (Q/Q), E552Q/K1072R (Q/R) and K429R/E1197Q (R/Q), were expressed in the yeast *Pichia pastoris* as recombinant proteins bearing an inframe polyhistidine tail (His_6) at the C-terminus. Protein purification from large-scale methanol-induced liquid cultures of *P. pastoris* was performed by detergent extraction from enriched membrane fractions, followed by affinity and anion-exchange chromatography on Ni^{2+}-NTA and DE52-cellulose resins, respectively (Lerner-Marmarosh *et al.*, 1999). Using this protocol, all proteins could be purified in large amounts (0.4 – 1.7 mg per 6 L culture) in a stable form and at a high degree of purity (>95%; Figure 5.1).

Steady-state ATP hydrolysis by the purified proteins activated with *Escherichia coli* lipids and dithiothreitol was determined by measuring Pi release (Van Veldhoven and Mannaerts, 1987), in the absence or presence of MDR drugs or Pgp inhibitors that are known to stimulate the ATPase activity of Pgp. Wild-type Abcb1a has low basal ATPase activity (0.13 $\mu mol\ min^{-1}\ mg^{-1}$), which can be strongly stimulated (12- to 18-fold) by verapamil and valinomycin (to 2.38 and 1.66 $\mu mol\ min^{-1}\ mg^{-1}$)(Carrier *et al.*, 2003). The nine Abcb1a mutants all showed very low ATPase activity with values comparable to those obtained in an assay in which all reagents were added except for the protein. In addition, this low basal activity was not stimulated by the addition of drug substrates (data not shown). Thus, all mutants appear to have no steady-state ATPase activity, although we cannot exclude the possibility that they retain very low levels of such

Figure 5.1:

Purification of NBD Mutants from P. pastoris membranes

Two micrograms of purified (concentrated DE52 eluate) wild-type and mutant Abcb1a variants E552A, D, N, E1197A, D, N, E552Q/E1197Q (Q/Q), E552Q/K1072R (Q/R), and K429R/E1197Q (R/Q) were subjected to SDS/PAGE, followed by staining with Coomassie Brilliant Blue. The position of the molecular mass markers is given on the left.

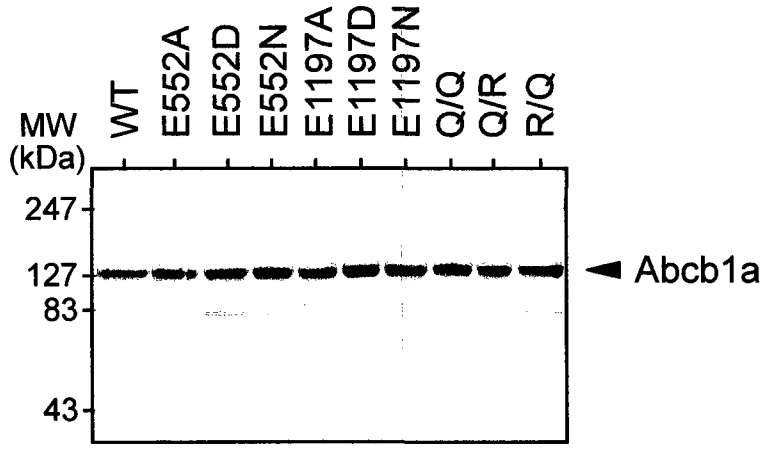
MW
(kDa)
WT
E552A
E552D
E552N
E1197A
E1197D
E1197N
Q/Q
Q/R
R/Q
247
127
83
43
Abcb1a

ATPase activity, as seen in Tombline *et al.* (Tombline *et al.*, 2004a). However, such levels would be below the threshold of accurate detection and reproducibility of our current assay; and would represent <1% of the activity of the wild-type enzyme.

We then determined, by photoaffinity labeling, whether any of the mutations altered the apparent binding affinity of Abcb1a for ATP. Purified and activated proteins were incubated with increasing amounts of 8-azido-[α^{32}P]ATP in the presence of Mg^{2+} (10 min on ice), followed by UV irradiation. Unincorporated ligand was removed by centrifugation and labeled proteins were resolved by SDS/PAGE. The gels were stained with Coomassie Brilliant Blue, to quantify amount of protein loaded (not shown), dried, and then subjected to autoradiography (Figure 5.2). Binding and 8-azido-[α^{32}P]ATP photo-crosslinking was specific to Abcb1a and increased proportionally with the amount of 8-azido-[α^{32}P]ATP present in the reaction. The [^{32}P] incorporation profile over several experiments was quantitatively similar for all mutants and was also very similar to that seen for the wild-type. These results suggest that the introduced mutations do not have a major effect on nucleotide binding to Abcb1a and are therefore unlikely to cause major non-specific structural changes in the NBDs. This agrees with previous studies of catalytic residue mutants of the Walker A and Walker B motifs and of the ICs (K429R, K1072R, D551N, D1196N, E552Q and E1197Q), which severely affect the catalytic activity of mouse Abcb1a but have little effect on the nucleotide-binding affinity of the protein (Urbatsch *et al.*, 1998; Vigano *et al.*, 2002; Carrier *et al.*, 2003). In addition, this confirms the notion that residues E552 and E1197 seem to participate in the catalytic steps after the initial binding of ATP to the NBDs.

Pgp ATPase activity can be stably inhibited by vanadate (Vi), a transition state analogue structurally related to phosphate (Pi) (Horio *et al.*, 1988). Trapping of nucleotide by Vi requires both hydrolysis of the bond between the β- and γ-phosphates of ATP and release of Pi. Vi can replace Pi once it is released, capturing ADP in the nucleotide-binding site and forming a long-lived intermediate that resembles the normal transition state {MgADP•Vi} (Urbatsch *et al.*, 1995b). When 8-azido-[α^{32}P]ATP is used as a substrate, this intermediate can be visualised by UV cross-linking (Urbatsch *et al.*, 1995b). Indeed, Vi-induced trapping of 8-azido-[α^{32}P]ADP under hydrolysis conditions (37°C) has been used as an alternative and highly sensitive method to monitor ATPase

Figure 5.2:

Direct Photolabeling of Purified Abcb1a NBD Mutants with Mg-8-azido-[α^{32}P]ATP

Purified and activated wild-type and mutant Abcb1a variants (E552Q/E1197Q, E552Q/K1072R, K429R/E1197Q, E552A, D, N, E1197A, D, and N) were UV-irradiated on ice in the presence of 3 mM $MgCl_2$ and 5, 20, and 80 μM 8-azido-[α^{32}P]ATP. Photolabeled samples were separated on 7.5% SDS polyacrylamide gels and stained with Coomassie Brilliant Blue followed by autoradiography (Materials and Methods). The position of the molecular mass markers is given on the left.

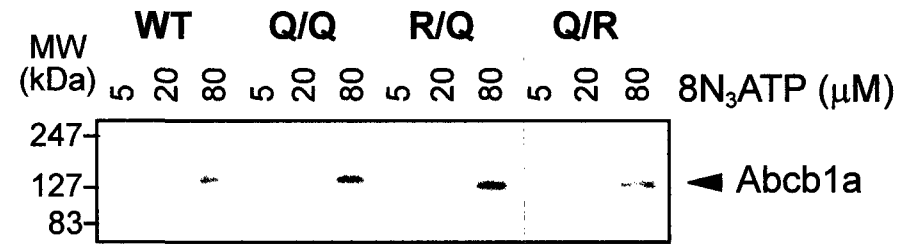
WT
Q/Q
R/Q
Q/R
MW
(kDa)
5 20 80 5 20 80 5 20 80 5 20 80
8N3ATP (μM)
247
127
83
Abcb1a

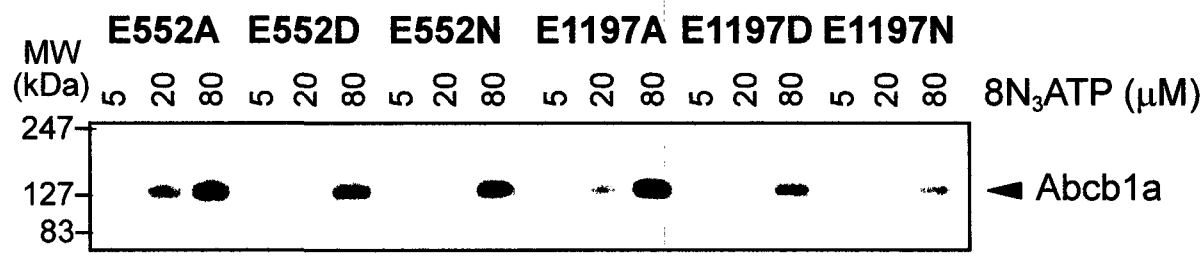
E552A
E552D
E552N
E1197A
E1197D
E1197N
MW
(kDa)
5 20 80 5 20 80 5 20 80 5 20 80 5 20 80 5 20 80
8N3ATP (μM)
247
127
83
Abcb1a

activity in wild-type and mutant Pgp (Urbatsch *et al.*, 1995b; Urbatsch *et al.*, 1998). For wild-type Abcb1a, nucleotide trapping is completely dependent on the presence of Vi and is strongly stimulated by verapamil and valinomycin (Figure 5.3). Despite the observed lack of ATPase activity of the nine mutants analysed (as measured by Pi release), 8-azido-nucleotide trapping is readily detectable in these mutants, with the notable exception of the Q/R double-mutant, which is only very weakly labeled (faint bands seen in the presence of drug upon overexposure; not shown). For the single-site mutants in both NBDs, nucleotide trapping either resembles wild-type (E552D and E1197D) or the previously analyzed E552Q (E552N and E552A) and E1197Q (E1197N and E1197A) mutants. In the double-mutants Q/Q, R/Q and Q/R, trapping appears to be drug stimulated but Vi independent and occurs most readily in the R/Q mutant. In fact, the Q/R enzyme traps nucleotide only to a very low extent and visibly only in the presence of drugs (±Vi). These results are reminiscent of previous studies of double-mutants of the IC in human and mouse enzymes (Sauna *et al.*, 2002; Tombline *et al.*, 2004b). It is interesting to note that the single K429R mutant could not trap 8-azido-nucleotide under any of the conditions tested (Urbatsch *et al.*, 1998), whereas introduction of the E1197Q mutation in its wild-type NBD now allows for 8-azido-nucleotide to be substantially trapped in the protein.

We next wanted to determine whether these mutant enzymes were able to hydrolyse the terminal phosphate of bound ATP and form ADP. For this, we used TLC to analyze the nucleotides tightly bound to the protein following trapping in the presence of Vi and drug, under hydrolysing (37°C) and non-hydrolysing (4°C) conditions. The appearance of a spot corresponding to 8-azido-[α^{32}P]ADP was monitored and indicated that hydrolysis did take place. As seen in figure 5.4, 8-azido-[α^{32}P]ADP can be detected following incubation with 8-azido-[α^{32}P]ATP and Vi under hydrolysis conditions (37°C) in all the single-site and double-mutants, with the exception of the Q/Q mutant. Production of 8-azido-[α^{32}P]ADP in all mutants (except Q/Q) was temperature sensitive, as determined by disappearance of the 8-azido-[α^{32}P]ADP spot when the trapping reaction was carried out at 4 °C, suggesting that the 8-azido-[α^{32}P]ADP spot appeared as a result of hydrolysis of 8-azido-[α^{32}P]ATP. Thus, although the spot corresponding to 8-azido-[α^{32}P]ADP detected in the Q/R mutant was faint, it was considered genuine.

Figure 5.3:

Photolabeling of Abcb1a NBD Mutants by Vanadate Trapping with Mg-8-azido-[α^{32}P]ATP

Purified and activated wild-type and mutant Abcb1a variants were pre-incubated for 20 min at 37°C with 5 μM 8-azido-[α^{32}P]ATP and 3 mM $MgCl_2$ in the absence or presence of 200μM vanadate. Verapamil (VER; 100 μM) and valinomycin (VAL; 100μM) were included as indicated above the lanes. Samples were processed for photolabeling as described in Materials and Methods and analysed by SDS/PAGE.

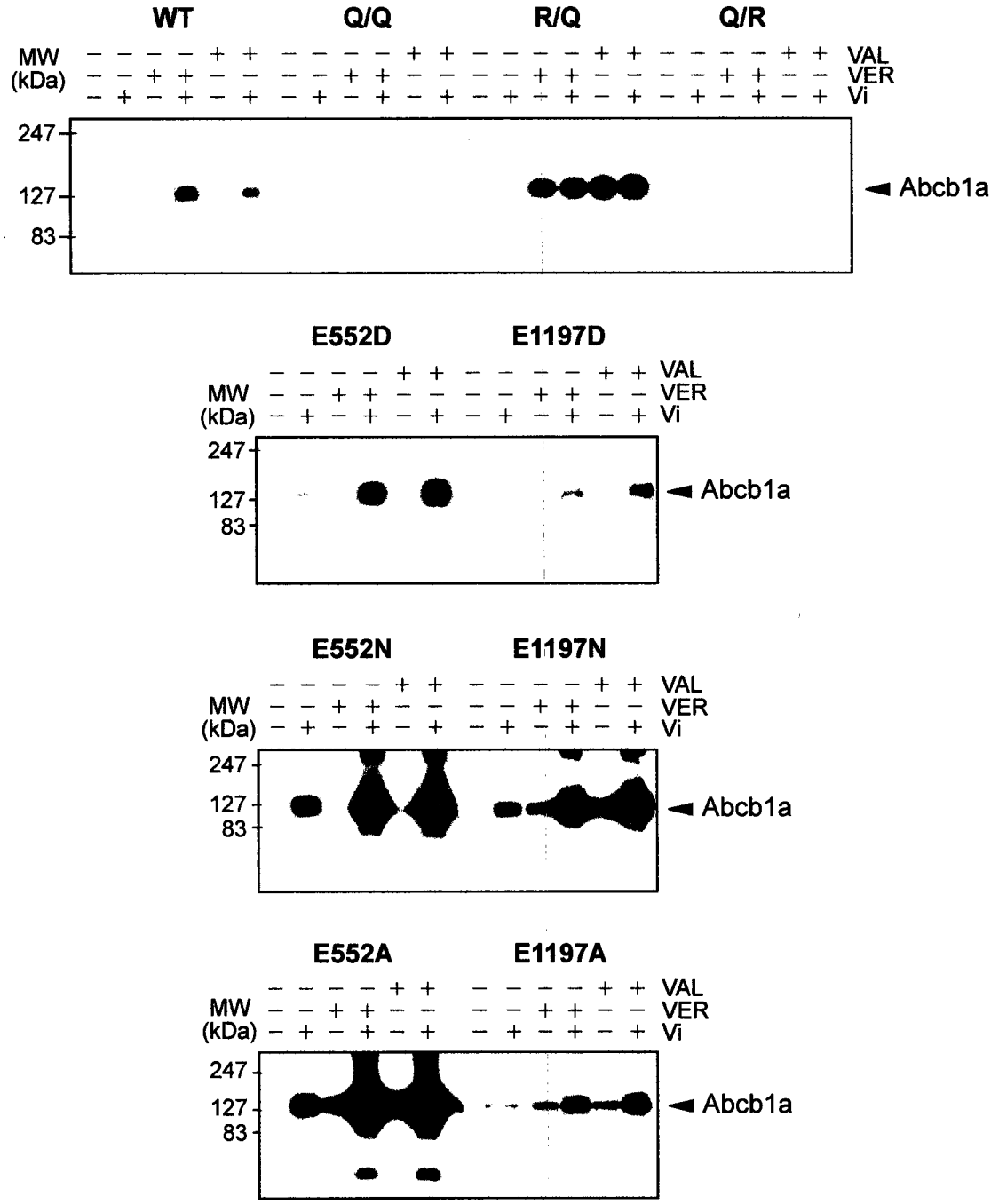
WT
Q/Q
R/Q
Q/R
MW
(kDa)
VAL
VER
Vi
247
127
83
Abcb1a
E552D
E1197D
E552N
E1197N
E552A
E1197A

Figure 5.4:

TLC Analysis of Vanadate-Trapped Nucleotides in Abcb1a NBD Mutants

Purified and activated wild-type and mutant Abcb1a variants were pre-incubated with 5 μM 8-azido-[α^{32}P]ATP and 3 mM $MgCl_2$ for 10 min at either 37 or 4°C in the presence of 200 μM Vi and 100 μM verapamil. Unbound ligands were removed by ultracentrifugation and washing. The protein pellets were then resuspended in 8-azido-ATP and precipitated by trichloroacetic acid. Supernatant (0.5 μL) and 125 dpm of standards were applied to a PEI-Cellulose plate following magnesium chelation with EDTA. The plate was developed in 3.2% (w/v) NH_4HCO_3 and exposed to film. The asterisk (*) indicates the position of a non-specific radioactive contaminant present in the commercial preparation of 8-azido-[α^{32}P]ATP.

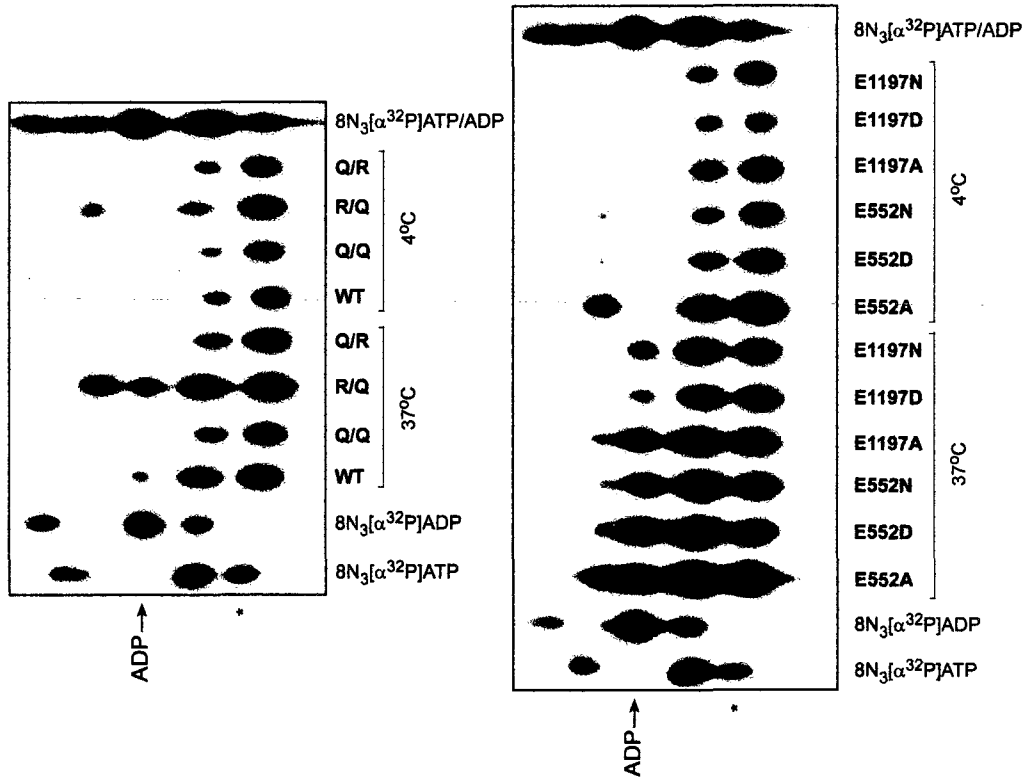
8N3[α32P]ATP/ADP
Q/R
R/Q
Q/Q
WT
4°C
Q/R
R/Q
Q/Q
WT
37°C
8N3[α32P]ADP
8N3[α32P]ATP
ADP→
*
8N3[α32P]ATP/ADP
E1197N
E1197D
E1197A
E552N
E552D
E552A
4°C
E1197N
E1197D
E1197A
E552N
E552D
E552A
37°C
8N3[α32P]ADP
8N3[α32P]ATP
ADP→
*

Because trapping in the double-mutants appears to be Vi independent, a dose-response assay (0, 0.05 μM ≤ Vi ≤ 100 μM) was carried out on the R/Q mutant. Figure 5.5 clearly demonstrates that, unlike E552Q and E1197Q, the R/Q double mutant does not respond to increasing concentrations of Vi.

Given that the R/Q and Q/Q double-mutants are photolabeled by 8-azido-[α^{32}P]-nucleotide and this photolabeling occurs in a Vi-independent fashion, we wanted to determine in which NBD the 8-azido-nucleotides were trapped in these proteins. To answer this question, we took advantage of the trypsin-sensitive region situated in the linker domain of Abcb1a. Following trapping in the absence or presence of Vi and mild-trypsin treatment, the trypsin degradation products of the two mutants R/Q and Q/Q were resolved by SDS/PAGE and immobilized on nitrocellulose membranes. Immunoblotting of the membranes by Pgp-specific antibody *C219* reveals that increasing concentrations of trypsin degrade the enzymes to different extents and the identity of the fragments could be determined by N- and C-terminal-specific antibodies (see Materials and Methods; data not shown). For the R/Q mutant, the two fragments corresponding to the N- and C-terminal halves of the protein cut at the linker region could be detected in lanes 2-4 (-Vi and +Vi). Thus, it is possible to observe that the trapped nucleotide(s) appears to be exclusively in the MD-7 reactive fragment which contains NBD2, both in the absence and presence of Vi (Figure 5.6). For the Q/Q mutant, the two fragments corresponding to the N- and C-terminal halves of the protein cut at the linker region could also be detected in lanes 2-4 (-Vi and +Vi) and the radiolabel could be detected in each fragment, both in the absence and presence of Vi (Figure 5.6). Because the trapping signal in the Q/R mutant was so low, we did not attempt this experiment with this enzyme.

Figure 5.5:

Photolabeling of Abcb1a NBD Mutants with Mg-8-azido-[α^{32}P]ATP and Varying Concentrations of Vanadate

Purified and activated Abcb1a variants K429R/E1197Q, E552Q and E1197Q were pre-incubated with 5 μM 8-azido-[α^{32}P]ATP, 3 mM $MgCl_2$ and 100 μM verapamil for 20 min at 37°C in the absence or presence of increasing concentrations of Vi, as indicated above the lanes. Samples were processed for photolabeling as described in Metarials and Methods and analyzed by SDS/PAGE. E552Q and E1197Q were included as controls since these mutants display varying degrees of Vi-dependence of photolabeling.

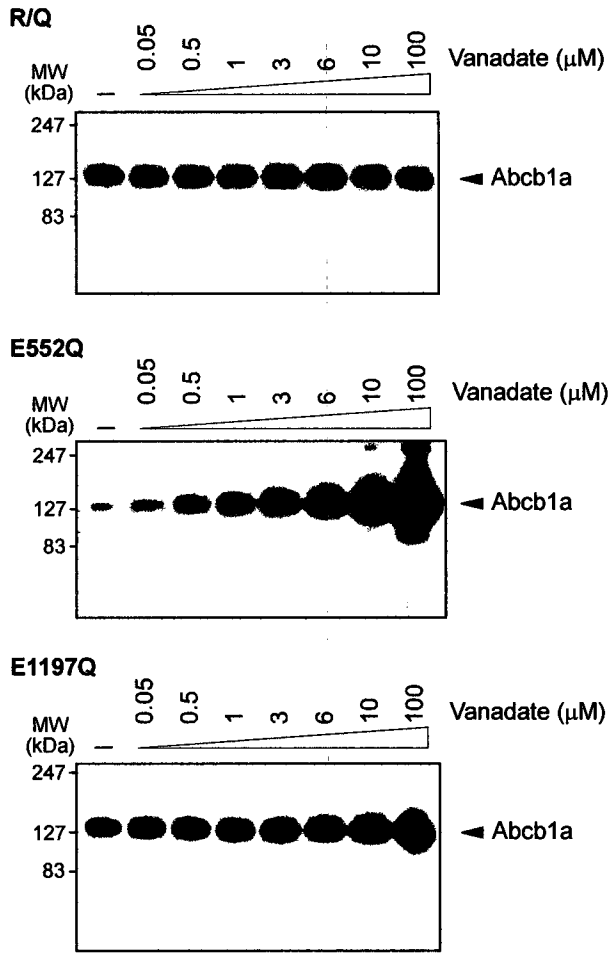
R/Q
MW (kDa)
—
0.05
0.5
1
3
6
10
100
Vanadate (μM)
247
127
83
Abcb1a
E552Q
MW (kDa)
—
0.05
0.5
1
3
6
10
100
Vanadate (μM)
247
127
83
Abcb1a
E1197Q
MW (kDa)
—
0.05
0.5
1
3
6
10
100
Vanadate (μM)
247
127
83
Abcb1a

Figure 5.6:

Trypsin Digestion of Abcb1a NBD Mutants Photolabeled with Mg-8-azido-[α^{32}P]ATP in the Absence or Presence of Vanadate

Purified and activated mutant Abcb1a variants K429R/E1197Q and E552Q/E1197Q were pre-incubated with 5 μM 8-azido-[α^{32}P]ATP, 3 mM $MgCl_2$ and 100 μM verapamil in the absence (upper) or presence (lower) of 200 μM Vi for 20 min at 37°C. Unbound ligands were removed by ultracentrifugation and washing, and the samples were then UV irradiated. The samples were promptly digested with trypsin (see Materials and Methods) at varying trypsin-to-protein ratios (lane 1, 1: 75; lane 2, 1:37.5; lane 3, 1:18.75; lane 4, 1:9.38; lane 5, 1:4.69; lane 6, 1:2.34) and photolabeled, trypsinized samples were separated by electrophoresis on 10% SDS-polyacrylamide gels, transferred onto nitrocellulose membranes and subjected to autoradiography. The membranes were then analyzed by immunoblotting using mouse anti-P-glycoprotein mAbs that recognize either the N-terminal half (*MD13*) or the C-terminal half (*MD7*), or both halves of Pgp (*C219*) (not shown) to identify fragments corresponding to NBD1 or NBD2, as indicated to the right.

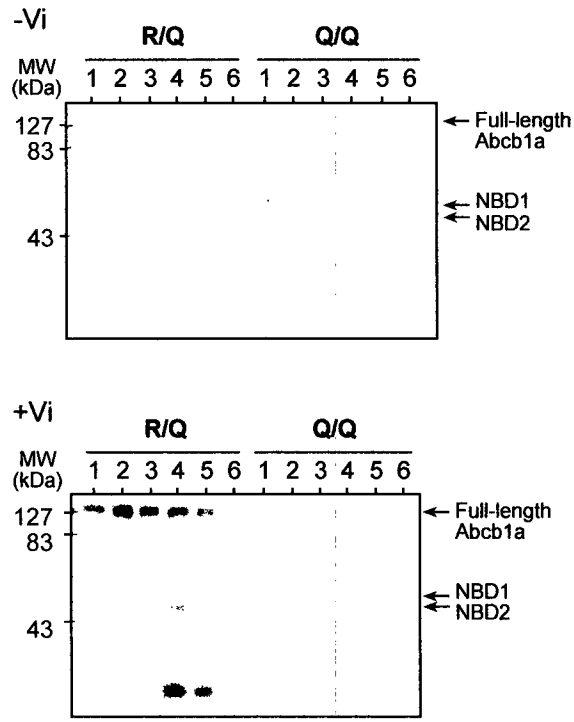
-Vi
R/Q
Q/Q
MW (kDa)
1 2 3 4 5 6 1 2 3 4 5 6
127
83
43
Full-length Abcb1a
NBD1
NBD2
+Vi
R/Q
Q/Q
MW (kDa)
1 2 3 4 5 6 1 2 3 4 5 6
127
83
43
Full-length Abcb1a
NBD1
NBD2

5.5 Discussion

Despite the fact that ABC transporters are highly clinically relevant and have been studied for well over 20 years, many questions about their mechanism of action remain partially elucidated. For example, the exact catalytic cycle, the functional symmetry or asymmetry of the NBDs and the types of signals produced throughout the protein to mediate allocrite transport, are still not fully understood. But using the increasing number of crystal structures available for ABC transporter family members, together with the results obtained following mutagenesis of key residues in various ABC enzymes, a general mechanism of action is beginning to emerge. One such key residue is the invariant carboxylate (IC, sometimes called the "catalytic carboxylate") that immediately follows the Walker B motif in each NBD. This residue was initially mutated in Abcb1a NBDs and identified a unique phenotype in which dependence on Vi for trapping of 8-azido-nucleotide was partially lost (Urbatsch *et al.*, 2000c). In mouse Abcb1a, these residues correspond to E552 and E1197 in NBD1 and NBD2, respectively. Subsequent studies with human and mouse enzymes, in which these two residues were mutated to other amino acids singly or together, or in combination with other mutations, have suggested that they are not classical catalytic residues, because cleavage of the γ-phosphate does occur in the NBD with the mutation at the IC (Sauna *et al.*, 2002; Carrier *et al.*, 2003; Tombline *et al.*, 2004a). Moreover, these and other studies suggest that the IC residues are involved in the formation of the NBD dimer, now recognized as a catalytic intermediate in the ATP hydrolysis pathway that leads to allocrite transport (Tombline *et al.*, 2004a; Tombline *et al.*, 2004b; Tombline *et al.*, 2005). In addition to the E552D, E1197D, E552A, E1197A, and E552Q/E1197Q mutants also analyzed in previous studies (mouse and human enzymes), we have created the following novel mutants: E552N, E1197N, E552Q/K1072R, and K429R/E1197Q, to further characterize the role of the IC residues in the catalytic mechanism of Abcb1a. As seen in figure 5.1, we were able to express and purify all mutants to high levels.

Studies on the Single-Site Mutants—Our results with the single-site mutants are reminiscent of those previously obtained with the glutamine mutation (E→Q) (Carrier *et al.*, 2003; Tombline *et al.*, 2004a). Indeed, although all single-site mutants show an absence of steady-state ATPase activity, as measured by Pi release, ATPase activity is not

completely abolished and the mutants can cleave ATP to ADP and Pi, in a temperature-dependent fashion (Figures 5.3 and 5.4). The apparent lack of turnover is not due to a major decrease in affinity by the enzymes for MgATP (Figure 5.2). As suggested by Tombline *et al.* (Tombline *et al.*, 2004a), very low turnover probably occurs in all the single-site enzymes, but we have not used a more sensitive assay to determine that. Thus, as for the glutamine mutants, a step in the catalytic pathway must be substantially slowed, such that normal turnover is not observed by measuring Pi-release by our assay. The results obtained with the aspartate transformation (E→D) are especially interesting since the 8-azidonucleotide-trapping properties of these enzymes with the mutation in NBD1 or NBD2 resemble the wild-type enzyme, but no steady-state ATPase activity was measured. Thus, the length of the IC residue side-chain is important for normal catalytic activity, but the presence of the charge seems to slow a step further along the catalytic pathway, because the dependence on Vi for trapping is almost normal. By contrast, when the charge is removed, as in the glutamine (length of side-chain maintained) and asparagine (shorter side-chain) mutants, then trapping in the absence of Vi now occurs (Carrier *et al.*, 2003 and Figure 5.3); this is also the case when the side-chain is almost completely removed as in the alanine mutants (Figure 5.3). These results thus emphasize the strict requirement for glutamate at this residue, with the negative charge playing a crucial role. Another notable feature of the single-site IC mutants (including the glutamine substitutions (Carrier *et al.*, 2003)) is the fact that, in the absence of Vi (± drugs) labeling of the enzymes with the mutation in NBD2 is consistently higher than labeling of the enzymes with the equivalent mutation in NBD1 (E→A mutation in the presence of drug is an exception). However, the reverse is true when Vi is present in the labelling reaction; i.e. labeling of the enzymes with the mutation in NBD1 is consistently higher than labeling of the enzymes with the equivalent mutation in NBD2. These observations hint at the fact that the two NBDs may not have the same affinity for nucleotide or that they may hydrolyse ATP at different rates or in a given order. In all single-site mutants, drug stimulation can be observed, suggesting that signal transduction between the drug binding site(s) and the NBDs is not affected by the mutations.

Studies on the Double-Mutants—In this study, we also analyzed three double-mutants. First, we created the double-mutant in which the IC residue is mutated to

glutamine (E→Q) in both NBDs (Q/Q). Second, we created a mutant in which NBD1 contains the E→Q mutation and NBD2 contains the ATPase-inactivating mutation of the Walker A lysine (K1072R) (Q/R). Finally, the third double-mutant contains the E→Q mutation in NBD2 and the ATPase-inactivating mutation of the Walker A lysine (K429R) is in NBD1(R/Q). As seen in Figure 5.3, these three double-mutants trap 8-azido-nucleotide in a drug-stimulated and Vi-independent fashion, but to very different extents. The R/Q mutant enzyme is most extensively labeled, followed by the Q/Q mutant enzyme and the Q/R mutant enzyme, which shows almost no labeling at all. Again, major changes in affinity for 8-azido-ATP cannot account for the differences in labeling with 8-azido-nucleotide (Figure 5.2) and as in the single-site mutants, drug stimulation can be observed (Figure 5.3), suggesting that signal transduction between the drug binding site(s) and the NBDs is not affected by the mutations.

When 8-azido-ADP production by the double-mutant enzymes is analyzed (Figure 5.4), it is possible to see that the R/Q and Q/R mutant enzymes do produce ADP and this process is temperature-sensitive, whereas the Q/Q mutant enzyme does not produce any ADP. Based on previous results, it is tempting to suggest that the Q/Q mutant enzyme is trapped in a stable dimer in which nucleotide (ATP) is sandwiched at the interface. Our results with this mutant support this explanation. First, 8-azido-nucleotide labeling of this mutant does occur and appears to be completely Vi insensitive (Figure 5.3). Second, this mutant appears not to produce ADP (Figure 5.4). Finally, trapped 8-azido-nucleotide is observed in both NBDs (Figure 5.6). The R/Q and Q/R mutants do not appear to be trapped in the same conformation as the Q/Q mutant. Deactivation of the "wild-type" NBD allows us to observe that upon NBD dimerization only NBD2 can enter the transition state. Thus, the results suggest that once the dimer is formed with nucleotide in each NBD, progression into the transition state induces asymmetry in the dimer (Ivetac *et al.*, 2007; Lawson *et al.*, 2008), such that NBD2 would be most likely to be committed to hydrolyse its ATP. The conformational change induced by hydrolysis at NBD2 would then be transmitted to NBD1, which in turn would be in the correct conformation to hydrolyse its ATP, leading to full destabilization of the dimer. This suggests that the NBDs are not symmetrical and NBD2 is first committed to hydrolyse upon dimerization. Such a scenario, in which hydrolysis is sequential in a closed dimer, does not invalidate

the theory of alternate catalysis, but it must be taken into consideration that a transport cycle involves dimerization of the NBDs with hydrolysis of two nucleotides per dimerization, and not, as previously believed, a continuous turnover comparable to a two-cylinder engine. Thus, the dimer closes with bound nucleotide in each active site, one NBD is committed to hydrolysis (presumably NBD2) and hydrolyses its nucleotide, then the other NBD (presumably NBD1) hydrolyses its nucleotide and these events cause conformational changes which lead to allocrite transport, destabilization of the NBD dimer and release of hydrolysis products, such that a new cycle can begin with the NBDs hydrolysing in the same order, giving the impression of alternate site catalysis.

Another very well-studied ABC transporter is the cystic fibrosis transmembrane conductance regulator (CFTR/ABCC7). Cystic fibrosis is a lethal disease that affects about 1 in 2900 Caucasians and is caused by mutations in the *CFTR/ABCC7* gene (Huang and Pan, 2007; Quinton, 2007). Although the CFTR protein is part of the ABC superfamily of proteins, it is not a classical ABC transporter, because it acts as a chloride channel. Despite or because of this peculiarity, recent observations obtained by mutating the IC in CFTR's NBD2 (Vergani *et al.*, 2005) seem to have unraveled some of the mystery behind the catalytic cycle of ABC transporters and also support our hypotheses. Thus, it appears that in CFTR, dimerization of the NBDs following binding of ATP at both sites propagates a signal which leads to the opening of the chloride channel (Vergani *et al.*, 2005). Subsequent hydrolysis of ATP at the active nucleotide-binding site in NBD2 initiates channel closure by destabilising the NBD dimer. But, unlike typical ABC transporters, CFTR's NBD1 is not ATPase active and a possible explanation for the inactivation of the catalytic activity with augmentation of affinity for ATP at NBD1 would be that this could maintain the NBDs in a closed dimer for longer, thus allowing the channel to be opened for a reasonable amount of time. The way in which NBD1 may prolong channel opening could either be by delaying hydrolysis at NBD2 or because once NBD2 has hydrolysed, NBD1 still holds ATP and full dimer dissociation is retarded. Transposing these observations to other ABC transporters, we can build the following hypothesis about catalytic activity: (a) ATP binds to both NBDs and forms a tight dimer, plausibly, this could be accelerated by drug binding to the TMDs, (b) as the dimer progresses towards the transition state, conformational changes propagate to the TMDs

and this allows the allocrite-binding site to "flip" the transport substrate from the high-affinity site to the low-affinity site, (c) ATP hydrolysis is quickly initiated at the NBDs and proceeds in a sequential fashion. Hydrolysis of ATP (one or both) may lead to further conformational changes required for full transport and release of allocrite. Presumably, ATP present at NBD1 induces ATP hydrolysis at NBD2 which is then followed by hydrolysis at NBD1. (d) When only ADP is present, dimer destabilization occurs and NBDs move apart, resetting the protein and releasing hydrolysis products (not Pi as it can diffuse out freely once formed).

Conclusions—From the results obtained in this study, we would like to suggest that once NBD dimerization has occurred with one ATP molecule bound at each active site, progression into the transition state induces asymmetry in the nucleotide-binding sites such that NBD2 is committed to hydrolysis.

Analyzing results of this and other studies, it seems that a dual role for the IC residues is starting to emerge; first the ICs appear to be important in NBD-NBD communication and transmission of the nucleotide state of one active site to the other; second, the ICs appear to be involved in catalysis by contributing to the catalytic dyad along with the highly conserved H-loop His.

5.6 Acknowledgements

We are grateful to Dr. Victor Ling (The B.C. Cancer Research Centre, Vancouver, Canada) for the generous gift of the mouse mAbs *MD13* and *MD7*. This study was supported by an FRSQ-FCAR-Santé scholarship to IC and by research grants to PG from the Canadian Institute of Health Research (CIHR). PG is a Career Scientist of the CIHR of Canada.

Chapter 6

Summary, Future Perspectives, and Conclusions

Section 6.1 – Summary and Future Perspectives

This thesis describes studies aimed at further understanding the role of conserved residues in the NBDs of Abcb1a. The information and conclusions obtained from these studies may potentially be important to other ABC proteins, especially the MDR transporters, for the elucidation of their respective function and mechanism of action. The large amount of published literature on ABC proteins has just begun to produce a uniform picture of the mechanism of action. Clarification of the complete mechanism of ABC proteins in general, and MDR transporters in particular, is critical to the development of new clinical strategies to circumvent the MDR phenotype mediated by many ABC transporters, and certain defects (such as processing and/or targeting defects) associated with deleterious mutations. This, in turn, can be achieved through a rational approach at designing better and more specific inhibitors or chemo-sensitizers, as well as processing chaperones.

Despite major advances in the understanding of ABC proteins, the exact mechanism of ATP hydrolysis remains an enigma. Although certain aspects of the mechanism had been elucidated when this thesis project was undertaken, such as 1) binding and hydrolysis occurs at both NBDs, 2) Walker A residues interact with the phosphate moiety of the bound nucleotide, 3) ATP is hydrolysed to ADP and Pi with a single K_M(ATP) which is around 0.5mM (implying low affinity binding sites), 4) the enzyme does not have a phosphorylated intermediate, 5) Mg^{2+} is an essential cofactor which is coordinated in part by the Walker B aspartate, 6) Pi analogues such as Vi inhibit ATPase activity, 7) allocrites stimulate ATPase activity and increase V_{max} but do not change K_M, and 8) hydrolysis by the two NBDs is cooperative and non-simultaneous, other aspects remained partially or completely obscure. These include: 1) what is the exact function of the conserved amino acid residues of the NBS? 2) What residues of the NBS are involved in nucleotide binding, and how is nucleotide specificity determined? 3) What residues are involved in the catalytic cleavage of the γ-phosphate of ATP? 4) What is the reaction path of ATP hydrolysis, i.e. does ATP hydrolysis occur via a catalytic base or is it substrate-assisted? 5) What is the nucleotide occupancy during the catalytic cycle? 6) How do the NBDs communicate between themselves and with the TMDs? And, 7) how many molecules of ATP need to be hydrolysed to effect one transport cycle? The

work presented in this thesis has addressed some of these issues, especially pertaining to the catalytic mechanism of the NBDs.

The studies described in Chapter 2 examine the role of the aromatic residue of the A-loop, situated approximately 25 residues upstream of the Walker A sequence, in Abcb1a. Although previous findings by several groups (Shyamala *et al.*, 1991; Sankaran *et al.*, 1997c; Zhao and Chang, 2004; Zaitseva *et al.*, 2005c) had hinted at the role for this conserved aromatic residue in nucleotide binding, high resolution structures confirmed its strategic location with respect to bound nucleotide. Indeed, in the high-resolution structures of NBDs crystallized in the presence of nucleotide, an aromatic residue (tyrosine, phenylalanine, or tryptophan) is seen to stack against the adenine moiety of the nucleotide (reviewed in Ambudkar *et al.*, 2006). Although most of the binding energy for ATP appears to be contributed by the phosphate groups (Berger and Welsh, 2000), the nucleotide specificity and further essential stabilization of nucleotide binding may be contributed by residues which interact with the nucleoside moiety. A large-scale data-mining study of ATP-bound crystal structures (including some members of the ABC-transporter family) by Mao and colleagues, determined that the molecular determinants for recognition of the adenine moiety of ATP by proteins includes hydrogen bonding, Van der Waals, π-π stacking, and cation-π stacking interactions, of which aromatic residues are good candidates for π-π stacking (Mao *et al.*, 2004). As Ambudkar and colleagues demonstrated, the aromatic residue of the A-loop of ABCB1 contributes to the positioning of ATP in the active site via π-π interactions with the adenine ring of ATP (Ambudkar *et al.*, 2006; Kim *et al.*, 2006). This was also the case for the ABCC1/MRP1 and HlyB proteins (Zhao and Chang, 2004; Zaitseva *et al.*, 2005c). Results obtained with mutants of the equivalent residues in Abcb1a (Y397 and Y1040) determined that the aromatic residues of the A-loop in this enzyme also contribute significantly to the positioning and maintaining of the nucleotide in the active site. Our results are thus in agreement with those obtained by Kim *et al.* and Zhao *et al.* with the eukaryotic enzymes ABCB1 (Kim *et al.*, 2006) and ABCC1 (Zhao and Chang, 2004), respectively. A major difference, though, is that in our eukaryotic enzyme, a simple substitution to a conserved amino acid produces a significant change in the catalytic properties of the enzyme, whereas these effects are only observed in ABCB1 and ABCC1 when non-conserved

substitutions are introduced in each NBD (ABCB1 and ABCC1) or when the conserved substitutions are introduced simultaneously in both NBDs (W in ABCB1) (Zhao and Chang, 2004; Kim *et al.*, 2006). Perhaps the mouse enzyme is less tolerant of substitutions at this position because the NBD is more rigid and/or because there aren't (as many) other residues which contribute to the stabilization of ATP binding via the adenine and ribose moieties, as may be the case in ABCB1 or ABCC1.

An important but poorly understood aspect of catalysis by ABC transporters is the nucleotide occupancy of the two active sites during a full cycle of ATP hydrolysis. Determining which amino acid side chains are in the vicinity of the adenine moiety of bound nucleotide under binding and hydrolysis conditions could identify appropriate positions for the insertion of probes for fluorescence analyses aimed at monitoring nucleotide occupancy during the catalytic cycle. Such analyses have been used successfully in F_1-ATPase to monitor the presence of and affinity for nucleotide in its three catalytic NBSs during the catalytic cycle of this multi-domain ATPase (Weber *et al.*, 1993; Dou *et al.*, 1998). Thus, in these studies it was determined that nucleotide occupancy of all three catalytic sites was necessary to yield V_{max} rates, and, that the affinity of the three sites for nucleotide was not equivalent. Identification of residues that are in the vicinity of the adenine moiety of ATP in the NBSs of hamster Abcb1 has been achieved with the use of the photo-activatable nucleotide analogue 8-azidoATP (Sankaran *et al.*, 1997b and Chapter 2). In Chapter 2, the equivalent tyrosine residues in Abcb1a (Y397, Y1040, Y618, and Y1263) were characterized for their functional role by replacing them with tryptophan. Although photolabelling experiments suggested that Y618 in NBD1, and by homology, Y1263 in NBD2 may be near the azido group of 8-azidoATP during nucleotide binding in the absence of vanadate, the activity of the enzyme was not affected by their substitution to tryptophan, implying that these residues do not seem to play a major role in nucleotide binding during catalysis. Mutagenesis to replace these residues by less conservative amino acids (for example alanine, leucine, and cysteine), singly or in combination, could determine whether they do actually have a role in catalysis. On the other hand, this also suggests that the Y618W and Y1263W mutants may turn out to be suitable fluorescent probes for nucleotide occupancy during the catalytic cycle, in tryptophan fluorescence assays, when re-introduced in the tryptophan-

free enzyme (Kwan *et al.*, 2000). If the fluorescence of these introduced tryptophan residues becomes altered by the presence of nucleotide then nucleotide occupancy during the catalytic cycle of Abcb1a could be followed in real-time. The fact that mutating the tyrosine residues of the A-loop to tryptophan (Y397W and Y1040W) affected significantly these mutant enzymes' function indicates that these residues may not be appropriate sites for insertion of fluorescent probes, as the catalytic properties of the enzyme are altered.

Tryptophan fluorescence analyses have also been used, in another ABC protein, to monitor NBD dimerization. In LolD-E171Q, mutation of the A-loop tyrosine to tryptophan (Y11W) had no effect on dimerization, as assayed by gel filtration, and thus allowed tryptophan fluorescence anisotropy measurements to be used to characterize dimerization of this otherwise tryptophan-free NBD (Smith *et al.*, 2002). The Y618W and Y1263W mutants, re-introduced in the tryptophan-free enzyme (Kwan *et al.*, 2000), could also serve as probes of dimer formation, if the fluorescence of these introduced tryptophan residues is altered upon dimer formation or dissociation. Dimerization could then be followed in real-time during the catalytic cycle of Abcb1a.

The studies described in Chapters 3, 4, and 5 examined the role of the conserved acidic amino acids (carboxylates: aspartate and glutamate) in the NBDs of Abcb1a. Since it was speculated that ABC transporters utilize a catalytic base to hydrolyse the γ-phosphate of ATP (Yoshida and Amano, 1995), a search for that residue was undertaken (Chapter 3). Both NBDs of Abcb1a contain several acidic amino acids (≥30 in each NBD), therefore, the first task was to identify those aspartates and glutamates that are most conserved in the two NBDs of Abcb1a and other ABC proteins which are related (≥30% sequence identity), thus indicating a possible conserved function. Seven acidic amino acids in each NBD of Abcb1a (at homologous positions in each NBD) were identified that were highly conserved in the NBDs of ABC proteins (i.e. present in more than 50% of the sequences aligned at that position). The importance of these conserved carboxylates was tested by mutagenesis, followed by functional analysis in yeast cells and after purification and reconstitution of the enzymes. A cluster of three acidic residues within and adjacent to the Walker B motif of each NBD were shown to be highly

mutation sensitive (NBD1/NBD2: D551/D1196, E552/E1197, and D558/D1203). D551 and D1196 are part of the well-described Walker B motif and have previously been mutated (e.g. Urbatsch *et al.*, 1998); by analogy to other ATPases, these aspartates are suggested to form a complex with Mg^{2+} of MgATP. When mutated to asparagine (N), D551N and D1196N showed complete loss of activity as demonstrated using both transport and ATPase assays (Pi release and Vi-trapping of 8-azidoATP). E552 and E1197, as well as D558 and D1203 are part of the extended Walker B motif or the D-loop typical of ABC transporters (Holland and Blight, 1999), and both sets of carboxylate residues are completely conserved in all ABC proteins that were analyzed. In addition, in the crystal structure of HisP, a glutamate (E179) is located within 4.3Å of ATP and has been suggested to position the water molecule for a hydrolytic attack on the γ-phosphate (Hung *et al.*, 1998); glutamates E552 and E1197 of Abcb1a map to the homologous position of E179 in HisP. When mutated to asparagine, D558N and D1203N showed reduced but real activity, either in the transport or ATPase assays. Thus, although these residues appeared to be important for catalysis, their role does not seem to involve catalytic cleavage of the γ-phosphate of ATP. Two interesting observations were made with the mutants D558N and D1203N. One, the biological activity in yeast seems to correlate well with the ATPase activity of the purified mutant enzymes; i.e., the biological assay shows sensitivity to impairment of ATPase. Overall, it appears that a drug-stimulated ATPase activity of ≤18%, as in D558N, is insufficient to energize drug transport and show biological activity in yeast. Two, the D1203N mutant retained a higher drug-stimulated ATPase activity (of 30%, which supported some biological activity) than D558N, indicating that interactions may be different for NBD1 and NBD2 since the mutant at the homologous residue in NBD1 had more severe effects. Possible functional differences between NBD1 and NBD2 will be discussed in a later section. When mutated to glutamine (Q), E552Q and E1197Q showed complete loss of activity in transport assays. On the other hand, although these mutants demonstrated a complete loss of steady-state ATP hydrolysis as assessed by Pi release, both mutants showed Vi-induced trapping of nucleotide which could be strongly stimulated by drugs such as verapamil and valinomycin. Surprisingly, both mutants also exhibited labelling by 8-azido-ATP even in the absence of Vi, both in the absence and presence of drug.

Upon further characterization of the E552Q and E1197Q mutants (Chapter 4), ADP could be recovered from the trapped enzymes. Additionally, the E552Q and E1197Q mutants showed characteristics similar to those of the wild-type (WT) enzyme with respect to 8-azido-[α^{32}P]ATP binding and 8-azido-[α^{32}P]nucleotide trapping, with the latter being both Mg^{2+} and temperature dependent. Importantly, drug-stimulated nucleotide trapping in E552Q was demonstrated to be stimulated by Vi, resembling the WT enzyme, while in E1197Q trapping was almost completely Vi-insensitive. Similar nucleotide trapping properties were observed when aluminum fluoride or beryllium fluoride was used as an alternate transition-state analogue. Partial proteolytic cleavage of photolabelled enzymes indicated that, in the absence of Vi, nucleotide trapping occurs exclusively at the mutant NBD, whereas in the presence of Vi, nucleotide trapping occurs at both NBDs. Together, these results suggested that there is single-site turnover occurring in the mutant NBD of E552Q and E1197Q and that ADP release from the mutant site, or another catalytic step, is impaired. Thus, these invariant carboxylates do not appear to function as classical catalytic carboxylates.

In order to characterize the exact role of these invariant carboxylate residues in Abcb1a catalysis (Chapter 5), we investigated the biochemical properties of the single-site mutants E552D, N and A in NBD1, and E1197D, N and A in NBD2, as well as the double-mutant E552Q/E1197Q. In addition, we investigated the biochemical properties of mutants in which the Walker A lysine to arginine (K→R) mutation, known to abolish ATPase activity (Urbatsch *et al.*, 1998), was introduced in the non-mutant NBD of E552Q and E1197Q (E552Q/K1072R and K429R/E1197Q). The results obtained with these mutants suggested that the length of the invariant carboxylate residue is important for the catalytic activity, whereas the charge of the side chain is critical for full turnover to occur. Moreover, in the double-mutants where the K→R mutation is introduced in the non-mutant NBD of the E→Q mutants, single-site turnover is observed, especially when NBD2 can undergo γ-Pi cleavage.

Studies carried out by other groups on ABCB1 and Abcb1a mutants of the invariant carboxylates are in agreement with these results and complement the dataset. The following will highlight the results and conclusions from these studies. Mutants E556Q or A, E1201Q or A and double mutants E552Q/E1197Q (Q/Q) and A/A in

ABCB1 (Sauna *et al.*, 2002) lack transport and steady-state ATPase activities but retain normal 8-azido-[α^{32}P]ATP binding. In these mutants, trapping of 8-azido-[α^{32}P]nucleotide in the presence and absence of Vi is observed, with slightly higher Vi-stimulation in E556X than E1201X mutants. In the double mutants Q/Q and A/A, Vi appeared to have no effect on the extent of 8-azido-nucleotide trapping, but drugs did stimulate trapping. In addition, the radio-label was almost equally distributed in each NBD in the double mutants Q/Q and A/A (with or without Vi). Conclusions from these studies were that in the single-site mutants, the second hydrolysis reaction responsible for resetting the protein to its resting-state is blocked and that ADP release is blocked in the double mutants. Thus, the invariant carboxylates are not catalytic residues, but rather they are involved in recruiting the second site after ATP hydrolysis at the first site. Mutants E552Q, A, D, or K and E1197Q, A, D, or K in Abcb1a (Tombline *et al.*, 2004a) appear to have extremely low but real drug-stimulated ATPase activity. Vi-trapping experiments with [α^{32}P]ATP showed that ADP is the trapped species in the E→Q mutants, whereas 26-47% of trapped nucleotide is ATP (with the rest being ADP) in the other mutants. Release of trapped nucleotide was demonstrated to be actually faster in all mutants than in WT, and subsequent rounds of trapping were not inhibited. Some asymmetric behaviour was observed in mutants of NBD1 versus mutants in NBD2. Conclusions from these studies were that mutation to Q, A, D, or K alter characteristics of the transition state but do not eliminate its formation. Also, there is strict requirement for glutamate at position 552 and 1197, and in the absence of glutamate, other residues in the catalytic site take over, albeit far less efficiently, as catalytic residues. Double mutants Q/Q, A/A, D/D, and K/K in Abcb1a (Tombline *et al.*, 2004b) also appear to have extremely low but real ATPase activity which is not stimulated by drugs. Vi-trapping experiments with [α^{32}P]ATP showed that Q/Q and A/A mutants trap significant amounts of nucleotide whereas D/D and K/K almost trap none. In addition, Vi had no effect on trapping but drugs did stimulate trapping (in the Q/Q and A/A mutants). Upon determination of the trapped nucleotides in the Q/Q and A/A mutants, it was shown that ATP accounted for more than half of the bound nucleotide, both in the absence and presence of Vi. Q/Q and A/A were also shown to release trapped nucleotide faster than the WT enzyme. Conclusions from these studies were that the double-mutants Q/Q and A/A retain ADP

and ATP following trapping and that this binding is tight (nucleotide occlusion). Moreover, these mutants do not form a normal transition-state complex with Vi, thus suggesting that the invariant carboxylates are involved in bond formation at the transition state, and a direct impairment of a hydrolysis step is the primary cause of low ATPase activity, as opposed to slow ADP release. The step that is impaired appears to be NBD dimerization and the mutants seem to promote formation and increase the stability of the NBD dimer structure, which allows nucleotide occlusion.

Thus, the most significant conclusions from the studies presented in chapters 3, 4, and 5, as well as those presented above, are that 1) the invariant carboxylates thought to activate the water molecule for attack on the γ-phosphate of ATP do not appear to be classical catalytic residues, 2) NBD dimerization is a step in the catalytic pathway, and 3) the two NBDs are not symmetric. A possible explanation for the role of the invariant carboxylates comes from biochemical and structural studies done on the NBDs of the ABC transporter Haemolysin B (HlyB-NBD) of *E. coli*. Mutational studies have revealed the importance of certain key residues in ATP-hydrolysis by the HlyB-NBD (Benabdelhak *et al.*, 2005). Most important for our understanding of the catalytic cycle were mutations of E631 and H662. An E631Q mutation resulted in NBDs retaining substantial amounts of ATPase activity (Zaitseva *et al.*, 2005a), as also observed in Abcb1a (this thesis) and other ABC transporters (Sauna *et al.*, 2002; Verdon *et al.*, 2003b; Tombline *et al.*, 2004a), thus casting doubt on the precise role of the glutamate. Another interesting residue of HlyB is the highly conserved H662 of the H-loop. While the E631Q mutation in HlyB retained around 10% ATPase activity, the H662A mutant was completely ATPase-deficient (up to a protein concentration of more than 20 mg/mL) (Zaitseva *et al.*, 2004). The precise molecular functions of E631 and H662 were established by re-introducing the histidine *in silico* in the high-resolution crystal structure of the HlyB-NBD-H662A mutant (Zaitseva *et al.*, 2005a), which resulted in a complex network of interactions (Figure 6.1 A). In the modelled structure, E631 forms a bidentate interaction with the backbone and the side chain of H662, thereby positioning H662 in a proper orientation to stabilize the transition state of the HlyB-NBD/MgATP complex. H662, on the other hand, acts as a linchpin that interacts with ATP and the D-loop of the

Figure 6.1:

The linchpin model of ATP-hydrolysis of the HlyB-NBD

(A) The figure demonstrates the key role of H662 in the pre-hydrolysis state through interactions with the γ-phosphate, the invariant carboxylate E631, and the D-loop. ATP is in stick representation, Mg^{2+} is a green sphere, and water molecules are blue spheres. Conserved motifs are coloured in red: Walker A, brown: Q-loop, blue: signature motif, magenta: Walker B, black: D-loop, and green: H-loop, and are labelled accordingly. Asterisks indicate conserved motifs of the *trans*-monomer. Figure reproduced with permission from (Zaitseva *et al.*, 2005b). (B) Schematic drawing of the substrate-assisted mechanism of ATP hydrolysis. Arrows indicate the molecular steps of the proposed MgATP-driven proton abstraction and the nucleophilic attack of the catalytic water. The red arrows indicate the rate-limiting step (P—O bond cleavage).

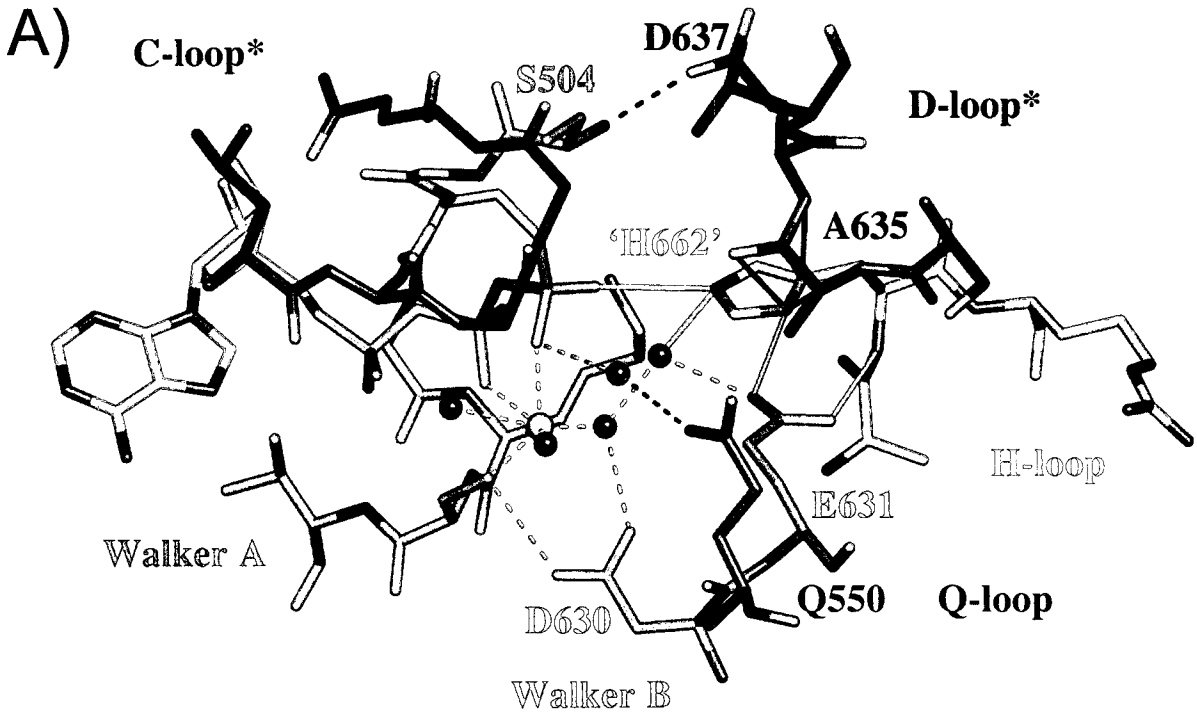
A)
C-loop*
S504
D637
D-loop*
'H662'
A635
H-loop
E631
Walker A
D630
Q550
Q-loop
Walker B

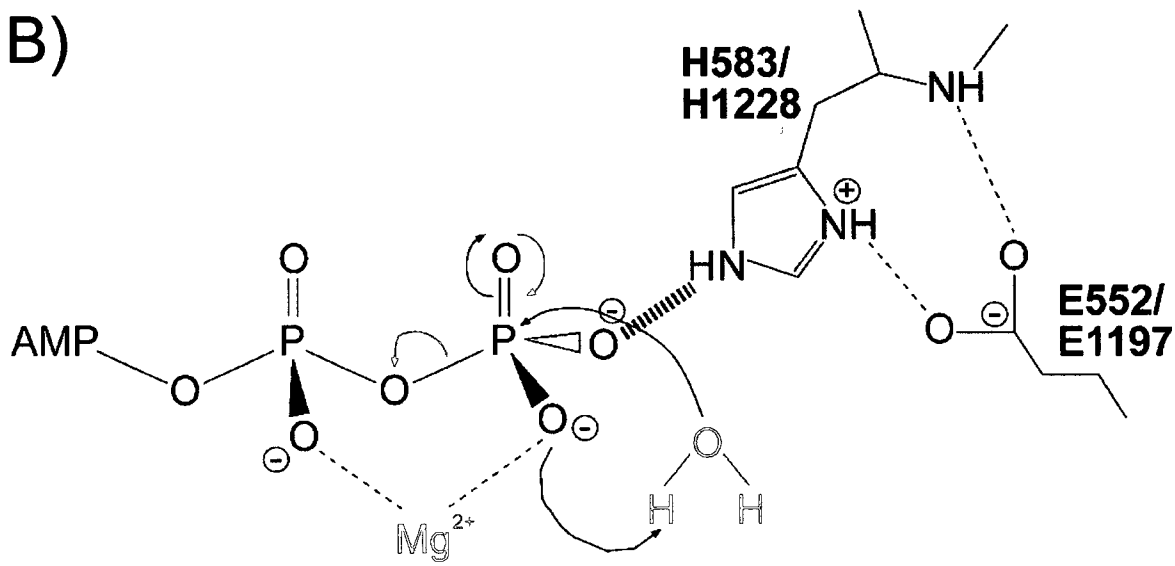
B)
H583/
H1228
NH
NH
HN
O
E552/
E1197
AMP
P
P
O
O
O
O
O
O
Mg2+
H
H

trans-monomer, and coordinates a water molecule which is in the proper position to act as the catalytic water. In this structure, E631 thus acts as a platform and without this glutamate the conformational restriction imposed on H662 is relaxed and the probability of obtaining the correct orientation is drastically reduced. However, the intrinsic flexibility of individual NBDs might explain the varying levels of residual ATPase activity found after mutation of the glutamate. In contrast, substitution of the histidine removes the linchpin, resulting in ATP not being fixed in space anymore, and loss of coordination of the catalytic water, thus abolishing ATPase activity. This model is supported by a variety of biochemical evidence (Zaitseva *et al.*, 2005a). First, ATPase activity in solutions of increasing viscosity revealed that the reaction velocity did not change, indicating that a chemical reaction is the rate-limiting step of the catalytic cycle rather than nucleotide association, dissociation or NBD-dimerization, since the latter depend on the diffusion rate, which is slowed in solutions of higher viscosity. Secondly, reaction velocities of the ATPase activity were insensitive to the presence of D_2O. This experiment allowed the elimination of general base catalysis as the rate-limiting reaction, since by definition such a process requires a proton abstraction or polarization step (Fersht, 1985). When a reaction is performed in D_2O, the zero-point energy changes, and the activation barrier for any proton-abstraction process is raised, with a consequent reduction in the reaction velocity. The absence of a deuterium isotope effect (Schowen and Schowen, 1982) clearly demonstrated that protons are not involved. This implies that ATP-hydrolysis might be the rate-limiting step of the catalytic cycle, i.e. that the step of bond cleavage has the highest activation barrier. This model is further supported by the fact that ATPase activity is modulated by the nature of the divalent ion present, going hand in hand with the pK_a value of the corresponding ion, rather than with the ionic radius. This suggests that the bound cofactor influences the pK_a value of the γ-phosphate moiety, resulting in modulation of the reaction velocity. As a consequence, the substrate (ATP) acts as a base and ATP hydrolysis by the HlyB-NBD should then follow substrate-assisted catalysis (Dall'Acqua and Carter, 2000) (Figure 6.1 B), a mechanism already described for another branch of P-loop enzymes, the GTPase ras^{p21} (Schweins *et al.*, 1995) or EcoRI and V (Jeltsch *et al.*, 1993).

Mutation of the conserved histidine of the H-loop in HisP (H211, Shyamala *et al.*, 1991) and MalK (H192, Davidson and Sharma, 1997) resulted in background steady-state ATPase activity and completely abrogated transport (Davidson and Sharma, 1997; Nikaido and Ames, 1999). In the case of the HlyB-NBD (Zaitseva *et al.*, 2004), substitution of H662 for alanine also reduced the steady-state ATPase activity to background levels (Zaitseva *et al.*, 2005a). (Since these three NBDs form homodimers, the mutation is present in both NBDs simultaneously). As mentioned above, in the half-transporter HlyB, structural and biochemical analyses placed the conserved histidine of the H-loop as a key player in catalysis, functioning as a linchpin for substrate-induced hydrolysis (Zaitseva *et al.*, 2005a). Mutagenesis of the histidine residue of the H-loop of Abcb1a should determine whether this residue also functions as the linchpin in catalysis in this enzyme. Thus, H583 in NBD1 and H1228 in NBD2 of Abcb1a could be substituted to alanine, arginine, leucine, and proline, singly and in combination, and characterized with respect to transport, ATP binding, and ATP hydrolysis.

Section 6.2 – Final Conclusions

Despite the increasing amount of knowledge about ABC protein structure and function, a number of key unresolved issues concerning the function of ABC transporters still need to be addressed. Questions that remain partially or completely unanswered include: 1) what is the mechanism of allocrite recognition and transport by the TMDs across the membrane lipid bilayer? 2) What are the exact structural determinants of the allocrite-binding site and how exactly is this allocrite-binding site organized in the membrane lipid bilayer? 3) How does allocrite-binding to the TMDs result in the activation of the NBDs for ATP hydrolysis? 4) Which regions of the protein are critical for this signalling process between the two domains? 5) How is the energy of ATP hydrolysis coupled to allocrite transport and what kind of conformational changes take place during this process? And 6) what is the nature of the mechanism by which the two NBDs hydrolyse ATP during the catalytic cycle? Clarification of these points is critical to the rational design of chemotherapeutic agents aimed at treating the numerous diseases and phenotypes associated with ABC transporter function. The large amount of published

literature on MDR transporters and other ABC proteins is starting to piece the puzzle together and a uniform picture and mechanism is beginning to emerge.

6.2.1 Mechanism of action of ABC transporters

Although it is well established that it is the energy of ATP hydrolysis at the NBDs that fuels allocrite transport by the TMDs, the actual mechanism of allocrite transport is still not well understood. Nonetheless, several models have been put forward, especially for the MDR transporters, and a general model for transport by all ABC transporters is beginning to emerge.

6.2.1.1 Alternating catalytic sites model

The first model for the catalytic cycle of ABC transporters was proposed by Senior and colleagues in 1995 for the MDR transporter P-gp (Senior *et al.*, 1995b). This model was based on the findings that Vi-trapping of nucleotide at either NBD blocks ATP hydrolysis at both sites, and that mutations and chemical modifications which inactivate one catalytic site also block catalysis at the other, intact site. Thus, it was proposed that ATP hydrolysis occurs alternately between the two NBSs. The alternating catalytic sites cycle is depicted in figure 6.2 and this scheme also incorporates a proposal for coupling of drug transport to ATP hydrolysis by P-gp. Senior and colleagues postulated that drug transport is coupled to relaxation of a high energy catalytic site conformation which is generated by the hydrolysis step.

P-gp differs from other transport ATPases in that it shows no high-affinity binding site for MgATP, nor does it utilize a covalent E~P catalytic intermediate. Changes in free energy associated with such species during the catalytic cycle are thought to be coupled to conformational changes at transport-substrate binding sites in other transport ATPases (Tanford, 1983). In P-gp, Pi binding occurs with relatively weak affinity, implying that a large free energy change occurs during catalysis, before the stage of Pi release. Thus, the ATP hydrolysis step itself must generate a P-gp.MgADP.Pi conformation of high chemical potential. Relaxation of this conformation, probably through intermediates, could be coupled to movement of a drug-binding site from inside-facing aspect of higher affinity to outside-facing aspect of lower affinity. Note that in this scheme, transport of one drug molecule would occur with every ATP hydrolysed.

Figure 6.2:

Alternating catalytic sites cycle of ATP hydrolysis by P-gp

Rectangles represent the two TMDs; circles, squares, and hexagon represent different conformations of the N- and C-catalytic sites (NBD1 and NBD2 respectively). Top left, the NBD1 site is empty, the NBD2 site has bound ATP, and drug is bound at inside-facing transport site. Top right, ATP binding at NBD1 allows ATP hydrolysis at NBD2, inducing a conformation at NBD2 which prohibits hydrolysis at NBD1. The conformation at NBD2 immediately after bond-cleavage is a high chemical potential state with bound ADP.Pi, shown as a *hexagon*. Bottom right, relaxation of the NBD2 conformation occurs, coupled to drug movement from inside-facing, higher-affinity to outside-facing, lower-affinity, and Pi is released. Bottom left, Drug and ADP dissociate. Drug binds at the inner side and in *top left* NBD1 and NBD2 have now reversed their relationship. In the next cycle, ATP hydrolysis will occur in NBD1. Figure reproduced with permission from (Senior *et al.*, 1995b).

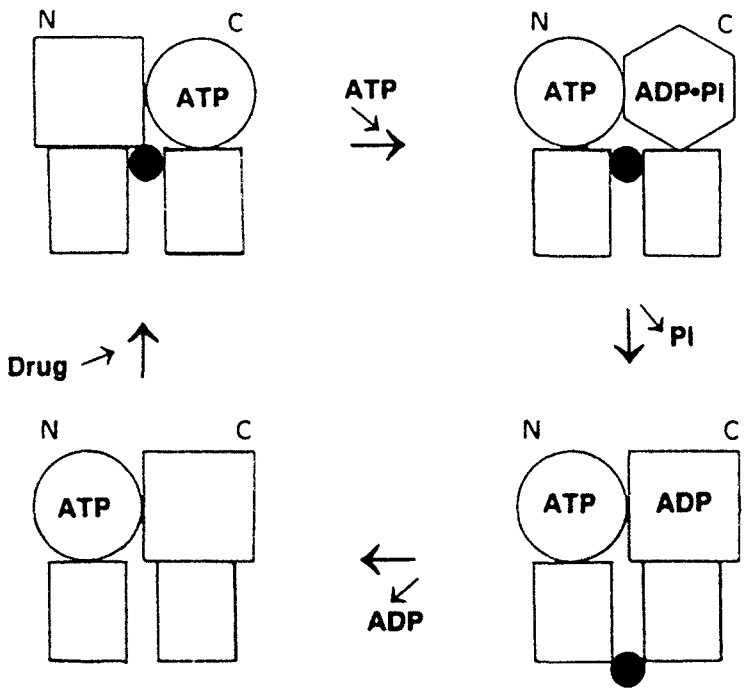
N
C
ATP
ATP
N
C
ATP
ADP•PI
Pi
Drug
N
C
ATP
ADP
N
C
ATP
ADP

6.2.1.2 Two-step model

This model was proposed by Sauna and Ambudkar in the year 2000 and is an extension of the model originally proposed by Senior and colleagues. Given that the two NBDs of ABC transporters hydrolyse ATP non-simultaneously; this model generally assumes that the two NBDs are coupled to distinct steps in the transport cycle. In other words, one ATP hydrolysis is used to translocate the allocrite, and the second is used to reset the transporter. Data which support this model include the observation that ATP hydrolysis by P-gp results in a conformational change in which the affinity of [^{125}I]iodoarylazidoprazosin (IAAP) for the transporter trapped in the transition-state conformation (P-gp.ADP.Vi) is substantially reduced (Sauna and Ambudkar, 2000). Additionally, transformation of P-gp from this intermediate state of low affinity for drug to the next catalytic cycle in which the enzyme now binds drug with high affinity requires conditions that permit ATP hydrolysis.

The essential features of the cycle are illustrated in figure 6.3. Drug and ATP first bind to P-gp (Step I) with no energetic requirement for the drug to bind. Studies have demonstrated, using the fluorescent probe MIANS, that prior binding of ATP is not essential for drug interaction with P-gp (Liu and Sharom, 1996). Additionally, drugs do not affect nucleotide binding. Thus, ATP binding could precede, follow, or accompany the binding of drug. The binding of nucleotide and drug is followed by the first hydrolysis event (Step II), which is accompanied by a large conformational change that (possibly besides other effects) reduces the affinity of both drug and nucleotide for P-gp (Dey *et al.*, 1997; Ramachandra *et al.*, 1998; Sauna and Ambudkar, 2000; Sauna and Ambudkar, 2001). This intermediate can be trapped by using Vi generating the stable Pgp.ADP.Vi complex (Steps IIIA and IIIB). Following hydrolyis, ADP is released (Step IV). This release occurs spontaneously and is not influenced by the presence of nucleotides. The dissociation of ADP is accompanied by a conformational change that allows nucleotide binding, but substrate binding continues to be reduced. A second ATP hydrolysis event is then initiated (Step V) which is kinetically indistinguishable from the first; at this point the substrate binding is still not regained. This event too can be captured as an intermediate by using Vi to trap the nucleotide (Steps VIA and VIB). The subsequent release of ADP (Step VII) completes one catalytic cycle, bringing the P-gp molecule back

Figure 6.3:

A proposed scheme for the catalytic cycle of ATP hydrolysis by P-gp

The ellipses represent the substrate binding sites, the "ON" and the "OFF" sites. The hexagon portrays the "ON" site with reduced affinity for the drug. Two circles represent the ATP sites and the circles are shown overlapping to indicate that both sites are required for ATP hydrolysis. The empty square with rounded edges represents the ATP site with reduced affinity for nucleotide. The release of ADP in Steps IV and VII (underlined) appears to be rate limiting, which is modulated by drug-substrate (Kerr *et al.*, 2001). Figure reproduced with permission from (Sauna *et al.*, 2001b).

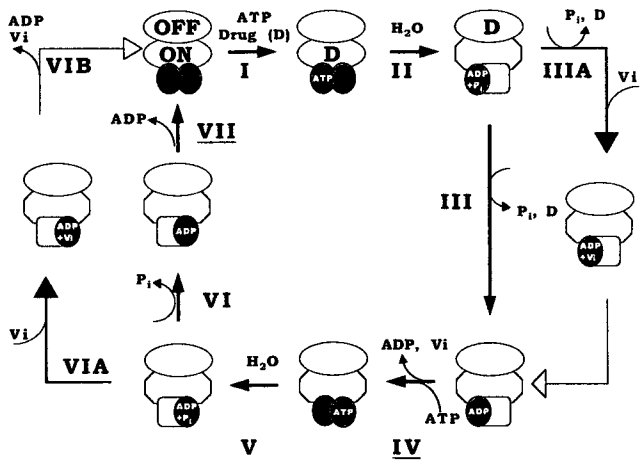
ADP
Vi
VIB
OFF
ON
ATP
Drug (D)
I
D
ATP
H2O
II
D
ADP
+Pi
Pi, D
IIIA
Vi
ADP
VII
III
Pi, D
ADP
+Vi
ADP
Pi
VI
Vi
VIA
H2O
ADP, Vi
ATP
ADP
V
IV

to the original state where it can bind both substrate and nucleotide to initiate the next cycle. In this model, the conformation of P-gp following ATP hydrolysis shows reduced affinity for the nucleotide (Steps II, III, IIIA, V, VI, and VIA). Additionally, following the second ATP hydrolysis event, the release of ADP from P-gp is essential to complete the catalytic cycle, i.e. to bring the molecule back to the state where it will bind the next molecule of drug (Steps VIB and VII). Finally, this model is consistent with findings that ADP release at Steps IV and VII appear to be the rate-limiting steps in the catalytic cycle (Kerr *et al.*, 2001). Note that in this scheme, transport of one drug molecule would occur with two ATP molecules hydrolysed.

6.2.1.2 Partitioning model

This model, postulated by al-Shawi and colleagues in 2004 for the ABC transporter P-gp (Omote *et al.*, 2004), tried to accommodate most of the kinetic data available to date in the literature for P-gp, while still incorporating the alternating catalytic cycle (Senior *et al.*, 1995b). In the partitioning model, two distinct transition states that could be assigned to basal ATPase activity and to drug-coupled transport activity, respectively, were identified using linear free energy analyses (al-Shawi *et al.*, 2003). From these analyses it was concluded that basal ATPase activity is a mechanistic property of the enzyme and constitutes a separate uncoupled pathway of ATP hydrolysis during which no endogenous or exogenous allocrite is carried across the transporter. In addition, both transition states were determined to involve major concerted conformational reorientations of the protein.

The model suggests that if there is insufficient drug and two ATP molecules bind the empty transporter, the enzyme partitions to the uncoupled cycle and hydrolyses ATP without any transport work (Figure 6.4, basal cycle: *shaded*). In this cycle, the drug sites are in a low-affinity unloading conformation. If there is sufficient drug present, the enzyme partitions to the coupled activity cycle (Figure 6.4, coupled cycle), which is the alternating catalytic cycle previously described (Senior *et al.*, 1995b). Results of transport studies obtained with SL-verapamil indicated that this cycle was tightly coupled and that net flux through this pathway ceased when the gradient of transported drug was in the range of the K_i/K_M(drug) ratio (Omote and al-Shawi, 2002). Therefore, drug binds first to a high-affinity loading site, followed by ATP, to form the ternary complex. After passing

Figure 6.4:

Catalytic and drug transport cycles of P-gp

A partitioning model of ABCB1 catalytic and transport cycles is shown. E refers to ABCB1 species. Inner-leaflet, high-affinity, drug-loading "ON-sites" are shown in green (loading site, ^{V}). Extracellular facing, low-affinity, drug-unloading "OFF-sites" are shown in orange (unloading site, $_{\Lambda}$). Red stars show the rate-limiting transition states for the two cycles. The centrally located species $_{ATP}E^{V}_{\Lambda}$ indicates a molecule of P-gp that has one bound ATP. This species is thought to be a mobile carrier form of the protein in which the unloaded high-affinity and unloaded low-affinity drug-binding sites are in equilibrium. Upper right cycle shows the drug-activated, coupled activity; lower left cycle (shaded) shows the uncoupled basal activity. Figure reproduced with permission from (al-Shawi and Omote, 2005).

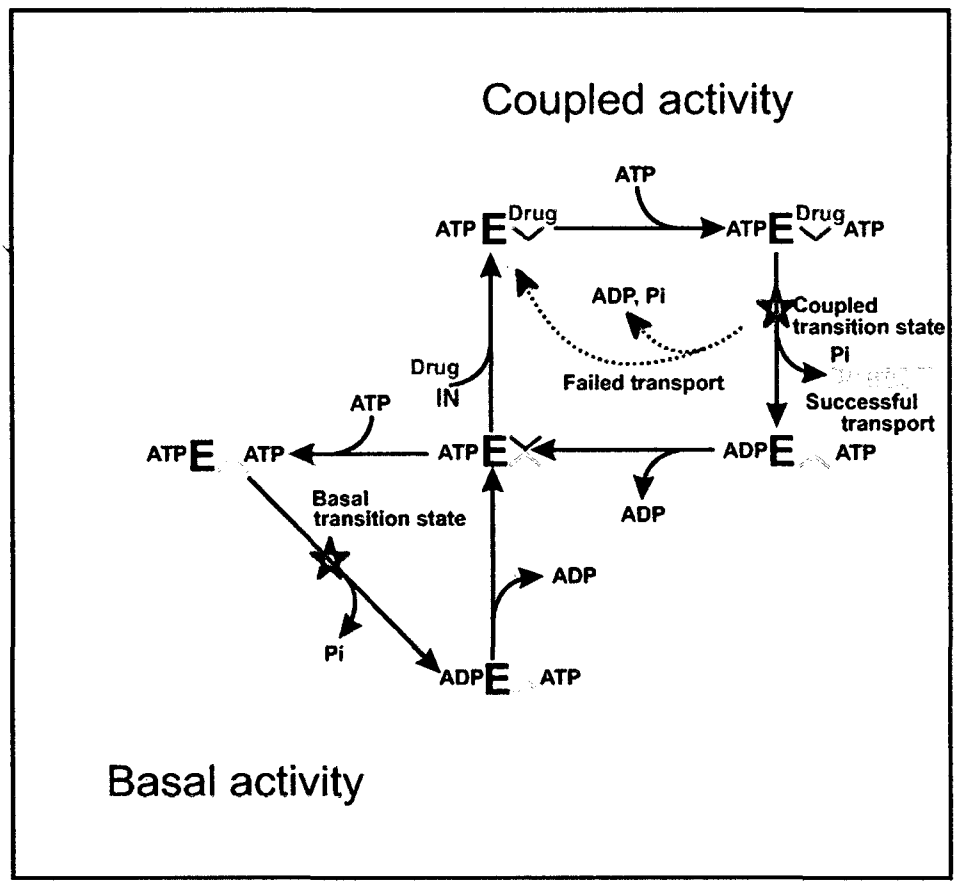
Coupled activity
ATP
ATP E Drug
ATP E Drug ATP
ADP, Pi
Coupled transition state
Pi
Drug IN
Failed transport
Successful transport
ATP
ATP E ATP
ATP E
ADP E ATP
ADP
Basal transition state
ADP
Pi
ADP E ATP
Basal activity

through the high-energy transition state, drug is released to the other side of the membrane (successful transport).

According to this model, the overall rate-limiting step of P-gp during transport is a concerted carrier reorientation step in which the carried allocrite is moved from a high-affinity drug-loading "ON" site to a low-affinity drug-unloading "OFF" site. Different drugs lead to different energy levels of the rate-limiting coupling transition state (al-Shawi *et al.*, 2003; Omote *et al.*, 2004). Due to the instability of the higher-energy transition states, there is a greater probability of non-productive transition state decay without drug transport for drugs with higher-energy transition states (Figure 6.4, failed transport). For example, failed transport is observed when WT P-gp is transporting colchicine or etoposide and the mutation G185V increases the strength of colchicine and etoposide interaction with the transition state and improves the transport of these drugs by reducing the level of failed transport (Omote *et al.*, 2004).

Regulation of ATPase activity between the two catalytic cycles would make P-gp an energy inefficient transporter. al-Shawi and colleagues believe that this unusual transport mechanism is absolutely required for P-gp's physiological function as a very broad drug specificity exporter. A large component of the drug selectivity of P-gp arises from partitioning of hydrophobic transport drugs into the inner leaflet, followed by protein binding. The partitioning between these two phases (membrane inner-leaflet and high-affinity drug-loading sites) is nearly iso-energetic (Seelig *et al.*, 2000). Thus, the interaction of the drug with P-gp is weak relative to the membrane. This may be a strict requirement for low drug selectivity by P-gp, to maximize the chemical entities that can be transported. Given the high toxicity of P-gp's natural xenobiotic allocrites, it has evolved to maximize successful drug transport. al-Shawi and colleagues further postulate that the central $_{ATP}E^{V}_{\Lambda}$ species of figure 6.4 (located on both the coupled and uncoupled cycles) is a mobile carrier form of the protein. In this species the high and low affinity drug-binding sites are in equilibrium and it is the only species that is competent to bind drugs for transport. Thus, its concentration must be maximized. If P-gp binds two ATP molecules in the presence of high ATP and low drug concentrations, the protein becomes kinetically incompetent for transport. Under such conditions the dissociation of ATP is slow. P-gp appears to have evolved the uncoupled ATPase cycle to return quickly to the

transport competent form $_{ATP}E^{V}_{\Lambda}$ and to maximize its concentration. In other words, P-gp appears to have evolved a parallel process that is always faster than a serial process, which is rate-limited by the slowest step. Thus, P-gp pays the price of this cellular protection vigilance with lowered overall coupling efficiency, thereby sacrificing efficiency to achieve higher drug clearance rates (al-Shawi *et al.*, 2003; Omote *et al.*, 2004). In this model, the stoichiometry of ATP molecules hydrolysed per allocrite transported is variable and depends on the concentration and nature of the allocrite.

6.2.1.3 ATP-switch model

By the end of 2004, three datasets caused the previous models to be revisited. First, biochemical data suggesting that ATP-binding, rather than ATP hydrolysis, can provide sufficient energy for transport. Second, structural data showing that the two NBSs are not independent and are located at the interface of an NBD dimer "sandwich", implying that the two NBDs act in concert at a single step rather than influencing distinct steps in the transport cycle. And third, the finding that the ATP binding and hydrolysis activities of the two catalytic sites of some ABC transporters can differ dramatically (e.g. ABCC7/CFTR and ABCC1/MRP1).

The ATP-switch model (Higgins and Linton, 2004) is based on structural and biochemical data from a number of ABC transporters and the critical fact of this model is that transport is a multistep process involving bidirectional communication, via conformational changes, between the NBDs and the TMDs. At the heart of the model is a switch between two principal conformations of the NBDs: formation of a closed dimer upon binding of two ATP molecules at the dimer interface, and dissociation to an open dimer facilitated by ATP hydrolysis and release of Pi and ADP (Figure 6.5). Thus, the switch between the open and closed NBD dimer conformations induces conformational changes in the TMDs necessary for transport (or, for some ABC proteins, biological processes other than transport), i.e. dimerization is the power-stroke for transport. The transport cycle is initiated by binding of allocrite to the TMDs with the NBDs in the open dimer conformation (step I). A conformational change is then transmitted to the NBDs facilitating ATP binding and closed dimer formation. In this model, substrate binding to the transporter must initiate the cycle, otherwise the binding and hydrolysis of ATP would occur independently of transport in a futile cycle. There are multiple lines of evidence

Figure 6.5:

Schematic of the ATP-switch model for the transport cycle of an ABC transporter

The schematic is for a drug exporter. The TMDs are shown as cylinders spanning the membrane; the NBDs as shapes at the cytoplasmic face of the membrane. The transporter in its basal state (top left) has the NBDs in the open-dimer configuration with low affinity for ATP and a high-affinity, allocrite-binding site in the TMDs (yellow star) exposed to the inner leaflet of the membrane. Step I: the transport cycle is initiated by binding of allocrite to its high-affinity site. This sends a signal to the NBDs, which facilitates co-operative binding of two molecules of ATP and closed NBD dimer formation, either by allowing *de novo* binding or by increasing the affinity for pre-bound ATP. Step II: the conformational changes required to form the closed NBD dimer are transmitted to the TMDs, such that the allocrite-binding site is exposed extracellularly and its affinity for allocrite is reduced (blue star). Allocrite is released extracellularly. Step III: ATP is hydrolysed to form a transition state intermediate. Hydrolysis of the two ATP molecules is normally sequential (although for some ABC transporters, only one ATP may be hydrolysed). Step IV: sequential release of Pi, and then ADP, restores the transporter to its basal configuration. Figure modified and reproduced with permission from (Linton and Higgins, 2007).

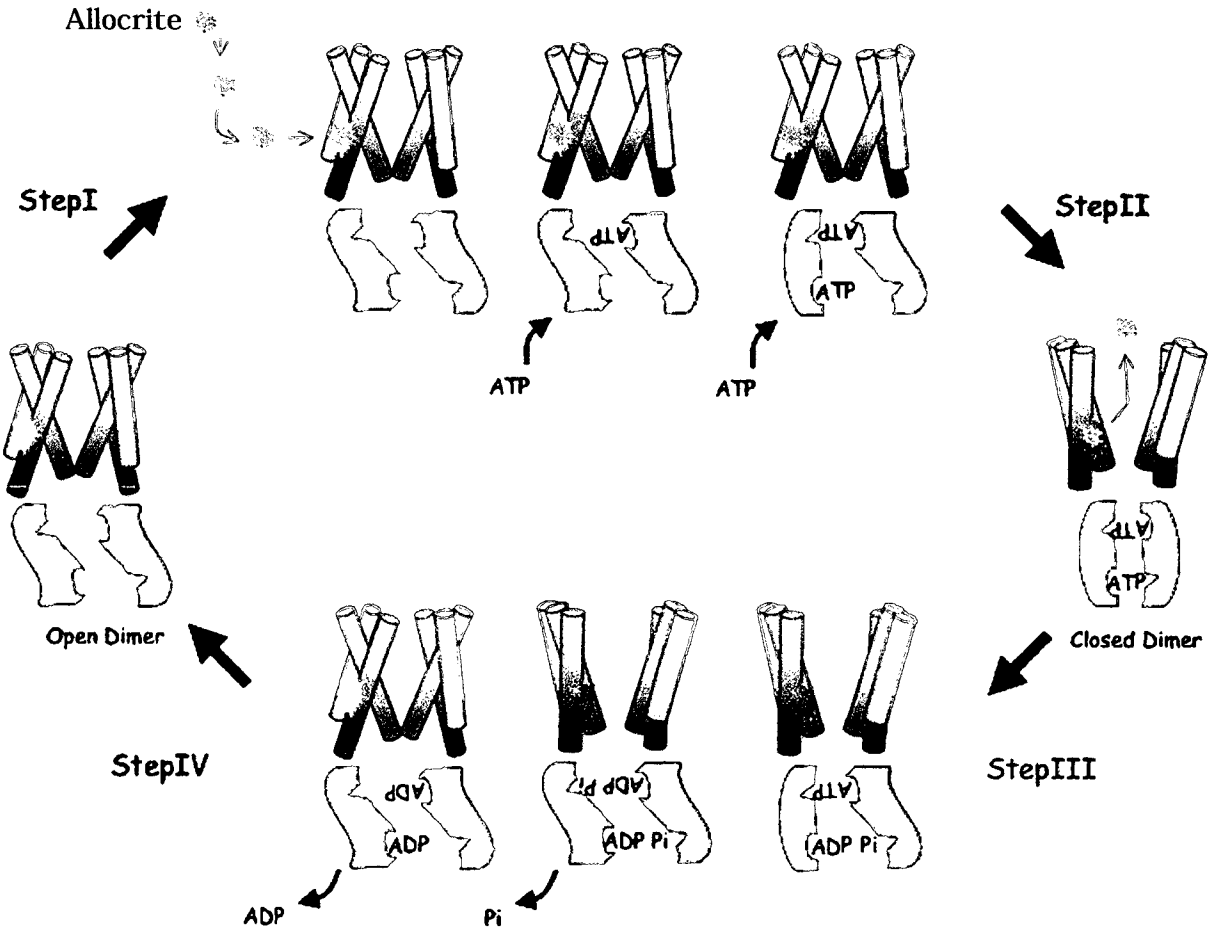
Allocrite
StepI
StepII
StepIII
StepIV
Open Dimer
Closed Dimer
ATP
ATP
ATP
ATP
ATP
ADP
ADP
ADP Pi
ADP Pi
ADP
Pi

showing that binding of the allocrite initiates the transport cycle and that this occurs by enhancing ATP binding to the NBDs (reviewed in Linton and Higgins, 2007). Although the nature of the conformational changes involved in transmitting a signal from the TMDs to the NBDs to enhance ATP binding and closed dimer formation remains speculative, it seems likely that this occurs via the transmission interface (see Section 1.5). Similarly, little is known about the conformational changes which facilitate ATP binding by the NBDs. It has been suggested from structures of both the GlcV NBD and the HlyB-NBD in their nucleotide-free forms (Verdon *et al.*, 2003a; Zaitseva *et al.*, 2006), that unusual conformations of the Walker A loop occlude the nucleotide-binding pockets and displacement of this loop in response to a signal transmitted from the TMDs might increase affinity for ATP. Alternatively, and perhaps more probably, ATP may always have access, and the ability to bind with low affinity, to the NBDs in the open dimer configuration, but a conformational change transmitted from the TMDs is required to align the signature motifs from the opposing NBDs to form nucleotide-binding pockets of high affinity and enable closed dimer formation. Formation of the closed dimer around the bound ATP molecules then induces a major conformational change in the TMDs to initiate allocrite translocation (step II). Export across a cell membrane requires that a high-affinity binding site for the transport substrate accessible from one face of the membrane is converted into a low-affinity site at the other face of the membrane. For an active transporter, these conformational changes require energy input (Mitchell, 1957), and until recently, it was generally assumed that the free energy of ATP hydrolysis drove these conformational changes. However, it is now becoming clear that ATP-binding and closed dimer formation, rather than hydrolysis, provides sufficient energy to induce the key conformational changes involved in substrate transport (reviewed in Higgins and Linton, 2004). ATP is now hydrolysed to initiate transition of the closed to the open dimer configuration (step III). ABC transporters normally hydrolyse ATP as part of the transport cycle. ATP hydrolysis destabilises the closed dimer, which initiates resetting of the transporter to its basal state. The trigger for ATP hydrolysis is unknown. Likely, ATP hydrolysis is an automatic consequence of closed dimer formation. The observation that stable closed dimers of isolated NBDs are difficult to obtain in the presence of ATP (Nikaido, 1997; Verdon *et al.*, 2003a) suggests that the NBDs may be autocatalytic.

Crystals of the isolated LolD (MJ0796) and HlyB-NBD homodimers with bound ATP could only be obtained once specific mutations preventing hydrolysis were introduced (Smith *et al.*, 2002; Zaitseva *et al.*, 2005a). Hydrolysis of ATP does not restore the transporter to its basal state, but is a necessary step in the restoration of the basal state. Release of Pi and then ADP restores the protein to its basal state ready to initiate another transport cycle (step IV). After ATP hydrolysis, Pi must be released before ADP because Vi is able to replace Pi and stabilise the NBD dimer in complex with ADP (Senior *et al.*, 1995b; Sharma and Davidson, 2000). How Pi is released from the post-hydrolytic complex is also debatable. Based on comparison of the electrostatic potential of monomeric and dimeric LolD, it has been proposed that electrostatic repulsion between the ADP coordinated by the catalytic domain of one NBD and the Pi coordinated by the signature motif of the other NBD destabilises the closed NBD dimer, leading to Pi and ADP release (Smith *et al.*, 2002). A different mechanism has been postulated for the isolated HlyB-NBD. Hydrophilic tunnels have been described for the mutant HlyB-NBDs with bound ATP (Zaitseva *et al.*, 2006), and it is suggested that these represent exit tunnels for the released Pi. The tunnels are asymmetric in the HlyB-NBD homodimeric structure. One tunnel provides a continuous passage from one γ-phosphate to the surface of the dimer; the other tunnel, extending from the γ-phosphate of the second ATP, is closed by a salt bridge providing an explanation for the observed, non-simultaneous hydrolysis of the two ATPs in the complex. Thus, it is postulated that Pi leaves the closed HlyB-NBD dimer via an exit tunnel without a build up of electrostatic charge. The remaining ADP is unable to stabilise the NBD dimer, and the dissociation of the NBDs results. This mechanism may not be common to all ABC NBDs, and indeed, for MutS, ADP appears to remain bound to one NBD until substrate binding induces a conformational change in the NBDs, such that ADP is displaced by ATP (Lamers *et al.*, 2003). For P-gp and MutS, it has been shown that ADP release provides a rate-limiting step in the ATPase cycle (Senior *et al.*, 1995b; Gradia *et al.*, 1999; Kerr *et al.*, 2001).

ABC transporters may differ in the details of the cycle. For example, in some cases, one NBD appears to provide the preferred site of ATP binding or hydrolysis, whilst for other ABC transporters, the selection may be random. For some transporters, hydrolysis of only one ATP molecule may be required. The point of allocrite release may

also vary. Nevertheless, despite such variations, the transition between open and closed NBD dimer, and associated conformational changes, provides a common mechanism for transport.

6.2.1.4 Reverse-tweezers model

As reviewed above, various distinct mechanisms have been proposed in the literature to rationalize ATP-driven transport through ABC transporters. The crystal structures of complete transporters obtained in the recent years have since helped to visualize how ATP binding and hydrolysis by the NBDs might be coupled to inward-facing or outward-facing conformations of the TMDs. The structures of ATP-bound, outward-facing (Sav1866 and MalFGK$_2$-MBP) and nucleotide-free, inward-facing (HI1470/1, ModBC, BtuCD-BtuF, and MsbA) conformations have been used to formulate a common mechanism of transport for ABC importers and exporters (Hollenstein *et al.*, 2007a). Given the distinct function of these proteins, it may seem unreasonable to suggest that they operate alike. However, because not only their motor domains but also critical transmission elements are architecturally conserved, a related *modus operandi* can reasonably be proposed.

The key to effective, unidirectional transport appears to be the ATP-driven closing of the NBDs (dimerization), which causes the distance between the coupling helices to be decreased by some 10-15Å when compared with the nucleotide-free state (Figure 6.6). The approaching coupling helices appear to trigger a flipping of the TMDs from an inward-facing to an outward-facing conformation, similar to the opening of reverse-tweezers when the base is squeezed together (here the base would be the NBDs). In this conformation, ABC importers may now accept allocrites from their cognate binding proteins, whereas ABC exporters may extrude already-bound allocrites to the environment. Upon ATP hydrolysis and the release of ADP and Pi, the transporter may flip back to an inward-facing conformation. Importers may now release their allocrites into the cytoplasm, whereas exporters may recruit new allocrites into high-affinity binding sites.

This proposed basic scheme is reminiscent of the "alternating access and release" mechanism that, while conceptually suggested about half a century ago (Jardetzky, 1966), is still a successful working hypothesis for the mechanism of transporters such as major

Figure 6.6:

ATP-induced conformational changes

The nucleotide-free structure of ModBC-ModA (left) reveals an inward-facing conformation of the TMDs, whereas AMP-PNP-bound Sav1866 (reflecting the ATP-bound state, right) reveals an outward-facing conformation. In ModBC, the NBDs adopt an open conformation, whereas in Sav1866, the NBDs adopt a closed, dimerized conformation with two nucleotide analogues sandwiched between the NBDs. The attached, architecturally conserved coupling helices are coloured black in both transporters for better visibility, and the change in distance between the two states is indicated below the ribbon diagrams. Compared with the nucleotide-free state of ModBC, the coupling helices approach one another by more than 10Å in the ATP-bound state of Sav1866. This is coupled to the TMDs flipping from an inward-facing to an outward-facing conformation. Figure reproduced with permission from (Hollenstein *et al.*, 2007a).

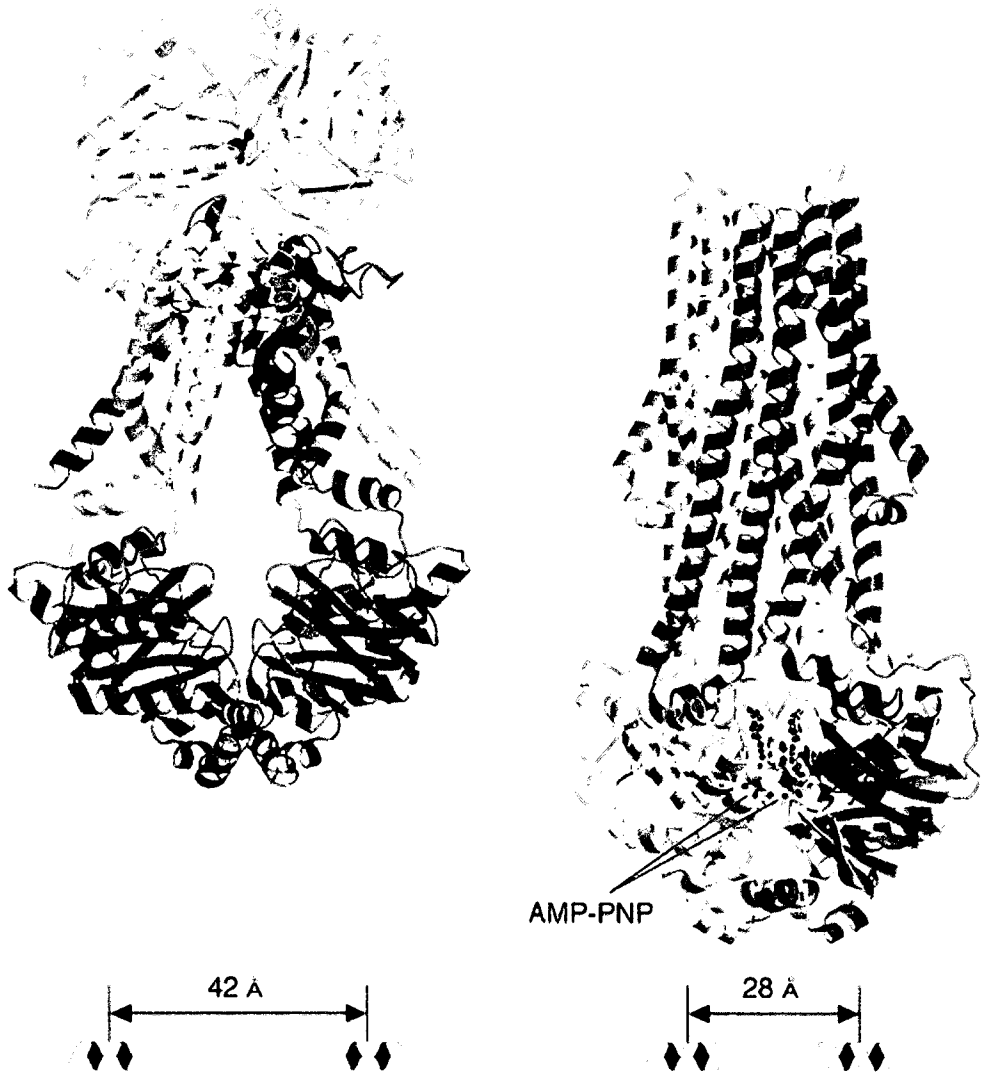
AMP-PNP
42 Å
28 Å

facilitators (e.g. Guan and Kaback, 2006). In ABC transporters, an important distinction is that ATP, not allocrite-binding, appears to control which side of the membrane the translocation pathway is accessible to (inward-facing or outward-facing). Also, the TMDs of ABC transporters may adopt additional conformations, in particular a state that is closed to both sides of the membrane simultaneously, as was observed in the structures of a major facilitator protein OxlT, the oxalate transporter (Hirai *et al.*, 2002).

6.2.2 Structural and functional equivalence or asymmetry of the two NBDs

The question of whether the two NBDs of ABC proteins are structurally and/or functionally equivalent and whether they play distinct roles during catalysis and transport (or other biological processes) is still being debated. In support of structural and functional equivalence of the two sites are the observations that 1) there is no evidence for binding site heterogeneity in ATP- and ADP-binding studies with purified transporters such as Abcb1a and ABCB1 (Sharom *et al.*, 1999; Urbatsch *et al.*, 2000a), 2) mutations in Walker A or B residues in either NBD completely abolish drug transport and ATPase activity in many transporters including Abcb1a (Urbatsch *et al.*, 1998), ABCB1 (Azzaria *et al.*, 1989), and $MalFGK_2$ (Davidson and Sharma, 1997), 3) each ABCB1 half shows low intrinsic ATPase activity (Loo and Clarke, 1994), 4) V_i inhibits ATP hydrolysis and can induce trapping of 8-azido-[α^{32}P]ADP·V_i in Abcb1a and ABCB1 with seemingly equal labelling of NBD1 and NBD2 (Urbatsch *et al.*, 1995a; Urbatsch *et al.*, 1995b; Sauna and Ambudkar, 2001), and 5) NEM inhibits ABCB1 ATPase activity by binding to a cysteine present in the Walker A motif of NBD1 and NBD2 (al-Shawi *et al.*, 1994; Sharom *et al.*, 1999), and NEM-sensitive ATPase activity is inhibited by similar ATP concentrations in single-cysteine ABCB1 mutants in NBD1 and NBD2 (Loo and Clarke, 1995a). Opposing data in support of structurally and/or functionally distinct NBDs include the observations that 1) NBD1 cannot be replaced by NBD2 without loss of transport function in Abcb1a (Beaudet and Gros, 1995), 2) median inhibition of ATPase activity in cysteine-less ABCB1 mutants bearing single-cysteine replacements in NBD1 or NBD2 occurs at different NEM concentrations (Loo and Clarke, 1995a), 3) in ABCB1 (Hrycyna *et al.*, 1999) 8-azido-[α^{32}P]ATP preferentially labels NBD1 under binding conditions (4°C), while under hydrolysis conditions (37°C and V_i) NBD2 is preferentially

labelled, 4) equivalent mutations in Walker B residues of NBD1 and NBD2 cause different conformational changes in Abcb1a as measured by trypsin sensitivity (Julien and Gros, 2000), 5) equivalent mutations in Walker A lysine residues in ABCB2/TAP1 and ABCB3/TAP2 cause different degrees of impairment of peptide transport (Lapinski *et al.*, 2001), and 6) functional studies of human ABCC7/CFTR (Szabo *et al.*, 1999; Aleksandrov *et al.*, 2001; Aleksandrov *et al.*, 2002; Powe Jr. *et al.*, 2002), of human ABCC1/MRP1 (Gao *et al.*, 2000; Hou *et al.*, 2000; Nagata *et al.*, 2000; Cui *et al.*, 2001; Hou *et al.*, 2002), of yeast Ste6 (Proff and Kolling, 2001), and of the NBDs of the bacterial arsenite transporter ArsA (Zhou and Rosen, 1997) show that NBD1 and NBD2 have different ATP-binding and hydrolysis properties.

Further evidence of structural symmetry has come from crystallization studies. High-resolution structures of NBD homodimers (in the presence of nucleotide) demonstrate that the two NBDs adopt highly similar conformations. For example, in the high-resolution structure of MutS (mismatch repair ABC protein) dimerized about a short mismatched DNA, five structural domains are observed in each monomer (Obmolova *et al.*, 2000). Each of the five domains is structurally identical between the two subunits, although the relative orientations of three domains (including the ABC-NBD) differ. In the LolD-E171Q homodimeric structure in the presence of ATP, a symmetrical ATP sandwich complex is observed (Smith *et al.*, 2002). Also, in the HlyB-NBD-H662A homodimeric structure in the presence of MgATP the r.m.s.d. between individual monomers is below 0.7Å for the 241 Cα atoms, displaying a highly symmetrical organization (Schmitt *et al.*, 2003).

On the other hand, evidence of structural and functional asymmetry was obtained recently when additional crystal structures of HlyB were solved. Structures of two mutated forms of the HlyB-NBD, H662A and E631Q, in complex with ATP, in the absence and presence of Mg^{2+} (dimers), and in complex with ADP (monomers), as well as the WT monomer protein in the absence and presence of bound ADP (Schmitt *et al.*, 2003; Zaitseva *et al.*, 2005a; Zaitseva *et al.*, 2006) were obtained and compared. A basic ABC catalytic cycle was described in structural detail, and important mechanistic insights as well as several novel features, including a structural asymmetry within the dimer in the presence of MgATP, were thus revealed (Zaitseva *et al.*, 2006). Whereas direct ATP-

protein interactions are rather symmetric in the dimer structures, symmetric and asymmetric protein-protein interactions do occur, in both the ATP- and the MgATP-bound states. The pattern of interactions in both states is qualitatively different, with a more prominent asymmetry in the presence of Mg^{2+}; the D-loop is heavily involved in asymmetric inter-monomer interactions in the MgATP-bound state. Detailed cavity analyses of the dimer structures revealed that Pi should not be able to diffuse freely out of the NBS, but rather, a conformational change would have to occur within the protein in order to open an exit path for the cleaved Pi. Hence, it was proposed that the asymmetry within the dimer represents one open and one closed phosphate exit tunnel. Presence of the phosphate tunnels could explain biochemical data which strongly suggested sequential ATP hydrolysis by the NBDs of ABC proteins (This thesis, and for example Janas *et al.*, 2003; Tombline *et al.*, 2005).

Our studies support a model in which the two NBDs of ABC transporters are not symmetrical and this asymmetry is observed in the sequence of hydrolytic events, i.e. upon nucleotide binding and dimer formation, the same NBD (NBD2) is committed to hydrolyse its ATP first during each catalytic cycle.

6.2.3 Last words and thoughts on the mechanism of ABC proteins

Additional crystallographic studies of ABC transporters trapped in distinct states will undoubtedly be a priority for the coming years and may reveal the conformational changes concomitant with substrate transport and ATP hydrolysis. Moreover, biochemical, biophysical, and modeling studies may fill the gaps between the snapshot pictures provided by the structures available to date. Meanwhile, a common mechanism for allocrite transport by ABC transporters can be postulated based on the models available so far. In this scheme, the transporter (importer or exporter) in its basal state in the membrane has its TMDs in an inward-facing conformation. The NBDs are in the open dimer conformation and ATP normally occupies the NBSs, since cellular concentrations of the nucleotide are usually greater than the apparent K_d for ATP (0.4-0.5mM, Liu and Sharom, 1996). In importers, the allocrite-laden PBP interacts with the TMDs; in exporters, allocrite binds to the high-affinity, and inward-facing binding site of the transporter. These interactions cause conformational changes in the TMDs which are

transmitted to the NBDs via the transmission interface and likely re-orient the helical domain so that the signature motif is aligned with the NBS of the opposite NBD. This causes dimerization around the two ATP molecules to occur. Dimerization of the NBDs brings the coupling helices of each TMD closer together, which leads to reorientation of the TM helices such that the TMDs are now in an outward-facing conformation. In importers, this pries open the PBP which releases its allocrite into the binding pocket in the TMDs; in exporters, the allocrite-binding site is now exposed to the other side of the membrane, and due to reduction in affinity for the allocrite, the latter is released to the extracellular space (or to the outer-leaflet of the membrane). Upon dimerization of the NBDs, the ATP molecules are hydrolysed and destabilization of the dimer ensues. Upon release of Pi and ADP the NBDs move apart and the coupling helices become separated, thus reorienting the TM helices in the membrane. In importers, the allocrite is now released to the intracellular space; this may be aided by conformational changes associated with release of hydrolysis products. The transporter is now reset and ready for a new transport cycle.

Hydrolysis at the NBDs has been established to occur non-simultaneously, but the exact mechanism of catalysis has not yet been fully elucidated. Indeed, two catalytic mechanisms for the hydrolysis of the γ-phosphate of ATP have been proposed based on NBS geometry observed in high-resolution structures of different ABC proteins. For example, the structure of the mutant LolD homodimer in its ATP-bound state shows a water molecule positioned with ideal geometry for hydrolytic attack on the γ-phosphate group of ATP, but which cannot be activated because the required H-bond acceptor, the catalytic base (invariant carboxylate) E171, has been mutated to stabilise the structure (Figure 6.7 A). Thus, in LolD, hydrolysis is thought to occur via a catalytic base mechanism. On the other hand, structures of similar mutants of HlyB-NBD with bound ATP have led to a different interpretation of the molecular mechanism of hydrolysis. Arguing that base catalysis would be possible in monomeric NBDs and that free NBDs in solution need to dimerize to hydrolyse ATP, substrate-assisted catalysis (SAC) has been proposed for HlyB (Figure 6.7 B). SAC requires the microenvironment of the closed NBD dimer to enable ATP itself to abstract a hydrogen atom from the catalytic water, thus activating it for nucleophilic attack on the γ-phosphate. Which mechanism is

Figure 6.7:

Possible mechanisms of ATP hydrolysis

(A) General base catalysis. The histidine of the H-loop donates a hydrogen bond to the γ-phosphate of ATP stabilizing its position. The invariant carboxylate is oriented towards the water from which it abstracts a proton (*arrow*), thus activating the water for nucleophilic attack on the γ-phosphate. (B) Substrate-assisted catalysis. The H-loop histidine donates the same hydrogen bond to the γ-phosphate of ATP, but the role of the invariant carboxylate is to accept two hydrogen bonds from the H-loop histidine stabilizing the position of the latter in the active site and thus forming a "catalytic dyad". Catalysis is substrate-assisted as the γ-phosphate acts as a base to abstract a proton from the hydrolytic water (*arrow*), activating it for nucleophilic attack. Such a substrate-assisted mechanism would be dependent on the pK_a of the ATP, which in turn would be dependent on the local environment of the active site. Only one NBD is shown for clarity; the side chains of Glu631 and His662, the proposed hydrolytic water and the ATP are shown in *stick form* and coloured *elementally*. The magnesium cofactor is shown as a *green sphere*. Figure modified and reproduced with permission from (Linton and Higgins, 2007).

A)

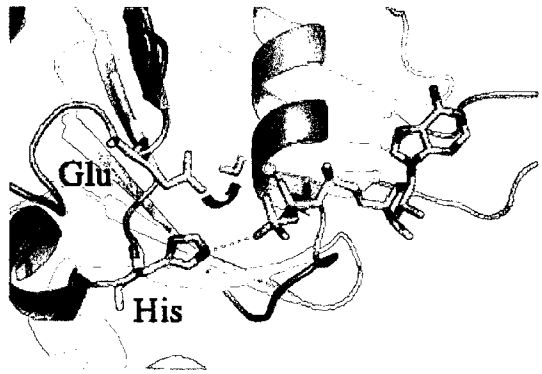

B)

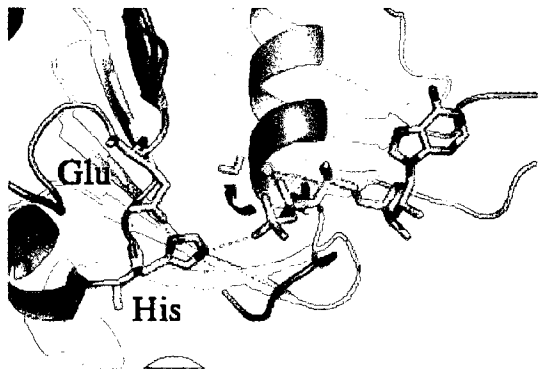

operative in ABC proteins remains to be identified, although our studies on the putative catalytic base (Chapters 3, 4, and 5) suggest that SAC is the employed mechanism.

Significant progress has been made in the studies of ABC transporters to understand their function and mechanisms of transport and catalysis. However, many details still remain unknown. Understanding the details of the mechanisms of allocrite recognition and transport, as well as ATP hydrolysis will be essential for a more rational approach to designing new compounds or methods to circumvent the action of MDR transporters or to alleviate phenotypes associated with targeting defects of certain ABC transporters. Even though high-resolution structures provide useful models, their static nature does not permit complete characterization of the nature of any dynamic interactions. The use of site-directed mutagenesis to study the function of key residues within enzymes remains a powerful tool in our endeavour to fully understand the function and mechanism of ABC proteins.

References

Abe-Dohmae, S., Ueda, K. and Yokoyama, S. (2006). ABCA7, a molecule with unknown function. *FEBS Lett.* **580**(4): 1178-82. Epub 2005 Dec 19.

Abrahams, J. P., Leslie, A. G., Lutter, R. and Walker, J. E. (1994). Structure at 2.8 A resolution of F1-ATPase from bovine heart mitochondria. *Nature.* **370**(6491): 621-8.

Ahn, K., Gruhler, A., Galocha, B., Jones, T. R., Wiertz, E. J., Ploegh, H. L., Peterson, P. A., Yang, Y. and Fruh, K. (1997). The ER-luminal domain of the HCMV glycoprotein US6 inhibits peptide translocation by TAP. *Immunity.* **6**(5): 613-21.

Ahn, K., Meyer, T. H., Uebel, S., Sempe, P., Djaballah, H., Yang, Y., Peterson, P. A., Fruh, K. and Tampe, R. (1996). Molecular mechanism and species specificity of TAP inhibition by herpes simplex virus ICP47. *EMBO J.* **15**(13): 3247-55.

Albrecht, C. and Viturro, E. (2007). The ABCA subfamily--gene and protein structures, functions and associated hereditary diseases. *Pflugers Arch.* **453**(5): 581-9. Epub 2006 Apr 4.

Aleksandrov, L., Aleksandrov, A. A., Chang, X. B. and Riordan, J. R. (2002). The First Nucleotide Binding Domain of Cystic Fibrosis Transmembrane Conductance Regulator Is a Site of Stable Nucleotide Interaction, whereas the Second Is a Site of Rapid Turnover. *J. Biol. Chem.* **277**(18): 15419-25.

Aleksandrov, L., Mengos, A., Chang, X., Aleksandrov, A. and Riordan, J. R. (2001). Differential interactions of nucleotides at the two nucleotide binding domains of the cystic fibrosis transmembrane conductance regulator. *J. Biol. Chem.* **276**(16): 12918-23.

Allen, J. D., Brinkhuis, R. F., van Deemter, L., Wijnholds, J. and Schinkel, A. H. (2000). Extensive contribution of the multidrug transporters P-glycoprotein and Mrp1 to basal drug resistance. *Cancer Res.* **60**(20): 5761-6.

Allikmets, R. (1997). A photoreceptor cell-specific ATP-binding transporter gene (ABCR) is mutated in recessive Stargardt macular dystrophy. *Nat Genet.* **17**(1): 122.

Allikmets, R. (2000). Further evidence for an association of ABCR alleles with age-related macular degeneration. The International ABCR Screening Consortium. *Am J Hum Genet.* **67**(2): 487-91. Epub 2000 Jul 3.

Allikmets, R., Raskind, W. H., Hutchinson, A., Schueck, N. D., Dean, M. and Koeller, D. M. (1999). Mutation of a putative mitochondrial iron transporter gene (ABC7) in X-linked sideroblastic anemia and ataxia (XLSA/A). *Hum Mol Genet.* **8**(5): 743-9.

Allikmets, R., Wasserman, W. W., Hutchinson, A., Smallwood, P., Nathans, J., Rogan, P. K., Schneider, T. D. and Dean, M. (1998). Organization of the ABCR gene: analysis of promoter and splice junction sequences. *Gene.* **215**(1): 111-22.

Alonso, E. M., Snover, D. C., Montag, A., Freese, D. K. and Whitington, P. F. (1994). Histologic pathology of the liver in progressive familial intrahepatic cholestasis. *J Pediatr Gastroenterol Nutr.* **18**(2): 128-33.

al-Shawi, M. K. and Omote, H. (2005). The remarkable transport mechanism of P-glycoprotein: a multidrug transporter. *J Bioenerg Biomembr.* **37**(6): 489-96.

al-Shawi, M. K., Polar, M. K., Omote, H. and Figler, R. A. (2003). Transition state analysis of the coupling of drug transport to ATP hydrolysis by P-glycoprotein. *J. Biol. Chem.* **278**(52): 52629-40.

al-Shawi, M. K. and Senior, A. E. (1993). Characterization of the adenosine triphosphatase activity of Chinese hamster P-glycoprotein. *J. Biol. Chem.* **268**(6): 4197-206.

al-Shawi, M. K., Urbatsch, I. L. and Senior, A. E. (1994). Covalent inhibitors of P-glycoprotein ATPase activity. *J. Biol. Chem.* **269**(12): 8986-92.

Ambudkar, S. V., Cardarelli, C. O., Pashinsky, I. and Stein, W. D. (1997). Relation between the turnover number for vinblastine transport and for vinblastine-stimulated ATP hydrolysis by human P-glycoprotein. *J. Biol. Chem.* **272**(34): 21160-6.

Ambudkar, S. V., Dey, S., Hrycyna, C., Ramachandra, M., Pastan, I. and Gottesman, M. M. (1999). Biochemical, cellular, and pharmacological aspects of the multidrug transporter. *Annu. Rev. Pharmacol. Toxicol.* **39**: 361-98.

Ambudkar, S. V., Gottesman, M. M., Abelson, J. and Simon, M. (1998). ABC Transporters: Biochemical, Cellular, and Molecular Aspects, Elsevier.

Ambudkar, S. V., Kim, I.-W., Xia, D. and Sauna, Z. E. (2006). The A-loop, a novel conserved aromatic acid subdomain upstream of the Walker A motif in ABC transporters, is critical for ATP binding. *FEBS Lett.* **580**(4): 1049-55.

Ambudkar, S. V., Lelong, I. H., Zhang, J., Cardarelli, C. O., Gottesman, M. M. and Pastan, I. (1992). Partial purification and reconstitution of the human multidrug-resistance pump: characterization of the drug-stimulatable ATP hydrolysis. *Proc. Natl. Acad. Sci. U.S.A.* **89**(18): 8472-6.

Ames, G. F. (1989). Reconstitution of periplasmic transport in inside-out membrane vesicles. Energization by ATP. *J. Biol. Chem.* **264**(7): 3998-4002.

Ames, G. F., Mimura, C. S., Holbrook, S. R. and Shyamala, V. (1992). Traffic ATPases: a superfamily of transport proteins operating from Escherichia coli to humans. *Adv Enzymol Relat Areas Mol Biol.* **65**: 1-47.

Andersen, D. S. and Leevers, S. J. (2007). The essential Drosophila ATP-binding cassette domain protein, pixie, binds the 40 S ribosome in an ATP-dependent manner and is required for translation initiation. *J Biol Chem.* **282**(20): 14752-60. Epub 2007 Mar 28.

Anderson, M. P., Gregory, R. J., Thompson, S., Souza, D. W., Paul, S., Mulligan, R. C., Smith, A. E. and Welsh, M. J. (1991). Demonstration that CFTR is a chloride channel by alteration of its anion selectivity. *Science.* **253**(5016): 202-5.

Anjard, C. and Loomis, W. F. (2002). Evolutionary analyses of ABC transporters of Dictyostelium discoideum. *Eukaryot Cell.* **1**(4): 643-52.

Annilo, T., Shulenin, S., Chen, Z. Q., Arnould, I., Prades, C., Lemoine, C., Maintoux-Larois, C., Devaud, C., Dean, M., Denefle, P., *et al.* (2002). Identification and characterization of a novel ABCA subfamily member, ABCA12, located in the lamellar ichthyosis region on 2q34. *Cytogenet Genome Res.* **98**(2-3): 169-76.

Annilo, T., Tammur, J., Hutchinson, A., Rzhetsky, A., Dean, M. and Allikmets, R. (2001). Human and mouse orthologs of a new ATP-binding cassette gene, ABCG4. *Cytogenet Cell Genet.* **94**(3-4): 196-201.

Assmann, G., von Eckardstein, A. and Brewer, H. B., Jr. (1995). Familial high density lipoprotein deficiency: Tangier disease. The metabolic and molecular bases of inherited disease. Scriver, C. A.*et al.* New York, McGraw-Hill: 2053–72.

Aubry, F., Mattei, M. G., Barque, J. P. and Galibert, F. (1996). Chromosomal localization and expression pattern of the RNase L inhibitor gene. *FEBS Lett.* **381**(1-2): 135-9.

Avendano, M. (2000). Multidrug-resistant tuberculosis: long term follow-up of 40 non-HIV-infected patients. *Canadian Respiratory Journal* **7**(5): 383-9.

Azzaria, M., Schurr, E. and Gros, P. (1989). Discrete mutations introduced in the predicted nucleotide-binding sites of the mdr1 gene abolish its ability to confer multidrug resistance. *Mol. Cell. Biol.* **9**(12): 5289-97.

Bakos, E. and Homolya, L. (2007). Portrait of multifaceted transporter, the multidrug resistance-associated protein 1 (MRP1/ABCC1). *Pfluegers Archives - European Journal of Physiology* **453**: 621-41.

Barthelme, D., Scheele, U., Dinkelaker, S., Janoschka, A., Macmillan, F., Albers, S. V., Driessen, A. J., Stagni, M. S., Bill, E., Meyer-Klaucke, W., *et al.* (2007). Structural organization of essential iron-sulfur clusters in the evolutionarily highly conserved ATP-binding cassette protein ABCE1. *J Biol Chem.* **282**(19): 14598-607. Epub 2007 Mar 12.

Baubichon-Cortay, H., Baggetto, L. G., Dayan, G. and Di Pietro, A. (1994). Overexpression and purification of the carboxyl-terminal nucleotide-binding domain from mouse P-glycoprotein. Strategic location of a tryptophan residue. *J Biol Chem.* **269**(37): 22983-9.

Beaudet, L. and Gros, P. (1995). Functional dissection of P-glycoprotein nucleotide-binding domains in chimeric and mutant proteins. Modulation of drug resistance profiles. *J. Biol. Chem.* **270**(29): 17159-70.

Beaudet, L., Urbatsch, I. L. and Gros, P. (1998a). High-level expression of mouse Mdr3 P-glycoprotein in yeast Pichia pastoris and characterization of ATPase activity. *Methods Enzymol.* **292**: 397-413.

Beaudet, L., Urbatsch, I. L. and Gros, P. (1998b). Mutations in the nucleotide-binding sites of P-glycoprotein that affect substrate specificity modulate substrate-induced adenosine triphosphatase activity. *Biochemistry* **37**(25): 9073-82.

Bebawy, M. and Chetty, M. (2008). Differential pharmacological regulation of drug efflux and pharmacoresistant schizophrenia. *Bioessays.* **30**(2): 183-8.

Beck, K., Hayashi, K., Dang, K., Hayashi, M. and Boyd, C. D. (2005). Analysis of ABCC6 (MRP6) in normal human tissues. *Histochem Cell Biol.* **123**(4-5): 517-28. Epub 2005 May 12.

Benabdelhak, H., Schmitt, L., Horn, C., Jumel, K., Blight, M. A. and Holland, I. B. (2005). Positive co-operative activity and dimerization of the isolated ABC ATPase domain of HlyB from Escherichia coli. *Biochem. J.* **386**(Pt 3): 489-95.

Berge, K. E., Tian, H., Graf, G. A., Yu, L., Grishin, N. V., Schultz, J., Kwiterovich, P., Shan, B., Barnes, R. and Hobbs, H. H. (2000). Accumulation of dietary cholesterol in sitosterolemia caused by mutations in adjacent ABC transporters. *Science.* **290**(5497): 1771-5.

Berger, A. L. and Welsh, M. J. (2000). Differences between Cystic Fibrosis Transmembrane Conductance Regulator and HisP in the Interaction with the Adenine Ring of ATP. *J. Biol. Chem.* **275**(38): 29407-12.

Bianchet, M. A., Ko, Y. H., Amzel, L. M. and Pedersen, P. L. (1997). Modeling of nucleotide binding domains of ABC transporter proteins based on a F1-ATPase/recA topology: structural model of the nucleotide binding domains of the cystic fibrosis transmembrane conductance regulator (CFTR). *J Bioenerg Biomembr.* **29**(5): 503-24.

Bienengraeber, M., Olson, T. M., Selivanov, V. A., Kathmann, E. C., O'Cochlain, F., Gao, F., Karger, A. B., Ballew, J. D., Hodgson, D. M., Zingman, L. V., *et al.* (2004). ABCC9 mutations identified in human dilated cardiomyopathy disrupt catalytic KATP channel gating. *Nat Genet.* **36**(4): 382-7. Epub 2004 Mar 21.

Bisbal, C., Martinand, C., Silhol, M., Lebleu, B. and Salehzada, T. (1995). Cloning and characterization of a RNAse L inhibitor. A new component of the interferon-regulated 2-5A pathway. *J Biol Chem.* **270**(22): 13308-17.

Bishop, L., Agbayani, R., Jr., SV, A., Maloney, P. C. and Ames, G. F. (1989). Reconstitution of a bacterial periplasmic permease in proteoliposomes and demonstration of ATP hydrolysis concomitant with transport. *Proc. Natl. Acad. Sci. U.S.A.* **86**(18): 6953-7.

Bither, P. P. and Berns, L. A. (1988). Stargardt's disease: a review of the literature. *J Am Optom Assoc.* **59**(2): 106-11.

Blight, M. A., Pimenta, A. L., Lazzaroni, J. C., Dando, C., Kotelevets, L., Seror, S. J. and Holland, I. B. (1994). Identification and preliminary characterization of temperature-sensitive mutations affecting HlyB, the translocator required for the secretion of haemolysin (HlyA) from Escherichia coli. *Mol Gen Genet.* **245**(4): 431-40.

Bliss, J. M., Garon, C. F. and Silver, R. P. (1996). Polysialic acid export in Escherichia coli K1: the role of KpsT, the ATP-binding component of an ABC transporter, in chain translocation. *Glycobiology.* **6**(4): 445-52.

Borst, P., de Wolf, C. and van de Wetering, K. (2007). Multidrug resistance-associated proteins 3, 4, and 5. *Pflugers Arch.* **453**(5): 661-73. Epub 2006 Apr 4.

Borst, P. and Elferink, R. O. (2002). Mammalian ABC transporters in health and disease. *Annu Rev Biochem.* **71**: 537-92. Epub 2001 Nov 9.

Borst, P., Evers, R., Kool, M. and Wijnholds, J. (2000). A family of drug transporters: the multidrug resistance-associated proteins. *J Natl Cancer Inst.* **92**(16): 1295-302.

Borst, P., van de Wetering, K. and Schlingemann, R. (2008). Does the absence of ABCC6 (Multidrug Resistance Protein 6) in patients with Pseudoxanthoma elasticum prevent the liver from providing sufficient vitamin K to the periphery? *Cell Cycle* **7**: 11.

Broccardo, C., Luciani, M. and Chimini, G. (1999). The ABCA subclass of mammalian transporters. *Biochim Biophys Acta.* **1461**(2): 395-404.

Broccardo, C., Osorio, J., Luciani, M. F., Schriml, L. M., Prades, C., Shulenin, S., Arnould, I., Naudin, L., Lafargue, C., Rosier, M., *et al.* (2001). Comparative analysis of the promoter structure and genomic organization of the human and mouse ABCA7 gene encoding a novel ABCA transporter. *Cytogenet Cell Genet.* **92**(3-4): 264-70.

Brooks-Wilson, A., Marcil, M., Clee, S. M., Zhang, L. H., Roomp, K., van Dam, M., Yu, L., Brewer, C., Collins, J. A., Molhuizen, H. O., *et al.* (1999). Mutations in ABC1

in Tangier disease and familial high-density lipoprotein deficiency. *Nat Genet.* **22**(4): 336-45.

Bruggemann, E. P., Currier, S. J., Gottesman, M. M. and Pastan, I. (1992). Characterization of the azidopine and vinblastine binding site of P-glycoprotein. *J Biol Chem.* **267**(29): 21020-6.

Bruggemann, E. P., Germann, U. A., Gottesman, M. M. and Pastan, I. (1989). Two different regions of P-glycoprotein [corrected] are photoaffinity-labeled by azidopine. [erratum appears in J Biol Chem 1990 Mar 5;265(7):4172.]. *J. Biol. Chem.* **264**(26): 15483-8.

Bryan, J., Munoz, A., Zhang, X., Dufer, M., Drews, G., Krippeit-Drews, P. and Aguilar-Bryan, L. (2007). ABCC8 and ABCC9: ABC transporters that regulate K+ channels. *Pflugers Arch.* **453**(5): 703-18. Epub 2006 Aug 8.

Bullard, J. E., Wert, S. E. and Nogee, L. M. (2006). ABCA3 deficiency: neonatal respiratory failure and interstitial lung disease. *Semin Perinatol.* **30**(6): 327-34.

Burke, M. A., Mutharasan, R. K. and Ardehali, H. (2008). The sulfonylurea receptor, an atypical ATP-binding cassette protein, and its regulation of the KATP channel. *Circ Res.* **102**(2): 164-76.

Buschman, E. and Gros, P. (1991). Functional analysis of chimeric genes obtained by exchanging homologous domains of the mouse mdr1 and mdr2 genes. *Mol. Cell. Biol.* **11**(2): 595-603.

Campling, B. G., Young, L. C., Baer, K. A., Lam, Y. M., Deeley, R. G., Cole, S. P. and Gerlach, J. H. (1997). Expression of the MRP and MDR1 multidrug resistance genes in small cell lung cancer. *Clin Cancer Res.* **3**(1): 115-22.

Carrier, I., Julien, M. and Gros, P. (2003). Analysis of Catalytic Carboxylate Mutants E552Q and E1197Q Suggests Asymmetric ATP Hydrolysis by the Two Nucleotide-Binding Domains of P-Glycoprotein. *Biochemistry* **42**: 12875-85.

Carson, M. R., Travis, S. M. and Welsh, M. J. (1995). The two nucleotide-binding domains of cystic fibrosis transmembrane conductance regulator (CFTR) have distinct functions in controlling channel activity. *J Biol Chem.* **270**(4): 1711-7.

Chan, H. S., Haddad, G., Thorner, P. S., DeBoer, G., Lin, Y. P., Ondrusek, N., Yeger, H. and Ling, V. (1991). P-glycoprotein expression as a predictor of the outcome of therapy for neuroblastoma. *N Engl J Med.* **325**(23): 1608-14.

Chang, G. (2003). Structure of MsbA from Vibrio cholera: a multidrug resistance ABC transporter homolog in a closed conformation - retracted. *J. Mol. Biol.* **330**(2): 419-30.

Chang, G. and Roth, C. B. (2001). Structure of MsbA from E. coli: a homolog of the multidrug resistance ATP binding cassette (ABC) transporters. - Retracted. *Science* **293**(5536): 1793-800.

Chapuy, B., Koch, R., Radunski, U., Corsham, S., Cheong, N., Inagaki, N., Ban, N., Wenzel, D., Reinhardt, D., Zapf, A., *et al.* (2008). Intracellular ABC transporter A3 confers multidrug resistance in leukemia cells by lysosomal drug sequestration. *Leukemia* **8**: 8.

Chassaing, N., Martin, L., Calvas, P., Le Bert, M. and Hovnanian, A. (2005). Pseudoxanthoma elasticum: a clinical, pathophysiological and genetic update including 11 novel ABCC6 mutations. *J Med Genet.* **42**(12): 881-92. Epub 2005 May 13.

Chen, C. J., Chin, J. E., Ueda, K., Clark, D. P., Pastan, I., Gottesman, M. M. and Roninson, I. B. (1986). Internal duplication and homology with bacterial transport proteins in the mdr1 (P-glycoprotein) gene from multidrug-resistant human cells. *Cell* **47**(3): 381-9.

Chen, H. L., Gabrilovich, D., Tampe, R., Girgis, K. R., Nadaf, S. and Carbone, D. P. (1996). A functionally defective allele of TAP1 results in loss of MHC class I antigen presentation in a human lung cancer. *Nat Genet.* **13**(2): 210-3.

Chen, J., Lu, G., Lin, J., Davidson, A. L. and Quiocho, F. A. (2003). A tweezers-like motion of the ATP-binding cassette dimer in an ABC transport cycle. *Mol. Cell* **12**(3): 651-61.

Chen, J., Sharma, S., Quiocho, F. A. and Davidson, A. L. (2001). Trapping the transition state of an ATP-binding cassette transporter: evidence for a concerted mechanism of maltose transport. *Proc Natl Acad Sci U S A.* **98**(4): 1525-30. Epub 2001 Feb 6.

Chen, K. G., Szakacs, G., Annereau, J. P., Rouzaud, F., Liang, X. J., Valencia, J. C., Nagineni, C. N., Hooks, J. J., Hearing, V. J. and Gottesman, M. M. (2005). Principal expression of two mRNA isoforms (ABCB 5alpha and ABCB 5beta) of the ATP-binding cassette transporter gene ABCB 5 in melanoma cells and melanocytes. *Pigment Cell Res.* **18**(2): 102-12.

Chen, Z. Q., Dong, J., Ishimura, A., Daar, I., Hinnebusch, A. G. and Dean, M. (2006). The essential vertebrate ABCE1 protein interacts with eukaryotic initiation factors. *J Biol Chem.* **281**(11): 7452-7. Epub 2006 Jan 18.

Cheong, N., Madesh, M., Gonzales, L. W., Zhao, M., Yu, K., Ballard, P. L. and Shuman, H. (2006). Functional and trafficking defects in ATP binding cassette A3 mutants associated with respiratory distress syndrome. *J Biol Chem.* **281**(14): 9791-800. Epub 2006 Jan 16.

Childs, S., Yeh, R. L., Georges, E. and Ling, V. (1995). Identification of a sister gene to P-glycoprotein. *Cancer Res.* **55**(10): 2029-34.

Choi, K. H., Chen, C. J., Kriegler, M. and Roninson, L. B. (1988). An altered pattern of cross-resistance in multidrug-resistant human cells results from spontaneous mutations in the mdr1 (P-glycoprotein) gene. *Cell* **53**(4): 519-29.

Chutkow, W. A., Samuel, V., Hansen, P. A., Pu, J., Valdivia, C. R., Makielski, J. C. and Burant, C. F. (2001). Disruption of Sur2-containing K(ATP) channels enhances insulin-stimulated glucose uptake in skeletal muscle. *Proc Natl Acad Sci U S A.* **98**(20): 11760-4. Epub 2001 Sep 18.

Chutkow, W. A., Simon, M. C., Le Beau, M. M. and Burant, C. F. (1996). Cloning, tissue expression, and chromosomal localization of SUR2, the putative drug-binding subunit of cardiac, skeletal muscle, and vascular KATP channels. *Diabetes.* **45**(10): 1439-45.

Cideciyan, A. V., Aleman, T. S., Swider, M., Schwartz, S. B., Steinberg, J. D., Brucker, A. J., Maguire, A. M., Bennett, J., Stone, E. M. and Jacobson, S. G. (2004). Mutations in ABCA4 result in accumulation of lipofuscin before slowing of the retinoid cycle: a reappraisal of the human disease sequence. *Hum Mol Genet.* **13**(5): 525-34. Epub 2004 Jan 6.

Coelho, C. M., Kolevski, B., Bunn, C., Walker, C., Dahanukar, A. and Leevers, S. J. (2005). Growth and cell survival are unevenly impaired in pixie mutant wing discs. *Development.* **132**(24): 5411-24. Epub 2005 Nov 16.

Cole, S. P., Bhardwaj, G., Gerlach, J. H., Mackie, J. E., Grant, C. E., Almquist, K. C., Stewart, A. J., Kurz, E. U., Duncan, A. M. and Deeley, R. G. (1992). Overexpression of a transporter gene in a multidrug-resistant human lung cancer cell line. *Science.* **258**(5088): 1650-4.

Cole, S. P., Sparks, K. E., Fraser, K., Loe, D. W., Grant, C. E., Wilson, G. M. and Deeley, R. G. (1994). Pharmacological characterization of multidrug resistant MRP-transfected human tumor cells. *Cancer Res.* **54**(22): 5902-10.

Cornwell, M. M., Tsuruo, T., Gottesman, M. M. and Pastan, I. (1987). ATP-binding properties of P glycoprotein from multidrug-resistant KB cells. *FASEB J.* **1**(1): 51-4.

Cui, L., Hou, Y. X., Riordan, J. R. and Chang, X. B. (2001). Mutations of the Walker B motif in the first nucleotide binding domain of multidrug resistance protein MRP1 prevent conformational maturation. *Arch. Biochem. Biophys.* **392**(1): 153-61.

Dall'Acqua, W. and Carter, P. (2000). Substrate-assisted catalysis: molecular basis and biological significance. *Protein Sci.* **9**(1): 1-9.

Dalmas, O., Orelle, C., Foucher, A. E., Geourjon, C., Crouzy, S., Di Pietro, A. and Jault, J. M. (2005). The Q-loop disengages from the first intracellular loop during the catalytic cycle of the multidrug ABC transporter BmrA. *J. Biol. Chem.* **280**(44): 36857-64.

Dassa, E. and Bouige, P. (2001). The ABC of ABCS: a phylogenetic and functional classification of ABC systems in living organisms. *Res Microbiol.* **152**(3-4): 211-29.

Davidson, A. L. and Chen, J. (2004). ATP-binding cassette transporters in bacteria. *Annu Rev Biochem.* **73**: 241-68.

Davidson, A. L., Laghaeian, S. S. and Mannering, D. E. (1996). The maltose transport system of Escherichia coli displays positive cooperativity in ATP hydrolysis. *J Biol Chem.* **271**(9): 4858-63.

Davidson, A. L. and Maloney, P. C. (2007). ABC transporters: how small machines do a big job. *Trends Microbiol.* **15**(10): 448-55. Epub 2007 Oct 24.

Davidson, A. L. and Nikaido, H. (1990). Overproduction, solubilization, and reconstitution of the maltose transport system from Escherichia coli. *J Biol Chem.* **265**(8): 4254-60.

Davidson, A. L. and Sharma, S. (1997). Mutation of a single MalK subunit severely impairs maltose transport activity in Escherichia coli. *J Bacteriol.* **179**(17): 5458-64.

Dawson, R. J., Hollenstein, K. and Locher, K. P. (2007). Uptake or extrusion: crystal structures of full ABC transporters suggest a common mechanism. *Mol Microbiol.* **65**(2): 250-7. Epub 2007 Jun 18.

Dawson, R. J. and Locher, K. P. (2006). Structure of a bacterial multidrug ABC transporter. *Nature.* **443**(7108): 180-5.

Dawson, R. J. and Locher, K. P. (2007). Structure of the multidrug ABC transporter Sav1866 from Staphylococcus aureus in complex with AMP-PNP. *FEBS Lett.* **581**(5): 935-8. Epub 2007 Feb 7.

Dayan, G., Baubichon-Cortay, H., Jault, J. M., Cortay, J. C., Deleage, G. and Di Pietro, A. (1996). Recombinant N-terminal nucleotide-binding domain from mouse P-

glycoprotein. Overexpression, purification, and role of cysteine 430. *J Biol Chem.* **271**(20): 11652-8.

de la Salle, H., Hanau, D., Fricker, D., Urlacher, A., Kelly, A., Salamero, J., Powis, S. H., Donato, L., Bausinger, H., Laforet, M., *et al.* (1994). Homozygous human TAP peptide transporter mutation in HLA class I deficiency. *Science.* **265**(5169): 237-41.

de Vree, J. M., Jacquemin, E., Sturm, E., Cresteil, D., Bosma, P. J., Aten, J., Deleuze, J. F., Desrochers, M., Burdelski, M., Bernard, O., *et al.* (1998). Mutations in the MDR3 gene cause progressive familial intrahepatic cholestasis. *Proc Natl Acad Sci U S A.* **95**(1): 282-7.

Dean, D. A., Davidson, A. L. and Nikaido, H. (1989). Maltose transport in membrane vesicles of Escherichia coli is linked to ATP hydrolysis. *Proc Natl Acad Sci U S A.* **86**(23): 9134-8.

Dean, M. (2002). The Human ATP-Binding Cassette (ABC) Transporter Superfamily, Bethesda (MD): National Library of Medicine (US), NCBI. **2008:** 50.

Dean, M. and Allikmets, R. (2001). Complete characterization of the human ABC gene family. *J Bioenerg Biomembr.* **33**(6): 475-9.

Dean, M. and Annilo, T. (2005). Evolution of the ATP-binding cassette (ABC) transporter superfamily in vertebrates. *Annu. Rev. Genomics Hum. Gen.* **6**: 123-42.

Dean, M., Hamon, Y. and Chimini, G. (2001a). The human ATP-binding cassette (ABC) transporter superfamily. *J Lipid Res.* **42**(7): 1007-17.

Dean, M., Rzhetsky, A. and Allikmets, R. (2001b). The human ATP-binding cassette (ABC) transporter superfamily. *Genome Res.* **11**(7): 1156-66.

Dean, M., White, M. B., Amos, J., Gerrard, B., Stewart, C., Khaw, K. T. and Leppert, M. (1990). Multiple mutations in highly conserved residues are found in mildly affected cystic fibrosis patients. *Cell.* **61**(5): 863-70.

Decottignies, A. and Goffeau, A. (1997). Complete inventory of the yeast ABC proteins. *Nat Genet.* **15**(2): 137-45.

Deeley, R. G. and Cole, S. P. (2006). Substrate recognition and transport by multidrug resistance protein 1 (ABCC1). *FEBS Lett.* **580**(4): 1103-11.

Delepelaire, P. (1994). PrtD, the integral membrane ATP-binding cassette component of the Erwinia chrysanthemi metalloprotease secretion system, exhibits a secretion signal-regulated ATPase activity. *J Biol Chem.* **269**(45): 27952-7.

Deleuze, J. F., Jacquemin, E., Dubuisson, C., Cresteil, D., Dumont, M., Erlinger, S., Bernard, O. and Hadchouel, M. (1996). Defect of multidrug-resistance 3 gene expression in a subtype of progressive familial intrahepatic cholestasis. *Hepatology.* **23**(4): 904-8.

Demirel, O., Waibler, Z., Kalinke, U., Grunebach, F., Appel, S., Brossart, P., Hasilik, A., Tampe, R. and Abele, R. (2007). Identification of a lysosomal peptide transport system induced during dendritic cell development. *J Biol Chem.* **282**(52): 37836-43. Epub 2007 Oct 31.

Devine, S. E., Ling, V. and Melera, P. W. (1992). Amino acid substitutions in the sixth transmembrane domain of P-glycoprotein alter multidrug resistance. *Proc. Natl. Acad. Sci. U.S.A.* **89**(10): 4564-8.

Dey, S., Ramachandra, M., Pastan, I., Gottesman, M. M. and Ambudkar, S. V. (1997). Evidence for two nonidentical drug-interaction sites in the human P-glycoprotein. *Proc. Natl. Acad. Sci. U.S.A.* **94**(20): 10594-9.

Diederichs, K., Diez, J., Greller, G., Muller, C., Breed, J., Schnell, C., Vonrhein, C., Boos, W. and Welte, W. (2000). Crystal structure of MalK, the ATPase subunit of the trehalose/maltose ABC transporter of the archaeon *Thermococcus litoralis*. *EMBO J.* **19**(22): 5951-61.

Dietrich, C. G., Geier, A. and Oude Elferink, R. P. (2003). ABC of oral bioavailability: transporters as gatekeepers in the gut. *Gut.* **52**(12): 1788-95.

Dippel, R. and Boos, W. (2005). The maltodextrin system of Escherichia coli: metabolism and transport. *J Bacteriol.* **187**(24): 8322-31.

Dixon, P. H., Weerasekera, N., Linton, K. J., Donaldson, O., Chambers, J., Egginton, E., Weaver, J., Nelson-Piercy, C., de Swiet, M., Warnes, G., *et al.* (2000). Heterozygous MDR3 missense mutation associated with intrahepatic cholestasis of pregnancy: evidence for a defect in protein trafficking. *Human Mol. Gen.* **9**(8): 1209-17.

Doige, C. A. and Sharom, F. J. (1992). Transport properties of P-glycoprotein in plasma membrane vesicles from multidrug-resistant Chinese hamster ovary cells. *Biochim. Biophys. Acta* **1109**(2): 161-71.

Donato, L., de la Salle, H., Hanau, D., Tongio, M. M., Oswald, M., Vandevenne, A. and Geisert, J. (1995). Association of HLA class I antigen deficiency related to a TAP2 gene mutation with familial bronchiectasis. *J Pediatr.* **127**(6): 895-900.

Dong, J., Lai, R., Nielsen, K., Fekete, C. A., Qiu, H. and Hinnebusch, A. G. (2004). The essential ATP-binding cassette protein RLI1 functions in translation by promoting preinitiation complex assembly. *J Biol Chem.* **279**(40): 42157-68. Epub 2004 Jul 23.

Dorin, J. R., Dickinson, P., Emslie, E., Clarke, A. R., Dobbie, L., Hooper, M. L., Halford, S., Wainwright, B. J. and Porteous, D. J. (1992). Successful targeting of the mouse cystic fibrosis transmembrane conductance regulator gene in embryonal stem cells. *Transgenic Res.* **1**(2): 101-5.

Dou, C., Fortes, P. A. and Allison, W. S. (1998). The alpha 3(beta Y341W)3 gamma subcomplex of the F1-ATPase from the thermophilic Bacillus PS3 fails to dissociate ADP when MgATP is hydrolyzed at a single catalytic site and attains maximal velocity when three catalytic sites are saturated with MgATP. *Biochemistry.* **37**(47): 16757-64.

Doyle, L. A., Yang, W., Abruzzo, L. V., Krogmann, T., Gao, Y., Rishi, A. K. and Ross, D. D. (1998). A multidrug resistance transporter from human MCF-7 breast cancer cells. *Proc Natl Acad Sci U S A.* **95**(26): 15665-70.

Duan, X. and Quiocho, F. A. (2002). Structural evidence for a dominant role of nonpolar interactions in the binding of a transport/chemosensory receptor to its highly polar ligands. *Biochemistry.* **41**(3): 706-12.

Efferth, T. (2001). The human ATP-binding cassette transporter genes: from the bench to the bedside. *Curr Mol Med.* **1**(1): 45-65.

Endo, K., Maehara, Y., Ichiyoshi, Y., Kusumoto, T., Sakaguchi, Y., Ohno, S. and Sugimachi, K. (1996). Multidrug resistance-associated protein expression in clinical gastric carcinoma. *Cancer.* **77**(8 Suppl): 1681-7.

Estevez, A. M., Haile, S., Steinbuchel, M., Quijada, L. and Clayton, C. (2004). Effects of depletion and overexpression of the Trypanosoma brucei ribonuclease L inhibitor homologue. *Mol Biochem Parasitol.* **133**(1): 137-41.

Evseenko, D. A., Murthi, P., Paxton, J. W., Reid, G., Emerald, B. S., Mohankumar, K. M., Lobie, P. E., Brennecke, S. P., Kalionis, B. and Keelan, J. A. (2007). The ABC transporter BCRP/ABCG2 is a placental survival factor, and its expression is reduced in idiopathic human fetal growth restriction. *FASEB J.* **21**(13): 3592-605. Epub 2007 Jun 26.

Eytan, G. D., Regev, R. and Assaraf, Y. G. (1996). Functional reconstitution of P-glycoprotein reveals an apparent near stoichiometric drug transport to ATP hydrolysis. *J Biol Chem.* **271**(6): 3172-8.

Fellay, J., Marzolini, C., Meaden, E. R., Back, D. J., Buclin, T., Chave, J. P., Decosterd, L. A., Furrer, H., Opravil, M., Pantaleo, G., *et al.* (2002). Response to antiretroviral treatment in HIV-1-infected individuals with allelic variants of the multidrug resistance transporter 1: a pharmacogenetics study. *Lancet.* **359**(9300): 30-6.

Fersht, A. R. (1985). Enzyme Structure and Mechanism, W.H. Freeman & Company.

Fetsch, E. E. and Davidson, A. L. (2002). Vanadate-catalyzed photocleavage of the signature motif of an ATP-binding cassette (ABC) transporter. *Proc. Natl. Acad. Sci. U.S.A.* **99**(15): 9685-90.

Fisher, A. J., Smith, A. C., Thoden, J. B., Smith, R., Sutoh, K., Holden, H. M. and Rayment, I. (1995). X-ray structures of the myosin motor domain of Dictyostelium discoideum complexed with MgADP.BeFx and MgADP.AlF4. *Biochemistry* **34**(28): 8960-72.

Fitzgerald, M. L., Xavier, R., Haley, K. J., Welti, R., Goss, J. L., Brown, C. E., Zhuang, D. Z., Bell, S. A., Lu, N., McKee, M., *et al.* (2007). ABCA3 inactivation in mice causes respiratory failure, loss of pulmonary surfactant, and depletion of lung phosphatidylglycerol. *J Lipid Res.* **48**(3): 621-32. Epub 2006 Dec 1.

Flugge, U. I. and van Meer, G. (2006). ABC Transporters. *FEBS Lett.* **580**(4): 997.

Fojo, A., Akiyama, S., Gottesman, M. M. and Pastan, I. (1985). Reduced drug accumulation in multiply drug-resistant human KB carcinoma cell lines. *Cancer Res.* **45**(7): 3002-7.

Forss-Petter, S., Werner, H., Berger, J., Lassmann, H., Molzer, B., Schwab, M. H., Bernheimer, H., Zimmermann, F. and Nave, K. A. (1997). Targeted inactivation of the X-linked adrenoleukodystrophy gene in mice. *J Neurosci Res.* **50**(5): 829-43.

Frank, N. Y., Margaryan, A., Huang, Y., Schatton, T., Waaga-Gasser, A. M., Gasser, M., Sayegh, M. H., Sadee, W. and Frank, M. H. (2005). ABCB5-mediated doxorubicin transport and chemoresistance in human malignant melanoma. *Cancer Res.* **65**(10): 4320-33.

Frank, N. Y., Pendse, S. S., Lapchak, P. H., Margaryan, A., Shlain, D., Doeing, C., Sayegh, M. H. and Frank, M. H. (2003). Regulation of progenitor cell fusion by ABCB5 P-glycoprotein, a novel human ATP-binding cassette transporter. *J Biol Chem.* **278**(47): 47156-65. Epub 2003 Sep 7.

Frasch, W. D. (2000). The participation of metals in the mechanism of the F(1)-ATPase. *Biochim Biophys Acta.* **1458**(2-3): 310-25.

Fromm, M. F. (2000). P-glycoprotein: a defense mechanism limiting oral bioavailability and CNS accumulation of drugs. *International Journal of Clinical Pharmacology & Therapeutics* **38**(2): 69-74.

Gao, M., Cui, H. R., Loe, D. W., Grant, C. E., Almquist, K. C., Cole, S. P. and Deeley, R. G. (2000). Comparison of the functional characteristics of the nucleotide binding domains of multidrug resistance protein 1. *J. Biol. Chem.* **275**(17): 13098-108.

Gaudet, R. and Wiley, D. C. (2001). Structure of the ABC ATPase domain of human TAP1, the transporter associated with antigen processing. *EMBO J.* **20**(17): 4964-72.

Gerloff, T., Stieger, B., Hagenbuch, B., Madon, J., Landmann, L., Roth, J., Hofmann, A. F. and Meier, P. J. (1998). The sister of P-glycoprotein represents the canalicular bile salt export pump of mammalian liver. *J Biol Chem.* **273**(16): 10046-50.

Gietz, R. D., Schiestl, R. H., Willems, A. R. and Woods, R. A. (1995). Studies on the transformation of intact yeast cells by the LiAc/SS-DNA/PEG procedure. *Yeast* **11**(4): 355-60

Goodno, C. C. (1982). Myosin active-site trapping with vanadate ion. *Methods Enzymol.* **85 Pt B**: 116-23.

Gottesman, M. M. (2002). Mechanisms of cancer drug resistance. *Annu. Rev. Med.* **53**: 615-27.

Gottesman, M. M. and Ambudkar, S. V. (2001). Overview: ABC transporters and human disease. *J. Bioenerg. Biomembr.* **33**(6): 453-8.

Gottesman, M. M., Fojo, T. and Bates, S. E. (2002). Multidrug resistance in cancer: role of ATP-dependent transporters. *Nat. Rev. Cancer* **2**(1): 48-58.

Gottesman, M. M. and Ling, V. (2006). The molecular basis of multidrug resistance in cancer: the early years of P-glycoprotein research. *FEBS Lett.* **580**(4): 998-1009. Epub 2005 Dec 28.

Gottesman, M. M. and Pastan, I. (1993). Biochemistry of multidrug resistance mediated by the multidrug transporter. *Annu. Rev. Biochem.* **62**: 385-427.

Gottesman, M. M., Pastan, I. and Ambudkar, S. V. (1996). P-glycoprotein and multidrug resistance. *Curr. Op. Gen. Dev.* **6**(5): 610-7.

Gradia, S., Subramanian, D., Wilson, T., Acharya, S., Makhov, A., Griffith, J. and Fishel, R. (1999). hMSH2-hMSH6 forms a hydrolysis-independent sliding clamp on mismatched DNA. *Mol Cell.* **3**(2): 255-61.

Grant, C. E., Valdimarsson, G., Hipfner, D. R., Almquist, K. C., Cole, S. P. and Deeley, R. G. (1994). Overexpression of multidrug resistance-associated protein (MRP) increases resistance to natural product drugs. *Cancer Res.* **54**(2): 357-61.

Greenberger, L. M. (1993). Major photoaffinity drug labeling sites for iodoaryl azidoprazosin in P-glycoprotein are within, or immediately C-terminal to, transmembrane domains 6 and 12. *J Biol Chem.* **268**(15): 11417-25.

Gros, P., Croop, J. and Housman, D. (1986). Mammalian multidrug resistance gene: complete cDNA sequence indicates strong homology to bacterial transport proteins. *Cell* **47**(3): 371-80.

Gros, P. and Hanna, M. (1996). The P-glycoprotein family and multidrug resistance: An overview. Handbook of Biological Physics. Konings, W. N.*et al.* Amsterdam, Elsevier. **2:** 137-63.

Guan, L. and Kaback, H. R. (2006). Lessons from lactose permease. *Annu Rev Biophys Biomol Struct.* **35**: 67-91.

Hamada, H. and Tsuruo, T. (1988). Purification of the 170- to 180-kilodalton membrane glycoprotein associated with multidrug resistance. 170- to 180-kilodalton membrane glycoprotein is an ATPase. *J Biol Chem.* **263**(3): 1454-8.

Hanekop, N., Zaitseva, J., Jenewein, S., Holland, I. B. and Schmitt, L. (2006). Molecular insights into the mechanism of ATP-hydrolysis by the NBD of the ABC-transporter HlyB. *FEBS Lett.* **580**(4): 1036-41.

Hengel, H., Koopmann, J. O., Flohr, T., Muranyi, W., Goulmy, E., Hammerling, G. J., Koszinowski, U. H. and Momburg, F. (1997). A viral ER-resident glycoprotein inactivates the MHC-encoded peptide transporter. *Immunity.* **6**(5): 623-32.

Herrmann, C. (2003). Ras-effector interactions: after one decade. *Curr Opin Struct Biol.* **13**(1): 122-9.

Higgins, C. F., Hiles, I. D., Salmond, G. P., Gill, D. R., Downie, J. A., Evans, I. J., Holland, I. B., Gray, L., Buckel, S. D., Bell, A. W., *et al.* (1986). A family of related ATP-binding subunits coupled to many distinct biological processes in bacteria. *Nature.* **323**(6087): 448-50.

Higgins, C. F., Hyde, S. C., Mimmack, M. M., Gileadi, U., Gill, D. R. and Gallagher, M. P. (1990). Binding protein-dependent transport systems. *J Bioenerg Biomembr.* **22**(4): 571-92.

Higgins, C. F. and Linton, K. J. (2004). The ATP switch model for ABC transporters. *Nature Structural & Molecular Biology* **11**(10): 918-26.

Hirai, T., Heymann, J. A., Shi, D., Sarker, R., Maloney, P. C. and Subramaniam, S. (2002). Three-dimensional structure of a bacterial oxalate transporter. *Nat Struct Biol.* **9**(8): 597-600.

Holland, I. B. and Blight, M. A. (1999). ABC-ATPases, adaptable energy generators fuelling transmembrane movement of a variety of molecules in organisms from bacteria to humans. *J. Mol. Biol.* **293**(2): 381-99.

Holland, I. B., Cole, S. P., Kuchler, K. and Higgins, C. F., Eds. (2003). ABC Proteins: From Bacteria to Man, Academic Press.

Hollenstein, K., Dawson, R. J. and Locher, K. P. (2007a). Structure and mechanism of ABC transporter proteins. *Curr Opin Struct Biol* **25**: 25.

Hollenstein, K., Frei, D. C. and Locher, K. P. (2007b). Structure of an ABC transporter in complex with its binding protein. *Nature.* **446**(7132): 213-6. Epub 2007 Feb 25.

Holmes, J. A. and West, R. R. (1994). The effect of MDR-1 gene expression on outcome in acute myeloblastic leukaemia. *Br J Cancer.* **69**(2): 382-4.

Hopfner, K. P., Karcher, A., Shin, D. S., Craig, L., Arthur, L. M., Carney, J. P. and Tainer, J. A. (2000). Structural biology of Rad50 ATPase: ATP-driven conformational control in DNA double-strand break repair and the ABC-ATPase superfamily. *Cell* **101**(7): 789-800.

Horio, M., Gottesman, M. M. and Pastan, I. (1988). ATP-dependent transport of vinblastine in vesicles from human multidrug-resistant cells. *Proc. Natl. Acad. Sci. U.S.A.* **85**(10): 3580-4.

Hou, Y., Cui, L., Riordan, J. R. and Chang, X. (2000). Allosteric interactions between the two non-equivalent nucleotide binding domains of multidrug resistance protein MRP1. *J. Biol. Chem.* **275**(27): 20280-7.

Hou, Y. X., Cui, L., Riordan, J. R. and Chang, X. B. (2002). ATP binding to the first nucleotide-binding domain of multidrug resistance protein MRP1 increases binding and hydrolysis of ATP and trapping of ADP at the second domain. *J. Biol. Chem.* **277**(7): 5110-9.

Hrycyna, C. A., Ramachandra, M., Ambudkar, S. V., Ko, Y. H., Pedersen, P. L., Pastan, I. and Gottesman, M. M. (1998). Mechanism of action of human P-glycoprotein ATPase activity. Photochemical cleavage during a catalytic transition state using orthovanadate reveals cross-talk between the two ATP sites. *J. Biol. Chem.* **273**(27): 16631-4.

Hrycyna, C. A., Ramachandra, M., Germann, U. A., Cheng, P. W., Pastan, I. and Gottesman, M. M. (1999). Both ATP sites of human P-glycoprotein are essential but not symmetric. *Biochemistry* **38**(42): 13887-99.

Hsu, W. Y., Chen, J. Y., Lin, W. L. and Tsay, C. H. (1989). [Harlequin fetus--a case report]. *Zhonghua Yi Xue Za Zhi (Taipei).* **43**(1): 63-6.

Huang, C. K. and Pan, Q. (2007). Validation of cystic fibrosis mutation analysis using ABI 3130XL genetic analyzer. *Diagn Mol Pathol.* **16**(1): 57-9.

Hung, L. W., Wang, I. X., Nikaido, K., Liu, P. Q., Ames, G. F. and Kim, S. H. (1998). Crystal structure of the ATP-binding subunit of an ABC transporter. *Nature* **396**(6712): 703-7.

Hunke, S., Landmesser, H. and Schneider, E. (2000a). Novel missense mutations that affect the transport function of MalK, the ATP-binding-cassette subunit of the Salmonella enterica serovar typhimurium maltose transport system. *J Bacteriol.* **182**(5): 1432-6.

Hunke, S., Mourez, M., Jehanno, M., Dassa, E. and Schneider, E. (2000b). ATP modulates subunit-subunit interactions in an ATP-binding cassette transporter (MalFGK2) determined by site-directed chemical cross-linking. *J Biol Chem.* **275**(20): 15526-34.

Hvorup, R. N., Goetz, B. A., Niederer, M., Hollenstein, K., Perozo, E. and Locher, K. P. (2007). Asymmetry in the structure of the ABC transporter-binding protein complex BtuCD-BtuF. *Science.* **317**(5843): 1387-90. Epub 2007 Aug 2.

Hyde, S. C., Emsley, P., Hartshorn, M. J., Mimmack, M. M., Gileadi, U., Pearce, S. R., Gallagher, M. P., Gill, D. R., Hubbard, R. E. and Higgins, C. F. (1990). Structural model of ATP-binding proteins associated with cystic fibrosis, multidrug resistance and bacterial transport. *Nature* **346**(6282): 362-5.

Inagaki, N., Gonoi, T., Clement, J. P., Wang, C. Z., Aguilar-Bryan, L., Bryan, J. and Seino, S. (1996). A family of sulfonylurea receptors determines the pharmacological properties of ATP-sensitive K+ channels. *Neuron.* **16**(5): 1011-7.

Inagaki, N., Gonoi, T., Clement, J. P. t., Namba, N., Inazawa, J., Gonzalez, G., Aguilar-Bryan, L., Seino, S. and Bryan, J. (1995). Reconstitution of IKATP: an inward rectifier subunit plus the sulfonylurea receptor. *Science.* **270**(5239): 1166-70.

Ivetac, A., Campbell, J. D. and Sansom, M. S. (2007). Dynamics and Function in a Bacterial ABC Transporter: Simulation Studies of the BtuCDF System and Its Components. *Biochemistry.* **46**(10): 2767-78. Epub 007 Feb 16.

Jackson, D. G. and Capra, J. D. (1993). TAP1 alleles in insulin-dependent diabetes mellitus: a newly defined centromeric boundary of disease susceptibility. *Proc Natl Acad Sci U S A.* **90**(23): 11079-83.

Janas, E., Hofacker, M., Chen, M., Gompf, S., van der Does, C. and Tampe, R. (2003). The ATP hydrolysis cycle of the nucleotide-binding domain of the mitochondrial ATP-binding cassette transporter Mdl1p. *J Biol Chem.* **278**(29): 26862-9. Epub 2003 May 13.

Jardetzky, O. (1966). Simple allosteric model for membrane pumps. *Nature.* **211**(5052): 969-70.

Jedlitschky, G., Burchell, B. and Keppler, D. (2000). The multidrug resistance protein 5 functions as an ATP-dependent export pump for cyclic nucleotides. *J Biol Chem.* **275**(39): 30069-74.

Jeltsch, A., Alves, J., Wolfes, H., Maass, G. and Pingoud, A. (1993). Substrate-assisted catalysis in the cleavage of DNA by the EcoRI and EcoRV restriction enzymes. *Proc Natl Acad Sci U S A.* **90**(18): 8499-503.

Jiang, Q. and Uitto, J. (2006). Pseudoxanthoma elasticum: a metabolic disease? *J Invest Dermatol.* **126**(7): 1440-1.

Jones, K., Bray, P. G., Khoo, S. H., Davey, R. A., Meaden, E. R., Ward, S. A. and Back, D. J. (2001). P-Glycoprotein and transporter MRP1 reduce HIV protease inhibitor uptake in CD4 cells: potential for accelerated viral drug resistance? *AIDS* **15**(11): 1353-8.

Jones, P. M. and George, A. M. (1999). Subunit interactions in ABC transporters: towards a functional architecture. *FEMS Microbiol Lett.* **179**(2): 187-202.

Jones, P. M. and George, A. M. (2002). Mechanism of ABC transporters: a molecular dynamics simulation of a well characterized nucleotide-binding subunit. *Proc Natl Acad Sci U S A.* **99**(20): 12639-44. Epub 2002 Sep 17.

Jones, P. M. and George, A. M. (2004). The ABC transporter structure and mechanism: perspectives on recent research. *Cell Mol Life Sci.* **61**(6): 682-99.

Jonker, J. W., Buitelaar, M., Wagenaar, E., Van Der Valk, M. A., Scheffer, G. L., Scheper, R. J., Plosch, T., Kuipers, F., Elferink, R. P., Rosing, H., *et al.* (2002). The breast cancer resistance protein protects against a major chlorophyll-derived dietary phototoxin and protoporphyria. *Proc Natl Acad Sci U S A.* **99**(24): 15649-54. Epub 2002 Nov 12.

Jonker, J. W., Smit, J. W., Brinkhuis, R. F., Maliepaard, M., Beijnen, J. H., Schellens, J. H. and Schinkel, A. H. (2000). Role of breast cancer resistance protein in the bioavailability and fetal penetration of topotecan. *J Natl Cancer Inst.* **92**(20): 1651-6.

Juliano, R. L. and Ling, V. (1976). A surface glycoprotein modulating drug permeability in Chinese hamster ovary cell mutants. *Biochim Biophys Acta.* **455**(1): 152-62.

Julien, M. and Gros, P. (2000). Nucleotide-induced conformational changes in P-glycoprotein and in nucleotide binding site mutants monitored by trypsin sensitivity. *Biochemistry* **39**(15): 4559-68.

Kage, K., Tsukahara, S., Sugiyama, T., Asada, S., Ishikawa, E., Tsuruo, T. and Sugimoto, Y. (2002). Dominant-negative inhibition of breast cancer resistance protein as drug efflux pump through the inhibition of S-S dependent homodimerization. *Int J Cancer.* **97**(5): 626-30.

Kaminski, W. E., Orso, E., Diederich, W., Klucken, J., Drobnik, W. and Schmitz, G. (2000). Identification of a novel human sterol-sensitive ATP-binding cassette transporter (ABCA7). *Biochem Biophys Res Commun.* **273**(2): 532-8.

Kaminski, W. E., Piehler, A., Pullmann, K., Porsch-Ozcurumez, M., Duong, C., Bared, G. M., Buchler, C. and Schmitz, G. (2001). Complete coding sequence, promoter region, and genomic structure of the human ABCA2 gene and evidence for sterol-dependent regulation in macrophages. *Biochem Biophys Res Commun.* **281**(1): 249-58.

Kaminski, W. E., Piehler, A. and Wenzel, J. J. (2006). ABC A-subfamily transporters: structure, function and disease. *Biochim Biophys Acta.* **1762**(5): 510-24. Epub 2006 Feb 28.

Karcher, A., Buttner, K., Martens, B., Jansen, R. P. and Hopfner, K. P. (2005). X-ray structure of RLI, an essential twin cassette ABC ATPase involved in ribosome biogenesis and HIV capsid assembly. *Structure* **13**(4): 649-59.

Karcz, S. R., Galatis, D. and Cowman, A. F. (1993). Nucleotide binding properties of a P-glycoprotein homologue from Plasmodium falciparum. *Mol Biochem Parasitol.* **58**(2): 269-76.

Karpowich, N., Martsinkevich, O., Millen, L., Yuan, Y. R., Dai, P. L., MacVey, K., Thomas, P. J. and Hunt, J. F. (2001). Crystal structures of the MJ1267 ATP binding cassette reveal an induced-fit effect at the ATPase active site of an ABC transporter. *Structure* **9**(7): 571-86.

Kast, C., Canfield, V., Levenson, R. and Gros, P. (1995). Membrane topology of P-glycoprotein as determined by epitope insertion: transmembrane organization of the N-terminal domain of mdr3. *Biochemistry* **34**(13): 4402-11.

Kast, C., Canfield, V., Levenson, R. and Gros, P. (1996). Transmembrane organization of mouse P-glycoprotein determined by epitope insertion and immunofluorescence. *J. Biol. Chem.* **271**(16): 9240-8.

Kaur, P. (2002). Multidrug resistance: can different keys open the same lock? *Drug Resist Updat.* **5**(2): 61-4.

Kelly, L., Karchin, R. and Sali, A. (2007). Protein interactions and disease phenotypes in the ABC transporter superfamily. *Pac Symp Biocomput.*: 51-63.

Kennedy, M. A., Barrera, G. C., Nakamura, K., Baldan, A., Tarr, P., Fishbein, M. C., Frank, J., Francone, O. L. and Edwards, P. A. (2005). ABCG1 has a critical role in mediating cholesterol efflux to HDL and preventing cellular lipid accumulation. *Cell Metab.* **1**(2): 121-31.

Kerr, K. M., Sauna, Z. E. and Ambudkar, S. V. (2001). Correlation between steady-state ATP hydrolysis and vanadate-induced ADP trapping in Human P-glycoprotein. Evidence for ADP release as the rate-limiting step in the catalytic cycle and its modulation by substrates. *J Biol Chem.* **276**(12): 8657-64.

Kim, I. W., Peng, X. H., Sauna, Z. E., FitzGerald, P. C., Xia, D., Muller, M., Nandigama, K. and Ambudkar, S. V. (2006). The conserved tyrosine residues 401 and 1044 in ATP sites of human P-glycoprotein are critical for ATP binding and hydrolysis: evidence for a conserved subdomain, the A-loop in the ATP-binding cassette. *Biochemistry.* **45**(24): 7605-16.

Kim, W. S., Fitzgerald, M. L., Kang, K., Okuhira, K., Bell, S. A., Manning, J. J., Koehn, S. L., Lu, N., Moore, K. J. and Freeman, M. W. (2005). Abca7 null mice retain normal macrophage phosphatidylcholine and cholesterol efflux activity despite alterations in adipose mass and serum cholesterol levels. *J Biol Chem.* **280**(5): 3989-95. Epub 2004 Nov 17.

Kiuchi, Y., Suzuki, H., Hirohashi, T., Tyson, C. A. and Sugiyama, Y. (1998). cDNA cloning and inducible expression of human multidrug resistance associated protein 3 (MRP3). *FEBS Lett.* **433**(1-2): 149-52.

Klein, I., Sarkadi, B. and Varadi, A. (1999). An inventory of the human ABC proteins. *Biochim. Biophys. Acta* **1461**(2): 237-62.

Klement, J. F., Matsuzaki, Y., Jiang, Q. J., Terlizzi, J., Choi, H. Y., Fujimoto, N., Li, K., Pulkkinen, L., Birk, D. E., Sundberg, J. P., *et al.* (2005). Targeted ablation of the abcc6 gene results in ectopic mineralization of connective tissues. *Mol Cell Biol.* **25**(18): 8299-310.

Klett, E. L., Lu, K., Kosters, A., Vink, E., Lee, M. H., Altenburg, M., Shefer, S., Batta, A. K., Yu, H., Chen, J., *et al.* (2004). A mouse model of sitosterolemia: absence of Abcg8/sterolin-2 results in failure to secrete biliary cholesterol. *BMC Med.* **2**: 5.

Klucken, J., Buchler, C., Orso, E., Kaminski, W. E., Porsch-Ozcurumez, M., Liebisch, G., Kapinsky, M., Diederich, W., Drobnik, W., Dean, M., *et al.* (2000). ABCG1 (ABC8), the human homolog of the Drosophila white gene, is a regulator of macrophage cholesterol and phospholipid transport. *Proc Natl Acad Sci U S A.* **97**(2): 817-22.

Ko, Y. H. and Pedersen, P. L. (1998). Overexpression, purification, and function of first nucleotide-binding fold of cystic fibrosis transmembrane conductance regulator. *Methods Enzymol.* **292**: 675-86.

Koch, J., Guntrum, R., Heintke, S., Kyritsis, C. and Tampe, R. (2004). Functional dissection of the transmembrane domains of the transporter associated with antigen processing (TAP). *J Biol Chem.* **279**(11): 10142-7. Epub 2003 Dec 15.

Konig, J., Nies, A. T., Cui, Y., Leier, I. and Keppler, D. (1999). Conjugate export pumps of the multidrug resistance protein (MRP) family: localization, substrate specificity, and MRP2-mediated drug resistance. *Biochim Biophys Acta.* **1461**(2): 377-94.

Kool, M., de Haas, M., Scheffer, G. L., Scheper, R. J., van Eijk, M. J., Juijn, J. A., Baas, F. and Borst, P. (1997). Analysis of expression of cMOAT (MRP2), MRP3, MRP4, and MRP5, homologues of the multidrug resistance-associated protein gene (MRP1), in human cancer cell lines. *Cancer Res.* **57**(16): 3537-47.

Koronakis, E., Hughes, C., Milisav, I. and Koronakis, V. (1995). Protein exporter function and in vitro ATPase activity are correlated in ABC-domain mutants of HlyB. *Mol Microbiol.* **16**(1): 87-96.

Kranitz, L., Benabdelhak, H., Horn, C., Blight, M. A., Holland, I. B. and Schmitt, L. (2002). Crystallization and preliminary X-ray analysis of the ATP-binding domain of the ABC transporter haemolysin B from Escherichia coli. *Acta crystallogr D Biol Crystallogr* **58**(Pt 3): 539-41.

Kruh, G. D., Guo, Y., Hopper-Borge, E., Belinsky, M. G. and Chen, Z. S. (2007). ABCC10, ABCC11, and ABCC12. *Pflugers Arch.* **453**(5): 675-84. Epub 2006 Jul 26.

Kubo, Y., Sekiya, S., Ohigashi, M., Takenaka, C., Tamura, K., Nada, S., Nishi, T., Yamamoto, A. and Yamaguchi, A. (2005). ABCA5 resides in lysosomes, and ABCA5 knockout mice develop lysosomal disease-like symptoms. *Mol Cell Biol.* **25**(10): 4138-49.

Kuss, B. J., Deeley, R. G., Cole, S. P., Willman, C. L., Kopecky, K. J., Wolman, S. R., Eyre, H. J., Lane, S. A., Nancarrow, J. K., Whitmore, S. A., *et al.* (1994). Deletion of gene for multidrug resistance in acute myeloid leukaemia with inversion in chromosome 16: prognostic implications. *Lancet.* **343**(8912): 1531-4.

Kwan, T. (1998). Mutational analysis of the P-glycoprotein first intracellular loop and flanking transmembrane domains. *Biochemistry* **37**(10): 3337-50.

Kwan, T., Loughrey, H., Brault, M., Gruenheid, S., Urbatsch, I. L., Senior, A. E. and Gros, P. (2000). Functional analysis of a tryptophan-less P-glycoprotein: a tool for tryptophan insertion and fluorescence spectroscopy. *Mol. Pharmacol.* **58**(1): 37-47.

Laemmli, U. K. (1970). Cleavage of structural proteins during the assembly of the head of bacteriophage T4. *Nature* **227**(259): 680-5.

Lamers, M. H., Georgijevic, D., Lebbink, J. H., Winterwerp, H. H., Agianian, B., de Wind, N. and Sixma, T. K. (2004). ATP increases the affinity between MutS ATPase domains. Implications for ATP hydrolysis and conformational changes. *J Biol Chem.* **279**(42): 43879-85. Epub 2004 Aug 4.

Lamers, M. H., Winterwerp, H. H. and Sixma, T. K. (2003). The alternating ATPase domains of MutS control DNA mismatch repair. *EMBO J.* **22**(3): 746-56.

Langmann, T., Klucken, J., Reil, M., Liebisch, G., Luciani, M. F., Chimini, G., Kaminski, W. E. and Schmitz, G. (1999). Molecular cloning of the human ATP-binding cassette transporter 1 (hABC1): evidence for sterol-dependent regulation in macrophages. *Biochem Biophys Res Commun.* **257**(1): 29-33.

Lapinski, P. E., Neubig, R. R. and Raghavan, M. (2001). Walker A Lysine Mutations of TAP1 and TAP2 Interfere with Peptide Translocation but Not Peptide Binding. *J. Biol. Chem.* **276**(10): 7526-33.

Larsen, T. A., Olson, A. J. and Goodsell, D. S. (1998). Morphology of protein-protein interfaces. *Structure.* **6**(4): 421-7.

Lawn, R. M., Wade, D. P., Garvin, M. R., Wang, X., Schwartz, K., Porter, J. G., Seilhamer, J. J., Vaughan, A. M. and Oram, J. F. (1999). The Tangier disease gene product ABC1 controls the cellular apolipoprotein-mediated lipid removal pathway. *J Clin Invest.* **104**(8): R25-31.

Lawson, J., O'Mara, M. L. and Kerr, I. D. (2008). Structure-based interpretation of the mutagenesis database for the nucleotide binding domains of P-glycoprotein. *Biochim Biophys Acta* **1778**(2): 376-91.

Le Beau, M. M., Larson, R. A., Bitter, M. A., Vardiman, J. W., Golomb, H. M. and Rowley, J. D. (1983). Association of an inversion of chromosome 16 with abnormal marrow eosinophils in acute myelomonocytic leukemia. A unique cytogenetic-clinicopathological association. *N Engl J Med.* **309**(11): 630-6.

Lee, C. G., Gottesman, M. M., Cardarelli, C. O., Ramachandra, M., Jeang, K. T., Ambudkar, S. V., Pastan, I. and Dey, S. (1998). HIV-1 protease inhibitors are substrates for the MDR1 multidrug transporter. *Biochemistry* **37**(11): 3594-601.

Lefevre, C., Audebert, S., Jobard, F., Bouadjar, B., Lakhdar, H., Boughdene-Stambouli, O., Blanchet-Bardon, C., Heilig, R., Foglio, M., Weissenbach, J., *et al.* (2003). Mutations in the transporter ABCA12 are associated with lamellar ichthyosis type 2. *Hum Mol Genet.* **12**(18): 2369-78. Epub 003 Jul 15.

Leggas, M., Adachi, M., Scheffer, G. L., Sun, D., Wielinga, P., Du, G., Mercer, K. E., Zhuang, Y., Panetta, J. C., Johnston, B., *et al.* (2004). Mrp4 confers resistance to topotecan and protects the brain from chemotherapy. *Mol Cell Biol.* **24**(17): 7612-21.

Lehner, P. J., Karttunen, J. T., Wilkinson, G. W. and Cresswell, P. (1997). The human cytomegalovirus US6 glycoprotein inhibits transporter associated with antigen processing-dependent peptide translocation. *Proc Natl Acad Sci U S A.* **94**(13): 6904-9.

Lerner-Marmarosh, N., Gimi, K., Urbatsch, I. L., Gros, P. and Senior, A. E. (1999). Large scale purification of detergent-soluble P-glycoprotein from Pichia pastoris cells and characterization of nucleotide binding properties of wild-type, Walker A, and Walker B mutant proteins. *J. Biol. Chem.* **274**(49): 34711-8.

Lewis, H. A., Buchanan, S. G., Burley, S. K., Conners, K., Dickey, M., Dorwart, M., Fowler, R., Gao, X., Guggino, W. B., Hendrickson, W. A., *et al.* (2004). Structure of nucleotide-binding domain 1 of the cystic fibrosis transmembrane conductance regulator. *EMBO J* **23**(2): 282-93.

Ling, V. and Thompson, L. H. (1974). Reduced permeability in CHO cells as a mechanism of resistance to colchicine. *J Cell Physiol.* **83**(1): 103-16.

Linton, K. J. (2007). Structure and Function of ABC Transporters. *Physiology (Bethesda).* **22**: 122-30.

Linton, K. J. and Higgins, C. F. (1998). The Escherichia coli ATP-binding cassette (ABC) proteins. [see comments.]. *Mol. Microbiol.* **28**(1): 5-13.

Linton, K. J. and Higgins, C. F. (2007). Structure and function of ABC transporters: the ATP switch provides flexible control. *Pflugers Arch* **453**(5): 555-67.

Litman, T., Brangi, M., Hudson, E., Fetsch, P., Abati, A., Ross, D. D., Miyake, K., Resau, J. H. and Bates, S. E. (2000). The multidrug-resistant phenotype associated with overexpression of the new ABC half-transporter, MXR (ABCG2). *J. Cell Sci.* **113**(Pt 11): 2011-21.

Liu, C. E. and Ames, G. F. (1997). Characterization of transport through the periplasmic histidine permease using proteoliposomes reconstituted by dialysis. *J Biol Chem.* **272**(2): 859-66.

Liu, C. E., Liu, P. Q. and Ames, G. F. (1997). Characterization of the adenosine triphosphatase activity of the periplasmic histidine permease, a traffic ATPase (ABC transporter). *J Biol Chem.* **272**(35): 21883-91.

Liu, P. Q. (1998). In vitro disassembly and reassembly of an ABC transporter, the histidine permease. *Proc. Natl. Acad. Sci. U.S.A.* **95**(7): 3495-500.

Liu, R. and Sharom, F. J. (1996). Site-directed fluorescence labeling of P-glycoprotein on cysteine residues in the nucleotide binding domains. *Biochemistry.* **35**(36): 11865-73.

Liu, R. and Sharom, F. J. (1997). Fluorescence studies on the nucleotide binding domains of the P-glycoprotein multidrug transporter. *Biochemistry.* **36**(10): 2836-43.

Locher, K. P., Lee, A. T. and Rees, D. C. (2002). The E. coli BtuCD structure: a framework for ABC transporter architecture and mechanism. *Science* **296**(5570): 1091-8.

Loe, D. W., Deeley, R. G. and Cole, S. P. (1996). Biology of the multidrug resistance-associated protein, MRP. *Eur J Cancer.* **32A**(6): 945-57.

Loo, T. W. and Clarke, D. M. (1994). Reconstitution of drug-stimulated ATPase activity following co-expression of each half of human P-glycoprotein as separate polypeptides. *J. Biol. Chem.* **269**(10): 7750-5.

Loo, T. W. and Clarke, D. M. (1995a). Covalent modification of human P-glycoprotein mutants containing a single cysteine in either nucleotide-binding fold abolishes drug-stimulated ATPase activity. *J. Biol. Chem.* **270**(39): 22957-61.

Loo, T. W. and Clarke, D. M. (1995b). Membrane topology of a cysteine-less mutant of human P-glycoprotein. *J. Biol. Chem.* **270**(2): 843-8.

Loo, T. W. and Clarke, D. M. (1995c). Rapid purification of human P-glycoprotein mutants expressed transiently in HEK 293 cells by nickel-chelate chromatography and characterization of their drug-stimulated ATPase activities. *J. Biol. Chem.* **270**(37): 21449-52.

Loo, T. W. and Clarke, D. M. (1999a). Determining the structure and mechanism of the human multidrug resistance P-glycoprotein using cysteine-scanning mutagenesis and thiol-modification techniques. *Biochim. Biophys. Acta* **1461**(2): 315-25.

Loo, T. W. and Clarke, D. M. (1999b). Identification of residues in the drug-binding domain of human P-glycoprotein. Analysis of transmembrane segment 11 by cysteine-scanning mutagenesis and inhibition by dibromobimane. *J. Biol. Chem.* **274**(50): 35388-92.

Loo, T. W. and Clarke, D. M. (1999c). Merck Frosst Award Lecture 1998. Molecular dissection of the human multidrug resistance P-glycoprotein. *Biochem. Cell Biol.* **77**(1): 11-23.

Loo, T. W. and Clarke, D. M. (2005). Recent progress in understanding the mechanism of P-glycoprotein-mediated drug efflux. *J Membr Biol.* **206**(3): 173-85.

Lorico, A., Rappa, G., Finch, R. A., Yang, D., Flavell, R. A. and Sartorelli, A. C. (1997). Disruption of the murine MRP (multidrug resistance protein) gene leads to increased sensitivity to etoposide (VP-16) and increased levels of glutathione. *Cancer Res.* **57**(23): 5238-42.

Lu, G., Westbrooks, J. M., Davidson, A. L. and Chen, J. (2005). ATP hydrolysis is required to reset the ATP-binding cassette dimer into the resting-state conformation. *Proc. Natl. Acad. Sci. U.S.A.* **102**(50): 17969-74.

Luciani, M. F. and Chimini, G. (1996). The ATP binding cassette transporter ABC1, is required for the engulfment of corpses generated by apoptotic cell death. *EMBO J.* **15**(2): 226-35.

Mack, J. T., Beljanski, V., Soulika, A. M., Townsend, D. M., Brown, C. B., Davis, W. and Tew, K. D. (2007). "Skittish" Abca2 knockout mice display tremor, hyperactivity, and abnormal myelin ultrastructure in the central nervous system. *Mol Cell Biol.* **27**(1): 44-53. Epub 2006 Oct 23.

Maliepaard, M., Scheffer, G. L., Faneyte, I. F., van Gastelen, M. A., Pijnenborg, A. C., Schinkel, A. H., van De Vijver, M. J., Scheper, R. J. and Schellens, J. H. (2001). Subcellular localization and distribution of the breast cancer resistance protein transporter in normal human tissues. *Cancer Res.* **61**(8): 3458-64.

Mannering, D. E., Sharma, S. and Davidson, A. L. (2001). Demonstration of conformational changes associated with activation of the maltose transport complex. *J Biol Chem.* **276**(15): 12362-8.

Mao, L., Wang, Y., Liu, Y. and Hu, X. (2004). Molecular Determinants for ATP-binding in Proteins: A Data Mining and Quantum Chemical Analysis. *J. Mol. Biol.* **336**: 787-807.

Marcil, M., Brooks-Wilson, A., Clee, S. M., Roomp, K., Zhang, L. H., Yu, L., Collins, J. A., van Dam, M., Molhuizen, H. O., Loubster, O., *et al.* (1999). Mutations in the ABC1 gene in familial HDL deficiency with defective cholesterol efflux. *Lancet.* **354**(9187): 1341-6.

Martinez-Mir, A., Bayes, M., Vilageliu, L., Grinberg, D., Ayuso, C., del Rio, T., Garcia-Sandoval, B., Bussaglia, E., Baiget, M., Gonzalez-Duarte, R., *et al.* (1997). A new locus for autosomal recessive retinitis pigmentosa (RP19) maps to 1p13-1p21. *Genomics.* **40**(1): 142-6.

Marton, M. J., Vazquez de Aldana, C. R., Qiu, H., Chakraburtty, K. and Hinnebusch, A. G. (1997). Evidence that GCN1 and GCN20, translational regulators of GCN4, function on elongating ribosomes in activation of eIF2alpha kinase GCN2. *Mol Cell Biol.* **17**(8): 4474-89.

Matsumura, Y., Sakai, H., Sasaki, M., Ban, N. and Inagaki, N. (2007). ABCA3-mediated choline-phospholipids uptake into intracellular vesicles in A549 cells. *FEBS Lett.* **581**(17): 3139-44. Epub 2007 Jun 6.

Matsuzaki, Y., Nakano, A., Jiang, Q. J., Pulkkinen, L. and Uitto, J. (2005). Tissue-specific expression of the ABCC6 gene. *J Invest Dermatol.* **125**(5): 900-5.

Mayer, R., Kartenbeck, J., Buchler, M., Jedlitschky, G., Leier, I. and Keppler, D. (1995). Expression of the MRP gene-encoded conjugate export pump in liver and its selective absence from the canalicular membrane in transport-deficient mutant hepatocytes. *J Cell Biol.* **131**(1): 137-50.

McNeish, J., Aiello, R. J., Guyot, D., Turi, T., Gabel, C., Aldinger, C., Hoppe, K. L., Roach, M. L., Royer, L. J., de Wet, J., *et al.* (2000). High density lipoprotein deficiency and foam cell accumulation in mice with targeted disruption of ATP-binding cassette transporter-1. *Proc Natl Acad Sci U S A.* **97**(8): 4245-50.

Michaelis, S. and Berkower, C. (1995). Sequence comparison of yeast ATP-binding cassette proteins. *Cold Spring Harb Symp Quant Biol.* **60**: 291-307.

Mildvan, A. S. (1997). Mechanisms of signaling and related enzymes. *Proteins.* **29**(4): 401-16.

Mimura, C. S., Holbrook, S. R. and Ames, G. F. (1991). Structural model of the nucleotide-binding conserved component of periplasmic permeases. *Proc Natl Acad Sci U S A.* **88**(1): 84-8.

Mitchell, P. (1957). A general theory of membrane transport from studies of bacteria. *Nature.* **180**(4577): 134-6.

Miyake, K., Mickley, L., Litman, T., Zhan, Z., Robey, R., Cristensen, B., Brangi, M., Greenberger, L., Dean, M., Fojo, T., *et al.* (1999). Molecular cloning of cDNAs which are highly overexpressed in mitoxantrone-resistant cells: demonstration of homology to ABC transport genes. *Cancer Res.* **59**(1): 8-13.

Moins-Teisserenc, H., Semana, G., Alizadeh, M., Loiseau, P., Bobrynina, V., Deschamps, I., Edan, G., Birebent, B., Genetet, B., Sabouraud, O., *et al.* (1995). TAP2 gene polymorphism contributes to genetic susceptibility to multiple sclerosis. *Hum Immunol.* **42**(3): 195-202.

Molday, L. L., Rabin, A. R. and Molday, R. S. (2000). ABCR expression in foveal cone photoreceptors and its role in Stargardt macular dystrophy. *Nat Genet.* **25**(3): 257-8.

Moody, J. E., Millen, L., Binns, D., Hunt, J. F. and Thomas, P. J. (2002). Cooperative, ATP-dependent association of the nucleotide binding cassettes during the catalytic cycle of ATP-binding cassette transporters. *J. Biol. Chem.* **277**(24): 21111-4.

Morbach, S., Tebbe, S. and Schneider, E. (1993). The ATP-binding cassette (ABC) transporter for maltose/maltodextrins of Salmonella typhimurium. Characterization of the ATPase activity associated with the purified MalK subunit. *J Biol Chem.* **268**(25): 18617-21.

Mosser, J., Douar, A. M., Sarde, C. O., Kioschis, P., Feil, R., Moser, H., Poustka, A. M., Mandel, J. L. and Aubourg, P. (1993). Putative X-linked adrenoleukodystrophy gene shares unexpected homology with ABC transporters. *Nature.* **361**(6414): 726-30.

Muir, M., Williams, L. and Ferenci, T. (1985). Influence of transport energization on the growth yield of Escherichia coli. *J Bacteriol.* **163**(3): 1237-42.

Muller, M., Bakos, E., Welker, E., Varadi, A., Germann, U. A., Gottesman, M. M., Morse, B. S., Roninson, I. B. and Sarkadi, B. (1996). Altered drug-stimulated ATPase activity in mutants of the human multidrug resistance protein. *J. Biol. Chem.* **271**(4): 1877-83.

Nadanaciva, S., Weber, J. and Senior, A. E. (1999a). Binding of the transition state analog MgADP-fluoroaluminate to F1-ATPase. *J. Biol. Chem.* **274**(11): 7052-8.

Nadanaciva, S., Weber, J. and Senior, A. E. (1999b). The role of beta-Arg-182, an essential catalytic site residue in Escherichia coli F1-ATPase. *Biochemistry* **38**(24): 7670-7.

Nagata, K., Nishitani, M., Matsuo, M., Kioka, N., Amachi, T. and Ueda, K. (2000). Nonequivalent nucleotide trapping in the two nucleotide binding folds of the human multidrug resistance protein MRP1. *J. Biol. Chem.* **275**(23): 17626-30.

Nagata, K., Yamamoto, A., Ban, N., Tanaka, A. R., Matsuo, M., Kioka, N., Inagaki, N. and Ueda, K. (2004). Human ABCA3, a product of a responsible gene for abca3 for fatal surfactant deficiency in newborns, exhibits unique ATP hydrolysis activity and generates intracellular multilamellar vesicles. *Biochem Biophys Res Commun.* **324**(1): 262-8.

Nayak, S. and Bryant, F. R. (1999). Differential rates of NTP hydrolysis by the mutant [S69G]RecA protein. Evidence for a coupling of NTP turnover to DNA strand exchange. *J Biol Chem.* **274**(37): 25979-82.

Nelson, B. D. and Traxler, B. (1998). Exploring the role of integral membrane proteins in ATP-binding cassette transporters: analysis of a collection of MalG insertion mutants. *J Bacteriol.* **180**(9): 2507-14.

Nikaido, K. (1997). Purification and characterization of HisP, the ATP-binding subunit of a traffic ATPase (ABC transporter), the histidine permease of Salmonella typhimurium. Solubility, dimerization, and ATPase activity. *J. Biol. Chem.* **272**(44): 27745-52.

Nikaido, K. and Ames, G. F. (1999). One intact ATP-binding subunit is sufficient to support ATP hydrolysis and translocation in an ABC transporter, the histidine permease. *J. Biol. Chem.* **274**(38): 26727-35.

Norris, M. D., Bordow, S. B., Marshall, G. M., Haber, P. S., Cohn, S. L. and Haber, M. (1996). Expression of the gene for multidrug-resistance-associated protein and outcome in patients with neuroblastoma. *N Engl J Med.* **334**(4): 231-8.

Obmolova, G., Ban, C., Hsieh, P. and Yang, W. (2000). Crystal structures of mismatch repair protein MutS and its complex with a substrate DNA. *Nature.* **407**(6805): 703-10.

Oldham, M. L., Khare, D., Quiocho, F. A., Davidson, A. L. and Chen, J. (2007). Crystal structure of a catalytic intermediate of the maltose transporter. *Nature.* **450**(7169): 515-21.

Oloo, E. O., Fung, E. Y. and Tieleman, D. P. (2006). The dynamics of the MgATP-driven closure of MalK, the energy-transducing subunit of the maltose ABC transporter. *J Biol Chem.* **281**(38): 28397-407.

Omote, H. and al-Shawi, M. K. (2002). A novel electron paramagnetic resonance approach to determine the mechanism of drug transport by P-glycoprotein. *J. Biol. Chem.* **277**(47): 45688-94.

Omote, H., Figler, R. A., Polar, M. K. and Al-Shawi, M. K. (2004). Improved energy coupling of human P-glycoprotein by the glycine 185 to valine mutation. *Biochemistry* **43**(13): 3917-28.

Orelle, C., Dalmas, O., Gros, P., Di Pietro, A. and Jault, J. M. (2003). The conserved glutamate residue adjacent to the Walker-B motif is the catalytic base for ATP hydrolysis in the ATP-binding cassette transporter BmrA. *J Biol Chem.* **278**(47): 47002-8. Epub 2003 Sep 10.

Orso, E., Broccardo, C., Kaminski, W. E., Bottcher, A., Liebisch, G., Drobnik, W., Gotz, A., Chambenoit, O., Diederich, W., Langmann, T., *et al.* (2000). Transport of lipids from golgi to plasma membrane is defective in tangier disease patients and Abc1-deficient mice. *Nat Genet.* **24**(2): 192-6.

Oswald, C., Holland, I. B. and Schmitt, L. (2006). The motor domains of ABC-transporters / What can structures tell us? *Naunyn-Schmiedeberg's Archives of Pharmacology* **372**(6): 385-99. Epub 2006 Mar 16.

Panagiotidis, C. H., Reyes, M., Sievertsen, A., Boos, W. and Shuman, H. A. (1993). Characterization of the structural requirements for assembly and nucleotide binding of an ATP-binding cassette transporter. The maltose transport system of Escherichia coli. *J Biol Chem.* **268**(31): 23685-96.

Patzlaff, J. S., van der Heide, T. and Poolman, B. (2003). The ATP/substrate stoichiometry of the ATP-binding cassette (ABC) transporter OpuA. *J Biol Chem.* **278**(32): 29546-51. Epub 2003 May 23.

Paulusma, C. C., Bosma, P. J., Zaman, G. J., Bakker, C. T., Otter, M., Scheffer, G. L., Scheper, R. J., Borst, P. and Oude Elferink, R. P. (1996). Congenital jaundice in rats with a mutation in a multidrug resistance-associated protein gene. *Science.* **271**(5252): 1126-8.

Paulusma, C. C. and Oude Elferink, R. P. (1997). The canalicular multispecific organic anion transporter and conjugated hyperbilirubinemia in rat and man. *J Mol Med.* **75**(6): 420-8.

Pavelka, M. S., Jr., Hayes, S. F. and Silver, R. P. (1994). Characterization of KpsT, the ATP-binding component of the ABC-transporter involved with the export of capsular polysialic acid in Escherichia coli K1. *J Biol Chem.* **269**(31): 20149-58.

Paytubi, S., Morrice, N. A., Boudeau, J. and Proud, C. G. (2008). The N-terminal region of ABC50 interacts with eukaryotic initiation factor eIF2 and is a target for regulatory phosphorylation by CK2. *Biochem J.* **409**(1): 223-31.

Petronilli, V. and Ames, G. F. (1991). Binding protein-independent histidine permease mutants. Uncoupling of ATP hydrolysis from transmembrane signaling. *J Biol Chem.* **266**(25): 16293-6.

Pinkett, H. W., Lee, A. T., Lum, P., Locher, K. P. and Rees, D. C. (2007). An inward-facing conformation of a putative metal-chelate-type ABC transporter. *Science* **315**(5810): 373-7.

Plosch, T., Bloks, V. W., Terasawa, Y., Berdy, S., Siegler, K., Van Der Sluijs, F., Kema, I. P., Groen, A. K., Shan, B., Kuipers, F., *et al.* (2004). Sitosterolemia in ABC-transporter G5-deficient mice is aggravated on activation of the liver-X receptor. *Gastroenterology.* **126**(1): 290-300.

Plosch, T., Kosters, A., Groen, A. K. and Kuipers, F. (2005). The ABC of hepatic and intestinal cholesterol transport. *Handbook of Experimental Pharmacology*(170): 465-82.

Pondarre, C., Campagna, D. R., Antiochos, B., Sikorski, L., Mulhern, H. and Fleming, M. D. (2007). Abcb7, the gene responsible for X-linked sideroblastic anemia with ataxia, is essential for hematopoiesis. *Blood.* **109**(8): 3567-9. Epub 2006 Dec 27.

Powe Jr., A. C., Al-Nakkash, L., Lin, M. and Hwang, T.-C. (2002). Mutation of walker-a lysine 464 in cystic fibrosis transmembrane conductance regulator reveals functional interaction between its nucleotide-binding domains. *J. Physiol.* **539.2**: 333-46.

Powis, S. H., Mockridge, I., Kelly, A., Kerr, L. A., Glynne, R., Gileadi, U., Beck, S. and Trowsdale, J. (1992). Polymorphism in a second ABC transporter gene located within the class II region of the human major histocompatibility complex. *Proc Natl Acad Sci U S A.* **89**(4): 1463-7.

Prades, C., Arnould, I., Annilo, T., Shulenin, S., Chen, Z. Q., Orosco, L., Triunfol, M., Devaud, C., Maintoux-Larois, C., Lafargue, C., *et al.* (2002). The human ATP binding cassette gene ABCA13, located on chromosome 7p12.3, encodes a 5058 amino acid protein with an extracellular domain encoded in part by a 4.8-kb conserved exon. *Cytogenet Genome Res.* **98**(2-3): 160-8.

Procko, E., Raghuraman, G., Wiley, D. C., Raghavan, M. and Gaudet, R. (2005). Identification of domain boundaries within the N-termini of TAP1 and TAP2 and their importance in tapasin binding and tapasin-mediated increase in peptide loading of MHC class I. *Immunol Cell Biol.* **83**(5): 475-82.

Proff, C. and Kolling, R. (2001). Functional asymmetry of the two nucleotide binding domains in the ABC transporter Ste6. *Mol Gen Genet.* **264**(6): 883-93.

Pujol, A., Ferrer, I., Camps, C., Metzger, E., Hindelang, C., Callizot, N., Ruiz, M., Pampols, T., Giros, M. and Mandel, J. L. (2004). Functional overlap between ABCD1 (ALD) and ABCD2 (ALDR) transporters: a therapeutic target for X-adrenoleukodystrophy. *Hum Mol Genet.* **13**(23): 2997-3006. Epub 2004 Oct 15.

Quinton, P. M. (2007). Too much salt, too little soda: cystic fibrosis. *Sheng Li Xue Bao* **59**(4): 397-415.

Ramachandra, M., Ambudkar, S. V., Chen, D., Hrycyna, C. A., Dey, S., Gottesman, M. M. and Pastan, I. (1998). Human P-glycoprotein exhibits reduced affinity for substrates during a catalytic transition state. *Biochemistry* **37**(14): 5010-9.

Ramakrishnan, C., Dani, V. S. and Ramasarma, T. (2002). A conformational analysis of Walker motif A [GXXXXGKT (S)] in nucleotide-binding and other proteins. *Protein Eng.* **15**(10): 783-98.

Rao, U. S. (1995). Mutation of glycine 185 to valine alters the ATPase function of the human P-glycoprotein expressed in Sf9 cells. *J Biol Chem.* **270**(12): 6686-90.

Raymond, M., Gros, P., Whiteway, M. and Thomas, D. Y. (1992). Functional complementation of yeast ste6 by a mammalian multidrug resistance mdr gene. *Science* **256**(5054): 232-4.

Raymond, M., Ruetz, S., Thomas, D. Y. and Gros, P. (1994). Functional expression of P-glycoprotein in Saccharomyces cerevisiae confers cellular resistance to the immunosuppressive and antifungal agent FK520. *Mol. Cell. Biol.* **14**(1): 277-86.

Rea, P. A. (2007). Plant ATP-binding cassette transporters. *Annu Rev Plant Biol.* **58**: 347-75.

Reyes, C. L. and Chang, G. (2005). Structure of the ABC transporter MsbA in complex with ADP.vanadate and lipopolysaccharide. *Science.* **308**(5724): 1028-31.

Riordan, J. R., Rommens, J. M., Kerem, B., Alon, N., Rozmahel, R., Grzelczak, Z., Zielenski, J., Lok, S., Plavsic, N., Chou, J. L., *et al.* (1989). Identification of the cystic fibrosis gene: cloning and characterization of complementary DNA. *Science.* **245**(4922): 1066-73.

Ritter, C. A., Jedlitschky, G., Meyer zu Schwabedissen, H., Grube, M., Kock, K. and Kroemer, H. K. (2005). Cellular export of drugs and signaling molecules by the ATP-binding cassette transporters MRP4 (ABCC4) and MRP5 (ABCC5). *Drug Metab Rev.* **37**(1): 253-78.

Robbiani, D. F., Finch, R. A., Jager, D., Muller, W. A., Sartorelli, A. C. and Randolph, G. J. (2000). The leukotriene C(4) transporter MRP1 regulates CCL19 (MIP-3beta, ELC)-dependent mobilization of dendritic cells to lymph nodes. *Cell.* **103**(5): 757-68.

Rost, B. (1996). PHD: predicting one-dimensional protein structure by profile-based neural networks. *Methods Enzymol.* **266**: 525-39.

Rost, B. and Sander, C. (1993). Prediction of protein secondary structure at better than 70% accuracy. *J Mol Biol.* **232**(2): 584-99.

Rost, B. and Sander, C. (1994). Combining evolutionary information and neural networks to predict protein secondary structure. *Proteins.* **19**(1): 55-72.

Rozet, J. M., Gerber, S., Souied, E., Perrault, I., Chatelin, S., Ghazi, I., Leowski, C., Dufier, J. L., Munnich, A. and Kaplan, J. (1998). Spectrum of ABCR gene mutations in autosomal recessive macular dystrophies. *Eur J Hum Genet.* **6**(3): 291-5.

Ruetz, S. and Gros, P. (1994). Phosphatidylcholine translocase: a physiological role for the mdr2 gene. *Cell* **77**(7): 1071-81.

Russel, F. G., Koenderink, J. B. and Masereeuw, R. (2008). Multidrug resistance protein 4 (MRP4/ABCC4): a versatile efflux transporter for drugs and signalling molecules. *Trends Pharmacol Sci.* **29**(4): 200-7. Epub 2008 Mar 18.

Safa, A. R. (1993). Photoaffinity labeling of P-glycoprotein in multidrug-resistant cells. *Cancer Invest.* **11**(1): 46-56.

Sanchez-Fernandez, R., Rea, P. A., Davies, T. G. and Coleman, J. O. (2001). Do plants have more genes than humans? Yes, when it comes to ABC proteins. *Trends Plant Sci.* **6**(8): 347-8.

Sankaran, B., Bhagat, S. and Senior, A. E. (1997a). Inhibition of P-glycoprotein ATPase activity by beryllium fluoride. *Biochemistry* **36**(22): 6847-53.

Sankaran, B., Bhagat, S. and Senior, A. E. (1997b). Inhibition of P-glycoprotein ATPase activity by procedures involving trapping of nucleotide in catalytic sites. *Arch. Biochem. Biophys.* **341**(1): 160-9.

Sankaran, B., Bhagat, S. and Senior, A. E. (1997c). Photoaffinity labelling of P-glycoprotein catalytic sites. *FEBS Lett.* **417**(1): 119-22.

Saraste, M., Sibbald, P. R. and Wittinghofer, A. (1990). The P-loop--a common motif in ATP- and GTP-binding proteins. *Trends Biochem Sci.* **15**(11): 430-4.

Sarkadi, B., Price, E. M., Boucher, R. C., Germann, U. A. and Scarborough, G. A. (1992). Expression of the human multidrug resistance cDNA in insect cells generates a high activity drug-stimulated membrane ATPase. *J. Biol. Chem.* **267**(7): 4854-8.

Sauerbrey, A., Zintl, F. and Volm, M. (1994). P-glycoprotein and glutathione S-transferase pi in childhood acute lymphoblastic leukaemia. *Br J Cancer.* **70**(6): 1144-9.

Sauna, Z. E. and Ambudkar, S. V. (2000). Evidence for a requirement for ATP hydrolysis at two distinct steps during a single turnover of the catalytic cycle of human P-glycoprotein. *Proc. Natl. Acad. Sci. U.S.A.* **97**(6): 2515-20.

Sauna, Z. E. and Ambudkar, S. V. (2001). Characterization of the catalytic cycle of ATP hydrolysis by human P-glycoprotein. The two ATP hydrolysis events in a single catalytic cycle are kinetically similar but affect different functional outcomes. *J. Biol. Chem.* **276**(15): 11653-61.

Sauna, Z. E., Muller, M., Peng, X. H. and Ambudkar, S. V. (2002). Importance of the conserved Walker B glutamate residues, 556 and 1201, for the completion of the catalytic cycle of ATP hydrolysis by human P-glycoprotein (ABCB1). *Biochemistry.* **41**(47): 13989-4000.

Sauna, Z. E., Smith, M. M., Muller, M. and Ambudkar, S. V. (2001a). Functionally similar vanadate-induced 8-azidoadenosine 5'-[alpha-(32)P]Diphosphate-trapped transition state intermediates of human P-glycoprotin are generated in the absence and presence of ATP hydrolysis. *J Biol Chem.* **276**(24): 21199-208.

Sauna, Z. E., Smith, M. M., Muller, M., Kerr, K. M. and Ambudkar, S. V. (2001b). The mechanism of action of multidrug-resistance-linked P-glycoprotein. *J Bioenerg Biomembr.* **33**(6): 481-91.

Scarborough, G. A. (1995). Drug-stimulated ATPase activity of the human P-glycoprotein. *J Bioenerg Biomembr.* **27**(1): 37-41.

Schinkel, A. H. (1999). P-Glycoprotein, a gatekeeper in the blood-brain barrier. *Adv Drug Deliv Rev.* **36**(2-3): 179-94.

Schinkel, A. H., Mayer, U., Wagenaar, E., Mol, C. A., van Deemter, L., Smit, J. J., van der Valk, M. A., Voordouw, A. C., Spits, H., van Tellingen, O., *et al.* (1997). Normal viability and altered pharmacokinetics in mice lacking mdr1-type (drug-transporting) P-glycoproteins. *Proc Natl Acad Sci U S A.* **94**(8): 4028-33.

Schinkel, A. H., Smit, J. J., van Tellingen, O., Beijnen, J. H., Wagenaar, E., van Deemter, L., Mol, C. A., van der Valk, M. A., Robanus-Maandag, E. C., te Riele, H. P., *et al.* (1994). Disruption of the mouse mdr1a P-glycoprotein gene leads to a deficiency in the blood-brain barrier and to increased sensitivity to drugs. *Cell.* **77**(4): 491-502.

Schinkel, A. H., Wagenaar, E., Mol, C. A. and van Deemter, L. (1996). P-glycoprotein in the blood-brain barrier of mice influences the brain penetration and pharmacological activity of many drugs. *J Clin Invest.* **97**(11): 2517-24.

Schmees, G., Stein, A., Hunke, S., Landmesser, H. and Schneider, E. (1999). Functional consequences of mutations in the conserved 'signature sequence' of the ATP-binding-cassette protein MalK. *Eur J Biochem.* **266**(2): 420-30.

Schmitt, L., Benabdelhak, H., Blight, M. A., Holland, I. B. and Stubbs, M. T. (2003). Crystal structure of the nucleotide-binding domain of the ABC-transporter haemolysin B: identification of a variable region within ABC helical domains. *J. Mol. Biol.* **330**(2): 333-42.

Schneider, E. and Hunke, S. (1998). ATP-binding-cassette (ABC) transport systems: functional and structural aspects of the ATP-hydrolyzing subunits/domains. *FEMS Microbiol. Rev.* **22**(1): 1-20.

Schneider, E. and Walter, C. (1991). A chimeric nucleotide-binding protein, encoded by a hisP-malK hybrid gene, is functional in maltose transport in Salmonella typhimurium. *Mol Microbiol.* **5**(6): 1375-83.

Schneider, E., Wilken, S. and Schmid, R. (1994). Nucleotide-induced conformational changes of MalK, a bacterial ATP binding cassette transporter protein. *J Biol Chem.* **269**(32): 20456-61.

Schowen, K. B. and Schowen, R. L. (1982). Solvent isotope effects of enzyme systems. *Methods Enzymol.* **87**: 551-606.

Schriml, L. M. and Dean, M. (2000). Identification of 18 mouse ABC genes and characterization of the ABC superfamily in Mus musculus. *Genomics.* **64**(1): 24-31.

Schumacher, M. A., Miller, M. C., Grkovic, S., Brown, M. H., Skurray, R. A. and Brennan, R. G. (2001). Structural mechanisms of QacR induction and multidrug recognition. *Science.* **294**(5549): 2158-63.

Schurr, E., Raymond, M., Bell, J. C. and Gros, P. (1989). Characterization of the multidrug resistance protein expressed in cell clones stably transfected with the mouse mdr1 cDNA. *Cancer Res.* **49**(10): 2729-33.

Schweins, T., Geyer, M., Scheffzek, K., Warshel, A., Kalbitzer, H. R. and Wittinghofer, A. (1995). Substrate-assisted catalysis as a mechanism for GTP hydrolysis of p21ras and other GTP-binding proteins. *Nat Struct Biol.* **2**(1): 36-44.

Seelig, A., Blatter, X. L. and Wohnsland, F. (2000). Substrate recognition by P-glycoprotein and the multidrug resistance-associated protein MRP1: a comparison. *Int J Clin Pharmacol Ther.* **38**(3): 111-21.

Seghers, V., Nakazaki, M., DeMayo, F., Aguilar-Bryan, L. and Bryan, J. (2000). Sur1 knockout mice. A model for K(ATP) channel-independent regulation of insulin secretion. *J Biol Chem.* **275**(13): 9270-7.

Seliger, B., Hohne, A., Jung, D., Kallfelz, M., Knuth, A., Jaeger, E., Bernhard, H., Momburg, F., Tampe, R. and Huber, C. (1997). Expression and function of the

peptide transporters in escape variants of human renal cell carcinomas. *Exp Hematol.* **25**(7): 608-14.

Senior, A. E., al-Shawi, M. K. and Urbatsch, I. L. (1995a). ATP hydrolysis by multidrug-resistance protein from Chinese hamster ovary cells. *J. Bioenerg. Biomembr.* **27**(1): 31-6.

Senior, A. E., al-Shawi, M. K. and Urbatsch, I. L. (1995b). The catalytic cycle of P-glycoprotein. *FEBS Lett.* **377**(3): 285-9.

Senior, A. E. and Bhagat, S. (1998). P-glycoprotein shows strong catalytic cooperativity between the two nucleotide sites. *Biochemistry* **37**(3): 831-6.

Shani, N., Sapag, A. and Valle, D. (1996). Characterization and analysis of conserved motifs in a peroxisomal ATP-binding cassette transporter. *J Biol Chem.* **271**(15): 8725-30.

Shani, N. and Valle, D. (1998). Peroxisomal ABC transporters. *Methods Enzymol.* **292**: 753-76.

Shapiro, A. B., Duthie, M., Childs, S., Okubo, T. and Ling, V. (1996). Characterization and epitope mapping of several new anti-P-glycoprotein monoclonal antibodies. *Int. J. Cancer* **67**(2): 256-63.

Shapiro, A. B. and Ling, V. (1994). ATPase activity of purified and reconstituted P-glycoprotein from Chinese hamster ovary cells. [erratum appears in J Biol Chem 1994 Jun 17;269(24):16983.]. *J. Biol. Chem.* **269**(5): 3745-54.

Shapiro, A. B. and Ling, V. (1995). Using purified P-glycoprotein to understand multidrug resistance. *J. Bioenerg. Biomembr.* **27**(1): 7-13.

Sharma, S. and Davidson, A. L. (2000). Vanadate-induced trapping of nucleotides by purified maltose transport complex requires ATP hydrolysis. *J Bacteriol.* **182**(23): 6570-6.

Sharom, F. J., Liu, R., Romsicki, Y. and Lu, P. (1999). Insights into the structure and substrate interactions of the P-glycoprotein multidrug transporter from spectroscopic studies. *Biochim. Biophys. Acta* **1461**(2): 327-45.

Sharom, F. J., Yu, X., Chu, J. W. and Doige, C. A. (1995). Characterization of the ATPase activity of P-glycoprotein from multidrug-resistant Chinese hamster ovary cells. *Biochem J.* **308**(Pt 2): 381-90.

Sharom, F. J., Yu, X. and Doige, C. A. (1993). Functional reconstitution of drug transport and ATPase activity in proteoliposomes containing partially purified P-glycoprotein. *J. Biol. Chem.* **268**(32): 24197-202.

Shulenin, S., Nogee, L. M., Annilo, T., Wert, S. E., Whitsett, J. A. and Dean, M. (2004). ABCA3 gene mutations in newborns with fatal surfactant deficiency. *N Engl J Med.* **350**(13): 1296-303.

Shuman, H. A. (1982). Active transport of maltose in Escherichia coli K12. Role of the periplasmic maltose-binding protein and evidence for a substrate recognition site in the cytoplasmic membrane. *J Biol Chem.* **257**(10): 5455-61.

Shustik, C., Dalton, W. and Gros, P. (1995). P-glycoprotein-mediated multidrug resistance in tumor cells: biochemistry, clinical relevance and modulation. *Mol. Aspects Med.* **16**: 1-78.

Shyamala, V., Baichwal, V., Beall, E. and Ames, G. F. (1991). Structure-function analysis of the histidine permease and comparison with cystic fibrosis mutations. *J. Biol. Chem.* **266**(28): 18714-9.

Siesjo, B. K. (1988). Hypoglycemia, brain metabolism, and brain damage. *Diabetes Metab Rev.* **4**(2): 113-44.

Sisodiya, S. M., Lin, W. R., Harding, B. N., Squier, M. V. and Thom, M. (2002). Drug resistance in epilepsy: expression of drug resistance proteins in common causes of refractory epilepsy. *Brain* **125**: 22-31.

Smit, J. J., Schinkel, A. H., Mol, C. A., Majoor, D., Mooi, W. J., Jongsma, A. P., Lincke, C. R. and Borst, P. (1994). Tissue distribution of the human MDR3 P-glycoprotein. *Lab Invest.* **71**(5): 638-49.

Smit, J. J., Schinkel, A. H., Oude Elferink, R. P., Groen, A. K., Wagenaar, E., van Deemter, L., Mol, C. A., Ottenhoff, R., van der Lugt, N. M., van Roon, M. A., *et al.* (1993). Homozygous disruption of the murine mdr2 P-glycoprotein gene leads to a complete absence of phospholipid from bile and to liver disease. *Cell.* **75**(3): 451-62.

Smith, C. A. and Rayment, I. (1996a). Active site comparisons highlight structural similarities between myosin and other P-loop proteins. *Biophys J.* **70**(4): 1590-602.

Smith, C. A. and Rayment, I. (1996b). X-ray structure of the magnesium(II).ADP.vanadate complex of the Dictyostelium discoideum myosin motor domain to 1.9 A resolution. *Biochemistry* **35**(17): 5404-17.

Smith, P. C., Karpowich, N., Millen, L., Moody, J. E., Rosen, J., Thomas, P. J. and Hunt, J. F. (2002). ATP binding to the motor domain from an ABC transporter drives formation of a nucleotide sandwich dimer. *Mol. Cell* **10**(1): 139-49.

Snouwaert, J. N., Brigman, K. K., Latour, A. M., Malouf, N. N., Boucher, R. C., Smithies, O. and Koller, B. H. (1992). An animal model for cystic fibrosis made by gene targeting. *Science.* **257**(5073): 1083-8.

Spahn-Langguth, H., Baktir, G., Radschuweit, A., Okyar, A., Terhaag, B., Ader, P., Hanafy, A. and Langguth, P. (1998). P-glycoprotein transporters and the gastrointestinal tract: evaluation of the potential in vivo relevance of in vitro data employing talinolol as model compound. *Int J Clin Pharmacol Ther.* **36**(1): 16-24.

Spoerner, M., Herrmann, C., Vetter, I. R., Kalbitzer, H. R. and Wittinghofer, A. (2001). Dynamic properties of the Ras switch I region and its importance for binding to effectors. *Proc Natl Acad Sci U S A.* **98**(9): 4944-9.

Sreekrishna, K., Potenz, R. H., Cruze, J. A., McCombie, W. R., Parker, K. A., Nelles, L., Mazzaferro, P. K., Holden, K. A., Harrison, R. G., Wood, P. J., *et al.* (1988). High level expression of heterologous proteins in methylotrophic yeast Pichia pastoris. *J Basic Microbiol.* **28**(4): 265-78.

Stein, A., Hunke, S. and Schneider, E. (1997). Mutational analysis eliminates Glu64 and Glu94 as candidates for 'catalytic carboxylate' in the bacterial ATP-binding-cassette protein MalK. *FEBS Lett.* **413**(2): 211-4.

Stenham, D. R., Campbell, J. D., Sansom, M. S., Higgins, C. F., Kerr, I. D. and Linton, K. J. (2003). An atomic detail model for the human ATP binding cassette transporter P-glycoprotein derived from disulfide cross-linking and homology modeling. *FASEB J.* **17**(15): 2287-9.

Stockel, B., Konig, J., Nies, A. T., Cui, Y., Brom, M. and Keppler, D. (2000). Characterization of the 5'-flanking region of the human multidrug resistance

protein 2 (MRP2) gene and its regulation in comparison withthe multidrug resistance protein 3 (MRP3) gene. *Eur J Biochem.* **267**(5): 1347-58.

Story, R. M. and Steitz, T. A. (1992). Structure of the recA protein-ADP complex. *Nature.* **355**(6358): 374-6.

Strautnieks, S. S., Bull, L. N., Knisely, A. S., Kocoshis, S. A., Dahl, N., Arnell, H., Sokal, E., Dahan, K., Childs, S., Ling, V., *et al.* (1998). A gene encoding a liver-specific ABC transporter is mutated in progressive familial intrahepatic cholestasis. *Nat Genet.* **20**(3): 233-8.

Sullivan, G. F., Amenta, P. S., Villanueva, J. D., Alvarez, C. J., Yang, J. M. and Hait, W. N. (1998). The expression of drug resistance gene products during the progression of human prostate cancer. *Clin Cancer Res.* **4**(6): 1393-403.

Szabo, K., Szakacs, G., Hegeds, T. and Sarkadi, B. (1999). Nucleotide occlusion in the human cystic fibrosis transmembrane conductance regulator. Different patterns in the two nucleotide binding domains. *J. Biol. Chem.* **274**(18): 12209-12.

Szabo, K., Welker, E., Bakos, Muller, M., Roninson, I., Varadi, A. and Sarkadi, B. (1998). Drug-stimulated nucleotide trapping in the human multidrug transporter MDR1. Cooperation of the nucleotide binding domains. *J Biol Chem.* **273**(17): 10132-8.

Szakacs, G., Ozvegy, C., Bakos, E., Sarkadi, B. and Varadi, A. (2001). Role of glycine-534 and glycine-1179 of human multidrug resistance protein (MDR1) in drug-mediated control of ATP hydrolysis. *Biochem J.* **356**(Pt 1): 71-5.

Tanaka, Y., Yamada, K., Zhou, C. J., Ban, N., Shioda, S. and Inagaki, N. (2003). Temporal and spatial profiles of ABCA2-expressing oligodendrocytes in the developing rat brain. *J Comp Neurol.* **455**(3): 353-67.

Tanford, C. (1983). Mechanism of free energy coupling in active transport. *Annu Rev Biochem.* **52**: 379-409.

Thiebaut, F., Tsuruo, T., Hamada, H., Gottesman, M. M., Pastan, I. and Willingham, M. C. (1987). Cellular localization of the multidrug-resistance gene product P-glycoprotein in normal human tissues. *Proc Natl Acad Sci U S A.* **84**(21): 7735-8.

Thomas, A. C., Cullup, T., Norgett, E. E., Hill, T., Barton, S., Dale, B. A., Sprecher, E., Sheridan, E., Taylor, A. E., Wilroy, R. S., *et al.* (2006). ABCA12 is the major harlequin ichthyosis gene. *J Invest Dermatol.* **126**(11): 2408-13. Epub 006 Aug 10.

Thomas, P. M., Cote, G. J., Wohllk, N., Haddad, B., Mathew, P. M., Rabl, W., Aguilar-Bryan, L., Gagel, R. F. and Bryan, J. (1995). Mutations in the sulfonylurea receptor gene in familial persistent hyperinsulinemic hypoglycemia of infancy. *Science.* **268**(5209): 426-9.

Tombline, G., Bartholomew, L. A., Tyndall, G. A., Gimi, K., Urbatsch, I. L. and Senior, A. E. (2004a). Properties of P-glycoprotein with mutations in the "catalytic carboxylate" glutamate residues. *J. Biol. Chem.* **279**(45): 46518-26.

Tombline, G., Bartholomew, L. A., Urbatsch, I. L. and Senior, A. E. (2004b). Combined mutation of catalytic glutamate residues in the two nucleotide binding domains of P-glycoprotein generates a conformation that binds ATP and ADP tightly. *J. Biol. Chem.* **279**(30): 31212-20.

Tombline, G., Muharemagic, A., White, L. B. and Senior, A. E. (2005). Involvement of the "occluded nucleotide conformation" of P-glycoprotein in the catalytic pathway. *Biochemistry* **44**(38): 12879-86.

Trezise, A. E. and Buchwald, M. (1991). In vivo cell-specific expression of the cystic fibrosis transmembrane conductance regulator. *Nature.* **353**(6343): 434-7.

Tsui, L. C. (1992). The spectrum of cystic fibrosis mutations. *Trends Genet.* **8**(11): 392-8.

Tsui, L. C. (1995). The cystic fibrosis transmembrane conductance regulator gene. *Am J Respir Crit Care Med.* **151**(3 Pt 2): S47-53.

Tusnady, G. E., Sarkadi, B., Simon, I. and Varadi, A. (2006). Membrane topology of human ABC proteins. *FEBS Lett.* **580**(4): 1017-22.

Tyzack, J. K., Wang, X., Belsham, G. J. and Proud, C. G. (2000). ABC50 interacts with eukaryotic initiation factor 2 and associates with the ribosome in an ATP-dependent manner. *J Biol Chem.* **275**(44): 34131-9.

Ueda, K., Taguchi, Y. and Morishima, M. (1997). How does P-glycoprotein recognize its substrates? *Semin Cancer Biol.* **8**(3): 151-9.

Urbatsch, I. L., al-Shawi, M. K. and senior, A. E. (1994). Characterization of the ATPase activity of purified Chinese hamster P-glycoprotein. *Biochemistry* **33**(23): 7069-76.

Urbatsch, I. L., Beaudet, L., Carrier, I. and Gros, P. (1998). Mutations in either nucleotide-binding site of P-glycoprotein (Mdr3) prevent vanadate trapping of nucleotide at both sites. *Biochemistry* **37**(13): 4592-602.

Urbatsch, I. L., Gimi, K., Wilke-Mounts, S. and Senior, A. E. (2000a). Conserved walker A Ser residues in the catalytic sites of P-glycoprotein are critical for catalysis and involved primarily at the transition state step. *J. Biol. Chem.* **275**(32): 25031-8.

Urbatsch, I. L., Gimi, K., Wilke-Mounts, S. and Senior, A. E. (2000b). Investigation of the role of glutamine-471 and glutamine-1114 in the two catalytic sites of P-glycoprotein. *Biochemistry* **39**(39): 11921-7.

Urbatsch, I. L., Julien, M., Carrier, I., Rousseau, M. E., Cayrol, R. and Gros, P. (2000c). Mutational analysis of conserved carboxylate residues in the nucleotide binding sites of P-glycoprotein. *Biochemistry* **39**(46): 14138-49.

Urbatsch, I. L., Sankaran, B., Bhagat, S. and Senior, A. E. (1995a). Both P-glycoprotein nucleotide-binding sites are catalytically active. *J. Biol. Chem.* **270**(45): 26956-61.

Urbatsch, I. L., Sankaran, B., Weber, J. and Senior, A. E. (1995b). P-glycoprotein is stably inhibited by vanadate-induced trapping of nucleotide at a single catalytic site. *J. Biol. Chem.* **270**(33): 19383-90.

Urbatsch, I. L. and Senior, A. E. (1995). Effects of lipids on ATPase activity of purified Chinese hamster P-glycoprotein. *Arch. Biochem. Biophys.* **316**(1): 135-40.

van de Ven, R., de Jong, M. C., Reurs, A. W., Schoonderwoerd, A. J., Jansen, G., Hooijberg, J. H., Scheffer, G. L., de Gruijl, T. D. and Scheper, R. J. (2006). Dendritic cells require multidrug resistance protein 1 (ABCC1) transporter activity for differentiation. *J Immunol.* **176**(9): 5191-8.

van der Klei, I. J., Harder, W. and Veenhuis, M. (1991). Biosynthesis and assembly of alcohol oxidase, a peroxisomal matrix protein in methylotrophic yeasts: a review. *Yeast.* **7**(3): 195-209.

van Helvoort, A., Smith, A. J., Sprong, H., Fritzsche, I., Schinkel, A. H., Borst, P. and van Meer, G. (1996). MDR1 P-glycoprotein is a lipid translocase of broad

specificity, while MDR3 P-glycoprotein specifically translocates phosphatidylcholine. *Cell.* **87**(3): 507-17.

Van Kaer, L., Ashton-Rickardt, P. G., Ploegh, H. L. and Tonegawa, S. (1992). TAP1 mutant mice are deficient in antigen presentation, surface class I molecules, and CD4-8+ T cells. *Cell.* **71**(7): 1205-14.

van Veen, H. W., Callaghan, R., Soceneantu, L., Sardini, A., Konings, W. N. and Higgins, C. F. (1998). A bacterial antibiotic-resistance gene that complements the human multidrug-resistance P-glycoprotein gene. *Nature.* **391**(6664): 291-5.

van Veen, H. W., Venema, K., Bolhuis, H., Oussenko, I., Kok, J., Poolman, B., Driessen, A. J. and Konings, W. N. (1996). Multidrug resistance mediated by a bacterial homolog of the human multidrug transporter MDR1. *Proc Natl Acad Sci U S A.* **93**(20): 10668-72.

Van Veldhoven, P. P. and Mannaerts, G. P. (1987). Inorganic and organic phosphate measurements in the nanomolar range. *Anal. Biochem.* **161**(1): 45-8.

Veenhuis, M., Van Dijken, J. P. and Harder, W. (1983). The significance of peroxisomes in the metabolism of one-carbon compounds in yeasts. *Adv Microb Physiol.* **24**: 1-82.

Venter, H., Shahi, S., Balakrishnan, L., Velamakanni, S., Bapna, A., Woebking, B. and van Veen, H. W. (2005). Similarities between ATP-dependent and ion-coupled multidrug transporters. *Biochem Soc Trans.* **33**(Pt 5): 1008-11.

Verdon, G., Albers, S. V., Dijkstra, B. W., Driessen, A. J. and Thunnissen, A. M. (2003a). Crystal structures of the ATPase subunit of the glucose ABC transporter from Sulfolobus solfataricus: nucleotide-free and nucleotide-bound conformations. *J. Mol. Biol.* **330**(2): 343-58.

Verdon, G., Albers, S. V., van Oosterwijk, N., Dijkstra, B. W., Driessen, A. J. and Thunnissen, A. M. (2003b). Formation of the productive ATP-Mg2+-bound dimer of GlcV, an ABC-ATPase from Sulfolobus solfataricus. *J. Mol. Biol.* **334**(2): 255-67.

Vergani, P., Lockless, S. W., Nairn, A. C. and Gadsby, D. C. (2005). CFTR channel opening by ATP-driven tight dimerization of its nucleotide-binding domains. *Nature* **433**: 876-80.

Verrelle, P., Meissonnier, F., Fonck, Y., Feillel, V., Dionet, C., Kwiatkowski, F., Plagne, R. and Chassagne, J. (1991). Clinical relevance of immunohistochemical detection of multidrug resistance P-glycoprotein in breast carcinoma. *J Natl Cancer Inst.* **83**(2): 111-6.

Vetter, I. R. and Wittinghofer, A. (2001). The guanine nucleotide-binding switch in three dimensions. *Science.* **294**(5545): 1299-304.

Vigano, C., Julien, M., Carrier, I., Gros, P. and Ruysschaert, J.-M. (2002). Structural and functional asymmetry of the nucleotide-binding domains of P-glycoprotein investigated by attenuated total reflection fourier transform infrared spectroscopy. *J. Biol. Chem.* **277**(7): 5008-16.

Vogan, K. J. and Gros, P. (1997). The C-terminal subdomain makes an important contribution to the DNA binding activity of the Pax-3 paired domain. *J. Biol. Chem.* **272**(45): 28289-95.

Vulevic, B., Chen, Z., Boyd, J. T., Davis, W., Jr., Walsh, E. S., Belinsky, M. G. and Tew, K. D. (2001). Cloning and characterization of human adenosine 5'-triphosphate-

binding cassette, sub-family A, transporter 2 (ABCA2). *Cancer Res.* **61**(8): 3339-47.

Wada, M., Toh, S., Taniguchi, K., Nakamura, T., Uchiumi, T., Kohno, K., Yoshida, I., Kimura, A., Sakisaka, S., Adachi, Y., *et al.* (1998). Mutations in the canilicular multispecific organic anion transporter (cMOAT) gene, a novel ABC transporter, in patients with hyperbilirubinemia II/Dubin-Johnson syndrome. *Hum Mol Genet.* **7**(2): 203-7.

Walker, J. E., Saraste, M., Runswick, M. J. and Gay, N. J. (1982). Distantly related sequences in the alpha- and beta-subunits of ATP synthase, myosin, kinases and other ATP-requiring enzymes and a common nucleotide binding fold. *EMBO J.* **1**(8): 945-51.

Wanders, R. J., Visser, W. F., van Roermund, C. W., Kemp, S. and Waterham, H. R. (2007). The peroxisomal ABC transporter family. *Pflugers Arch.* **453**(5): 719-34. Epub 2006 Oct 13.

Wang, N., Yvan-Charvet, L., Lutjohann, D., Mulder, M., Vanmierlo, T., Kim, T. W. and Tall, A. R. (2007). ATP-binding cassette transporters G1 and G4 mediate cholesterol and desmosterol efflux to HDL and regulate sterol accumulation in the brain. *Faseb J* **26**: 26.

Wang, R., Salem, M., Yousef, I. M., Tuchweber, B., Lam, P., Childs, S. J., Helgason, C. D., Ackerley, C., Phillips, M. J. and Ling, V. (2001). Targeted inactivation of sister of P-glycoprotein gene (spgp) in mice results in nonprogressive but persistent intrahepatic cholestasis. *Proc Natl Acad Sci U S A.* **98**(4): 2011-6. Epub 01 Feb 6.

Ward, A., Reyes, C. L., Yu, J., Roth, C. B. and Chang, G. (2007). Flexibility in the ABC transporter MsbA: Alternating access with a twist. *Proc Natl Acad Sci U S A.* **104**(48): 19005-10. Epub 2007 Nov 16.

Weber, J. and Senior, A. E. (1997). Catalytic mechanism of F1-ATPase. *Biochim Biophys Acta.* **1319**(1): 19-58.

Weber, J., Wilke-Mounts, S., Lee, R. S., Grell, E. and Senior, A. E. (1993). Specific placement of tryptophan in the catalytic sites of Escherichia coli F1-ATPase provides a direct probe of nucleotide binding: maximal ATP hydrolysis occurs with three sites occupied. *J Biol Chem.* **268**(27): 20126-33.

Weiner, J. H., Furlong, C. E. and Heppel, L. A. (1971). A binding protein for L-glutamine and its relation to active transport in E. coli. *Arch Biochem Biophys.* **142**(2): 715-7.

Weng, J., Mata, N. L., Azarian, S. M., Tzekov, R. T., Birch, D. G. and Travis, G. H. (1999). Insights into the function of Rim protein in photoreceptors and etiology of Stargardt's disease from the phenotype in abcr knockout mice. *Cell.* **98**(1): 13-23.

Wijnholds, J., Evers, R., van Leusden, M. R., Mol, C. A., Zaman, G. J., Mayer, U., Beijnen, J. H., van der Valk, M., Krimpenfort, P. and Borst, P. (1997). Increased sensitivity to anticancer drugs and decreased inflammatory response in mice lacking the multidrug resistance-associated protein. *Nat Med.* **3**(11): 1275-9.

Wijnholds, J., Mol, C. A., van Deemter, L., de Haas, M., Scheffer, G. L., Baas, F., Beijnen, J. H., Scheper, R. J., Hatse, S., De Clercq, E., *et al.* (2000). Multidrug-resistance protein 5 is a multispecific organic anion transporter able to transport nucleotide analogs. *Proc Natl Acad Sci U S A.* **97**(13): 7476-81.

Winzeler, E. A., Shoemaker, D. D., Astromoff, A., Liang, H., Anderson, K., Andre, B., Bangham, R., Benito, R., Boeke, J. D., Bussey, H., *et al.* (1999). Functional characterization of the S. cerevisiae genome by gene deletion and parallel analysis. *Science.* **285**(5429): 901-6.

Wolters, J. C., Abele, R. and Tampe, R. (2005). Selective and ATP-dependent translocation of peptides by the homodimeric ATP binding cassette transporter TAP-like (ABCB9). *J Biol Chem.* **280**(25): 23631-6. Epub 2005 Apr 29.

Yamanaka, Y., Akiyama, M., Sugiyama-Nakagiri, Y., Sakai, K., Goto, M., McMillan, J. R., Ota, M., Sawamura, D. and Shimizu, H. (2007). Expression of the keratinocyte lipid transporter ABCA12 in developing and reconstituted human epidermis. *Am J Pathol.* **171**(1): 43-52.

Yamano, G., Funahashi, H., Kawanami, O., Zhao, L. X., Ban, N., Uchida, Y., Morohoshi, T., Ogawa, J., Shioda, S. and Inagaki, N. (2001). ABCA3 is a lamellar body membrane protein in human lung alveolar type II cells. *FEBS Lett.* **508**(2): 221-5.

Yarunin, A., Panse, V. G., Petfalski, E., Dez, C., Tollervey, D. and Hurt, E. C. (2005). Functional link between ribosome formation and biogenesis of iron-sulfur proteins. *EMBO J.* **24**(3): 580-8. Epub 2005 Jan 20.

Yasui-Furukori, N., Saito, M., Nakagami, T., Kaneda, A., Tateishi, T. and Kaneko, S. (2006). Association between multidrug resistance 1 (MDR1) gene polymorphisms and therapeutic response to bromperidol in schizophrenic patients: a preliminary study. *Progress in Neuro-psychopharmacology & Biological Psychiatry* **30**(2): 286-91. Epub 2006 Jan 4.

Yoshida, M. and Amano, T. (1995). A common topology of proteins catalyzing ATP-triggered reactions. *FEBS Lett.* **359**(1): 1-5.

Yoshiura, K., Kinoshita, A., Ishida, T., Ninokata, A., Ishikawa, T., Kaname, T., Bannai, M., Tokunaga, K., Sonoda, S., Komaki, R., *et al.* (2006). A SNP in the ABCC11 gene is the determinant of human earwax type. *Nat Genet.* **38**(3): 324-30. Epub 2006 Jan 29.

Young, A. M., Allen, C. E. and Audus, K. L. (2003). Efflux transporters of the human placenta. *Adv Drug Deliv Rev.* **55**(1): 125-32.

Young, J. and Holland, I. B. (1999). ABC transporters: bacterial exporters-revisited five years on. *Biochim Biophys Acta.* **1461**(2): 177-200.

Young, L. C., Campling, B. G., Voskoglou-Nomikos, T., Cole, S. P., Deeley, R. G. and Gerlach, J. H. (1999). Expression of multidrug resistance protein-related genes in lung cancer: correlation with drug response. *Clin Cancer Res.* **5**(3): 673-80.

Young, S. G. and Fielding, C. J. (1999). The ABCs of cholesterol efflux. *Nat Genet.* **22**(4): 316-8.

Yuan, Y. R., Blecker, S., Martsinkevich, O., Millen, L., Thomas, P. J. and Hunt, J. F. (2001). The crystal structure of the MJ0796 ATP-binding cassette. Implications for the structural consequences of ATP hydrolysis in the active site of an ABC transporter. *J. Biol. Chem.* **276**(34): 32313-21.

Zaitseva, J., Holland, I. B. and Schmitt, L. (2004). The role of CAPS buffer in expanding the crystallization space of the nucleotide-binding domain of the ABC transporter haemolysin B from Escherichia coli. *Acta crystallogr D Biol Crystallogr* **60**(Pt 6): 1076-84.

Zaitseva, J., Jenewein, S., Jumpertz, T., Holland, I. B. and Schmitt, L. (2005a). H662 is the linchpin of ATP hydrolysis in the nucleotide-binding domain of the ABC transporter HlyB. *EMBO J* **24**(11): 1901-10.

Zaitseva, J., Jenewein, S., Oswald, C., Jumpertz, T., Holland, I. B. and Schmitt, L. (2005b). A molecular understanding of the catalytic cycle of the nucleotide-binding domain of the ABC transporter HlyB. *Biochemical Society transactions* **33**(Pt 5): 990-5.

Zaitseva, J., Jenewein, S., Wiedenmann, A., Benabdelhak, H., Holland, I. B. and Schmitt, L. (2005c). Functional characterization and ATP-induced dimerization of the isolated ABC-domain of the haemolysin B transporter. *Biochemistry* **44**(28): 9680-90.

Zaitseva, J., Oswald, C., Jumpertz, T., Jenewein, S., Wiedenmann, A., Holland, I. B. and Schmitt, L. (2006). A structural analysis of asymmetry required for catalytic activity of an ABC-ATPase domain dimer. *EMBO J.* **25**(14): 3432-43. Epub 2006 Jul 6.

Zelcer, N., van de Wetering, K., Hillebrand, M., Sarton, E., Kuil, A., Wielinga, P. R., Tephly, T., Dahan, A., Beijnen, J. H. and Borst, P. (2005). Mice lacking multidrug resistance protein 3 show altered morphine pharmacokinetics and morphine-6-glucuronide antinociception. *Proc Natl Acad Sci U S A.* **102**(20): 7274-9. Epub 2005 May 10.

Zhang, F., Zhang, W., Liu, L., Fisher, C. L., Hui, D., Childs, S., Dorovini-Zis, K. and Ling, V. (2000). Characterization of ABCB9, an ATP binding cassette protein associated with lysosomes. *J Biol Chem.* **275**(30): 23287-94.

Zhang, K., Mack, P. and Wong, K. P. (1998). Glutathione-related mechanisms in cellular resistance to anticancer drugs. *Int J Oncol.* **12**(4): 871-82.

Zhao, Q. and Chang, X. (2004). Mutation of the Aromatic Amino Acid Interacting with Adenine Moiety of ATP to a Polar Residue Alters the Properties of Multidrug Resistance Protein 1. *J. Biol. Chem.* **279**(47): 48505-12.

Zhou, C., Zhao, L., Inagaki, N., Guan, J., Nakajo, S., Hirabayashi, T., Kikuyama, S. and Shioda, S. (2001). Atp-binding cassette transporter ABC2/ABCA2 in the rat brain: a novel mammalian lysosome-associated membrane protein and a specific marker for oligodendrocytes but not for myelin sheaths. *J Neurosci.* **21**(3): 849-57.

Zhou, C. J., Inagaki, N., Pleasure, S. J., Zhao, L. X., Kikuyama, S. and Shioda, S. (2002a). ATP-binding cassette transporter ABCA2 (ABC2) expression in the developing spinal cord and PNS during myelination. *J Comp Neurol.* **451**(4): 334-45.

Zhou, S., Morris, J. J., Barnes, Y., Lan, L., Schuetz, J. D. and Sorrentino, B. P. (2002b). Bcrp1 gene expression is required for normal numbers of side population stem cells in mice, and confers relative protection to mitoxantrone in hematopoietic cells in vivo. *Proc Natl Acad Sci U S A.* **99**(19): 12339-44. Epub 2002 Sep 6.

Zhou, T. and Rosen, B. P. (1997). Tryptophan fluorescence reports nucleotide-induced conformational changes in a domain of the ArsA ATPase. *J. Biol. Chem.* **272**(32): 19731-7.

Zhou, Y., Gottesman, M. M. and Pastan, I. (1999). Studies of human MDR1-MDR2 chimeras demonstrate the functional exchangeability of a major transmembrane

segment of the multidrug transporter and phosphatidylcholine flippase. *Mol. Cell. Biol.* **19**(2): 1450-9.

Zimmerman, C., Klein, K. C., Kiser, P. K., Singh, A. R., Firestein, B. L., Riba, S. C. and Lingappa, J. R. (2002). Identification of a host protein essential for assembly of immature HIV-1 capsids. *Nature.* **415**(6867): 88-92.

Zolnerciks, J. K., Wooding, C. and Linton, K. J. (2007). Evidence for a Sav1866-like architecture for the human multidrug transporter P-glycoprotein. *Faseb J* **12**: 1-12.

Original Contributions to Knowledge

1. Identification of an important role in Abcb1a catalysis for an aromatic residue which is part of a conserved motif, the A-loop, upstream of the Walker A sequence in each NBD. Tyrosine 397 and 1040 are thus responsible for π-stacking with the adenine moiety of bound nucleotide in the NBSs of Abcb1a and contribute to nucleotide specificity and stability.

2. Identification of residues (Y618 and Y1263) that could serve as appropriate fluorescent probes, when mutated to tryptophan in the tryptophan-free Abcb1a enzyme, in tryptophan fluorescence assays to monitor nucleotide occupancy and/or NBD dimerization during the catalytic cycle of Abcb1a.

3. Identification of mutation-sensitive conserved residues (invariant carboxylates E552 and E1197 in NBD1 and NBD2, respectively, of Abcb1a) with novel and unique phenotypes, featuring lack of transport and steady-state ATPase activities with retention of the capacity to trap 8-azido[α^{32}P]ATP both in the presence and absence of vanadate and/or drug.

4. Determination that formation of the catalytic transition state does occur in the mutant site in the single-site mutants E552X and E1197X, and steps after formation of the transition state are severely impaired in these mutant enzymes.

5. Detection of functional asymmetry between NBD1 and NBD2, as demonstrated by the radically different trapping properties of mutants K429R/E1197Q and E552Q/K1072R.

6. Identification that for E552 and E1197 the length of the side-chain is important for the catalytic activity, whereas the charge is critical for full turnover to occur.